

Spatial cells in the Subiculum; Influence of boundary manipulations

Sarah Stewart BSc (Hons) MSc

Submitted in accordance with the requirements for the degree of
Doctor of Philosophy

The University of Leeds
Institute of Psychological Sciences, Faculty of Medicine and Health

March 2013

The candidate confirms that the work submitted is her own and that appropriate credit has been given where reference has been made to the work of others.

This copy has been supplied on the understanding that it is copyright material and that no quotation from the thesis may be published without proper acknowledgement.

The right of Sarah Stewart to be identified as the Author of this work has been asserted by her in accordance with the Copyright, Designs and Patents Act 1988.

© 2012 The University of Leeds and Sarah Stewart

Acknowledgements

I would like to dedicate this thesis to my little cousin Beth. Beth was a pragmatic and curious girl who was fascinated by everything. By the age of 10 she had already decided that when she grew up she wanted to be a scientist like me. Last year we lost Beth to Leukaemia. I would therefore like to dedicate this work to Beth, who we all miss and who will always be in my heart.

I would like to give thanks to Dr Colin Lever. I could not have asked for a more enthusiastic and inspirational supervisor. I am grateful to Colin for encouraging my interest in science and for taking me on as PhD student. Colin's maintained enthusiasm meant that after every meeting I was always left excited and with fresh ideas, for that I am indebted. Further I would like to thank Colin's wife Kate and his children Rose and Moss for putting up with my home visits for our out of hours supervisory meetings. On a light note, I would also like to thank Colin for not laughing in my face when I first told him I thought I had recorded subicular grid cells.

I would also like to thank Professor John Rodgers for his unerring support and for his time and assistance over the years. After Colin had moved from Leeds to Durham John became my first supervisor and took over all of Colin's administrative roles. For that and for keeping me organised I will be eternally grateful.

There are also many other people who have helped with various aspects of my PhD. I would like to thank Neil, Lisa, Mark, Mark and Rob for their assistance and help with all lab-related things. A big thank you also goes to Vincent Douchamps for helping me set up my lab and for constant technical support. I would also like to thank my Colleagues at UCL for help with histology and analyses. Ali Jeewajee, Tom Wills and Francesca Cacucci I would like to thank for their help with the grid cell analyses and useful discussion. Particular thanks must be given to Stephen Burton, who not only was of great help with histology, but also entertained and looked after me during all of my trips to UCL. I would like to also give special thanks to Brian and Agnes Wallwork, for firstly hand-making all of my testing environments, and for secondly becoming treasured friends. Brian and Agnes' friendship and correspondence has continued to make me smile since our very first meeting three years ago.

I would like to give thanks to the friends I have made during my time at IPS; Neil Boyle, Ian Flatters, Emily Norris, Rebecca Graber, Nathan Illman, Anna Rossiter and Sarah Smith. It has been a pleasure working with them and I am so thankful for their support and companionship. In particular I would like to thank Fay Twiston-Davies, Suzi Morson and Christine Wells. I give specific thanks to Fay and Christine for being my lab companions. Both of whom kept me smiling during the long hours of testing, and often kept me from going mad during the dark trials. I would like to thank Suzi for her unofficial role as my PA. Truly without her I would have never got anything done. Thank you also to Suzi and Christine for the continuous supply of wine and cheese nights, without you my PhD would have been impossible. It has been an emotional journey the last few years and I am so grateful and thankful that we were together through it.

Lastly I would like to thank my family for their encouragement and for taking my mind off work whenever I visited home. Thank you to my Dad and my brother for being there when I needed them. Thank you to my grandparents Betty, Peter and Barclay for our long phone calls which were always able to cheer me. Also I would like to thank my granny Sally who I miss deeply. Most importantly I thank my Mum who is my rock and whose continued love and support humbles me almost every day. Without my families continued and unwavering support I would not have been able to reach this point.

Abstract

External space is mapped by a widespread brain circuit located in interconnected sub regions of the hippocampal-parahippocampal cortices. To date there have been 4 functionally specialised cell types identified providing information about location (place cells), heading direction (head direction cells), self-motion (grid cells) and boundaries (boundary vector cells and border cells).

In the present thesis I present novel research identifying and characterising spatial cells located in the subiculum, an under explored region within the hippocampal formation. The subiculum is a key output structure from CA1 but also provides strong projections to the entorhinal cortex and pre- and parasubiculum, placing it ideally within the brain circuitry to contribute to the representations of external space. This thesis presents evidence for a variety of functionally and morphologically diverse spatial cells located in the subiculum.

Critically I present the first ever report of subicular grid cells. These were recorded alongside boundary-responsive cells and head direction cells. The thesis characterises the basic properties of subicular grid cells, as tested in a variety of environmental manipulations. This thesis explores grid cell relationships to the environment and in particular to boundary manipulations.

Among the key results in this thesis is the discovery that grid scale increases along the anterior-posterior axis of the subiculum, similar to MEC grid scale. This thesis also shows that subicular grid cell patterns can be disrupted with environmental manipulation. Wall removal caused grid patterns to shift orientation and increase grid scale. The grid scale expansion was related to novelty, which supports previous findings from MEC grid cells (Barry et al., 2007; 2012). This thesis also shows that grid patterns were disrupted by barrier insertion e.g. causing an inhibition to grid fields. When recorded in total darkness the grid cell patterns remained stable, suggesting that vision is not required for maintenance of the grid pattern structure. Taken together these findings provide evidence that grid cell firing patterns are at least partially determined by environmental boundaries.

In addition this thesis extended upon the work of Lever et al., (2009), by presenting a detailed investigation and characterisation of subicular boundary vector cells (BVCs). I developed an empirical classification criterion, and utilised numerous manipulations to address the issue of what a BVC treats as a boundary. I also identified a new type of boundary related cell: the boundary-off cell. These cells have firing patterns which can be considered very similar to the

inverse of the BVC. The inhibitory response of boundaries on these cells may provide a mechanism to explain the field inhibition seen in grid cells with barrier insertion.

The data in this thesis presents novel research identifying and characterising spatial cells located in the subiculum. Of particular importance, is the discovery of grid cells in this structure that are intermingled with HD and boundary-responsive cells. The thesis focuses on characterising and investigating the importance of environment boundaries to subicular cell firing patterns. The results are discussed in relation to what is known about spatial representation in the hippocampal and parahippocampal regions, and the neural circuitry which comprises this representation.

Abbreviations

AC	Alternating current
BVC	Boundary vector cell
CA	Cornu ammonis
Cm	Centimetre
COP	Circular open platform
DG	Dentate Gyrus
EC	Entorhinal cortex
EEG	Electroencephalography
HD	Head direction
Hz	Hertz
i.m.	Intramuscular
i.p .	Intraperitoneal
ITI	inter trial interval
Kg	Kilograms
LEC	Lateral entorhinal cortex
LED	Light Emitting Diode
LH	Left hemisphere
LWC	Large walled circle
LWS	Large walled square
M	Metres
MEC	Medial entorhinal cortex
µm	Microns
µs	Microseconds
µv	Microvolts
ml	Millilitres
ms	Milliseconds
RH	right hemisphere
s.c.	Subcutaneous
SE	Standard error
SEM	Standard error of the mean
SWS	Small walled square

Contents

Abstract	iii
Contents	vi
Figure contents	xiii
Chapter 1 Introduction part 1: Anatomy of the hippocampal formation	1
1.1 Nomenclature.....	1
1.2 Gross morphology	2
1.3 Organization of the hippocampal formation and parahippocampal region..	3
1.4 Cytoarchitectonic organisation.....	5
1.4.1 Laminar organisation of the CA fields	5
1.4.2 Laminar organisation of the dentate gyrus (DG).....	5
1.4.3 Laminar organisation of the subiculum.....	6
1.4.4 Laminar organisation of the entorhinal cortex (EC)	6
1.4.5 Laminar organisation of the pre- and parasubiculum.....	6
1.5 General connectivity.....	6
1.5.1 Afferents to the hippocampal formation.....	7
1.5.2 Intrinsic connectivity of the hippocampal formation	9
1.5.3 Subcortical afferents to the hippocampal formation	9
1.5.4 Efferents from the hippocampal formation	10
1.6 The entorhinal cortex.....	10
1.6.1 Entorhinal afferents.....	11
1.6.2 Entorhinal efferents.....	11
1.7 Parasubicular and presubicular afferents and efferents	12
1.8 Subiculum	12
1.8.1 Intrinsic subicular connections.....	12
1.8.2 Extrinsic subicular projections	12
1.8.2.1 Subicular afferents.....	12
1.8.2.2 Reciprocal connection with entorhinal cortex.....	14
1.8.2.3 Subicular efferent connections	14
1.8.2.4 Subicular cell types.....	15
1.8.2.5 Subiculum summary.....	15

Chapter 2	Introduction part 2: Spatial cells	17
2.1	The spatial world	17
2.2	Spatial cells	20
2.2.1	Place cells	20
2.2.1.1	Located in the hippocampal formation	20
2.2.1.2	Field shape and size.....	21
2.2.1.3	Place cells receive sensory input from two systems.....	21
2.2.1.4	Place field formation	22
2.2.1.5	Place cell remapping	22
2.2.1.6	The influence of boundaries.....	23
2.2.2	Head-direction cells	26
2.2.2.1	Anatomical location of Head-direction cells.....	26
2.2.2.2	Head-direction cells provide a universal directional code..	26
2.2.2.3	Head-direction cells integrate external and idiothetic cues	27
2.2.3	Grid cells	29
2.2.3.1	Basic properties of grid cells.....	30
2.2.3.2	Spatial scale varies along the dorsal-ventral axis	32
2.2.3.3	Directionality in grid cells.....	32
2.2.3.4	Grid cells develop quickly in young rats	32
2.2.3.5	Does grid scale change?	35
2.2.3.6	Development of the grid pattern requires cue integration.	37
2.2.3.7	Grid cells in different regions	40
2.3	Boundary-related cells and the BVC model	41
2.3.1	BVCs have been recorded from the subiculum.....	42
2.3.1.1	What is a boundary?.....	46
2.3.1.2	The subiculum as an output area.....	47
2.3.2	Border cells.....	48
2.3.2.1	Border cell response to environment manipulation.....	49
2.3.2.2	Role for boundary-cells.....	50
2.4	Aims of the thesis	53
Chapter 3	Methods	55
3.1	Ethics.....	55
3.2	Subjects	55

3.3	Recording apparatus	56
3.3.1	Recording electrodes.....	56
3.3.2	Microdrives.....	56
3.4	Surgery.....	57
3.5	Data recording.....	59
3.5.1	Head position and orientation, and running speed	59
3.5.2	EEG and single-unit.....	60
3.5.2.1	EEG	Error! Bookmark not defined.
3.5.2.2	Single-units	Error! Bookmark not defined.
3.6	Materials.....	61
3.6.1	Laboratory layout	61
3.6.2	Test environments and materials	63
3.7	Experimental procedure.....	65
3.7.1	Screening and training before formal testing	65
3.8	General procedure.....	65
3.8.1	Task.....	65
3.8.2	Trial length	66
3.8.3	Inter trial interval (ITIs).....	66
3.9	Manipulations.....	68
3.9.1	Boundary insertion	68
3.9.2	Wall no-wall manipulation.....	69
3.9.3	Barrier insertion within the wall removal manipulation	70
3.9.4	Together-apart.....	71
3.9.5	Context change.....	72
3.9.6	Darkness	73
3.9.7	Object insertion	74
3.9.8	Ridge insertion.....	75
3.9.9	Together-apart variation	76
3.9.9.1	Summary.....	76
3.10	Histology.....	77
3.11	Data processing	77
3.11.1	Cluster-cutting and general cell identification.....	77
3.11.1.1	Cluster cutting using peak-to-trough amplitude	78

3.11.1.2	Cluster cutting using peak-to-trough time interval.....	78
3.11.1.3	Recording stability	80
3.12	Data analysis	81
3.12.1.1	Waveform analysis	81
3.12.2	Figures showing spatial firing.....	82
3.12.3	Quantitative measures of temporal and spatial firing characteristics	86
3.12.3.1	Temporal firing characteristics.....	86
3.12.3.2	Directional information.....	86
3.12.3.3	Comparing locational and directional information in boundary cells	87
3.13	Grid cell specific analysis.....	88
3.13.1	Spatial autocorrelogram.....	88
3.13.2	Grid cell classification.....	89
3.13.3	Grid scale expansion	92
3.13.3.1	Measuring grid scale change	92
3.13.3.2	Measuring shifts in orientation.....	92
3.13.4	Field inhibition in grid cells with barrier insertion	93
3.14	BVC specific analyses.....	94
3.14.1	BVC classification criteria	94
3.14.2	Quantifying the effect of wall removal on BVC fields	96
Chapter 4	Classification, basic properties and comparison of subicular spatial cells	97
4.1	Overview of the dataset.....	97
4.1	Grid cells.....	99
4.1.1	Grid cell classification criteria	99
4.1.2	Histology and tetrode localization.....	108
4.1.2	Gridness: The spatial periodicity of the grid pattern	110
4.1.3	Neighbouring grid cells share a common orientation	110
4.1.4	Grid scale varies across the grid cell sample	111
4.1.4.1	Grid scale is determined by anatomical location.....	111
4.1.5	Gridness correlates with theta modulation.....	113
4.1.5.1	The correlation between gridness and theta modulation is not due to other factors	114
4.2	Boundary Vector cells (BVCs).....	115

4.2.1	BVC classification criteria.....	115
4.2.2	Histology and tetrote localization.....	128
4.2.3	BVCs carry more locational than directional information.....	130
4.3	Head direction cells were sometimes recorded simultaneously with grid cells and BVCs.....	131
4.4	Comparison between grid cells, BVCs and HD cells	137
4.4.1	No BVCs met the gridness threshold	138
4.4.2	In general HD cells also did not met the gridness thershold	139
4.4.3	The spike waveforms of grid cells are shorter in duration then those of BVCs.....	139
4.4.3.1	Subicular BVCs and grid cells carry less directional information then HD cells.....	141
4.4.3.2	Grid cells do not carry more directional information and selectivity then BVCs	142
4.4.4	Theta modulation.....	143
Chapter 5	Responses to environmental manipulations.....	145
5.1	Grid cell responses to wall removal.....	145
5.1.1	Grid scale expanded upon wall removal	147
5.1.2	Grid scale expansion may be modulated by novelty	155
5.1.2.1	The relationship between the familiar grid scale and the magnitude of novelty-induced grid expansion.....	158
5.1.3	Orientation of the grid pattern shifts between walled and un-walled environments.....	159
5.1.3.1	Grid cell firing patterns are maintained in complete darkness.....	161
5.1.4	Barriers can cause field inhibition in grid cells.....	163
5.1.5	Summary of grid cell responses to environment manipulation.....	169
5.2	BVCs respond to environment boundaries	170
5.2.1	BVCs respond to environment walls.....	170
5.2.1.1	BVC fields are largely insensitive to context change	172
5.2.2	BVC fields are maintained in darkness	174
5.2.3	BVCs respond to internal barriers and objects.....	176
5.2.3.1	BVC firing may depend upon boundary height.....	179
5.2.4	BVCs respond to objects of varying heights and widths as boundaries: summary	179
5.2.5	BVCs maintain their firing fields with wall removal	181

5.2.6	BVCs respond to traversable gaps as boundaries	184
5.2.6.1	BVCs respond to traversable gaps as small as 3cm.....	186
5.2.7	Summary of BVC responses to environment manipulations	188
5.3	New class of boundary-correlated cell: Boundary-off cells.....	189
5.3.1	Boundary-off cells maintain their firing fields in darkness.....	193
5.3.2	Boundary-off cells carry more locational than directional information.....	194
5.3.3	Boundary-off cells have basic properties which are distinct from other spatially recorded cells.....	196
5.3.4	Boundary-off cell summary	196
Chapter 6	Discussion.....	199
6.1	Overview of results	199
6.2	Wealth of spatial cells in the subiculum	201
6.2.1	The different spatial cells were functionally and morphologically distinct.....	201
6.3	Grid cells exist in the subiculum	202
6.3.1	Subicular grid cells share properties with grid cells recorded from the parahippocampal formation.....	203
6.3.1.1	Subicular grid cells can be identified using gridness scores	203
6.3.1.2	Neighbouring grid cells share a common orientation.....	204
6.3.1.3	Spatial scale increases along the subicular anterior- posterior axis	204
6.3.2	Gridness correlates with theta modulation.....	205
6.3.3	Grid cells respond to environment manipulation	205
6.3.3.1	Wall removal alters grid cell firing patterns	206
6.3.3.2	Grid rescaling is related to environment novelty.....	207
6.3.3.3	Why rescaling had not been seen in previous studies	208
6.3.3.4	Addition of a barrier also disrupts grid patterns	209
6.4	Boundary responsive cells exist in the subiculum	210
6.4.1	Development of a BVC classification criteria.....	210
6.4.2	What is a boundary?	211
6.4.3	BVCs vs. border cells.....	213
6.4.4	New class of boundary cell: boundary-off cells	214
6.5	Research implications.....	214

6.5.1	The importance of boundary information for spatial signalling of spatial cells located in the hippocampal formation.....	214
6.5.1.1	Boundaries and arguably BVCs control place cell fields	215
6.5.1.2	Boundaries may be important for anchoring the grid pattern to the environment.	216
6.5.2	Implications for the spatial representation network.....	218
6.6	Methodological issues.....	220
6.6.1	Gridness score.....	220
6.6.1.1	Problems with spatial autocorrelogram.....	220
6.6.1.2	Gridness thresholds.....	220
6.6.2	Task design.....	221
6.7	Future directions.....	222
	References.....	225

Figure contents

Figure 1.2.1. Three-dimensional drawing illustrating the position of the hippocampal formation in the rodent brain from a lateral point of view.	2
Figure 1.3.1. Horizontal section through the hippocampal formation and parahippocampal region of the rodent brain.....	4
Figure 1.5.1. A diagram of the internal connections of the hippocampal-parahippocampal regions, plus cortical input and output to these regions.	8
Figure 2.1.1: Apparatus and procedure used to investigate the existence of a cognitive representation of a rats environment by Tolman (1948).....	17
Figure 2.2.1. Effect of wall removal on place cell firing.	25
Figure 2.2.2. Grid cells have multiple firing fields which tessellate the environment.	29
Figure 2.2.3. Spatial autocorrelation is used to determine the parameters of the grid pattern.....	31
Figure 2.2.4. Simultaneously recorded CA3 place cells and MEC grid cells in darkness.	39
Figure 2.3.1: A BVC responds maximally when a boundary is at a preferred distance and allocentric direction (irrespective of heading) from the rat.....	41
Figure 2.3.2. Firing fields of 14 subicular BVCs in different environments	44
Figure 2.3.3. BVC produce a second firing field for the insertion of an additional boundary.....	45
Figure 2.3.4: Border cells show a variety of responses to inserted barriers.	51
Figure 2.3.5. Border cells wall preference shifts between walled and un-walled environments.	52
Figure 3.3.1: Illustration of a microdrive framework.	57
Figure 3.6.1. Bird’s eye view of testing room.....	62
Figure 3.6.2. Key testing environments.....	63
Figure 3.6.3. Inserted objects and barriers	64
Figure 3.9.1. Barrier insertion manipulation trial series.	68
Figure 3.9.2. Wall no-wall manipulation trial series.....	69
Figure 3.9.3. Barrier insertion within the wall no-wall manipulation	70
Figure 3.9.4. Together-Apart manipulation trial series.....	71
Figure 3.9.5. Context change manipulation	72
Figure 3.9.6. Darkness manipulation trial series	73
Figure 3.9.7. Objects vs. barrier manipulations trial series.....	74
Figure 3.9.8. Ridges manipulation trial series	75
Figure 3.9.9. Together-apart variation manipulation trial series.....	76
Figure 3.11.1. Examples of cluster-cutting.....	79

Figure 3.12.1. Waveform illustration	81
Figure 3.12.2. Example locational rate maps and polar plots for spatial cells.	83
Figure 3.13.1. Spatial autocorrelation is used to determine the parameters of the grid pattern.	90
Figure 3.13.2. Gridness scores depend upon which spatial autocorrelation analysis is used.	91
Figure 3.14.1: Representative BVCs demonstrating the selection process used to classify boundary cells as BVCs.....	95
Figure 3.14.2. Do BVC field peaks move with the boundary when the walls are removed?	96
Figure 4.1.1. Periodic non-grid cells: putative grid cells with multiple peaks which did not reach the 0.25 gridness score threshold.....	100
Figure 4.1.2. Basic characterisation of all grid cells; subiculum (page 1/7).....	101
Figure 4.1.3. Estimated recording locations of grid cells.	109
Figure 4.1.4: Grid cell orientation is fairly constant within rat but varies between rats....	111
Figure 4.1.5. Anatomical position along the anterior-posterior axis determines grid scale.	112
Figure 4.1.6. Gridness positively correlates with theta modulation.....	113
Figure 4.2.1. BVCs develop extra locational fields following the insertion of an appropriately-oriented barrier.	117
Figure 4.2.2. BVCs can respond to environment drops and traversable gaps as well as walls.	119
Figure 4.2.3. Two BVCs had long-range fields.....	120
Figure 4.2.4. Non-BVC boundary cells: Boundary cells which did not show sufficient field doubling with boundary insertion were classed as non-BVC boundary cells.	121
Figure 4.2.5. Basic characterisation of all BVCs (page 1/6).....	122
Figure 4.2.6. Estimated recording locations of BVCs.	129
Figure 4.3.1. Head direction cells were sometime recorded simultaneously on the same tetrodes as grid cells and BVCs.	132
Figure 4.3.2. Basic characterisation of all HD cells (page 1/4).....	133
Figure 4.4.1. The BVC sample has significantly lower gridness scores then grid cells.....	138
Figure 5.1.1. Grid scale expands with wall removal (page 5/5).....	154
Figure 5.1.2. There is a positive relationship between grid scale and novelty.....	157
Figure 5.1.3. There is a trend towards a positive linear relationship between grid scale in the walled environment and the grid scale increase in the un-walled environment.	158
Figure 5.1.4. Grid orientation significantly shifted between walled and un-walled environments.	160
Figure 5.1.5. Grid cell firing patterns do not change between light and dark trials.....	161
Figure 5.1.6. The insertion of the barrier causes some grid cell patterns to shift/deform	165

Figure 5.1.7. Some grid cells show field inhibition with the insertion of a free-standing barrier.	166
Figure 5.1.8. Quantifying field inhibition with barrier insertion.	167
Figure 5.1.9. Grid fields continue to show inhibited firing relative to other nodes irrespective of exploration direction.	168
Figure 5.2.1. BVCs respond to perimeter walls of differently shaped environments.	170
Figure 5.2.2. BVCs vary in distal and directional preference.	171
Figure 5.2.3: BVCs are not sensitive to context change.	173
Figure 5.2.4: BVC firing properties are not disrupted between light and dark trials.	175
Figure 5.2.5: BVCs code for objects as well as for linear boundaries.	177
Figure 5.2.6. BVCs can produce second firing fields in darkness.	178
Figure 5.2.7: The height and width of a traversable barrier determines whether it is treated as a boundary.	180
Figure 5.2.8: BVCs respond for environment drops as well as walls.	183
Figure 5.2.9: BVCs can treat traversable drops as boundaries.	185
Figure 5.2.10. The size of the traversable drop determines whether BVCs treat it as a boundary.	187
Figure 5.3.1: Boundary-off cells were sometimes simultaneously recorded with other spatial cells.	190
Figure 5.3.2: Boundary-off cells show an inhibitory response to barrier insertion.	191
Figure 5.3.3. Basic characterisation of all boundary-off cells.	192
Figure 5.3.4: Boundary-off cells like BVCs and grid cells maintain their firing patterns in the absence of visual cues.	193

Table contents

Table 3.4.1: Target implant co-ordinates for all rats	59
Table 3.8.1. Trial lengths for trials in each environment.	67
Table 3.12.1 Table of measures used to characterise cell firing.....	84
Table 4.1.1. Spatial cells recorded and analysed in this thesis	98
Table 4.1.1. Gridness correlates with theta modulation but not other factors.	114
Table 4.2.1. The number of boundary cells classified as BVCs changes if the threshold of barrier coverage by the second field is varied.....	116
Table 4.2.2. BVCs carry more locational than directional information.	130
Table 4.4.1. Comparison of characteristics between grid cells, BVCs and HD cells.....	137
Table 4.4.2. BVCs have longer waveform durations than grid cells and higher amplitudes than HD cells.	140
Table 4.4.3. HD cells carry more directional information than Grid cells and BVCs.....	141
Table 4.4.4. Grid cells carry more directional information than BVCs.	142
Table 4.4.5. Grid cells are significantly more theta modulated than either HD or BVC cells.	143
Table 5.1.1. Grid cell properties in walled vs un-walled conditions.	146
Table 5.1.2. Spatial scale expands when the environment walls are removed.....	148
Table 5.1.3. Grid cell same day subset: Spatial scale expands when the environment walls are removed.....	149
Table 5.1.4 There was a significant difference in the number of exposures to walled and un-walled environments	156
Table 5.1.5. Removing visual cues did not interrupt grid cell firing properties.....	162
Table 5.2.1. Removing visual cues does not interrupt BVC firing properties.	174
Table 5.3.1. Boundary-off cells carry more locational than directional information.	194
Table 5.3.2. Boundary-off cells carry less spatial information per spike and less spatial selectivity than BVCs.....	195
Table 5.3.3. Boundary-off cells are distinct from other spatial cells.	197

Chapter 1 Introduction part 1: Anatomy of the hippocampal formation

The view that the hippocampal formation is important for memory began with the observations of brain damaged patients by William Scoville and Brenda Milner in 1957. The most famous of their patients was HM who following surgery to help manage his severe epilepsy had a large part of the hippocampal formation (and some of the surrounding cortical regions removed). HM developed profound global amnesia and could not remember any episode post-surgery or anything directly before surgery. HM's amnesia spurred efforts to find an animal model of amnesia. Early studies looking at primates (Orbach et al, 1960; Correll and Scoville, 1967) and rats (Morris, 1982) failed to find a convincing memory deficit following hippocampal damage. Alternatively a variety of other deficits emerged including changes to exploration and habituation to novelty, increased hyperactivity, and impaired spontaneous alternation (Kaada et al 1961; Kimble 1963; Isaacson and Kimble, 1972; Anderson et al, 2007). In the 1970's as it was realised that there was more than one type of memory, the view of the hippocampus and its role in memory changed and developed. It was decided that the previous methods used to test hippocampal functioning (in animals) was not optimal. This led to the design of the behavioural tasks used to this day, and the development of the method of single cell recording. It is now generally considered that the hippocampus (and the hippocampal formation) plays crucial roles in general learning and memory, and more specifically for spatial memory (Anderson et al., 2007).

1.1 Nomenclature

There is some debate regarding the definition of the hippocampus proper and the hippocampal formation (Amaral & Lavenex, 2007). This thesis adopts the nomenclature whereby the *hippocampus* includes the cornu ammonis (CA) fields (CA1, CA2 & CA3) and the dentate gyrus (DG). The *hippocampal formation* includes the hippocampus and the subiculum, which is also (having only three layers like the DG and CA fields). The *parahippocampal region* (para = alongside/near) includes the entorhinal cortex and the pre- and parasubiculum (Scharfman et al., 2000).

The above definitions are based on connectivity and laminar organisation. The hippocampal formation is distinctive in having a trilaminar (three-layered) allocortical organisation. Whilst the entorhinal cortex and

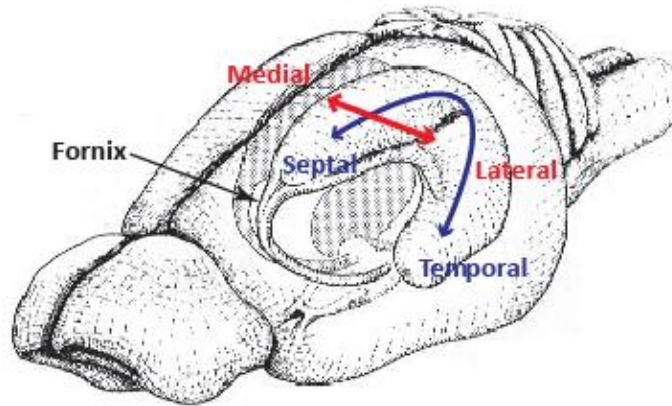


Figure 1.2.1. Three-dimensional drawing illustrating the position of the hippocampal formation in the rodent brain from a lateral point of view.

The septo-temporal axis (blue arrows) runs between the septal and temporal poles (labelled). The transverse axis (red arrows) runs from medial to lateral. Drawing adapted from Amaral and Witter (1995).

the pre- and parasubiculum have a multilaminar organisation similar to neocortical structures. The parahippocampal region can be viewed as the transition from allocortex to neocortex (Amaral and Lavenex, 2007). An additional difference between the parahippocampal region and the hippocampal formation is the distinctive nature of hippocampal connectivity, which is largely unidirectional. The parahippocampal region on the other hand is much more neocortical in terms of connectivity, with at least two sets of reciprocal connections. One between peri- and postrhinal cortices and the entorhinal cortex, and the other between the pre- and parasubiculum and entorhinal cortex.

1.2 Gross morphology

In rodents the hippocampal formation comprises a large proportion of the brain and the hippocampus proper is almost half the brain's cortical volume. In humans the more developed cerebral cortex has caused the human hippocampus to be located more ventral in the medial temporal lobe (Amaral and Lavenex, 2007). The dorsal hippocampus in the rat brain, is equivalent to the posterior hippocampus in primates.

Figure 1.2.1 illustrates the positioning of the hippocampal formation within the rat brain. The occipital and temporal neocortex has been removed to provide a view to the allocortex. The hippocampal formation is

the curving 'C' shaped structure. Its long axis the septo-temporal axis (more often referred to as the dorso-ventral axis) extends from close to the midline (near the septal nuclei) over and behind the thalamus to the temporal lobe. Orthogonal to this is the transverse axis which runs medial to lateral. These axes are important landmarks to the structural connectivity of the hippocampal formation which is arbitrarily split into 3 portions, dorsal, (located behind the septum), posterior (located at the ventrolateral curve) and ventral (located in the temporal portion).

The Fimbria-fornix is the pathway connecting the hippocampal formation with the basal forebrain, hypothalamic and brain stem regions (Amaral and Lavenex 2007). The ventral (septal) portion of the hippocampus is covered by the alveus a thin sheet of afferent and efferent fibres. These fibres collect at the ventral (temporal) hippocampal formation and become thicker through to the dorsal hippocampus. They become the fornix as they leave the hippocampus to descend into the forebrain. The fornix fibres are also a source of input to the hippocampus. These inputs include the afferent projections from the septum and raphe nuclei.

1.3 Organization of the hippocampal formation and parahippocampal region

Figure 1.3.1 shows a horizontal section of the hippocampal formation and parahippocampal region. This illustrates the trilaminar organization of the hippocampal formation as well as clear borders between areas. The darkly stained interlocking C structures represent the pyramidal layers of the hippocampus proper and the granule layer of dentate gyrus (DG). Below this is the relatively cell free layer called the stratum oriens. The widening of the tail of the CA1 field becomes the subiculum. To the right of the subiculum is the pre- and parasubiculum. The parahippocampal region is signaled by a sudden increase in layers. The subicular pre-parasubicular border is characterized by the emergence of a cortical sheet, consisting of the pre- and parasubiculum superficial layers. The deep layers are separated from the superficial layers by a cell-free zone (the lamina dissecans) which should be layer IV. At the border between the entorhinal and perirhinal or postrhinal/parahippocampal cortex the lamina dissecans disappears giving way to a more neocortical-like structure with 6 layers. The exception to this within the parahippocampal region is the peri and postrhinal cortices which only have 5 layers, lacking the granule cell layer IV.

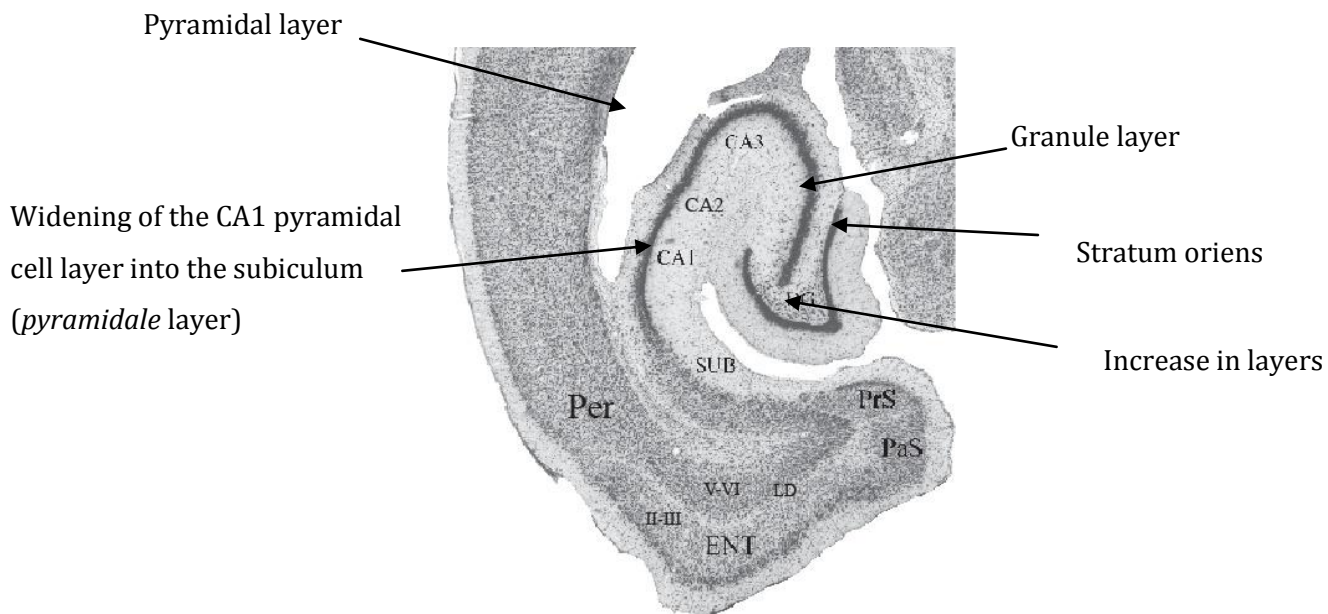


Figure 1.3.1. Horizontal section through the hippocampal formation and parahippocampal region of the rodent brain.

The trilaminar (three layered) structures that comprise the hippocampal formation are CA1, CA2, CA3, DG and subiculum. The layers can be differentiated by their staining; the darker the staining the more densely packed the cell layers. The parahippocampal region is composed of the presubiculum (PrS), parasubiculum (PaS), entorhinal cortex (EC) and perirhinal cortex (Per). The parahippocampal region begins where there is an abrupt increase in the number of layers. Layers II and III form the superficial parts of these structures while the deep layers (V-VI) are a continuation of the subiculum. Adapted from Witter et al., (2000).

1.4 Cytoarchitectonic organisation

1.4.1 Laminar organisation of the CA fields

The principal cellular layer of the CA fields is the *pyramidal cell layer*, which is densely packed in CA1 but less so in CA2 and CA3. Beneath this there is a narrow relatively cell-free layer called the *stratum oriens*. This contains the basal dendrites of the pyramidal cells and also some interneurons. It is also the region where some of the CA3 autoassociational connections and CA3 to CA1 Schaffer collateral connections are located. The extra layer in the CA3 field is the *stratum lucidum*, which is a narrow acellular zone situated just above the pyramidal layer. This is where mossy fibres originating from DG terminate. The *stratum radiatum* is located above the *stratum lucidum* in CA3 and immediately above the pyramidal cell layer in CA1 and CA2. This layer contains some interneurons and is where again some of the CA3 autoassociational connections and CA1 to CA3 Schaffer collateral connections are situated. The last layer is the superficial layer the *stratum lacunosum-moleculare* which is located deep to the *stratum radiatum*. This layer also contains interneurons and is where the perforant pathway fibres from neurons of the superficial layers of the entorhinal cortex terminate. These terminate on the distal apical dendrites of CA1 pyramidal cells (the distal dendrites project into the *stratum lacunosum-moleculare*). Afferent projections from other regions including thalamic regions such as the reuniens nucleus also terminate in the *stratum lacunosum-moleculare* (Amaral & Lavenex, 2007).

1.4.2 Laminar organisation of the dentate gyrus (DG)

The dentate gyrus (DG) comprises three layers. The principal cellular layer is the *stratum granulosum*. This layer contains granule cells and is densely-packed, similar to the CA principal cellular layers. These are the principal type of dentate cells and are the only ones to project outside the DG. They synapse with the CA3 dendrites in the *stratum lucidum*. Above the *stratum granulosum* is the superficial layer, the *stratum moleculare* which is closest to the hippocampal fissure. This is where the granule cell dendrites are located. Granule cells are unipolar, there are no granule cell dendrites on the other side of the granule layer. The dense projection to the DG from entorhinal cortex targets the granule cell dendrites in the molecular layer. The third layer, the *hilus*, (often referred to as the polymorphic cell layer of the DG) contains several types of neuron are situated within this layer, including the mossy cells that project back to the granule cells. (Amaral & Lavenex, 2007).

1.4.3 Laminar organisation of the subiculum

Similar to the CA fields the subiculum has 3 distinguishable layers. The CA1/Subiculum border is identifiable by the widening of the pyramidal cell layer. The principle cell layer is the *pyramidale*, which encloses the pyramidal cells somas, this layer is less well packed than the CA1 pyramidal layer. These neurons extend their apical dendrites into the *molecular* layer above and some extend to reach the hippocampal fissure (Harris et al., 2001). This is continuous with the CA1 *stratum lacunosum-moleculare* and *stratum radiatum* layers. The superficial portion of the *molecular* layer receives entorhinal projections whilst the deep part of the *molecular* layer is innervated by the CA1. The third layer, *oriens* is polymorphic and contains the basal dendrites (Amaral & Lavenex, 2007).

1.4.4 Laminar organisation of the entorhinal cortex (EC)

The EC contain six layers, which are often grouped into 2 categories the superficial (layers I-III) and deep (IV-VI) layers. The EC superficial layers contain stellate (layer II) and pyramidal (layers II and III) cells. The neurons from the layer II project to the DG and CA3, and those of layer III, to CA1 and the subiculum. The CA1 and the subiculum project back to the EC, onto its deep layers which contain various cellular types (Amaral & Lavenex, 2007).

1.4.5 Laminar organisation of the pre- and parasubiculum

The dorsal Presubiculum has clearly distinguishable superficial and deep layers. The most superficial cells are densely packed (layer II), whereas the cells located deeper in the presubiculum are more loosely arranged (layer III). In the ventral portion however, they are not so clearly distinguishable from the deep EC layers or the subiculum principle layer. The parasubiculum lies adjacent to the Presubiculum. Layers II and III consist of densely packed large pyramidal cells which is one of the major features used to distinguish the pre- and parasubiculum. As with the Presubiculum the deeper layers are continuous with the EC (Amaral & Lavenex, 2007).

1.5 General connectivity

Intrahippocampal circuitry is largely unidirectional which significantly differs from that of the neocortex, which in contrast has strong, reciprocal innervations between the neocortical regions (Felleman and Van Essen, 1991). There are 3 principal synaptic connections involving the hippocampal formation.

The first connection is between layers II and III of the EC and the DG, CA3 and CA1 via the '*perforant path*'. It is through this path that the EC provides the major source of input to the hippocampus. These are not reciprocal connections; they are unidirectional from the EC to the hippocampal fields. Secondly there are the *intrahippocampal* unidirectional projections comprising of the DG's sole projection to the CA3 via mossy fibres and the projection from CA3 to CA1 via the Schaffer collaterals. Lastly the CA1 projects out to both the subiculum and the deep layers of the EC. The subiculum also projects to the EC, presubiculum and parasubiculum. Therefore, the hippocampal processing loop begins in the superficial layers (II & III) of the entorhinal cortex which projects to DG, CA3 and CA1, and ends with projections from the CA1 and Subiculum into the deep layers (V & VI) of the entorhinal cortex (Amaral & Lavenex, 2007).

The following sections address (i) the intrinsic connectivity within; (ii), the major afferents (inputs) and (iii) the major efferents (outputs) of the hippocampal formation, entorhinal cortex and the subiculum. Figure 2.3 summarises these connections.

1.5.1 Afferents to the hippocampal formation

The major source of neocortical input to the hippocampus is from the superficial layers II and III of the EC through the perforant pathway. Much of the entorhinal input originates from postrhinal and perirhinal cortices, but these all project to the hippocampus (Figure 1.5.1). The perforant pathway from the EC into the hippocampus can be subdivided into two streams, one originating from layer II and one from layer III.

The projections originating in layer II of the EC project to DG, CA3 and CA2. The Projections to DG mainly terminate on granule cell dendrites, and projections to CA3 and CA2 terminate in the *stratum lacunosum-moleculare*. The projections from layer III project to the CA1 and subiculum. The projections to CA1 terminate in the *stratum lacunosum-moleculare*. EC input to CA1 varies depending on EC region with projections from lateral EC terminate in distal CA1 (close to the subiculum) and projections from medial EC terminate in proximal (close to CA2). Projections from EC layer III to the subiculum terminate in the *molecular* layer (Witter, 1993).

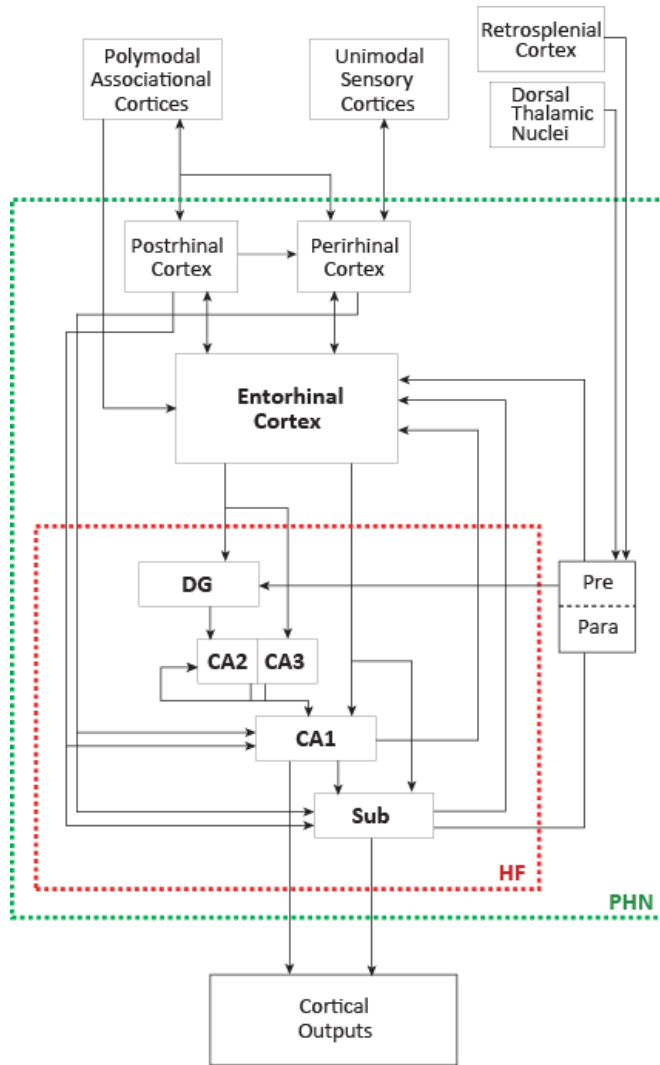


Figure 1.5.1. A diagram of the internal connections of the hippocampal-parahippocampal regions, plus cortical input and output to these regions.

The figure shows the connections between areas, and the directions of those connections using arrows. The red dashed box distinguishes the Hippocampal formation (HF) and the green box includes the Parahippocampal network (PHN). Adapted from (Wills et al., 2005).

1.5.2 Intrinsic connectivity of the hippocampal formation

There are 5 major connections within the hippocampal formation (as highlighted by the contents of the red dashed box in (Figure 1.5.1). The first is the DG projection to the CA3 via the mossy fibres. The fibres arise from the dentate granule cells and terminate just above the CA3 pyramidal layer. All DG cells project to CA3, and this projection stops at the border of CA3 and CA2, which is one main distinction between CA3 and CA2 pyramidal cells. The second is the recurrent collaterals between CA2 and CA3. The third is the recurrent collaterals of CA3 pyramidal cells. These strong autoassociational connections mean that a large proportion of CA3 pyramidal cells have excitatory synaptic contact with each other. The fourth is the schaffer collaterals projecting from CA3 and CA2 to CA1. Last are the projections from CA1 to subiculum. The subiculum itself does not project directly back into the hippocampus, but rather has strong reciprocal connections to the EC, which receives the majority of the subiculum output (Amaral and Witter, 1995).

1.5.3 Subcortical afferents to the hippocampal formation

There are several major subcortical inputs to the hippocampal formation, from the medial septum, the supramammillary nucleus, the brain stem, the amygdala and the thalamus.

The septum is part of the basal forebrain. The septal projection to the hippocampus originates mainly in the medial septal nucleus and an associated region called the nucleus of the diagonal band of Broca (Amaral & Lavenex, 2007). Septal fibres terminate in all areas of the hippocampal formation, but are particularly prominent in the DG, where cholinergic fibres from the medial septum innervate mossy cells. The medial septum is also a major source of subcortical input to CA3, and there is also some input to CA1 (Amaral and Witter, 1995).

The supramammillary nucleus is part of the hypothalamus. It consists of a population of large cells which partially surround the medial mammillary nuclei of the hypothalamus (Amaral and Lavenex, 2007). The termination patterns of projections from the supramammillary nucleus in the hippocampus are relatively specific, and target the DG and CA2 in particular, only projecting weakly (if at all) to CA1 and CA3 (Amaral & Lavenex, 2007).

The brain stem reticular formation consists of several structures including the rostral pontine region, pedunculopontine tegmental nucleus, and the raphe nuclei. The raphe nuclei are responsible for

serotonergic innervations of the rest of the brain, and the median raphe directly innervates GABAergic interneurons in the DG, CA1 and CA3 (Freund et al., 1990). Monoaminergic input from the brain stem is primarily restricted to noradrenergic and serotonergic input. Noradrenergic input is quite dense to all regions of hippocampus and subiculum, while serotonergic input is most dense to the lateral EC, DG and layer 1 of the pre- and parasubiculum (Amaral and Witter, 1995).

Lastly basolateral amygdalar input to hippocampus is largely restricted to CA1 and to its temporal third in particular (Amaral and Witter, 1995). In addition, CA1 receives a direct and massive input from the nucleus reunions of the thalamus (Wouterlood et al., 1990), largely directed at the *stratum lacunosum-moleculare* and to the middle septo-temporal levels of CA1.

1.5.4 Efferents from the hippocampal formation

Both the CA1 and the subiculum project to the deep layers of the EC (V and VI), and also give rise to a number of other efferents, to both cortical and subcortical regions. The CA1 and subiculum both project to the medial prefrontal cortex, retrosplenial cortex and perirhinal cortex. CA1 subcortical projections include medial and lateral septum. Specifically the ventral CA1 projects to areas including basal amygdale, olfactory bulb, anterior and dorsomedial hypothalamus. The subiculum is a major output region of the hippocampal formation, particularly to subcortical efferents including lateral septum, nucleus accumbens, medial mammillary nuclei and medial thalamic nuclei (Amaral and Lavenex 2007).

In summary, information enters the hippocampus via the superficial layers of the EC, is processed within the hippocampal formation and is then relayed via CA1 and the subiculum to the deep layers of the EC. From there it can be fed back into the hippocampus through associational connections between the deep and superficial EC layers, or be relayed to the cortical mantle, either directly (from a very specific region of EC) or indirectly through peri- and postrhinal cortices (Amaral and Witter, 1995).

1.6 The entorhinal cortex

The EC is the gateway for the main cortical inputs to the hippocampal formation, and is also the main region for relaying processed information back to the neocortex. The EC is therefore crucial to the functioning of the hippocampal formation. The EC can be subdivided into lateral (LEC) and medial (MEC) portions, which are cytoarchitectonically and functionally distinct. The lateral area layer II is more distinct than the medial

layer II, with lateral layer II cells being smaller, more densely packed and clustered into islands (Amaral and Witter, 1995). The MEC contains a high proportion of spatial cells, whereas the LEC does not (Amaral and Witter, 1995; Witter and Moser 2006).

1.6.1 Entorhinal afferents

As mentioned previously the EC provides the majority of the cortical input to the hippocampal formation via the perforant pathway. The peri- and postrhinal cortices provide the majority of input to EC, which is mostly received from inputs by unimodal and polymodal neocortical association areas, suggesting that the hippocampal formation receives highly-processed information from neocortex. Each cortical area has some associated specialisation of inputs. For example prominent unimodal afferents are olfactory and visual. The perirhinal cortex receives stronger olfactory inputs and the postrhinal cortex receives stronger visual and visuo-spatial inputs. However, it is the polymodal associational cortices which provide the majority of cortical input to the rhinal cortices, in particular the ventral temporal areas. The peri- and postrhinal cortices project differently to the EC, with the postrhinal cortex projecting preferentially to the MEC, and the perirhinal cortex projecting more to the LEC which is elucidated through a disassociation of functions between these 2 portions of the EC (Burwell and Amaral, 1998a). Visuo-spatial input, which originates in the retrosplenial, cingulate and posterior parietal cortices, also forms a robust projection directly to the EC (Burwell and Amaral, 1998b).

The pre- and parasubiculum also project to the EC and receives strong projections from visuo-spatial neocortical areas. They receive similar cortical inputs and, in addition, both receive input from the subiculum. The fact that they receive strong input from the subiculum, which is the major output area of the CA1 and also project heavily to the EC, suggests that pre- and parasubiculum lie at the crossroad between output and input. It is thought that this functional loop may be important in re-directing hippocampally-processed information back into the hippocampus (Amaral & Lavenex, 2007).

1.6.2 Entorhinal efferents

The projections into deep EC layers from CA1 and subiculum indicate that the deep layers are crucial in relaying hippocampal information to cortical regions. EC subcortical efferents overlap with those from subiculum and CA1, projecting to the septum (especially the lateral septum). EC also projects to the amygdala, and in particular the basal nucleus. Other important efferents include the nucleus accumbens

and olfactory tubercle. Evidence suggests that there is a restricted portion of layer V neurons in LEC which also project to lateral frontal (motor), parietal (somatosensory), temporal (auditory), occipital (visual), anterior insular and cingulate cortices (Insausti et al., 1997). The EC does not appear to project to the thalamus or brain stem (Amaral and Witter, 1995).

1.7 Parasubicular and presubicular afferents and efferents

Neither the parasubiculum nor the presubiculum appears to be an important output region. However, both have subicular afferents (these are discussed in the next section). The parasubiculum projects to the hippocampal formation, and its efferents to the thalamus project back to the hippocampal formation. The presubiculum has efferent projections to the hippocampal formation, and provides some projections to the retrosplenial and perirhinal cortices.

1.8 Subiculum

1.8.1 Intrinsic subicular connections

The subiculum gives rise to longitudinal associational projections extending from the level of the cells origin ventrally to much of the subiculum. Associational fibres terminate diffusely throughout the subiculum. This projection appears to be largely unidirectional, and it does not appear to produce or receive commissural connections. Pyramidal cells provide strong local input to the principal layer and to the apical dendrite superficial to it. The density of this connection is much higher than in the CA1. There are 2 types of principal cells, bursting and regular. Bursting cells have a columnar organisation whereby their axonal distribution remains in the region and is confined by their apical dendrites. Whereas the regular spiking cells generally have a more disseminated distribution along the traverse axis (Amaral 2005).

1.8.2 Extrinsic subicular projections

1.8.2.1 Subicular afferents

The subiculum is considered the major output area of the hippocampus (Naber et al., 2000). CA1 sends its primary projections to the Subiculum. This projection is considered to be simply organised. All CA1 regions

project to and are received by all portions of the subiculum (Amaral et al., 2001; O'Mara et al., 2009). Distal CA1 (the portion on the subiculum border) projects to proximal subiculum (area bordering CA1), proximal CA1 (bordering CA3) projects to the distal subiculum (bordering presubiculum) and the mid portion of the CA1 projects to the mid portion of the subiculum. Fibres beginning from the proximal CA1 travel to the subiculum via the alveus and the deepest portion of the *stratum oriens*, whereas fibres originating in mid-CA1 do not enter the alveus but project to the subiculum through the deep parts of *stratum oriens*. The axons of distal CA1 cells travel directly to subiculum from all parts of *stratum oriens* (Amaral et al., 2001; O'Mara et al., 2005; 2009). These projections are confirmed by neurophysiological depth profiles of this projection by stimulation of different sites by a bipolar stimulating electrode in the rat *in vivo* (O'Mara et al., 2001). This projection is generally considered to be monosynaptic from the CA1 (combined morphological and single unit studies; Gigg et al., 2000), however there is some evidence that the subiculum returns a minor oligosynaptic projection to CA1 (sequence of only a few neurons; Commins et al., 2002).

Other afferent projections include input from all areas of the anteroventral (AV) and anteromedial (AM) nuclei of the thalamus (see Risold et al., 1997; Canteras and Swanson, 1992; Kohler et al., 1990). Other projections include weak cholinergic projections from the septal nucleus and nucleus of the diagonal band. Also there are modulatory inputs from the brain stem, including the locus coeruleus (noradrenergic) and the raphe nuclei (serotonergic). Of particular note is that the subiculum receives dense mesencephalic dopaminergic projections from the ventral tegmental area (VTA) (Descarries et al. 1987; Gasbarri et al. 1994) and express high levels of D1- and D2-like DA receptors (Bruinink and Bischoff 1993; Fremeau et al. 1991).

The subiculum also receives input from many of the same cortical areas which project to the EC as well as direct input from the EC itself. Of particular note are the modest projections from the pre- and parasubiculum.

There are inconsistent reports of projections from the anterior cingulate cortex to the subiculum (White et al 1990). The subiculum also receives projections from the amygdaloid complex. In particular the parvocellular portion of the basal nucleus, posterior cortical nucleus and the amygdaloid hippocampal area (Amaral and Lavenex 2007). These projections terminate at the proximal portion of the subiculum and innervate the molecular layer. They are reciprocated, arising from the temporal third of the subiculum to various areas of the amygdaloid complex.

The Perirhinal and postrhinal cortices also project to the subiculum (Witter and Moser, 2006). The Perirhinal projects to the most proximal-to-CA1 portion of the dorsal subiculum and the postrhinal projects to the most distal-to-CA1 portion of the dorsal subiculum (bordering the presubiculum). These projections are reciprocal.

1.8.2.2 Reciprocal connection with entorhinal cortex

Witter et al., (2006) show evidence that the subiculum receives EC projection fibres directed towards transverse portions of subiculum which terminate in molecular layer. Perforant path fibres traverse the subiculum on the way to the DG and the hippocampus. Projections originate primarily from layer III of the EC (and possibly V), but also some may come from layer II as they traverse the subiculum to DG and CA3. Entorhinal fibres target dendritic spines of assumed principle neurons with asymmetrical synapses (80%) and the rest terminate on the dendritic shaft, probably belonging to interneurons. The symmetrical synapses on dendritic shafts mean that the interneurons may receive some inhibitory perforant path input (Amaral and Lavenex 2007).

This projection is reciprocated from the subiculum with fibre termination throughout the deep layers of the EC and being particularly dense in layer V. The reciprocal projection is organised similarly to the CA1-subiculum projection, with the proximal-to-CA1 subiculum projecting to the distal portion of the EC (LEC) and the distal-to-CA1 subiculum projects to the proximal EC (MEC). Subiculum fibres generally form asymmetrical synapses with spines and dendrites located in the EC. However, in accordance with the subiculum's excitatory influence on the EC, some of these form symmetrical synapses suggesting some inhibitory input from the subiculum to layer V. There is also a notable projection extending superficially to the acellular *lamina dissecans* in EC layer III (Amaral and Lavenex 2007).

1.8.2.3 Subicular efferent connections

The subiculum is considered the major source of efferent projections from the hippocampal formation. The subiculum does not project back to the CA1, but, projecting axon collaterals target other cortical and subcortical areas including the EC and the pre- and parasubiculum.

Projections from the Subiculum to pre- and parasubiculum are topographically organised, with the dorsal subiculum projecting to the dorsal and septal portions of both (Witter, 2006). Amaral and Lavenex (2007)

consider that this projection is the last stage in the process passing information out of the hippocampal formation to cortical and subcortical areas. However, an alternative view is that this information may also be feeding back into the entorhinal cortex via the pre- and parasubiculum. Subicular fibres predominantly terminate in layer I of the presubiculum. Projections to the dorsal presubiculum terminate deeper to layer II. Projections to the parasubiculum mainly terminate in layer I and the superficial portion of layer II.

There are also prominent connections to medial and ventral orbitofrontal cortices, the prelimbic and infralimbic cortices (Verwer et al., 1997), the retrosplenial cortex (Wyss and Van Groen, 1992) and the perirhinal cortex. There are also less substantial projections to the anterior cingulate cortex (Witter, 2006).

1.8.2.4 Subicular cell types

The subicular principle cell layer contains large pyramidal neurons (similar to CA cells; Harris et al., 2001), as well as many smaller neurons (Amaral and Witter, 1995). Subicular pyramidal cells are considered to be relatively uniform compared to the more extensively researched CA1 cells. There are 2 types which differ regarding their firing properties and distribution within the principle cell layer; regular spiking cells located superficially and intrinsically bursting cells which are located deeper (Greene and Totterdell, 1997; Amaral and Lavenex, 2007). These cells do not differ morphologically and both project outside the subiculum. However, some evidence suggests that only bursting cells project to the entorhinal cortex (Amaral and Lavenex, 2007). Therefore they may differ regarding connectivity. Little is known regarding the smaller neurons beyond being considered the interneurons of the subiculum. Their similarity to CA1 interneurons however is relatively unknown.

Staff et al., (2000) compared subicular and CA1 pyramidal neurons. Subicular neurons have fewer branches in the basal and apical dendrites trees. However, there was no difference in regular spiking and bursting neurons in the subiculum (Taube, 1993; Greene and Totterdell, 1997; Staff et al., 2000; Harris et al., 2001). Similar to CA1 cells, the subicular dendrites are studded also with spines.

1.8.2.5 Subiculum summary

The subiculum receives strong unidirectional input from CA1 and sends divergent output projections to many other parts of the brain. Subsequently the subiculum is considered the major output area of the hippocampus (Naber et al., 2000). Among its various cortical and subcortical output areas the subiculum

notably has strong reciprocal projects to the EC and strong projections to the pre- and parasubiculum. Whilst the projections from the CA1 are unidirectional, the subiculum could arguably feed-back information to the entorhinal cortex and subsequently to the hippocampus via its projections to the EC and the pre- and parasubiculum.

Chapter 2 Introduction part 2: Spatial cells

2.1 The spatial world

Navigation is a vital tool for survival. For example navigation allows animals to find food, mates, and avoid danger. Navigation is essentially the process/ activity of accurately ascertaining one's current location and route planning and following future routes. Early behavioural work by Tolman (1948) has been highly influential in the research field of navigation. He suggested that the ability to navigate requires specific cognitive processes allowing the animal to mentally represent space. He considered that "in the course of learning, something like a field map of the environment [is] established in the rat's brain". During early observations Tolman noted that rats would use 'short cut' behaviour to reach a goal location instead of following their trained route. He devised a task to test this behaviour. Initially he trained the rats to reach point B from starting point A (Figure 2.1.1). After training in an maze with only one route (Figure 2.1.1 *left*) he then put the rats in a sun-burst maze providing multiple routes to the goal location (Figure 2.1.1 *right*). Typically the rats tended to choose the shortest route (path 6), despite having no previous experience of the apparatus. This led him to conclude that the rats must have produced a cognitive representation of space through latent learning. This sort of learning goes beyond stimulus-response as it requires the creation of a mental representation of the environment rather than just associative learning techniques. He termed this

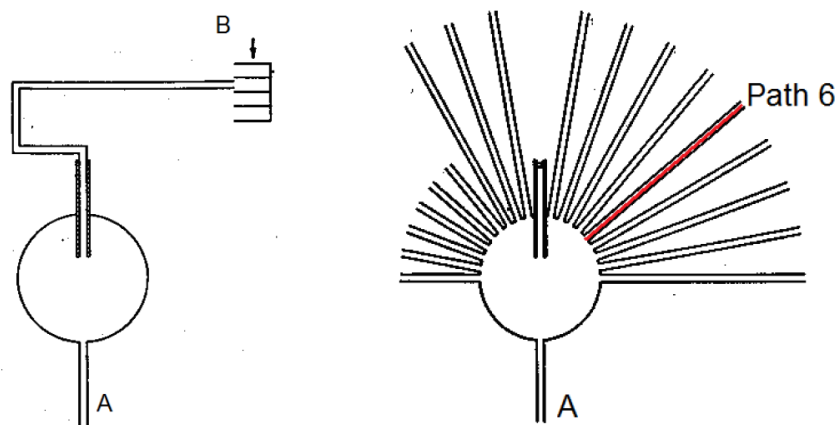


Figure 2.1.1: Apparatus and procedure used to investigate the existence of a cognitive representation of a rat's environment by Tolman (1948).

On the left is the training apparatus, where rats were trained to run from location A to location B. On the right is the sun burst maze, used as the test apparatus. After training in the single route maze, most rats were able to accurately choose the shortcut route highlighted in red (path 6).

mental representation a 'cognitive field map'.

Behavioural evidence compatible with the use of a cognitive map came with the development of the popular 'Morris water maze' task (Morris, 1981). Inside a pool of cloudy water, rats had to locate a platform hidden beneath the surface. This platform was not visible and so they had to locate it without relying on any intramaze cues. During training they were released into the pool from the same starting location which arguably allowed them to use either a cognitive map or an associative-based strategy to find the platform (e.g. body turns, time of swimming). In the test trials post-training the rats were released from random sites in the pool. If the rats were relying on an associative-based strategy then they would have been unable to locate the platform. However, Morris (1981) found that even when released from different starting positions the rats could still locate the platform, supporting the idea that the rats used a representation of the environment (cognitive map) rather than a response strategy.

Morris et al., (1982) later replicated this work using rats which had undergone hippocampal lesioning (lesions to the hippocampus, DG and the subiculum). In comparison to control rats lesioned animals performed poorly when released from different start locations. Morris et al, (1990) report that the hippocampus and subiculum lesions caused impairment to the initial postoperative acquisition of place navigation but did not prevent eventual learning to similar levels of performance by the controls. The effects of 'pure' subicular lesions on spatial learning with no damage to the hippocampus, were interpreted as deficits in heading and bearing on a target, and a deficit in precise localization of the hidden platform position.

This implies that the hippocampal formation may play a vital role in utilising a mental representation for navigation. Since this early work the cognitive map has been widely investigated (for a review see McNaughton et al., 2006).

They also report that lesions of the subiculum alone did not lead to deficits in spatial learning in the same fashion as do lesions of the hippocampus proper; rather,

The idea that the hippocampus was the substrate of a cognitive map was derived from O'Keefe's discovery of place cells. In 1971 O'Keefe and Dostrovsky recorded single cells from the hippocampus (CA1) during natural behaviour (grooming, walking sleeping etc) and in responses to various stimuli (e.g. odours, noises and light cues). Their early work identified a group of cells which exhibited spatially-related firing. These

cells appeared to remain silent unless the rat was walking through or was situated in a particular portion of the environment. It was the discovery of these location-specific cells which provided the first single-cell evidence supporting the idea of a kind of Tolmanian 'cognitive field map' representing allocentric space. These cells were called 'place cells' after their characteristic firing for a specific place within an environment (O'Keefe and Dostrovsky, 1971; O'Keefe, 1976; O'Keefe and Burgess, 1996).

It was the discovery of place cells that led to the development of the cognitive map theory of hippocampal functioning. The theory held that the hippocampus creates an intuitive, innate and Euclidean framework of allocentric space with place cells at the centre, allowing spatial memories to be encoded and stored in a map-like way (O'Keefe, 1976). O'Keefe and Nadel (1978) adopted a Kantian stance on space, emphasising the apriori abstract nature of space.

"The constituents of space are places, and thus an alternative definition of a map is the representation of a set of connected places which are systematically related to each other by a group of spatial transformation rules. ... The absolute space defined by Kant exists in the absence of objects." (O'Keefe and Nadel, 1978, p.78). "

The original theory (1978) held key suppositions concerned with; representation and navigation of environments, encoding and storing of spatial information and the evolution of a spatial memory system that can be related to human memory processes (e.g. semantic and episodic). Specifically, O'Keefe and Nadel proposed that hippocampal pyramidal cells represented 'place', that directional information existed within the hippocampus and that somehow speed and/or distance information could be generated for the workings of the cognitive mapping system.

2.2 Spatial cells

Since the initial proposition of the cognitive map theory, it is now clear that the hippocampal formation and the parahippocampal region contain at least 4 types of spatially responsive cells. The following section will provide a general consideration of cells with spatial signalling which have thus far been identified. These spatial cells will be discussed in order of discovery.

2.2.1 Place cells

A place cell is a complex-spike (pyramidal) cell that fires when the rat enters a certain location within the environment, referred to as its place field (O'Keefe & Dostrovsky, 1971). The cell, silent outside of its place field, sees an increase of its firing rate as the rat enters the field, peaking at its centre and decreasing as the rat exits the field. Place cells are typically omnidirectional and so this pattern of firing can be seen from whichever directions the rat enters and exits its place field.

2.2.1.1 Located in the hippocampal formation

Place cells are primarily recorded in the CA1 and CA3 of the hippocampus. Thompson and Best (1989) tried to make an accurate estimate of the place cell population in the CA1. They identified complex-spiking cells under light barbiturate anaesthesia, and then tested the rats in three environments (Radial Arm Maze and cylindrical and rectangular environments). Over a third of the cells identified under anaesthesia were also recorded in at least one of the environments. Almost all other cells recorded had very low spontaneous rates and were classed as silent cells. Only 14% had fields in two or three of the environments. Many of the cells with fields in one environment were as silent cells in the others.

Place cells have also been found in the subiculum and the EC, both of which are areas that are integral to inputting and receiving information from the CA1. In comparison to CA1 place cells subicular and entorhinal place cells had larger fields which were less spatially compact and were less sensitive to environment shape (Sharp et al., 1999; Quirk et al., 1992). Place cells located in these areas have not been as thoroughly characterised as hippocampal place cells. In the present thesis only CA1 and CA3 place cells will be referred to unless otherwise specified.

2.2.1.2 Field shape and size

The size and shape of place fields typically vary with the size and shape of the environment (Leutgeb et al., 2005; Fenton et al., 2008; Lever et al., 2002a; O'Keefe & Burgess, 1996). Interestingly, field size depends on the cells recording location along the hippocampal dorsoventral axis (Jung et al., 1994; Kjelstrup et al., 2008; Maurer et al., 2005). Whilst the ventral portion of the hippocampus is less well explored some ventral neurons have been reported to have place fields double the size of dorsal place cells (Maurer et al., 2005) or even four times those of the dorsal region (Marcelin et al., 2012). These larger place fields could cover the entire environment and act as the spatial context. This is relevant for interpreting experimental results involving the hippocampus in non-spatial functions, like conditioning or sensory processing without apparent spatial signalling. Therefore the place cells with large firing fields which signal the entirety of a specific environment may provide a spatial context for non-spatial activity. Interestingly unlike neocortical cells hippocampal place cells are not topographically organized (reviewed O'Keefe et al., 1998; Ranck et al., 2001). Exceptionally Hampson et al., (1999) showed that place cells located topographically close together (100-300µms apart) showed high cross-correlations of place field firing, whereas further away (400-1000µm apart) showed a much reduced cross-correlation. However, this finding has not been replicated (e.g. Redish et al., 2001).

There is limited evidence that place fields can be controlled by environment size. Muller and Kubie (1987) showed that place fields in small environments expanded when recorded in larger environments. This scaling was not parametric however, as the increase in field size was considerably less than the increase in environment area. Fenton et al., (2008) showed similar results.

2.2.1.3 Place cells receive sensory input from two systems

Evidence suggests that place fields are controlled by a combination of exteroceptive sensory and interoceptive idiothetic cues (O'Keefe, 2007). Allocentric exteroceptive information comes from the environment (visual, olfactory and auditory) and provides highly-processed multimodal sensory information. It is considered that only a subset of these cues would be required to identify location in a familiar environment using pattern completion (Wiebe et al., 1997; Wills et al., 2005).

Interoceptive idiothetic cues provide egocentric information including proprioceptive, vestibular and motor signals as well as information necessary for a path-integration mechanism (McNaughton et al, 2006a).

The advantage of combining these two systems is that the animal can orient itself in the absence of sensory cues using idiothetic vestibular and proprioceptive information (for example, in the dark). Evidence suggests that reliance on interoceptive cues alone is not efficient and can only be successfully used for short periods because the path integration mechanism can rapidly accumulate errors (e.g., McNaughton et al., 1996; 2006; Burak and Fiete, 2009).

2.2.1.4 Place field formation

When exposed to a novel environment or a novel extension of a familiar environment, hippocampal place fields are usually formed rapidly. The fields stabilise quickly with some cells stabilizing within 2-3 minutes, and the rest in around 5-6 minutes (Frank et al., 2004; O'Keefe, 2007). However, stability does seem to require a minimum exposure time. For example Frank et al., (2004) observed that if the duration of the first exposure was less than 4 minutes cells were much less stable upon re-exposure. The cues which determine the establishment of new place fields is still unclear (e.g. external or idiothetic) but evidence is clear that experience is certainly an important factor (McNaughton et al., 2006).

2.2.1.5 Place cell remapping

Once initially stabilised, place fields are very stable over time when re-exposed to a familiar environment (O'Keefe & Nadel, 1978; Thompson & Best, 1989; Lever et al., 2002a). However, they are not stable across different environments (Lever et al., 2002a). When the sensory qualities of two environments differ sufficiently hippocampal place cells are well known to remap (Muller and Kubie, 1987). Remapping is a phenomena whereby the place cell firing field transforms e.g. moves, morphs or disappears due to environmental change. The extent of remapping depends on the amount of changes between the familiar and the changed environments (Anderson & Jeffery, 2003; Lee et al., 2004; Leutgeb et al., 2005; 2007; Lever et al., 2002a). Three types of remapping are generally acknowledged. Minor environment changes are thought to produce 'partial remapping' where the place field may move location (Anderson & Jeffery, 2003; Shapiro et al., 1997) or 'rate remapping'

which is a change in firing rate but not field location (Leutgeb et al., 2005). Large differences between environments can cause 'global remapping' where the place field to completely disappear (Colgin et al., 2008).

Remapping is evident between geometrically altered environments but can also be produced by non-geometric manipulations. Other triggers include motivation (hunger, thirst; Kennedy and Shapiro, 2009), past emotional experience (Moita et al., 2004) and task (Markus et al., 1995). Colgin et al. (2008) hypothesised that responses to non-spatial changes would be reflected in the variation of the firing rate, and so would produce 'rate remapping'. Partial remapping, in which only some cells change the location of their place field, might reflect a change in some of the reference frames used to navigate in the same environment. In these cases some cells would be stable because they are fixed to unchanged distal cues, whilst other cells remap because they are fixed to proximal environmental cues which changed between environments (Colgin et al., 2008; Paz-Villagrán et al., 2004).

2.2.1.6 The influence of boundaries

There appears to be something special about boundary cues beyond other environmental cues. For example place fields tend to be localised more often around the environment walls (Hetherington & Shapiro, 1997; Hartley et al., 2000) and the insertion of a barrier can cause the doubling of place fields (Muller and Kubie, 1987; Barry et al., 2006).

Comparing recordings from the same place cells made in rectangular environments O'Keefe and Burgess (1996) noted that the location of peak firing typically maintained a constant position to the nearest walls. The rectangular environment was stretched and compressed causing several fields to parametrically stretch with the walls. For some place cells the changes to the environment shape made some place fields bimodal (separating into multiple peaks) in the larger rectangular environments. Similar parametric responses to geometric changes to an environment have been also seen across a variety of different shaped environments (Lever et al., 1999). O'Keefe and Burgess (1996) proposed that place cells receive inputs that are tuned to respond to the presence of a barrier at a given distance along a given allocentric direction. The presence of these inputs could explain the strong influence of environmental change upon place cell firing. It also would explain the

remapping, seen with environmental shape changes. The speculation of these inputs led to the development of the boundary vector cell (BVC) model discussed later.

The influence of boundaries on place fields is not limited to perimeter walls, inserted barriers can also affect place fields. Muller and Kubie (1987) showed that bisecting a place field with a barrier would often cause the cell to stop firing, without affecting more distant place fields. Barry et al., (2006) replicated this result and also demonstrated that the addition of a barrier can promote the addition, deletion or duplication of place fields adjacent to the barrier. Rivard et al., (2004) also showed that some place cells may signal the proximity of additional free-standing barriers. For these place cells changes to the barrier disrupted firing. They moved and rotated with the barrier, and disappeared if the barrier was removed. In contrast to the influence of extended barriers, Cressant et al., (1997) showed that isolated objects within the environment failed to affect place cell firing unless moved to the edge of the environment, (where they acted as orientation cues), or put in a line to form an extended barrier. In short, it seems that impediments to movement, be they the walls of the environment, a free standing barrier or even a sheer drop at the edge of a platform (Lever et al., 2002a), play a key role in defining place cell firing.

One interesting study indicating the importance of boundaries to firing patterns looked at place cell behaviour in a denuded environment. Barry et al., (2006) used their laboratory floor to place cells firing patterns with boundary removal (Figure 2.2.1). They covered the testing room in black drapes and all light but a single point near the ceiling was extinguished. During the experiment a burst of punishing white noise was used to prevent the rat reaching the room perimeters. The experiment had a number of wall removal conditions, where each wall was removed until only one of the pillars which connected the walls together was left as a solitary landmark. Of the 25 place cells recorded, only 3 showed localised firing in the single pillar condition, and these cells followed the pillar if it was moved rather than remaining fixed. Over the course of the experiment, many of the place fields broke down. In general, it appeared that the boundary changes made place fields 'less coherent and more diffuse' see (Figure 2.2.1). Whilst this finding stands alone and requires further investigation; it certainly highlights the importance of boundaries in modulating place cell firing.

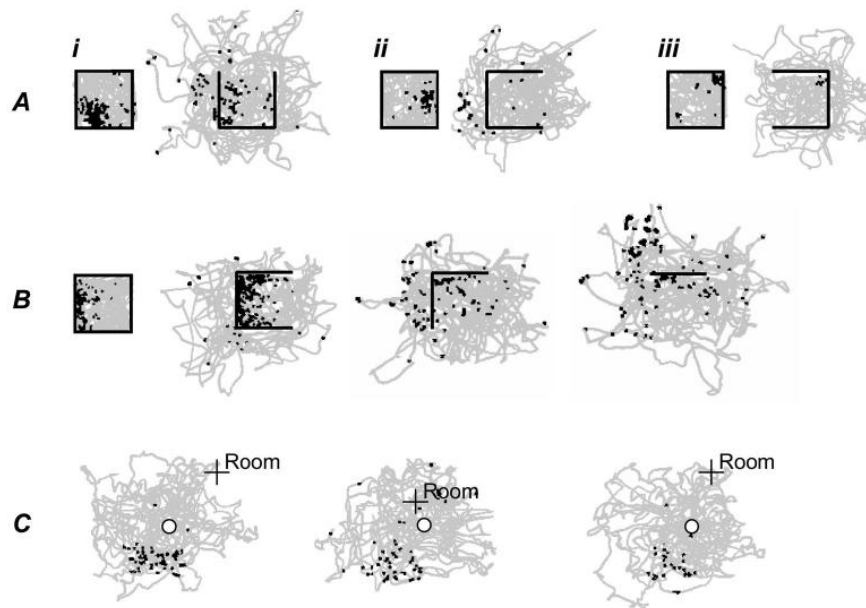


Figure 2.2.1. Effect of wall removal on place cell firing.

Figure shows A) Effect of removing one wall on 3 place cells (i-iii). Plots show the locations at which spikes were fired (black squares) and the path of the rat (grey). Walls are shown as black lines. B) Shows one place cell and the effect of successive removal of walls on the fields. Removal of one wall produced limited change, but the removal of the second and third walls caused a profound break down in spatial firing. C) shows a rare place cell (one of two) with a coherent field in the pillar-only condition (after removal of all 4 walls). The location of the pillar is shown by 'o', a fixed point within the room is shown by '+ Room'. When the pillar was moved around the room, the place cells field shifted in concert. Figure adapted from Barry et al., (2006).

2.2.2 Head-direction cells

It is generally acknowledged that directional information is provided by head-direction (HD) cells. HD cells code for direction of heading independent of the rat's position within the environment (Taube 1990a; Muller and Kubie, 1994; Burgess et al., 2005; Jeffery, 2007). HD cells fire maximally when the animal's head is pointing in a given compass direction (Taube et al., 1990). The orientation does not relate to geomagnetism and so the camera orientation is generally used to determine 'north'. There is no preferred direction in the distribution of HD cells; as a population they evenly signal the full 360° available. Similarly to place cells HD cells are not organised topographically; neighbouring neurons do not necessarily fire for the same direction (Taube et al., 1998; Taube and Muller, 1998).

2.2.2.1 Anatomical location of Head-direction cells

Head-direction cells have been found in the anterior and laterodorsal thalamus, lateral mammillary bodies, dorsal tegmental nucleus, anterior cingulate, retrosplenial cortex, postsubiculum, presubiculum, subiculum and entorhinal cortex (EC; Taube et al., 1998; 2007; Sargolini et al., 2006). HD cells are densely populated in the dorsal presubiculum which has strong anatomical connections to the hippocampus via the EC. HD cells are typically not found in the hippocampus proper. However, Leutgeb et al., (2000) reports recording a few CA1 head-direction cells.

2.2.2.2 Head-direction cells provide a universal directional code

Head-direction cells provide a universal directional metric. Unlike place cells whose firing is controlled by environment changes, HD cells generally maintain their firing patterns across environments (Taube et al., 1990; 1998). However, the orientation of the directional tuning can in some instances be controlled by geometric changes. Golob and Taube (1997) found that changing testing enclosure shapes altered preferred direction for a small number of HD cells (recorded from the postsubiculum and anterior thalamus). 20% of HD cells changed their directional preference by $>18^\circ$ from cylinder to square and this could be increased to $>36^\circ$ with more radical shape changes it may be that some HD cells are more influenced by external cues than others.

The direction vector of the HD cells is anchored to environment cues and the orientation of the directional field can be altered with cue rotation, similar to place cell firing (Muller and Kubie, 1987). Rotation of

internal or external cue cards (on the environment wall or on the testing room walls) can cause the HD population to produce a consummate rotation with the cue. Cue card rotation makes obvious the obligatory coupling of the HD cells. Whereby, when the preferred direction rotates the angular distance between pairs of cells is maintained, i.e. when a cell rotates 20° for environment change both cells rotate by the same amount. Shifts of directional preference with cue rotation is rapid. Zugaro et al., (2003) showed that the reorientation of directional preference with cue card rotation (90°) can occur within 100ms of the rotated cue card being visually perceptible. This provides evidence for a 'hardwired network of HD cells' which act in concert. This allows the HD cell population to give an accurate and clear-cut representation of heading direction.

Whilst HD cells anchor their orientation to environmental cues, not all cues have equal influence. To anchor firing HD cells can use both distal cues (e.g. cue cards on the lab room walls) or proximal intra-environment cues (e.g. object rotation). When both are available the HD system typically relies on distal cues. In the absence of distal cues Zugaro et al., (2001), showed that HD cells rotated in concert with rotated proximal cues. However if the distal cues were available and the proximal cues were rotated the HD orientation was relatively unaltered, supporting the dominance of distal over proximal cues to control HD responses.

2.2.2.3 Head-direction cells integrate external and idiothetic cues

HD cells also receive path integrative information (vestibular and visual motion signals). If visual motion and landmark cues contradict each other, HD cells will often average the signals from both cues (Blair and Sharp 1996). Clear evidence that path integration supports HD firing is suggested by the disruption produced by vestibular lesions which cause HD cells to lose their preferred direction (Stackman and Taube, 1997).

Whilst the orientation of the HD field is dependent upon external cues, the activation of HD cells is not solely dependent on external cues. In an early study by Taube et al., (1990) cue removal caused two thirds of the HD cells to shift preferred orientation. However, even for those cells which shifted there was no change to the width of firing field or the peak firing rate. It is suggested that this may be because these properties are dependent on intrinsic computations of the cell and or idiothetic cues from the vestibular and proprioceptive systems than external environmental stimuli (O'Keefe, 2007).

HD cells integrate information from idiothetic cues (from the vestibular and proprioceptive systems), however similar to place cells it is the general opinion that idiothetic information cannot maintain HD

activation independently. For example in darkness olfactory and idiothetic cues likely work together to preserve stable orientation (Save et al, 2000). Knerim et al., (1995) considers that in novel environments path integrative cues dominate with first exposure. With subsequent exposure environmental cues take over control once the environmental cues have achieved a stable relationship to the path integration system. Disorientating the animal and thus disrupting the vestibular and proprioceptive systems daily (for several weeks) before testing can also cause the cells to be less stable and less well controlled by explicit visual cues (Kneirim et al.,1995). Further evidence suggests that very little exposure time is needed in a novel environment before the cue cards take control. Goodridge et al., (1998) showed that HD cells generally became dependent on the external cue cards within 8 minutes, with some cells taking as little as 1 minute. Also, Zugaro et al., (2000) showed that preferred direction shifted to a new stable orientation within 15 second of cue card rotation; supporting the short time period required for HD stabilisation.

The path integration system is subject to cumulative errors, and fixing the HD system to environmental cues may provide a means of correcting these errors. The HD system could use path integration to assign stability and a direction to the visual cue, whilst the cue can then correct any drifts in the path integration system. This integration would require rapid association of cues to a stable pre-existing frame work (O'Keefe, 2007).

2.2.3 Grid cells

Grid cells were first recorded in layers II & III of the medial entorhinal cortex (MEC; Fyhn et al., 2004; Hafting et al., 2005). They are cells with similar sharply tuned spatial firing to that of place cells but with multiple firing fields (often referred to as vertices or nodes) which form an equally spaced hexagonal grid across the environment (Figure 2.2.2). This systematic distribution makes these cells perfectly suited to provide self-motion information. If projected to CA1 this information could contribute to the creation of place cells and determine the distances and directions between the place fields. It has been observed that grid cells in the same part of the MEC have similar grid scales (distances between fields) and orientations (Hafting et al., 2005; Barry et al., 2007; Boccara et al., 2010). Orientation has in fact been shown to be relatively constant within recording location, and in general grids cells recorded from each rat generally seem to share a common orientation (Hafting et al., 2005; Barry et al., 2007; Boccara 2010). However the placement of the grid cells fields are not topographic (Hafting et al., 2005). Also similar to place cells there is a clear linear increase in grid scale along the dorsal-ventral axis of the MEC (Fyhn et al., 2004; Hafting et al., 2005; Barry et al., 2007; Brun et al., 2008).

Grid cells provide information about position, distance and direction and have therefore been presented as a suitable candidate for providing a metric system for navigation (Hafting et al., 2005; Moser and Moser, 2008). The MEC is an obvious candidate for providing metric information to the hippocampus as most pyramidal cell in layers II and III of the EC project directly to the hippocampus (Witter and Amaral, 2004; Moser and Moser, 2008).

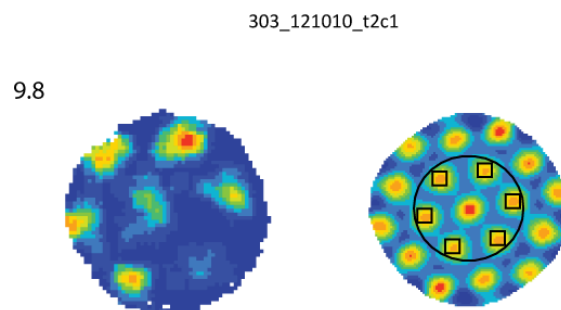


Figure 2.2.2. Grid cells have multiple firing fields which tessellate the environment.

The figure presents a grid cell from the dataset recorded for the present thesis. The cell identification number is given at the top. On the left is the rate map with the peak rate above it. As with all the rate maps shown red indicates maximum firing and dark blue indicates zero firing. Pixels not sampled by the rat during foraging are white. To the right is the spatial autocorrelation map. The black squares show the six peaks surrounding the central peak used to define gridness scores, grid scale and orientation.

2.2.3.1 Basic properties of grid cells

Grid cells were first recorded in the dorsocaudal MEC (Fyhn et al., 2004; Hafting et al., 2005) and have since also been recorded in the presubiculum and parasubiculum (Boccaro et al., 2010).

Grid cells are characterized by multiple peaks of firing which tessellate the environment (Figure 2.2.2). These firing fields have a hexagonal arrangement. Each field can be clearly delineated from background firing (Hafting et al., 2005). The regularity, orientation and distance between the fields creating the grid pattern are calculated through spatial autocorrelation of the rate maps (Figure 2.2.2). The periodicity of the pattern is represented as a 'gridness score'. This measure quantifies the extent to which the spatial autocorrelogram contains field peaks distributed at 60° increments around a central peak (see Figure 2.2.3a). The gridness score is varied between -1 and +1; the higher the score the more regular the pattern (see methods for full details).

Grid scale represents the separation of the peaks, and is calculated using the hexagonal pattern of the spatial autocorrelation maps. This is a measure of the median average distance from the central peak to the 6 surrounding peaks (see Figure 2.2.3b). Hafting et al., 2005 found that the distances between the central peak and the 6 surrounding peaks was nearly constant with a small standard deviation. The orientation of the grid was calculated as the angle between a camera- defined reference line and a vector to the nearest peak of the inner hexagon (counter-clockwise direction; see Figure 2.2.3c).

The location of the grid fields across the environment is called the grid phase, this is calculated by correlating field locations in pairs of rate maps. Neighbouring grid cells which may share spatial scale are likely to be 'offset' to one another (illustrated in Figure 2.2.3d). The location of the fields across the environment is referred to as the phase of the grid cell. The relationship between each cells field locations and the field locations of other cells is called the offset. The offset of individual cells to one another is not topographic but it is predetermined and persists with environment change (Hafting et al., 2005; Fyhn et al., 2007). So if the phase was to be altered, then the phase would change for all the cells whilst the offset would remain constant. If the grids of a small number of neighbouring cells (which share grid scale) were to be superimposed on each other, the entire environment could be covered by a few neurons, suggesting the entire environment could be coded locally by only a small subset of neurons (Moser and Moser 2008).

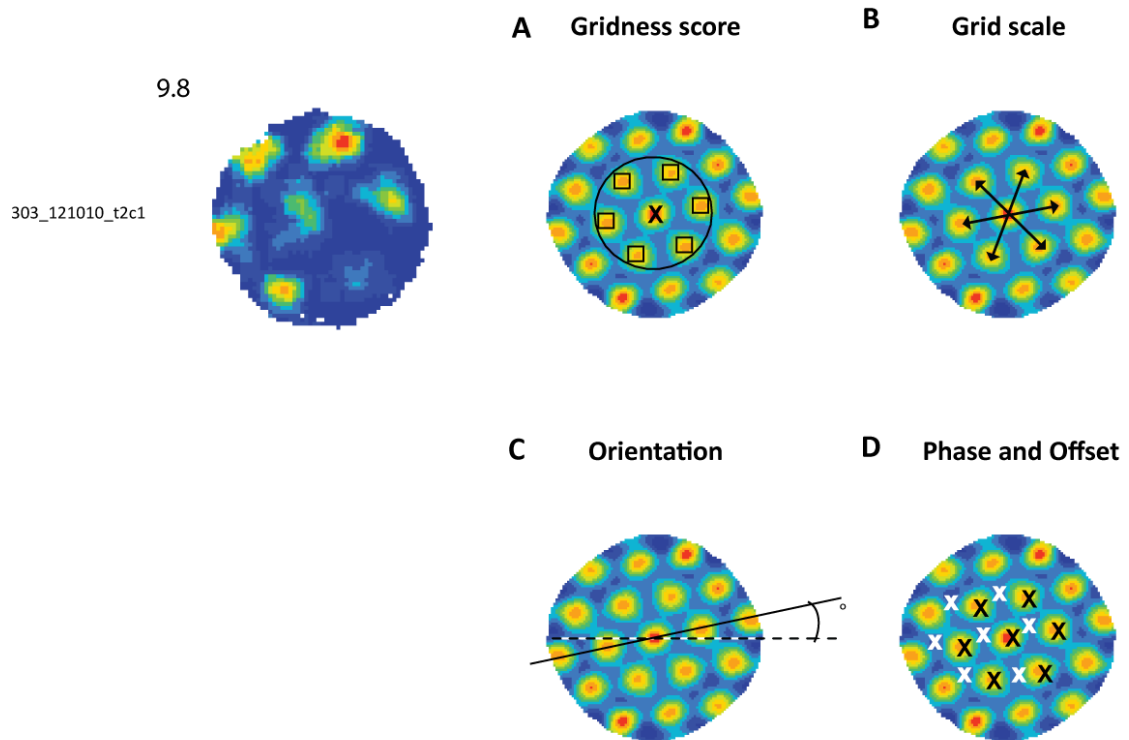


Figure 2.2.3. Spatial autocorrelation is used to determine the parameters of the grid pattern.

The figure shows an example grid cell recorded from rat 303. On the left is the rate map and with peak rate (Hz). To the right are the spatial autocorrelation maps, which had been adapted for illustrative purposes. A) Gridness score is calculated as the regularity of the grid pattern. The gridness measure tells us how closely the 6 peaks (black squares) round the central peak (black cross) are distributed at 60° increments. B) The grid scale is the spacing of the grid. This is calculated as the distance between any field and its 6 surrounding fields. C) The orientation of the grid is defined by the lines that intersect the grid fields. Each grid has three such axes. The grid orientation is the angle between a horizontal reference line (dotted line) and the axis with the smallest angle relative to this reference line (black). D) The spatial phase is the position of the grid fields in the environment. Two possible phases are indicated with crosses, one set in black and one in white.

2.2.3.2 Spatial scale varies along the dorsal-ventral axis

Grid scale increases along the dorsal-ventral axis in the rat MEC (Hafting et al., 2005; Brun et al., 2008; Stensola et al., 2012). As mentioned above the distance between fields (grid scale) within individual cells was near constant. Neighbouring neurons in the MEC also share similar grid scales, however grid scales from different locations across the dorsoventral axis of the MEC were strikingly different (Hafting et al., 2005; Brun et al., 2008; Stensola et al., 2012). Hafting et al., (2005) recorded cells along the dorsoventral axis as they lowered the electrodes through layers I and II. The dorsal MEC was sampled first and as the electrodes were advanced they reached the ventral MEC. Moving just 100microns deeper showed an increase in spatial scale. As with place cells the field size increased along the dorsoventral axis; the more ventrally a cell is recorded the larger the field size and the larger the spacing between fields. In Hafting et al., (2005) the grid scale varied between 39-73 cm from dorsal to ventral, accompanied by a variation in field size between 326 and 709cm². In a more recent study using larger recording environments Stensola et al., (2012) recorded grid cells with spatial scales of up to 171cm and Brun et al., (2008) recorded grid cells with spatial scales of up to 3metres. Stensola et al., (2012) reported large numbers of simultaneously recorded grid cells and provided evidence suggesting that the grid scale increase along the dorsal-ventral axis appears to be in discrete steps rather than gradually.

2.2.3.3 Directionality in grid cells

Grid cells are considered to be largely nondirectional (Moser and Moser, 2008). However, a class of grid cells called conjunctive grid x direction cells have both locational and directional signalling. These have been identified in the middle and deep MEC layers (Sargolini et al., 2006). These layers also contain a substantial proportion of HD cells. The MEC receives strong projections from the dorsal presubiculum (van Haeften et al., 1997) which is densely populated by directionally-modulated cells. There is considerable speculation that the signals from the presubicular HD cells may be controlling and accounting for the directional modulation of the grid cells located in the middle and deeper MEC layers (Moser and Moser, 2008).

2.2.3.4 Grid cells develop quickly in young rats

Wills et al., (2012) report that grid cells first emerge in young rats at around 3 weeks of age. Once they appear the grid cells seem to develop their functional properties rapidly. This is similar to the emergence age and development seen in previous studies by Langston et al., (2010) and Wills et al., (2010). Both

studies report that as soon as grid cells were detected, they seemed to possess most of the properties that adult grid cells possess. The grid patterns appear to be universal, as with adult grid cells, with the grid cells maintaining their phase offset between cells, even when the field positions were not stable.

Wills et al., (2012) and Langston et al., (2010) both show that in comparison to head direction and place cells that grids cells were the slowest to develop. These results have implications for the inputs and the dependence of information in the spatial representation circuit. For example it may be that grid cell development is dependent upon stable spatial signal originating from CA1 place cells and the head direction system (Burgess et al., 2007; Hasselmo et al., 2008a).

2.2.3.4.1 The appearance of the grid pattern in novel environments

Early work on grid cells suggested that the formation of the grid pattern does not require extensive training (Hafting et al, 2005). Similar to place cells, grid cells seem to require a minimum period of exposure to an environment before stabilization. Hafting et al., (2005) compared the field firing rates at 2 minute intervals (blocks) through 20 minutes of a 30 minute trial. The last 10 minutes was used to calculate the final peak rate for each of the fields. They found that the firing locations during the first 2 minute blocks were significantly correlated with firing locations at the end of the trial. The correlations were weaker for the earlier 2 minute blocks than the later blocks suggesting that the grid cells required a period of stabilization. Hafting et al., (2005) suggest this delay may reflect the time needed to set the phase and orientation of the grid in relation to environmental landmarks (allocentric exteroceptive cues). In all however, the influence of novelty was relatively mild, and there were no obvious signs of scale change in the original Hafting et al., (2005) report.

Later work has shown a larger influence of novelty. In 2007 Barry et al. investigated the grid pattern between familiar and novel environments. The novel environments were made such through the expansion/contraction of the familiar environment walls. Barry et al. found that environment manipulation caused a parametric expansion/ contraction the grid scale, which was related to novelty. More recently Barry et al., (2012) showed that non-geometric novelty also had an influential affect on grid scale. These studies and the influence of novelty on grid scale will be discussed in more detail in section 2.2.3.5 below.

2.2.3.4.2 Grid cell responses to environment manipulation

The grid pattern persists with the removal of visual cues and is present in all environments (Hafting et al., 2005). Early studies considered that gridness, grid scale and offset were maintained with environment change, and only orientation and phase were altered across environments.

Grid cell patterns are stable across trials in the same environment. Hafting et al., (2005) argue that this stability suggests that environmental cues play a significant role to anchor the grid pattern. Certainly this can be seen in particular grid responses to environment manipulation. Cells in the same animal share a common orientation (Hafting et al., 2005; Barry et al., 2007; Boccara et al., 2010). If environmental changes induce a shift in orientation, then all grids will maintain their rigid relationship (offset relative to one another) and will rotate together (much like head-direction cells). This can be seen in Hafting et al. (2005) when all external cues were masked and an internal cue card was rotated. This is also evident across rooms, all the grid cells typically rotated (in concert with HD cell rotation) whilst still maintaining their relationship to each other (Hafting et al., 2005). Evidence suggests grid phase can also depend on environmental cues. Solstad et al. (2008) demonstrated a phase shift in MEC grids with wall removal in the absence of HD cell rotation or grid cell orientation shift. Phase can also change in conjunction with orientation shifts between testing rooms. It is the general consensus that phase and orientation are determined by landmarks and boundaries (Moser and Moser, 2008).

How the fields of the grid are anchored to environment boundaries and landmarks of the environment is not known. Moser and Moser (2008) suggest that this anchoring may be due to back projections from the CA1 to the deep and superficial layers of the EC (Iijima et al., 1996; van Haeften et al., 1997; Kloosterman et al., 2000; 2003; Witter and Amaral, 2004). They consider that outputs from hippocampal place cells may reset the entorhinal path integrator as errors accumulate during movement. It maybe also that grid maps are aligned from one trial to the next through associations with landmarks. They highlight that the contextual specificity of the hippocampal representations, and, the enormous storage capacity of its intrinsic networks point to the hippocampus as a possible storage site for associations between the path integrator and environment features (Moser and Moser, 2008; Hafting et al., 2005; O'Keefe and Burgess, 2005). In agreement with these suggestions, grids have been shown to destabilize after inactivation of the hippocampus. Evidence shows that hippocampal inactivation gradually and selectively extinguished the grid pattern (Bonnievie et al., 2013). The authors consider these results suggest an excitatory drive from the

hippocampus to the MEC, as one prerequisite for the formation and translocation of grid patterns in the MEC.

2.2.3.5 Does grid scale change?

The stability of the grid pattern across multiple trials in the same environment suggested that external cues exert a significant influence over the maintenance of the grid pattern. When introduced to a novel environment the grid pattern was evident almost immediately and was maintained across environments. The persistence of the grid structure is reminiscent of the coherence across environments expressed by HD cells (Taube, 1998; Kneirim et al., 1995). The maintenance of grid structure in the absence of visual cues and in novel environments suggests path integration maybe the mechanism driving the grid cells rigid spatial periodicity (Hafting et al., 2005).

Hafting et al. (2005) looked at the influence of scaling the environment upon the grid structure of MEC layer II grid cells. They reduced a 2m diameter circular environment down to a 1m diameter circular environment. They found that the grid scale was unchanged, and the only obvious change was a slight increase in grid field size in the small circle. These results suggested that the metric of grid cells was only minimally influenced by the distance to the boundaries of the environment. The authors considered that this reinforced the view that external cues contributed little to the grid structure and that grid cell patterns are universal, regardless of the particular features of the external environment. However more recent evidence suggests plasticity of grid scale. In 2007 Fyhn et al. observed changes in MEC layer II grid cell spatial scale between square and circular environments. The spatial scale expanded by 4.9% when introduced to the circular environment from the square. This expansion was small but significant and was seen in 25% of the grid cells.

In 2007 Barry et al. investigated the environmental manipulation upon MEC grid cell spatial scale with the expansion/contraction of walls within familiar environments. Barry et al. observed that MEC grid scale could be varied parametrically with changes to environment size and shape. The paradigm involved running the grid cells in five 20min trials; with two baseline trials either side of two trials where one axis was changed (enlarged or shrunk) and one where both axis were changed (enlarged/shrunk). The grid cells rescaled parametrically with a 47.9% change with the enlarged/shrunk dimension and a 7.9% change in the unchanged dimension. As part of a study characterising border cells in the MEC Solstad et al., (2008) also

identified a small number of MEC grid cells which showed grid scale expansion when a square environment was extended in one direction to form a rectangular environment. The grid scale expanded parametrically along the extended dimension similar to that seen in Barry et al., (2007).

Barry et al., (2007) shows that the grid scale expansion was not a factor of running speed, directional modulation or recording site. However, rescaling did correlate with environment experience. The novelty of the test trials correlated with the expansion/contraction of the grid scale. Further, the rescaling was negatively correlated in cells recorded over multiple sessions, with the scale deformation reducing with continued experience. This suggests that the system reverted back to an intrinsic grid scale with experience. The authors suggest that this rescaling seems to occur over a similar timescale as it takes place cells to settle in altered environments (Lever et al., 2002a). This suggests that grid cells become associated with the features and boundaries of the environment, therefore explaining the parametric change in grid scale when the shape of the environment is manipulated.

This result has been recently replicated. In 2012 Barry et al. recorded 22 MEC grid cells from 8 animals in a study exploring the influence of novelty upon grid scale. They used a paradigm whereby a 1m x 1m square environment was run in a series of 5 trials per day for as long as one grid cell was being recorded. Three novel trials were run in between 2 familiar trials. There were 4 variations of the novel environment, with variations in colour, material, scent and lighting. The average expansion in the first ever recorded novel trial (trial 2, day 1) was 37.3% (13.8cm) in comparison to the familiar trials. They note that the expansion was similar between large and small scale grid cells, suggesting perhaps that the expansion may have been set at a fixed amount for all cells. However, there were not enough simultaneous recordings of small and large scaled grid cells to look at this further. Expansion persisted across days, but reduced in magnitude with experience as in Barry et al. (2007). The grid scales reverted back towards the baseline scale seen in the novel environment over the first 3 days of testing. By day 5, grid scales in the novel environments were no longer significantly different to familiar environments.

Barry et al., (2012) also looked at other changes to grid cell parameters between familiar and novel environments. Orientation remained stable between familiar trials and was significantly rotated between familiar and novel trials. This rotation did not revert over time to the baseline orientation, and is consistent with evidence that orientation is environment-dependent (Hafting et al., 2005). The grid cell firing pattern was also less regular and the fields were less circular and more elliptical. This was reflected by the

significant reduction in gridness. Like grid scale the gridness scores returned to normal with increased familiarity over 5 days. This increase in regularity was steadier (over 5 days) than the return of spatial scale.

Overall these results suggest that in a familiar environment grid cells become associated with environmental features. This association of the intrinsic grid pattern to environmental cues causes parametric alterations to grid scale in concert with environmental changes. This is consistent with place cell responses to environment change, and provides further support for the input of environmental information. The location of these inputs which anchor grid patterns to the environment boundaries is not yet known. However, there is speculation that they may arise from the associations of place and landmark from place cells (O'Keefe and Burgess, 2005) and/or from inputs from boundary-related cells (Solstad et al., 2008; Lever et al., 2009; Boccara et al., 2010).

2.2.3.6 Development of the grid pattern requires cue integration

The rigid periodicity of the grid pattern suggests grid cells may provide metric information to the navigation system and to the neural network representing space (Hafting et al., 2005; Fuhs and Touretzky 2006; McNaughton et al., 2006). Like place cells grid cells also require an integration of cues from different modalities. Early research considered that grid cells assimilate path integrative interoceptive information to create and maintain the rigid grid pattern independently of landmarks and environmental cues (Hafting et al., 2005). However this pattern is reproducible and stable across trials, indicating an association to environmental information. In general the grid pattern is considered to be anchored to the environment, via the integration of exteroceptive cues. It has been speculated that this external sensory information could be mediated by feedback from place cells whose location-specific firing is reliant on environmental information (O'Keefe and Burgess, 2005), or from BVCs which provide boundaries specific information (Lever et al., 2009; Moser and Moser, 2008). A more detailed discussion of grid cell responses to environmental manipulation is presented below.

Evidence suggests that the grid cell structure (spacing and field size) can exist independently of allocentric external cues. The periodic firing pattern is maintained in spite of changes to running speed and heading direction, suggesting the grids rely on the integration of changes in velocity and heading over time to enable a constant representation of the spatial relationship between positions (Moser and Moser, 2008). Further, the grid pattern can be maintained even with the removal of all visual cues. Hafting et al., (2005) recorded

33 grid cells from 4 rats in complete darkness, all lights were extinguished 10 minutes into a 40 minute trial. The removal of all visual cues had no significant effect on grid scale, firing rate or spatial information indicating the grid structure can exist independently of allocentric information. However, there was a moderate decrease in the spatial correlation between the rate maps which was exhibited as a weak dispersal/displacement of the fields (shift in phase). This is consistent with the theory that external cues are necessary for determining the phase, as they align the grid to the external reference frame (Hafting et al., 2005).

In a more recent study (Fhyn et al., 2007) where the rats were trained in both light and dark trials, two animals showed alternative responses to the removal and reintroduction of visual cues (Figure 2.2.4). In this study CA3 place cells and MEC grid cells were simultaneously recorded. Between light and dark trials the entorhinal cells were displaced (phase shift) and rotated (orientation shift), whilst the place cells showed global remapping (Figure 2.2.4). In one rat when the lights were turned on the hippocampal cells suddenly remapped to the light trial firing locations (Figure 2.2.4A). This was accompanied by equally fast realignment of the grid cells to the phase and orientation seen in the light trials. In a second rat the field locations for both the place and grid cells did not alter with the lights being turned on (figure 8B). The rat had to be removed from the environment and replaced one minute later for the cells to remap and realign to re-establish the firing patterns associated with the light trials. The authors consider this response may reflect the continued influence of self-motion information (idiothetic cues) upon the firing patterns. The temporary disruption of the rats running by removing it from the environment could then interrupt the path-integrative mechanisms, and allow the cells to reset.

Originally it was considered that this integration of external and idiothetic cues occurred locally within the MEC. The direct input to the MEC of directional and visuospatial information from the presubiculum and postrhinal cortex (respectively), puts the MEC in a privileged position to perform these computations (Hafting et al., 2005). However, in recent years grid cells have since been recorded from the presubiculum, and parasubiculum providing possible alternative regions which may perform the integrative computations (Boccarda et al., 2010). The continued stability of grid cells in the absence of visual cues, implies that there is a strong input from vestibular-kinesthetic feedback from the animals self-motion (Hafting et al., 2005). However, the maintenance of the grid pattern across trials, and the recent revelations that grid scale can expand with environment expansion and novelty, highlights the valuable input from environmental cues for anchoring the grid pattern, and creating a universal metric across environment.

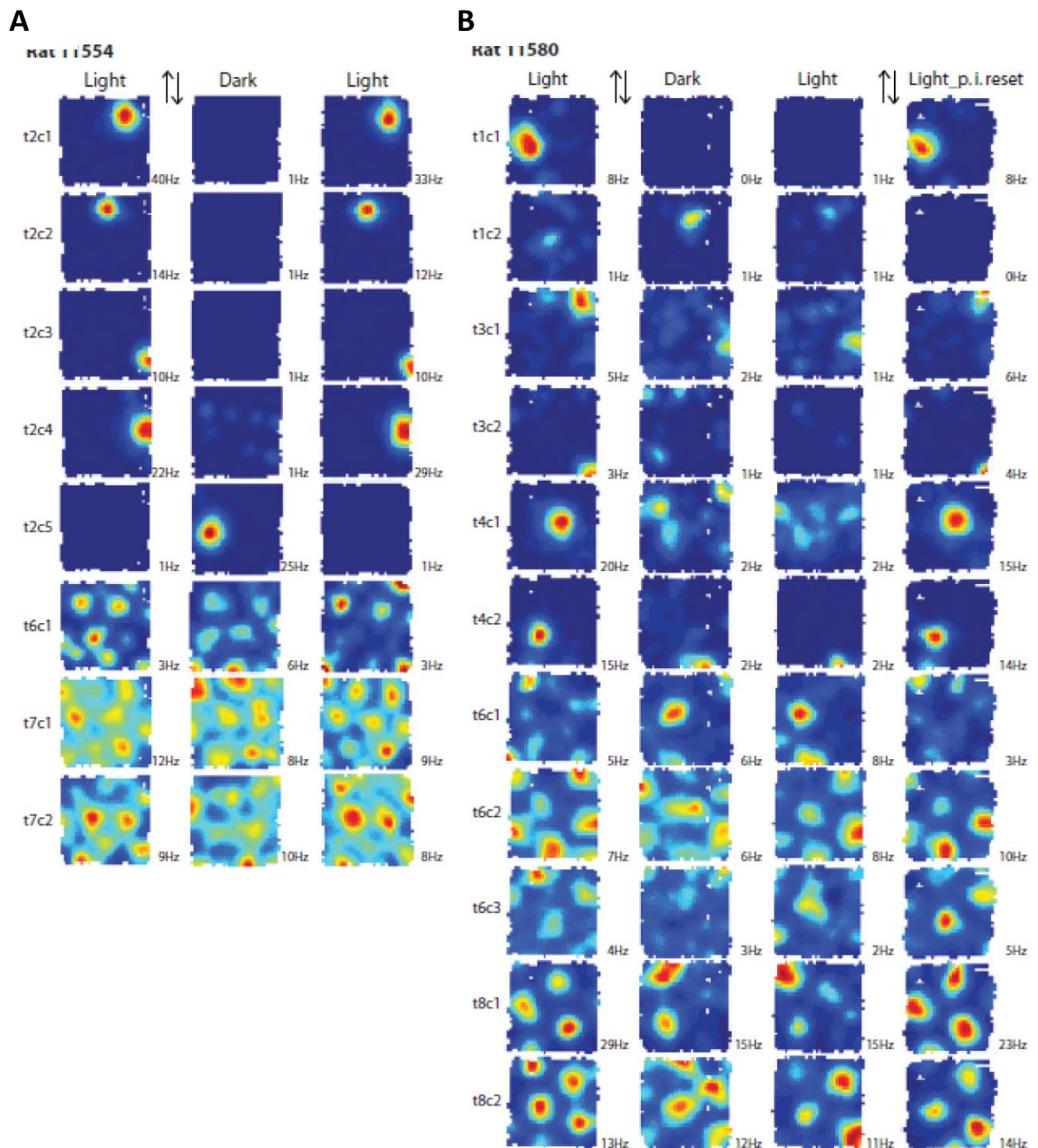


Figure 2.2.4. Simultaneously recorded CA3 place cells and MEC grid cells in darkness.

Figure shows simultaneously recorded CA3 place cells and MEC grid cells in darkness in 2 rats. Each row is a cell. A) In darkness the place cells locational fields disappeared or moved demonstrating global remapping. The simultaneously recorded grid cell firing patterns were coherent but displaced and rotated between the light and dark trials. B) Also shows this, but when the light was turned back on after the dark trial neither the CA3 place nor MEC grid representations reset back to the firing patterns shown in the first light trial (third column). The rat had to be removed and reintroduced after 1 minute to the environment to reset the representations (shown in the right hand column). Adapted from Fhyn et al., (2007).

2.2.3.7 Grid cells in different regions

Grid cells have been recorded predominantly from the superficial layers II and III and the deeper layers; V and VI of the dorsocaudal MEC (Hafting et al., 2005; Fyhn et al., 2007; Solstad et al., 2008; Barry et al., 2007; 2012). The function of the lateral portion of the EC is unclear. There is an absence of spatial cells which is consistent with the lack of input from HD cells in the presubiculum (Witter and Moser, 2006).

Grid cells have also been discovered in the pre- and parasubiculum (Boccarda et al., 2010). The local organization of the grid cells recorded from the pre- and parasubiculum shared many features with MEC grid cells. Neighbouring grid cells were generally offset from each other and spacing and orientation were relatively constant in comparison to MEC cells. Previous studies recording from the pre- and parasubiculum may not have found grid cells because the testing environments were too small. Many of the grid cells located in these areas were highly directional and were similar to the conjunctive grid x direction cells recorded in the deep MEC (layers III to VI; Sargolini et al., 2006).

There was a distinguishable difference in gridness between parahippocampal regions. Gridness was highest in layer II of the MEC and was reduced in the deeper layers of the MEC, and in the pre and para-subiculum. Gridness was lowest in the presubiculum and in layer V and VI of the MEC (Boccarda et al., 2010).

That grid cells are located in different regions raises the question of what mechanisms produce grid patterns. The origin and directional flow of information is not yet known. It could be argued that the multiplicity of spatial patterns in the pre- and parasubiculum could be inherited passively from parent cells in the MEC. However the projection from the MEC and these areas is relatively weak. Considering the strength of the projections it is more likely that the pre- and parasubiculum impose their firing patterns on MEC cells (Amaral and Witter, 2005).

2.3 Boundary-related cells and the BVC model

The most recently discovered spatial cells are those that signal environment boundaries. Prior to discovery their existence was speculated to account for the input of boundary-information to place cells. In 1996 O'Keefe and Burgess, identified environmental features which influenced place cell firing. They demonstrated that stretching a familiar rectangular environment along one axis resulted in a stretching of place fields along the same axis (O'Keefe and Burgess, 1996). To explain this finding the existence of "boundary vector cells" (BVCs) was predicted. These cells would input boundary information to the place cells (O'Keefe and Burgess, 1996, Burgess et al., 2000; Hartley et al., 2000).

The Boundary Vector Cell (BVC) model was outlined first in Burgess et al. (2000) and Hartley et al. (2000). It was considered that a BVC would fire whenever an environmental boundary intersected a receptive field located at a specific distance from the rat in a specific allocentric direction (Figure 2.3.1A). The BVC firing fields peak at the boundary creating a 'vector' from the rat (see Figure 2.3.1a).

The firing of a BVC depends solely on the rat's location relative to environmental boundaries and is independent of the rat's heading direction. BVCs with receptive fields peaked farther from the animal have broader fields than those peaked closer to it. Figure 2.3.1C shows the BVC firing field being generated by a specific BVC receptive field.

Barry et al., (2006) simulated BVC activity, and developed a number of predictions that would

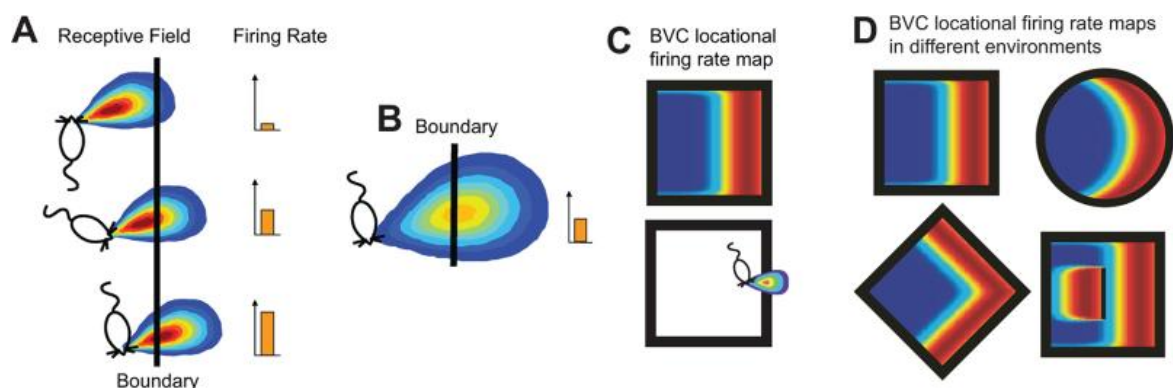


Figure 2.3.1: A BVC responds maximally when a boundary is at a preferred distance and allocentric direction (irrespective of heading) from the rat.

A) An example of a BVC receptive field tuned to respond to a barrier at a short distance east-northeast from a rat. B) BVCs tuned to respond to barriers farther from the animal will have broader receptive fields. C) Shows the firing field (shown as a rate map; top) for a BVC with a receptive field tuned to respond to a boundary at a short distance to the east (bottom). D) Shows the predicted firing fields in different environments for the BVC shown in C. Of particular note the insertion of a barrier causes a doubling of the field (bottom right). Figures are adapted from Lever et al., (2009).

characterise BVC firing. The model aimed to explain the shifts in field size and location that occurred in place cell firing fields with changes to the environment and to provide a candidate to account for boundary inputs to place cells.

Firstly, it is predicted that a BVCs firing field will follow the boundary (e.g. Figure 2.3.1D). For example in cylindrical environments the firing field will follow the boundary curve, producing a crescent shaped field. Secondly it is predicted is that the insertion of a barrier would produce a doubling of the BVC firing fields. For example, a BVC that fires maximally for an eastern boundary, will also fire along a barrier entered along the north-south axis (for example, see Figure 2.3.1D). The model suggests that the addition of a barrier provides additional loci at which short-range BVCs will fire (Lever et al., 2009). Barrier insertion has been shown to cause central place cell fields to vanish (Muller and Kubie, 1987), it may be that as an inserted barrier occludes the environment perimeter it disrupts BVC input to place cells. The third prediction is that when an environment is stretched, BVC fields also stretch continuing to fire along the entire boundary, this is similar to place cell responses to environment expansion (O'Keefe and Burgess, 1996). Fourthly it is predicted that BVCs would preserve their firing patterns in novel environments. This stability of firing across environments is predicted because BVCs provide signalling for any boundary which intersects the BVCs receptive field, independent of its qualities. Lastly it was predicted that like place cells BVCs would not be influenced by heading direction.

2.3.1 BVCs have been recorded from the subiculum

The discovery of subicular BVCs (Barry et al., 2006; Lever et al., 2009) is consistent with previous reports claiming that subicular firing is often driven by boundaries (Sharp et al., 1994; Sharp, 1997; 1999; 2006). Sharp (1997) recorded subicular 'location-cells'. These cells had larger locational fields and retained their firing patterns compared to hippocampal place cells across differently sized environments. Many of these cells showed a preference for the environment edges. Sharp concluded that these characteristics suggested that environment boundary information must play an important role in subicular firing.

In 2006, Barry et al. presented 10 putative subicular BVCs. These cells were recorded in only a single environment. Then in 2009, Lever et al. recorded a further 36 subicular BVCs. These BVCs were tested against the functional constraints of the BVC model. Out of the Lever et al., (2009) BVC sample, 24 were recorded in environments other than the standard recording square (see figure 10 for examples). The BVC firing fields followed the environment boundaries and fired irrespective of heading direction as predicted. Four rats had CA1/subiculum double implants which allowed for simultaneous recording of place cells and BVCs. Whilst place cells showed strong remapping between environments a, b and c, the

BVCs were consistently stable over time and across environments (see Figure 2.3.2). For example cell 2a (*second from the left*) responds to the west boundary of both the square, circular and un-walled environments.

As predicted the firing fields of BVCs were a function of distance and allocentric direction to the boundaries of the local environment. The long axes of the firing fields reflected the shape of the boundaries, tending to be straight in square environments and curved in circular environments (Figure 2.3.2). BVCs with directional preferences between the perpendiculars to adjacent walls fire along both walls (e.g. Figure 2.3.1, cell 5c). BVCs with receptive fields peaked close to the animal and oriented perpendicular to the walls of the environment fired predominantly when the rat was close to the wall in the BVCs preferred direction (Figure 2.3.2). BVCs with receptive fields peaked farther from the animal's head had firing fields that were broader but often still lay directly against a wall. Lever et al recorded some BVCs which had fields peaked so far from the rat, that the firing fields were offset from the wall. Lever et al considered that some of the larger firing fields may be from BVCs that were responding to distal rather than proximal walls.

As detailed above a key constraint of the BVC model is that BVCs should not only signal for perimeter boundaries, but should also signal for internal boundaries. When a free-standing appropriately-oriented barrier was inserted into the environment the cells demonstrated a clear doubling of their fields (Figure 2.3.3).

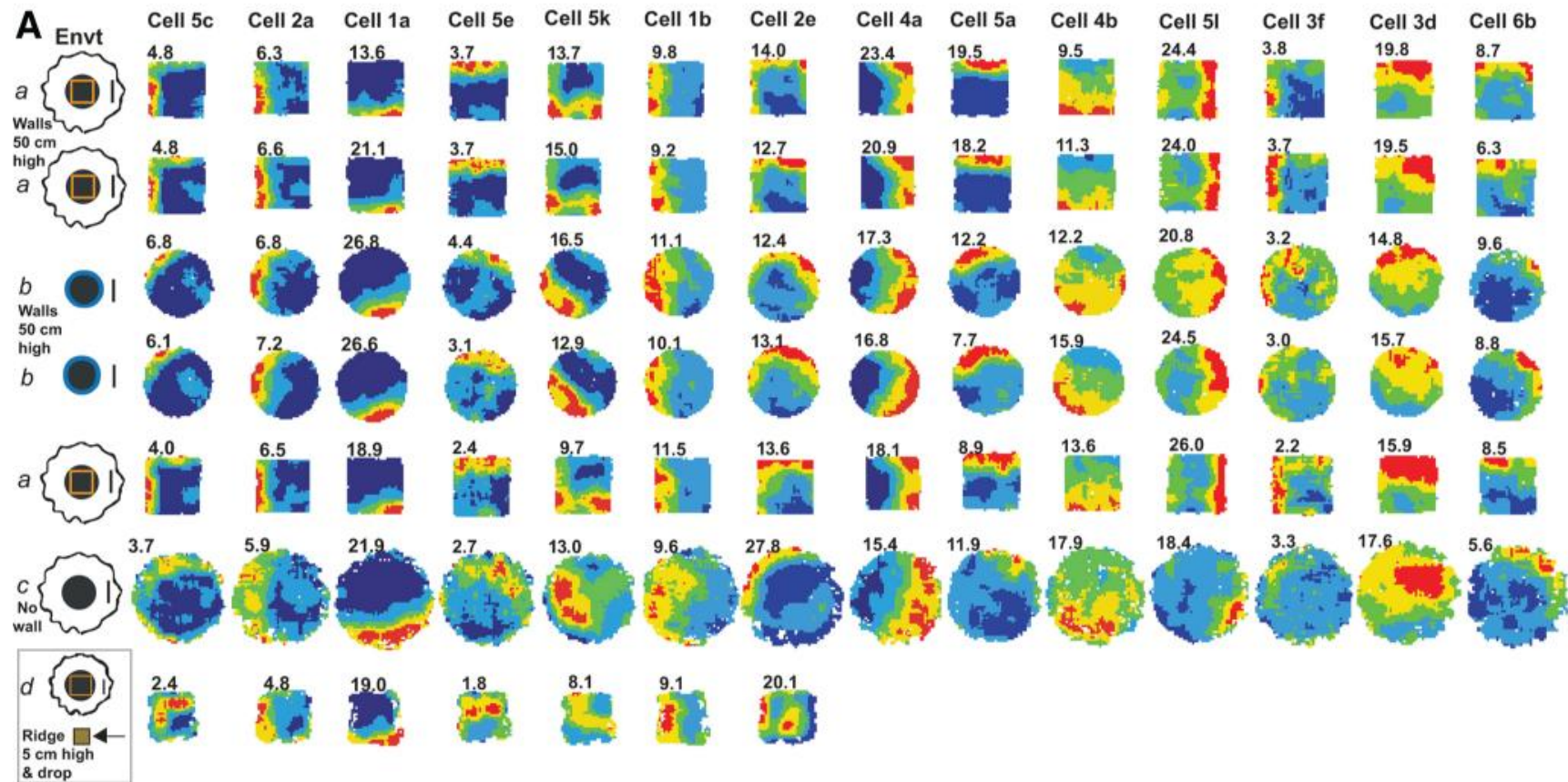


Figure 2.3.2. Firing fields of 14 subicular BVCs in different environments

Environment a, 62 x 62 x 50-cm-high beige square box made of morph material; Environment b, 79-cm-diameter, circular-walled, wooden light-gray enclosure; Environment c, the 90-cm-diameter floor of Environments a and b; Environment d, 39x39 cm square holding platform with 5-cm-high ridges. BVC fields followed the shape of the boundary and showed stable distal and directional preferences across environments. Figure adapted from Lever et al., (2009).

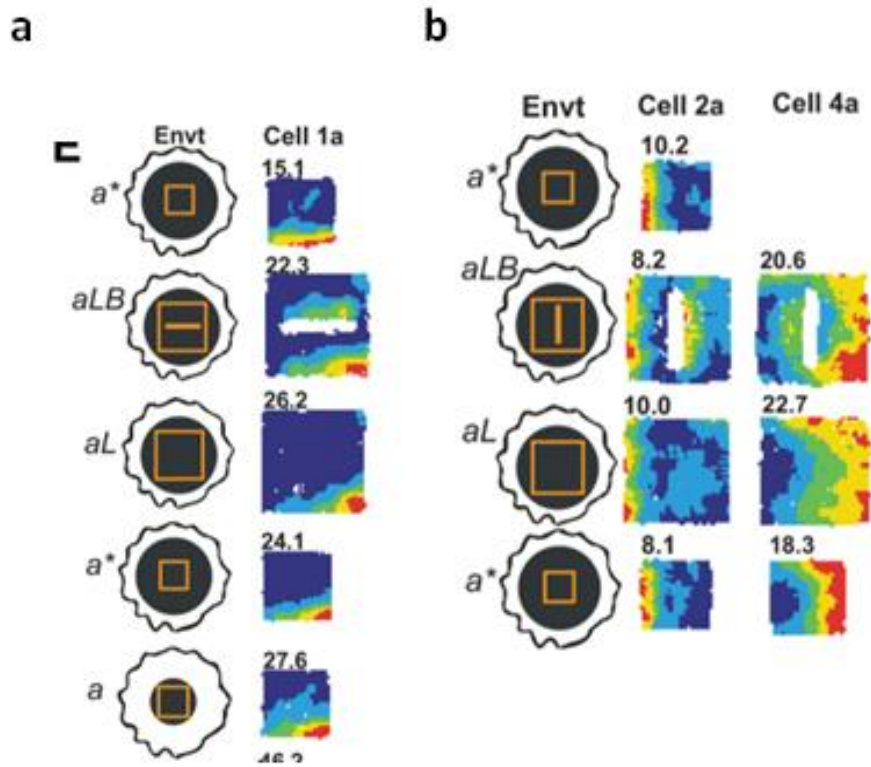


Figure 2.3.3. BVC produce a second firing field for the insertion of an additional boundary.

The figure shows 3 cells which were tested with the addition of an appropriately orientated barrier. For all cells this caused a doubling of the BVC firing fields. Figure adapted from Lever et al., (2009).

2.3.1.1 What is a boundary?

Remarkably despite their perceptual differences, BVCs can treat walls and drops similarly. Lever et al., (2009) demonstrated that to a BVC a boundary is not limited to environment walls (continuous vertical surfaces), as they can also respond to wall-less environment drops. Interestingly, wall-removal creates two perceivable boundaries, the wall-less platform edge and the extent over the edge that the rat can reach. Figure 2.3.2 shows that the BVCs seem to respond to either. For example cells 5e and 5k have fields that peak off from the edge of the rate map suggesting that they are responding to the environment edge. Cells 1a and 5a on the other hand have fields peaked along the edge of the rate map suggesting that they are coding for the extent of the rats explorable range (Figure 2.3.2).

The main determinant of BVC firing is the distal and directional vector from the rat to the boundary regardless of the boundary qualities e.g. shape, size and colour. Lever demonstrated that most BVCs produced firing fields in un-walled environments that were generally consistent with those in the walled environments. This seems to suggest that BVCs can respond to both extended vertical surfaces and to drops. Lever et al recorded one cell which produced a second field for a traversable drop between two wall-less environments. The rat was given a rectangular open platform made of two square platforms pressed together followed a trial where the square platforms were pulled apart 13cm. This gap was such that the rat could traverse across it, or be manually carried over. A traversable gap is qualitatively different to a wall or a drop from an open platform. It is not necessarily an environment boundary but it does impose some limitations to movement.

So, what do these results suggest constitutes a boundary? It may be that BVCs are responding to the visual perception of a boundary; whether it is open space or a wall. To test this Lever et al recorded 3 BVCs in complete darkness. The removal of visual input did not prevent BVC boundary responses. BVCs seem to respond to qualitatively different boundaries, and this suggests visual perception of a boundary alone cannot account for BVC responses. Lever et al concluded that 'a boundary is an abstract concept that may reflect sensory properties of environment features such as the sight or feel of a wall or an extended edge, as well as impediments to movement.' Also, as suggested by the diversity in the differing representations of the un-walled environment Lever et al consider that the relative importance of these factors may vary across the BVC population.

2.3.1.2 The subiculum as an output area

One difficulty for the BVC model and the discovery of subicular BVCs is that the subiculum is generally considered a CA1 output area with little to no back projection (Amaral and Witter, 1995; O'Mara et al., 2009). As an output structure the role played by the subiculum in spatial processing has always been considered limited. That said the subiculum is a relatively under investigated region (Witter and Amaral, 2006). If the subiculum is regarded as solely an output area, it may be that the boundary-signals are in fact just shadows of hippocampal activity. However, if this were the case then surely the characteristic remapping seen by place cells would also be seen in subicular cells. Derdikman and Moser (2009) in response to Lever et al., (2009) consider it to be crucial task towards understanding the relationship of CA1 place cells and BVCs by recording them both in a paradigm which causes place cells to remap.

The EC is the main input structure to the CA1 and the communication between the subiculum and the CA1 is generally considered to be via a strong uni-directional projection from the subiculum to the EC (Kloosterman et al., 2003). Subicular boundary-information could therefore reach hippocampal place cells via EC projections. Furthermore the appearance of boundary-related cells in the EC (outlined below) lends support to this route of input as BVCs could provide their inputs to CA1 via the MEC border cells.

The discovery of border cells in the MEC has also led to the suggestion that subicular BVCs are entorhinal axons (Solstad et al., 2008). This seems unlikely though as the waveforms of subicular BVCs are similar to pyramidal cell waveforms. It has also been suggested that subicular BVCs could be merely reflections of entorhinal border cell (Solstad et al., 2008). Lever et al. (2009) consider the anatomical distribution of the subicular BVCs argue against this. The MEC projects to the distal- to-CA1 part of the subiculum. If subicular BVC fields were actually copies of border cell firing, then the majority of BVCs would surely be located in this projection area. However, Lever et al. (2009) report that a high proportion of the BVCs are actually located in the proximal-to-CA1 portion of the subiculum.

2.3.2 Border cells

Boundary-related cells have recently been recorded in the MEC and the pre- and parasubiculum (Solstad et al., 2008; Savelli et al., 2008; Boccara et al., 2010). As mentioned above, the MEC is a more likely candidate than the subiculum for housing cells which would provide boundary-information to the hippocampus. The MEC projects directly to the CA1, whereas subiculum does not (Witter et al., 2006). Cells recorded by Solstad et al. (2008), and Savelli et al. (2008) were classed as ‘border cells’ and ‘putative boundary cells’ respectively. Solstad et al. describe border cells as cells which had ‘firing fields that line up along selected geometric borders of the proximal environment, irrespective of their length and continuity with other borders’.

Solstad et al. (2008) recorded border cells alongside HD and grid cells. Border cells comprised 10% of the spatial cells recorded throughout all layers of the MEC. Solstad et al. (2008) considered that the border cells may have a functional role in planning navigation trajectories and anchoring grid cells and place cells to a geometric reference frame.

In an attempt to quantify the border cells the Trondheim lab (Solstad et al., Boccara et al., 2010) created a ‘border score’. This was calculated by:

A border score was defined by comparing the mean firing distance (d_m) with the maximum coverage of any wall by a single field (c_m). For all experiments the coverage of a given wall of by a field was estimated as the fraction of pixels along the wall that was occupied by the field. c_m was defined as the maximum coverage of any single field over any of the four walls of the environment. The mean firing distance d_m was computed by averaging the distance to the nearest wall over all pixels in the map belonging to its fields, weighted by the firing rate. To achieve this, the firing rate was normalized by its sum over all pixels belonging to its field, resembling a probability distribution. Finally, d_m was normalized by half of the shortest side of the environment (i.e. the largest possible distance to its perimeter) so as to obtain a fraction between 0 and 1.

The border scores potentially ranged from -1 (cells with central firing fields) to +1 (cells that perfectly line up along an entire wall). Whilst the score takes some account of the thickness of the field it is more indicative of the length of the field along a wall. This measure fails (saturates) for thicker fielded border cells because there are too many high firing pixels located away from the nearest wall. To be classed as a border cell the cells had to achieve a border score of over 0.5 and be stable across trials.

2.3.2.1 Border cell response to environment manipulation

Solstad et al. (2008) thus far provides the only characterisation of border cell behaviour across environments. The following section will look at the border cell characteristics and responses to environmental manipulation and consider them in relation to the characteristics of BVC cells.

The authors report that in general border cell fields stretch parametrically with environment extension. They report 44 cells in this manipulation all of which had border scores of over 0.5. When a 1x1m box is extended in one axis to create a 1x2m box, the border cells with preference to the extended wall show that their fields extend with it. Solstad et al show overall that border cell boundary-tuning was maintained across rooms and differently shaped environments (square, 1x1m or 1.5x1.5m; circle, 1m or 1.5m diameter). Also in a simple cue card rotation experiment where the card was rotated 90° (in between 2 baseline trials with no rotation) they demonstrate that border cells rotated in concert with the co-recorded grid cells and HD cells.

Like with the subicular BVCs, activity seems to be determined by the walls of the environment rather than by other variables. To see if border cells were primarily tuned for periphery walls or for boundaries more generally, the border cells were recorded with inserted free-standing barriers (Figure 2.3.4). The cells were given 2 trials with an inserted barrier one oriented to the field and one in the orthogonal orientation. Of particular note, the border cells showed varying responses to the inserted barriers. Some showed clear doubling of fields similar to the subicular BVCs whereas some did not (Figure 2.3.4). Twelve of the 22 border cells recorded in this manipulation showed a preference for a single boundary. Typically these border cells showed clear field doubling for the appropriately oriented barrier (Figure 2.3.4 e.g. *top row left column*). Those responding to multiple walls had more diffuse fields, making the responses to the additional barriers unclear (Figure 2.3.4e.g. *bottom row right column*). For one cell the

height of the inserted barrier was reduced to 5cm (using a 5cm fence and 5cm table) making the barrier traversable. The cell's extra field persisted even though the rat could now explore and walk over it.

Solstad et al. (2008) also looked at border cell responses to wall removal (Figure 2.3.5). The authors note that in general, border fields could still be identified, and that the persistence of activity along the edges suggests that the border cells respond to a variety of boundaries. Certainly the border cells still show boundary signaling with wall removal however Figure 2.3.5 shows that the border cells typically remapped with wall preference shifting between the walled and un-walled environments. In contrast the subicular BVCs presented by Lever et al., (2009) showed stable fields with wall removal (Figure 2.3.2). The differences in responses between these 2 classes of boundary cells may give some clues to their functional differences.

2.3.2.2 Role for boundary-cells

Solstad et al. (2008) consider that because border cells are located throughout the MEC, the boundary information they provide should be available to MEC grid cells and to external target regions involved in path planning (Whitlock et al., 2008). The neural mechanisms for the representation of self-location in grid cells have yet to be ascertained. However, as discussed earlier in the introduction, general opinion is that the mechanisms likely involve interactions between self-motion cues and learned associations with the environment. Boundary-related cells could provide the geometric input to this system (Solstad et al. 2008; Moser and Moser, 2008; Hafting et al., 2005).

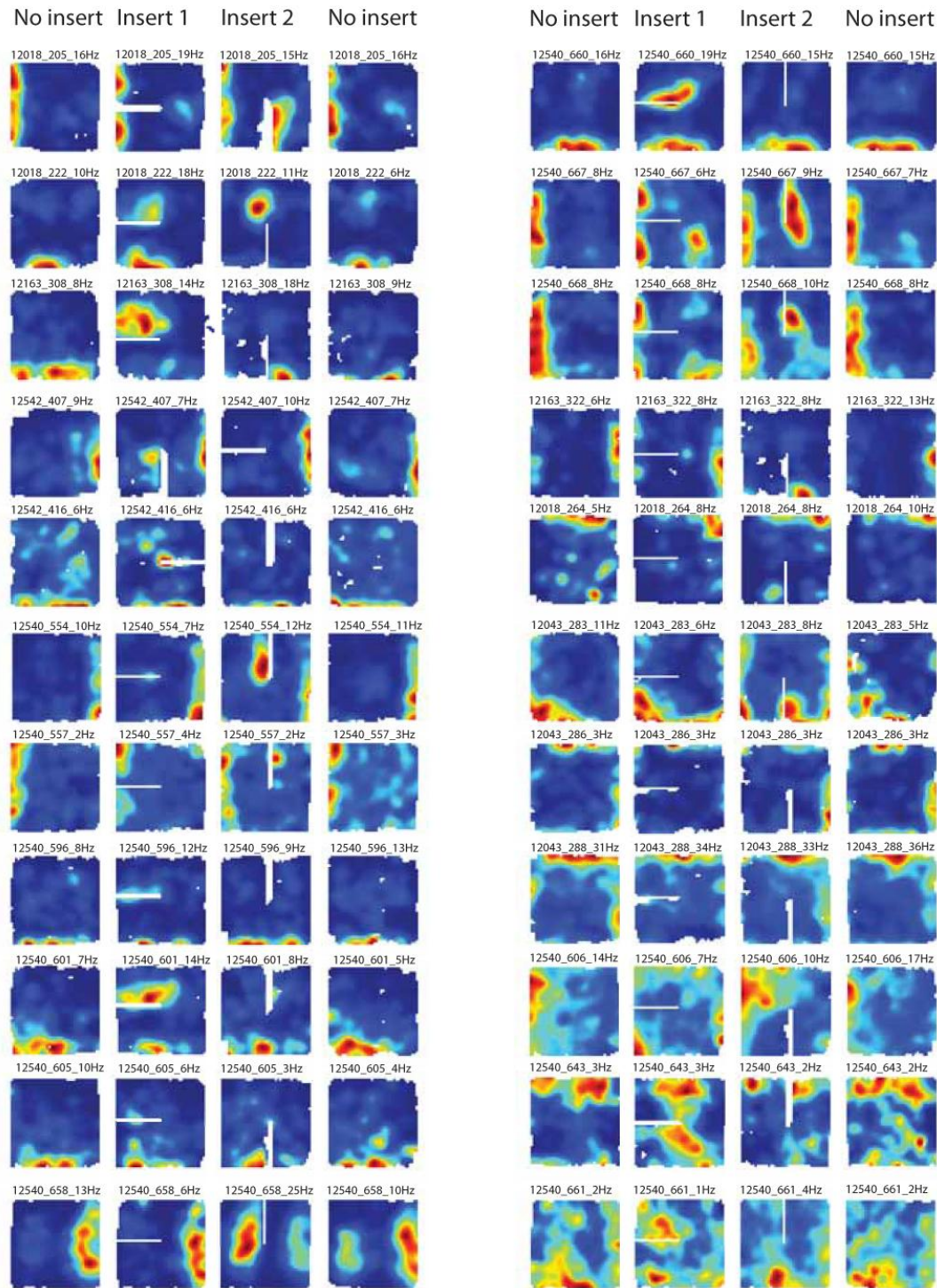


Figure 2.3.4: Border cells show a variety of responses to inserted barriers.

The figure presents the entire sample of border cells recorded by Solstad et al. (2008). Each row of the two columns is one cell. The barrier (shown as the white lines) was inserted horizontally in one trial and vertically in the other. The animal numbers (5 digits), cell numbers (3 digits) and peak rates are given above each trial. As with all the rate maps red indicates maximum firing and dark blue is zero firing. Pixels not sampled by firing are white. Border cells with fields along a single wall in the baseline trial, typically showed a field doubling for the appropriately orientated barrier. In cells with fields on multiple walls, additional fields were often unclear. Figure adapted from Solstad et al. (2008).

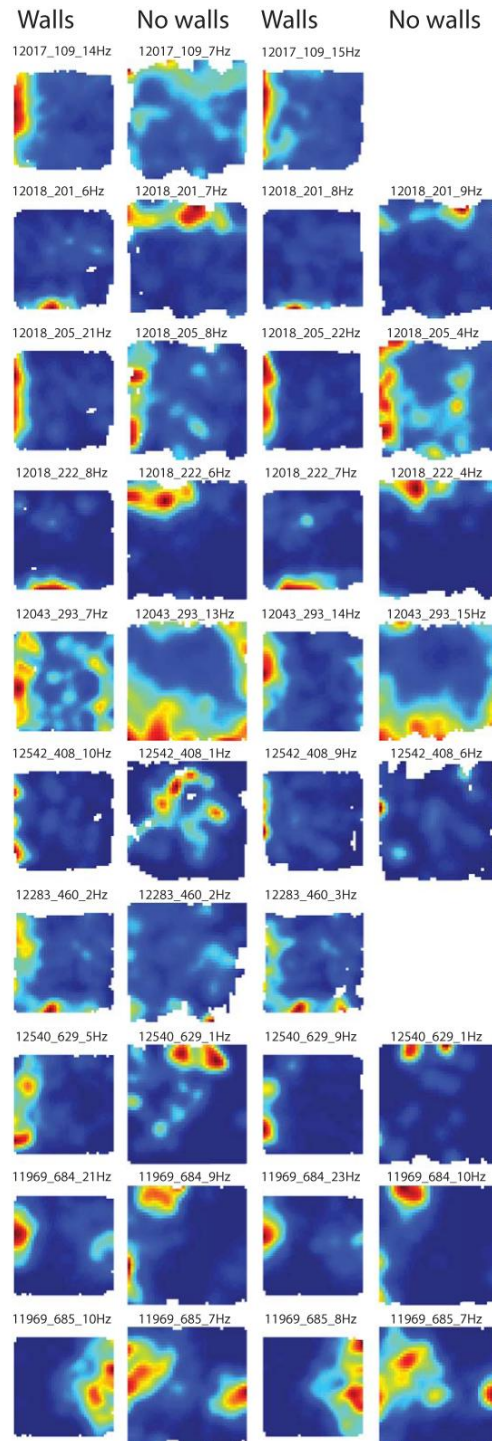


Figure 2.3.5. Border cells wall preference shifts between walled and un-walled environments.

Figure showing the entire sample of border cells recorded before and after removal of the walls. The animal numbers (5 digits), cell numbers (3 digits) and peak rates are given above each trial. As with all the rate maps red indicates maximum firing and dark blue is zero firing. Pixels not sampled by firing are white. Where there is a white gap (e.g. row 1 and row 7) this means that the cell was not recorded in that trial. Each row is a cell. The sequence of testing is from left to right. Border fields were often but not always maintained after removal of the external walls. Typically the border cells maintained boundary signalling, but the fields moved to a different environment edge. Adapted from Solstad et al., (2008).

2.4 Aims of the thesis

The present thesis aimed to extend the work of Lever et al., (2009) to further characterise the electrophysiological, neuroanatomical, temporal and spatial properties of subicular spatial cells. Originally the focus of this PhD was to extend upon Lever et al., (2009) by just recording subicular BVCs. However, whilst recording I made the remarkable discovery of co-localised grid cells. This thesis therefore provides the first ever account of these cells recorded from the subiculum.

The thesis has two main tasks:

- 1) To present the first ever characterisation and investigation of subicular grid cell properties and the influence of geometric manipulation upon grid cell firing.

and

- 2) To build upon the initial characterisation of BVCs by Lever et al., (2009), to investigate further what constitutes a boundary and what sensory inputs drive boundary- responsive cells.

Chapter 3 Methods

This chapter describes the methods used in the experiments for this thesis. It outlines the surgical procedures, the testing/ recording procedures, the specifics of the environmental manipulations and the analysis methods.

3.1 Ethics

All experiments and procedures were conducted in accordance with the Animals (Scientific Procedures) Act 1986. Experiments were performed under Dr Colin Lever's Home Office project licence (PPL 40/2935) and a personal licence held by Sarah Stewart (40/9456).

3.2 Subjects

All experiments used male lister-hooded rats (Charles River, Kent, UK), weighing between 300g and 420g at time of surgery. Subjects were maintained on a 12:12 hour light: dark cycle (lights off at 1300). Water was *ad libitum* and the subjects were food restricted to 85-90% of their free-feeding weight to encourage foraging during testing.

Subjects were given at least 7days habituation to the lab and at least one week of daily handling before surgery. Animals lived in their home cage groups until selected for surgery. Cage dimensions pre-surgery 50 x 32 x 18.5cm. Post-surgery the subjects were housed individually in cages 62 x 38 x 30 cm. Cage substrate was woodchip bedding and blue paper towelling for nesting. Food restriction (85-90% bodyweight) recommenced 1 week post-surgery.

3.3 Recording apparatus

3.3.1 Recording electrodes

Electrodes were constructed using HM-L-coated platinum iridium wire (90%/20%) (California Fine wire, Grover Beach, CA). The electrodes were configured into a tetrode formation, which is considered to improve the quality of the signal discrimination based on the spatial position of the neurons (Recce and O'Keefe, 1989; Harris et al., 2001). Tetrodes were all made from 25 μ m wire electrodes. They were made by measuring out a length of wire, and creating a loop (taping the ends together), which was then draped over a rod. The loop and the taped ends were then held together with a bent weighted needle, to create 2 loops and 4 pieces of wire. The wires were then twisted together using a magnetic spinner (20 times per cm of wire) and were cut to produce 4 spatially-proximal tips at one end and 4 loose ends which were stripped of insulation and were attached to the microdrive.

3.3.2 Microdrives

Four tetrodes were loaded into each moveable 16-channel microdrive. See Figure 3.3.1 for a diagram of a standard microdrive. Once the main body of the tetrodes were lowered into the cannula, each of the 4 loose ends of the tetrode were connected to (twisted around) one of the 16 channels (small metallic posts) present on the microdrive. These were then painted with silver conductive paint and then protected with nail varnish. Once loaded into the drive the electrodes were super-glued together (as far from the tips as possible to avoid getting super glue into the brain), to ensure a close configuration (<500 μ m).

Each rat was implanted with two drives; one per hemisphere. Once the electrodes had been lowered into the brain the 'feet' of the drive, were cemented to the screws attached to the skull. This aided the stability of the implants. In order to lower the tetrodes through the brain during screening and testing the cannula (containing the tetrodes) could be moved up or down by rotating the threaded post using the screw turner. One 360° anticlockwise turn would move the tetrodes bundle down by 200 μ m. To protect the cannula and tetrodes, a slightly longer sleeve was fitted over them. During surgery, this sleeve was pulled down and fixed to the skull with dental cement.

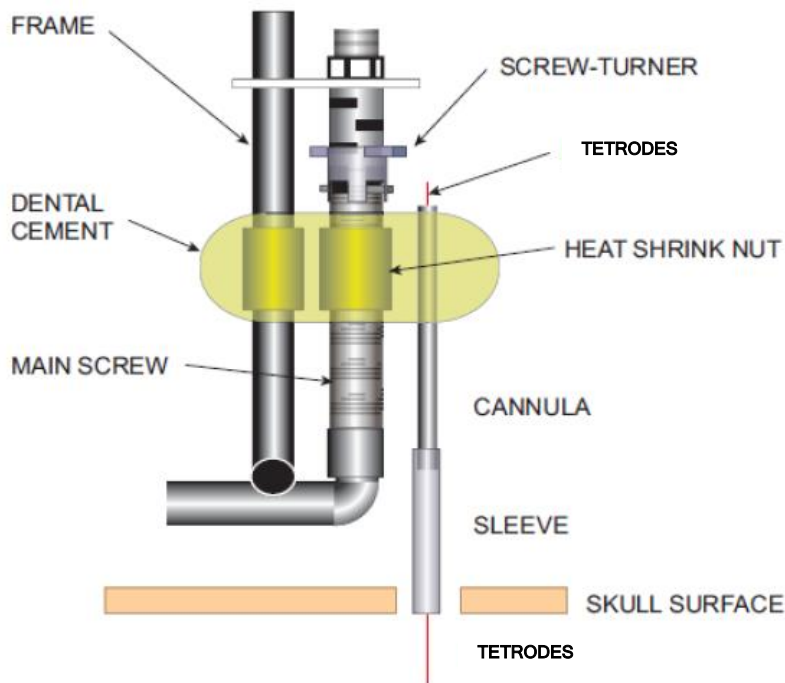


Figure 3.3.1: Illustration of a microdrive framework.

The microdrive was fixed to the skull using dental cement. Turning the screw-turner results in movement of the cannula containing the tetrodes. Adapted from a diagram by John Huxter.

3.4 Surgery

Under deep anaesthesia rats were chronically implanted with two 16-channel microdrives, with one in each hemisphere. General anaesthesia was induced by a combination of oxygen (flow rate: 3 l/min) and isoflurane (3% of the gas volume). Once the rat was anaesthetised, the surgery site was shaved and the rat was fitted into the stereotaxic frame. An analgesic [buprenorphine (Vetergesic; Reckitt Beckinsler, Hull, UK), 0.4ml-0.8ml, i.m.] and an antibiotic [enrofloxacin (Baytril; Bayer, Newbury, UK), 0.3ml, s.c.] were then administered. In order to assess the stability of the anaesthesia the isoflurane was reduced to 1-2% and the rats breathing was closely monitored. Before the incision was made the rat's eyes were covered with Vaseline to prevent them drying out, and the topical antiseptic Betadine (Seton Healthcare

LTD, Oldham, UK) was applied to the incision site. After wiping off the Betadine with 70% methanol, the skin was cut and the skull exposed to give a sufficient view of both the bregma and lamda brain plate joins. Between 7 and 9 screws (3-mm diameter, Precision Technology Supplies, East Grinstead, UK) were fitted into the skull, to assist the attachment of the microdrive and increase drive stability. Either one or 2 of the screws acted as the ground attachment using short pieces of pre-soldered wire. These were set deeper in the skull, and at the end of the surgery were soldered to the ground wire attached to the microdrive.

Following this, two holes (1.5-mm diameter) were drilled using a trephine drill bit, one over each hemisphere. The placement of these holes was determined by the tetrode co-ordinates (co-ordinates for each rat were given in Table 3.4.1). The microdrives were positioned and attached to the skull one at a time using dental cement. To protect the brain surface from both drying and dental cement the holes were plugged with a saline soaked sterile cotton bud. A loaded microdrive was stereotaxically positioned on the right hemisphere such that the tip of the tetrodes were at the target coordinates. After removing the cotton bud plug the tetrodes were slowly lowered into the brain (between 1.5-2.5mm deep depending upon the co-ordinates and brain location). The protective sleeve around the cannula was then lowered to rest upon the surface of the brain. The sleeve-brain junction was then covered in sterile Vaseline. To ensure a stable implant the microdrive was affixed to the skull using dental cement around the sleeve, drive feet, screws and skull. Once the dental cement dried, the same operation was carried out for the left hemisphere. Finally, each drive ground wire was carefully soldered to the ipsilateral ground screw and cemented to prevent the animal detaching the ground connections. A plastic screw was cemented to the front of the implant to protect the forward ground wires. Similarly a wing screw was also attached to the back of the implant by the same means, allowing connection to the headstage to the implant by a crocodile clip.

Table 3.4.1: Target implant co-ordinates for all rats

Co-ordinates for the implants were selected based upon those used previously by our lab, as well as new co-ordinates based on Paxinos and Watson, (2005). The table gives the rat number, hemisphere; LH left and RH right, the target area subiculum (sub), CA1, entorhinal cortex (EC). The co-ordinates are given in mm behind bregma, anterior-posterior (AP) along the midline and medial-lateral (ML) from the midline.

Rat no.	301		302		303		304		305		306	
Target Area	LH sub	RH sub	LH CA1	RH sub	LH sub	RH sub	LH sub	RH sub	LH sub	RH EC	LH sub	RH EC
AP	6.2	5.4	3.2	5.8	6.2	5.4	6.2	5.4	5.4	8.2	5.4	8.2
ML	3.2	2.0	2.1	2.9	3.2	1.8	3.2	1.8	1.8	3.2	1.8	3.2

3.5 Data recording

3.5.1 Head position and orientation, and running speed

The rats were attached to the recording system via the headstage. In order to track the subjects head position, orientation and running speed the rat was tracked using two groups of small, infrared light-emitting diodes (LEDs), one brighter and more widely projecting than the other attached to the rat's head (via the headstage). These LEDs were tracked using a video camera and position-detection hardware/software (DACQUSB, Axona, St Albans, UK). The two LED arrays were separated by ~10 cm, and were centred above the rat's skull. Offline analysis defined the point equidistant to the two LEDs groups as the position of the rats head (TINT, Axona, St Albans, UK). The tracking of these two arrays was based on their differential brightness and size. Position was sampled at a 50 Hz rate. Running speed was calculated from this 50-Hz position tracking data, with 400 μ s boxcar smoothing. Speeds above 2 m/s were discarded as being impossibly high and likely due to reflections of the LEDs or head shake. These values were replaced by interpolated values using adjacent points.

3.5.2 EEG and single-unit

During recording, each subject was connected to the recording system (Axona, St Albans, UK) by a headstage amplifier which could be plugged into the microdrive. The headstage cables were light and very flexible, thereby enabling the animal to move around freely. The headstage amplifiers were unity-gain buffers, which isolated the electrodes from the wires transmitting their signals to the recording system. The implanted electrodes were AC-coupled to these amplifiers. Lightweight wires 2-3metres long connected the headstage to a preamplifier. EEG signals were amplified 8-20k , and were filtered using a band pass filter which passed frequencies between 0.34-125Hz and rejected frequencies outside 0.34-125Hz . Positions were sampled at 50Hz. Cluster cutting to isolate single units was performed manually using custom made software (TINT, Axona, UK).

3.6 Materials

3.6.1 Laboratory layout

During screening and testing the room was lit with a lamp to the west of the environment and small wall lights on the cue cards (see Figure 3.6.1). The experiment used a number of environments, with the trials and order of trials being dependent upon the cells being recorded (outlined below).

For all trials bar one in the 'context change manipulation' the cue cards remained the same. These were 2 large card board sheets (75cm x 125cm) with distinguishable patterns. The cue cards are located on the north and south walls of the testing room (see Figure 3.6.1). Details of the cue card swap for the 'context change manipulation' can be seen below.

During screening and between trials the rats rested upon the holding platform located to the west of the testing environments. This was a shallow wooden platform (35cm x 35cm) containing woodchip bedding. The platform had ridged edges (5cm high 5cm thick) elevated 70cm from the floor. Rats were always passively transported by the experimenter into the test environment from west to east demonstrated by the pink arrow in Figure 3.6.1.

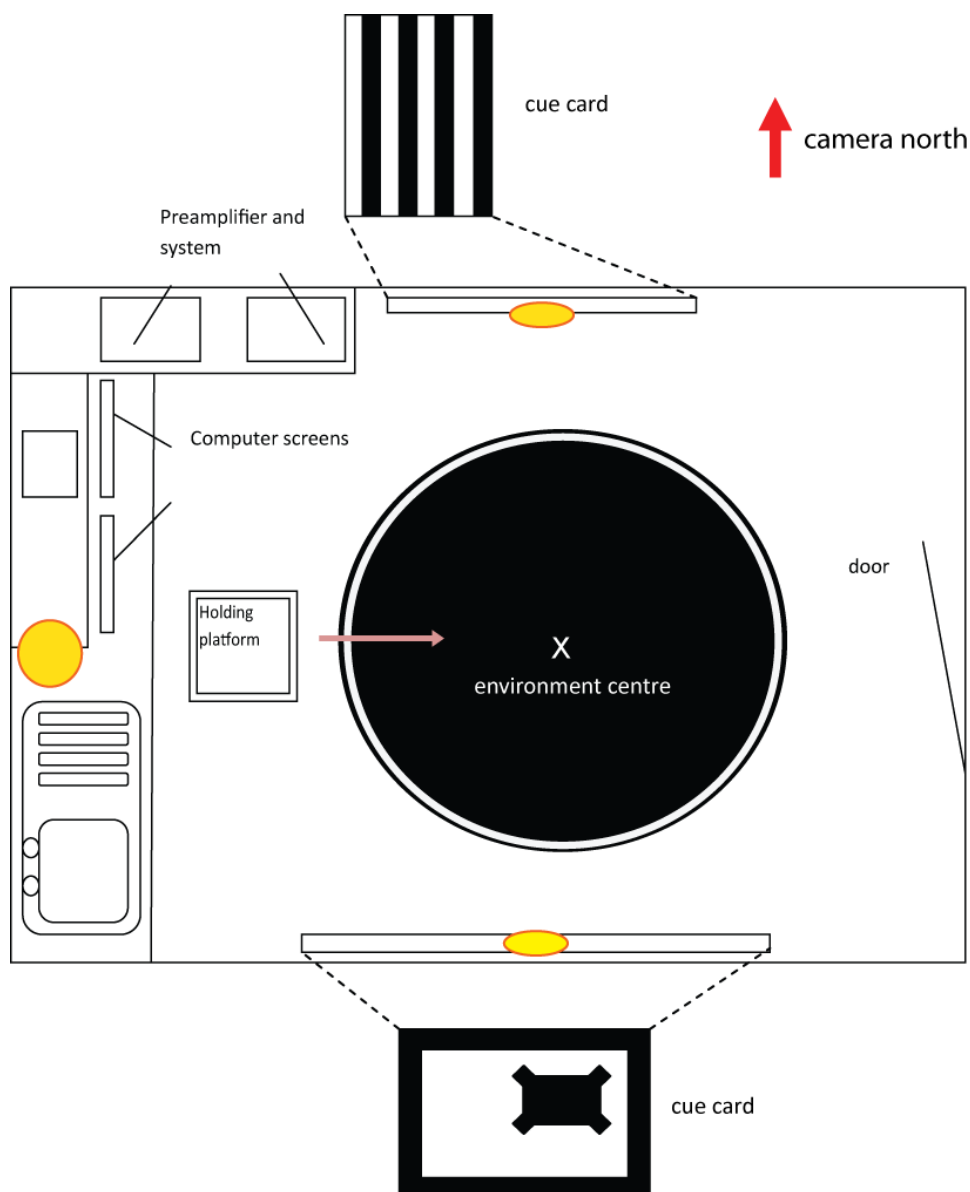


Figure 3.6.1. Bird's eye view of testing room

The diagram shows the large walled circle (white 50cm walls, 150cm diameter) sitting upon the circular open platform (black, 155cm diameter, elevated 30cm off the floor). Rats experienced all experimental trials in this room and were placed on the wooden holding platform during Inter-trial intervals and screening. Rats were always passively transported into the testing environments from west to east as indicated by the pink arrow. All environments were centred upon the 'X' marking the environment centre except the together apart trials (details below). Light sources are indicated as yellow ovals.

3.6.2 Test environments and materials

In order to identify and assess spatial cells of interest, a variety of environments were used. These were made especially for the experiment. Figure 3.6.2 shows the 5 key environments which were utilised in different combinations to create the manipulations.

For some of the manipulations objects were inserted into the environments. These include a free standing barrier, wine bottles as landmarks, and traversable ridges (Figure 3.6.3).

Key testing environments

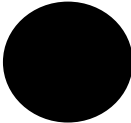
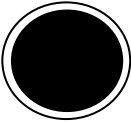
Illustration	Description
	The circular open platform (COP; 155cm diameter; elevated 30cm from the floor) this black and forms the base for most of the environments.
	The large walled circle (LWC; 150cm diameter, 50cm high walls), which has white walls, sits directly onto the base described above.
	The large walled square (LWS; 100cm x 100cm, with 50cm high walls), which has black walls, sits directly onto the base described above.
	The small walled circle (77cm diameter, 50cm high walls), which has white walls, sits directly onto the base described above.
	The small walled square (50cm x 50cm, 50cm high walls), which has black walls. This either sits on a white insert onto the base described above as a walled environment, or is placed on its side to make a 50cm x 50cm, open platform, elevated 50cm above the ground.
	

Figure 3.6.2. Key testing environments

Inserted objects and barriers

illustration	Description
 	<p>Barrier</p> <p>Black barrier (50cm long, 3cm wide and 50cm high) was typically inserted in an orientation parallel to the long axis of the BVC field. This was typically inserted into either the large walled circle or the large walled square environment.</p>
	<p>objects</p> <p>These were an array of 5 patterned bottles (8cm diameter and 30cm high) these were weighted with sand. These were ran as a linear array of 2 or more or singularly. There was also a 'Small object' this was a canonical measuring tube which was 2.5cm diameter and 15cm tall. Typically these were inserted into the large walled square environment.</p>
 	<p>Ridges</p> <p>Two ridges were used they were inserted into the large walled square.</p> <ol style="list-style-type: none"> 1. 4.5cm high black ridge (3 blocks together 20cm long and 10cm wide) 2. 5cm high unstained wooden ridge (2.5cm wide, 50cm long)

Figure 3.6.3. Inserted objects and barriers

3.7 Experimental procedure

3.7.1 Screening and training before formal testing

Rats were allowed one week of post-surgery recovery before screening. During screening the rat was placed on the holding platform and linked to the recording system by means of a light and very flexible cable attached to the headstage. This enabled the rat to move around freely. Over days/weeks the electrodes were vertically lowered towards the selected brain region. This was usually done in steps of between 100 and 25 μ m. In general larger steps were used until the electrodes were in the target region, and were then reduced to 25 μ m for the rest of the screening period and during testing. This slow, progressive lowering ensured better stability of the tetrodes within the surrounding tissue, allowing for the recording of the same cells across both multiple trials and multiple days.

Later in the screening phase the subject became accustomed to rice-foraging whist attached to the headstage. Each subject were tested in a minimum of 10 trials in the small circle (77cm diameter; walls 50cm) before the beginning of formal testing.

3.8 General procedure

The rat was brought into the laboratory and placed upon the holding platform, located to the west of the recording environments (Figure 3.6.1). The rat was then attached to the headstage for screening. For all testing trials regardless of environment the rat was placed (from laboratory west to east) into the centre of the environment facing laboratory east. For trials where the centre of the environment was unavailable, due to the presence of either a barrier, object or drop the rat was place as close as possible to the centre but still facing east. Generally, recording began within 0-15 seconds of placing the rat in the environment, and ended about 5-20 seconds before the rat was taken out of the environment.

3.8.1 Task

For all testing I used a standard foraging task (similar to the pellet-chasing paradigm developed by Muller and Kubie 1987). During all trials the rats were to forage for sweetened cooked rice. The experimenter walked around the environment during the trials, throwing rice in. The experimenter threw in

approximately $\frac{1}{2}$ a grain per minute. Whilst the majority of rice throwing was pseudo-randomly, if a portion of the environment appeared under sampled (especially near the end of a trial) the rat was encouraged to visit these portions by tactical rice throwing. The experimenter was able to monitor the path taken by the rat during the trial, through the LED tracking as captured by the recording software (DACQ USB, Axona, St Albans, UK).

3.8.2 Trial length

Trial length was determined by the environment size in order to maximise sampling. See Table 3.8.1 for all trial lengths. Trial length was proportional to the environment surface areas, Typically ~ 7 seconds was allowed per cm^2 , with the minimum trial length being 10 minutes. These trial lengths were generous and were longer than have previously been used (Lever et al., 2002a, Wills et al., 2005; Jeewajee et al., 2008 Solstad et al., 2008). The maximum trial length was 48 minutes which only applied to the darkness trial in the large square environment (procedure detailed below).

The typical trial length for a barrier insertion was 24 minutes in the large walled square and 42 minutes in the large walled circle (Table 3.8.1). However, for the manipulations in the large walled square environment with the insertion of objects and ridges and for the together-apart variation trials, trial length was reduced from 24 minutes to 15 minutes. This allowed 4.4 seconds per cm^2 . This reduction was due to the volume of trials required to complete these trial sequences. The reduction in trial length was not at the expense of adequate sampling. Previous studies which tested the influence of barrier insertion on spatial cell firing used similar environment sizes and trial lengths to those used here. In 2009 Lever et al., used a 94 x 94cm square environment with a trial length of 16minutes, and Solstad et al., (2008) used a 100cm x 100cm square environment with a 10 minute trial.

3.8.3 Inter trial interval (ITIs)

ITI's were between 10 -30 minutes. The standard ITI was 20minutes but for some trials where the trial length was shortened, the ITI was also reduced to 15minutes (this was based on ITI's used in previous studies, Lever et al, 2009; Solstad et al., 2008). Testing days could often be very long, and so if the subject was tiring (lying down/sleeping until prompted during trials) during the trials the ITI was extended to allow for extra rest.

Table 3.8.1. Trial lengths for trials in each environment.

The trial lengths were standardised for each environment. In cases where barriers were inserted the trial lengths remained the same for the large walled circle and large walled square.

Environment	Trial length
Large walled circle (+ barrier)	42 minutes
Circular open platform	42 minutes
Large walled square (+ barrier)	24 minutes
Small walled square	10 minutes
Small walled circle	10 minutes
Together-apart environments	Together trial: 24 minutes Apart trial: 27minutes
Large walled square variations:	
Darkness	48 minutes (24 minutes in the light and 24 minutes in the dark)
Inserted objects	15 minutes

3.9 Manipulations

Testing consisted of a variety of 9 environmental manipulations. The sequence the manipulations were selected was determined by the type of cell being recorded. Desirable cells would be identified during screening in the first trials of the day; typically in the small circle (77cm diameter white walls, black floor). Once identified, different manipulations were run depending upon the cell type, until the cell had been tested on all the relevant manipulations or the cell moved away from the recording electrode. Optimally manipulations were run on as few days as possible. Unless stated the trials were always run in the order presented in the tables.

3.9.1 Boundary insertion

If potential BVCs were identified online (whilst the rat was linked to the recording system) during screening then the first manipulation to be run was the 'Barrier insertion'; see Figure 3.9.1 . This manipulation was used online (and offline) to identify putative BVCs. As shown by Lever et al (2009) when BVCs were presented with a second boundary (in their preferred orientation) their firing fields doubled (data from 3 BVCs). This manipulation typically consisted of 3 large walled circle trials. The first and third trials acted as baseline trials. The second trial had a high barrier inserted so that its length intersected the BVCs preferred allocentric direction, therefore creating a second boundary. For some BVCs the large walled circle was unavailable and therefore the same was done using the large walled square. Further for some of the cells (particularly from early rats) didn't have the back to baseline trial.

Barrier insertion manipulation



Large walled circle with white walls and Black floor (50cm diameter 50cm high walls). Trial length: 42 minutes.



Large walled circle with with black Barrier (50cm long, 3cm wide and 50cm high) inserted in the correct orientation to the BVC barrier. Trial length: 42 minutes.



Back to baseline with the Large walled circle; white walls and Black floor (50cm diameter 50cm high walls). Trial length: 42 minutes.

Figure 3.9.1. Barrier insertion manipulation trial series.

3.9.2 Wall no-wall manipulation

Similar to BVC identification grid cells were detected during the first screening trial of the day. As a rule BVCs took priority, therefore BVC-specific manipulations were often run before the grid cell manipulations. The key manipulation for grid cells was the 'wall-no wall' manipulation; see Figure 3.9.2. Two large walled square trials were used as baseline trials. These were run either side of the circular open platform trial. Some cells were tested in the wall no-wall manipulation using the large walled circle instead of the square. For some cells there was also sometimes no return to baseline trial.

Wall vs. no-wall manipulation



Large walled square with black walls and floor (100cm x100cm with 50cm high walls).
Trial length: 24 minutes.

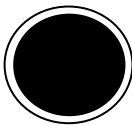


Circular open platform; this is black and is elevated 30cm from the ground (150cm diameter). Trial length: 42 minutes.



Large walled square with black walls and floor (100cm x100cm with 50cm high walls).
Trial length: 24 minutes.

Or



Large walled circle with white walls and black floor (150cm diameter with 50cm high walls). Trial length: 48 minutes.



Circular open platform; this is black and is elevated 30cm from the ground (150cm diameter). Trial length: 42 minutes.



Large walled circle with white walls and black floor (150cm diameter with 50cm high walls). Trial length: 48 minutes.

Figure 3.9.2. Wall no-wall manipulation trial series.

This manipulation was run with either or both the large walled circle and large walled square environments as baseline trials.

3.9.3 Barrier insertion within the wall removal manipulation

The influence of barrier insertion upon grid cell firing was also of interest; see Figure 3.9.3. Unless the grid cell was being recorded simultaneous with a putative BVC the barrier was either oriented north-south or east-west in the environment. 24/55 of grid cells were exposed to the ‘barrier insertion manipulation’ above (Figure 3.9.1) when recorded simultaneously with putative BVCs. For those grid cells which were recorded without BVCs then a large square trial with barrier inserted trial was added to the wall no wall manipulation detailed below.

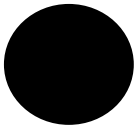
Barrier insertion within the wall removal manipulation



Large square with black walls and floor (100cm x100cm with 50cm high walls). Trial length: 24 minutes.



Large square with black walls and floor (100cm x100cm with 50cm high walls) with black barrier (50cm long, 3cm wide and 50cm high) inserted in the correct orientation of the BVC field. Trial length: 24 minutes. This trial is typically inserted into the ‘wall-no wall’ manipulation above or is run after a large square trial on a different day.



Circular open platform; this is black and is elevated 30cm from the ground (150cm diameter). Trial length: 42 minutes



Large square with black walls and floor (100cm x100cm with 50cm high walls). Trial length:24 minutes.

Figure 3.9.3. Barrier insertion within the wall no-wall manipulation

3.9.4 Together-apart

In order to investigate cell firing response to wall-less boundaries/ traversable boundaries the ‘together-apart’ manipulation was run; see Figure 3.9.4. This was a 2 trial manipulation. The first trial is 3 black boxes on their sides sat tight together to create a rectangular open platform. For boundary-related cells the long axis of the three boxes was typically oriented perpendicular to the preferred-direction component of the boundary vector. For the second trial the 3 boxes were moved 10cm away from each other creating two 10cm gaps; providing 3 ‘drops in the BVCs preferred orientation. The 10cm gaps were traversable and therefore provide a different quality of ‘drop’. For 2 cells a tripling of firing field was used to identify cells as BVCs.

Together-Apart manipulation



3 black boxes (50cmx50cmx50cm) were placed on their sides with no gaps between them to create a rectangular open platform (150cmx50cm). This is placed so that one of the 50cm edges is oriented for the BVC field. Trial length: 24minutes.



After the ITI the 3 black boxes (50cmx50cmx50cm) were pulled apart so that there is a 10cm gap between them. This then creates 3 50cm edges oriented to the BVC field. Trial length: 27 minutes.

Figure 3.9.4. Together-Apart manipulation trial series

3.9.5 Context change

In order to look at the effect of novelty upon BVC firing the ‘context change manipulation’ was run; see Figure 3.9.5. This involved running 2 trials of the ‘familiar’ small walled circle (white walls, black floor) environment, then changing the environment to a ‘novel’ environment (small square (black walls, white floor) with different external cue cards, then back to the ‘familiar’ small walled circle.

Context change manipulation

- 
 Small walled circle (white walled; 77cm diameter) as used in baseline trials. Trial length: 10 minutes.
 - 
 Repeat of small walled circle (white walled; 77cm diameter) as used in baseline trials. Trial length: 10 minutes.
 - 
 Change of environment to small black walled white floored square (50cmx50cm with 50cm walls). Trial length: 10minutes. Change of cue cards:
 - 


 The north wall stripy cue card is changed to the south walled ‘off square’ cue card
 - 


 The south wall ‘off square’ cue card is changed to a new ‘shiny triangle’ cue card
 - 
 Return to small walled circle (white walled; 77cm diameter) as used in baseline trials. Trial length: 10 minutes.
-

Figure 3.9.5. Context change manipulation

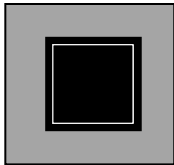
3.9.6 Darkness

To look at whether boundary-related cells and grid cells require ocular input the darkness manipulation was run; see Figure 3.9.6. This consisted of 2 trials. The first trial ran as a double length large walled square trial. Halfway through the trial all light was extinguished for the remainder of the trial. the two halves of the trial (light-dark) were analysed separately. Followed by another large walled square trial to return to baseline. Noise from the oscilloscope was not extinguished during this trial as the aim was not to disrupt the Head-direction system but to purely investigate the role of visual input.

Darkness manipulation



Large square with black walls floor (100cm x 100cm with 50cm high walls). Trial length: 24 minutes.



The trial is extended to 48minutes with all of the lights etc extinguished at 24minutes. Data is analysed as 2 separate trials. After the double trial the rat is removed from the environment for the ITI.



Return to a standard trial in the large square to go back to baseline. Trial length: 24 minutes.

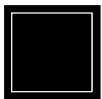
Figure 3.9.6. Darkness manipulation trial series

3.9.7 Object insertion

A number of BVC cells were run with extra manipulations to investigate correlates of BVC firing. The 'landmark vs. Barrier' (Figure 3.9.7), 'ridges' (Figure 3.9.8) and 'together-apart variation' (Figure 3.9.9) manipulations were run to investigate the difference in BVC response to different sizes/qualities of barriers. Within this manipulation the type of barrier/ barrier qualities were altered.

For the 'objects vs. Barrier' manipulation (below; Figure 3.9.7) 5 bottles were placed together in a line, oriented for the BVC field to create a continuous barrier. Subsequent trials had 1 to 4 bottles in the array. If a doubling of the firing field was absent for 1 bottle then the next trial had 2 bottles (together to lengthen the boundary), and so on until firing was restored.

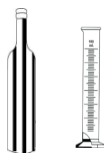
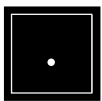
Objects vs. Barrier manipulation



Start with a large square, with black walls and floor (100cm x 100cm with 50cm high walls). This can be used from the last trial of a different manipulation therefore it can be 24 minutes long. If the ridges manipulation is started independently then the trial is shortened to 15minutes. ITI is also shortened to 15minutes.



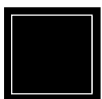
Insert the 5 wine bottles into the environment in a linear array (randomised order). Trial length: 15minutes.



Remove all the wine bottles bar the middle one. If the cell shows firing for the singular bottle, another trial with a thin measuring tube was ran. Trial length: 15minutes.



If the cell doesn't show double firing then add wine bottles back into the array one trial at a time until double firing is restored. Trial length: 15minutes.



Back to the baseline with an empty large square with black walls and floor (100cm x 100cm with 50cm high walls). Trial length: 15minutes.

Figure 3.9.7. Objects vs. barrier manipulations trial series

3.9.8 Ridge insertion

The 'ridge manipulation' involves inserting a traversable 'barrier'; see Figure 3.9.8. Two heights of ridge (4.5cm and 2.5cm) were used. If the cell shows a doubling of firing field with the 4.5cm ridge then a trial was run with the smaller 2.5cm ridge. For some trials both ridges were inserted into the large square during the same trial.

Ridges manipulation



Start with a large square, with black walls and floor (100cm x 100cm with 50cm high walls). This can be used from the last trial of a different paradigm therefore it can be 1440s long. If the ridges manipulation is started independently then the trial is shortened to 900s. ITI is also shortened to 900s.



A 4.5cm high ridge (3 blocks together 20cm long and 10cm wide) is inserted into Large square with black walls and floor (100cm x 100cm with 50cm high walls). The ridge is oriented for the BVC field. Trial length 900s.



If run in a sequence then a large square baseline trial is then run



A 2.5cm high (2.5cm wide, 50cm long) wooden ridge was inserted into the large walled square. The ridge is oriented for the BVC field. Trial length 900s.



Return to baseline with large square, with black walls and floor (100cm x 100cm with 50cm high walls).

Figure 3.9.8. Ridges manipulation trial series

3.9.9 Together-apart variation

The last extra manipulation is the together-apart variation; see Figure 3.9.9. This involved using 2 black boxes on their sides to form 2 x 50cm x 50cm square open platforms. For the baseline trials these were pushed together to form a rectangular open platform. One of the short edges was oriented for the BVC being record. Similar to the together-apart manipulation detailed above, the platforms were separated to produce a traversable gap oriented to the BVCs field. Throughout the manipulation the gap was varied. Typically this meant running trials with gaps from 1cm up to 10cm depending upon the cells response to the gap sizes.

3.9.9.1 Summary

The above section gives the list of manipulations used to test recorded cells. BVCs were tested using all the manipulations above with a focus on barrier insertion, context change and the together apart manipulations. Grids cells on the other hand were tested primarily in the barrier insertion, wall no-wall and darkness manipulations.

Together-apart variation manipulation



2 black boxes (50cm x 50cm x50 cm) were placed on their sides with no gap between them to create a rectangular open platform (100cm x 50xm) This is place so that one of the short edges is oriented for the BVC field. Trial length 900seconds.



After the ITI of 900seconds the 2 black boxes were separated so that there was a gap between them. This created two 50cm edges oriented to the BVC field. Trial length 900seconds.



In this manipulation the gaps were varied. Typically the manipulation ran: baseline-no gap, 1cm gap, 3cm gap, 10cm gap, and then back to baseline with no gap.



Return to baseline with 2 black boxes together creating a rectangular open platform (100cm x 50xm). Trial length 900seconds.

Figure 3.9.9. Together-apart variation manipulation trial series

3.10 Histology

After completion of the experiment, each rat was killed with an overdose of sodium pentobarbital [(Euthalal), Merial, Harlow, UK; 1ml i.p.] and perfused transcardially with saline solution, followed by 4% paraformaldehyde. Brains were extracted and sliced coronally into 40- μ m-thick sections, which were mounted and stained using cresyl violet solution to aid visualization of the tetrode tracks and tips. The target implant co-ordinates are given in Table 3.4.1.

To determine tetrode location I used cresyl violet staining. This highlights histological landmarks to help identify recording sites. In the anterior rat brain the dorsal commissure connects the hemispheres and is a clear cytoarchitectonic landmark. The posterior end of the dorsal commissure was used as a reference point. The breaking of the dorsal commissure between hemispheres corresponds to the Paxinos and Watson coordinate 5.28mm behind bregma (Paxinos and Watson, 2007). The brain was cut into 40 micron slices using the cryostat. This allowed us to count how many slices and estimate the microns behind the cessation of the posterior dorsal commissure (bPC) the tetrodes were located. Using the Paxinos and Watson rat brain atlas as a guide I estimated a 10% shrinkage of the brain post-perfusion.

3.11 Data processing

3.11.1 Cluster-cutting and general cell identification

Cluster-cutting involves isolating action potentials (spikes) with similar features from all action potentials recorded on a tetrode during a trial. The resulting isolated clusters with similar features were assumed to represent single cells. This analysis was performed manually using the custom-made software TINT (Axona, St Albans, UK). The software allowed for a separation of clusters by drawing around their edges directly on cluster plots. No automatic cluster cutting algorithms were used.

A tetrode records 4 simultaneous action potentials from each cell (one on each electrode channel), which create cluster plots in TINT. These cluster plots were two-dimensional scatter plots where each spike is represented as a dot whose abscissa and ordinate were each the value of a spike feature on one of the tetrode channels. The plot axis represents the amplitude of 2 electrode channels, allowing each spike to be represented across 6 cluster plots comparing each of the 4 electrode channels (see Figure 3.11.1.). The

differing peak-to-trough amplitudes (the difference between the maximum and minimum voltages of the action potential) of individual cells leads to each cell's cluster to having a different profile across the plots, lending to discrimination between cells. This is due to the tetrode design. Even if two neurons are spatially very close, their position relative to the tips of the tetrode will differ, entailing slight differences in the recorded action potentials from each cell. The spikes from these cells will therefore occupy a different position on at least one of the cluster plots.

3.11.1.1 Cluster cutting using peak-to-trough amplitude

The basic method behind cluster-cutting requires the experimenter to draw a polygon around a cluster to define the cell. The main parameter for cluster cutting is the peak-to-trough amplitude using the amplitude plots mentioned above. The cluster shape for pyramidal cells is generally ovoid because these neurons tend to fire in bursts, with the spike amplitude decreasing with each subsequent action potential of the spike train (Ranck, 1973). However clusters for other cellular forms may not be so clearly elliptical. The benefit of having 6 plots comparing the 4 channels means that if a cell isn't well isolated on one scatter plot it may be more isolated on another.

3.11.1.2 Cluster cutting using peak-to-trough time interval

Not all cells were well isolated and easy to 'cut' on the basis of amplitude (A). In these cases cells can be identified and separated on the basis of a second parameter; waveform shape. This is the time interval (and slope) between the peak and trough of the waveform. In order to do this TINT can generate a graph plotting the voltage of spikes at a particular time point (V_t) or a combination of both V_t and A. To reduce error, clusters that do not appear to be well-isolated were ignored. Once all the desired spikes had been selected, noise and erroneous spikes which do not belong to the cell could be removed using the same methods.

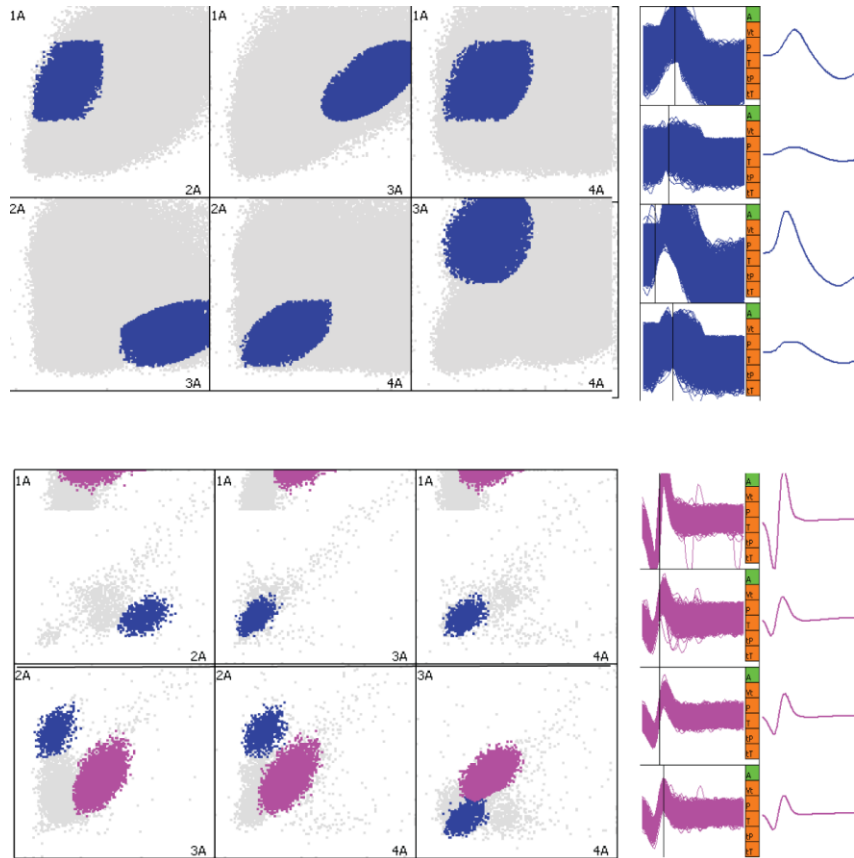


Figure 3.11.1. Examples of cluster-cutting.

Examples of cluster-cutting from rat 301 top (BVC; 301_170810_t4c1) and 304 bottom (Grid cell; 304_310311_t3c4). Each cluster (colour) is assumed to represent a different neuron (left). Each cluster plot illustrates the amplitude (A) of the spikes on two channels simultaneously; six plots are necessary to represent all the pairs of channels. The right windows displays for one cluster, the waveforms of all their spikes (and their average next to them). The tetraode shown for rat 301 top is tetraode 4 (day 170810, trial b in the large walled circle). The tetraode shown for rat 304 bottom is tetraode 4 (day 310311, trial b in the large walled circle).

3.11.1.3 Recording stability

A good stability of signal was often observed across trials/ days, manifested by the clusters occupying a similar position on the respective cluster plots. If too much change in the global pattern of activity (i.e., most clusters occupied a noticeably different position in the cluster plots) was noticed between trials the cell was considered to have moved away from the tetrode.

Clusters were cut based on a reference trial. This was typically a large walled circle trial, however if no large walled circle was run, then a trial testing the large square was used. The clusters were isolated (cut) using this trial, and this cut was then used as a template to cut the other recording trials. This was primarily a template of action for the experimenter to refer to. Often the cells were well isolated and so this was easily achieved by eye, but in cases where the cluster edges were less obvious, the scatter plot of the template trial could be super imposed over the top, to enable the experimenter to trace the cluster shapes.

Superimposition of the current trial on top of the reference trial was done using the transparency-enabling software glass 2k. Any cutting on the Vt plots was mimicked across trials accordingly. It was not permitted to fine-tune a trial's template generated cluster cut, by cutting individual spikes, noise etc. If the cut seemed obviously misleading, it was only permitted to change the general template, and start again.

3.12 Data analysis

3.12.1.1 Waveform analysis

Waveforms were calculated for each cell. These are presented in the basic properties figures in the results section. Generally they waveforms were calculated using the first large walled circle or square of the day trials. This was the case for the BVCS, HD cells and the Boundary-off cells. For the grid cells the waveforms were calculated using the large walled circle or square trial with the largest gridness score. To investigate differences in waveform amplitude and interval; the peak-to-trough measurements were looked at (Figure 3.12.1A). These were taken from the negative peak to the positive peak (Figure 3.12.1B). In the basic properties figures in the results section the peak amplitude are given the highest positive-to-negative or negative-to-positive amplitude (μV). And the waveform interval was given as the negative peak-to-trough interval (μs). Some cells presented inverted waveforms e.g. Figure 3.12.1C. These were judged as such if the positive peak was greater than the negative peak. For these cells the positive-to-negative peaks were used to calculate waveform amplitude and duration. This happened for a total of 8 cells (4 subicular grid cells; 1 non subicular grid cell; 2 BVCs and 1 HD).

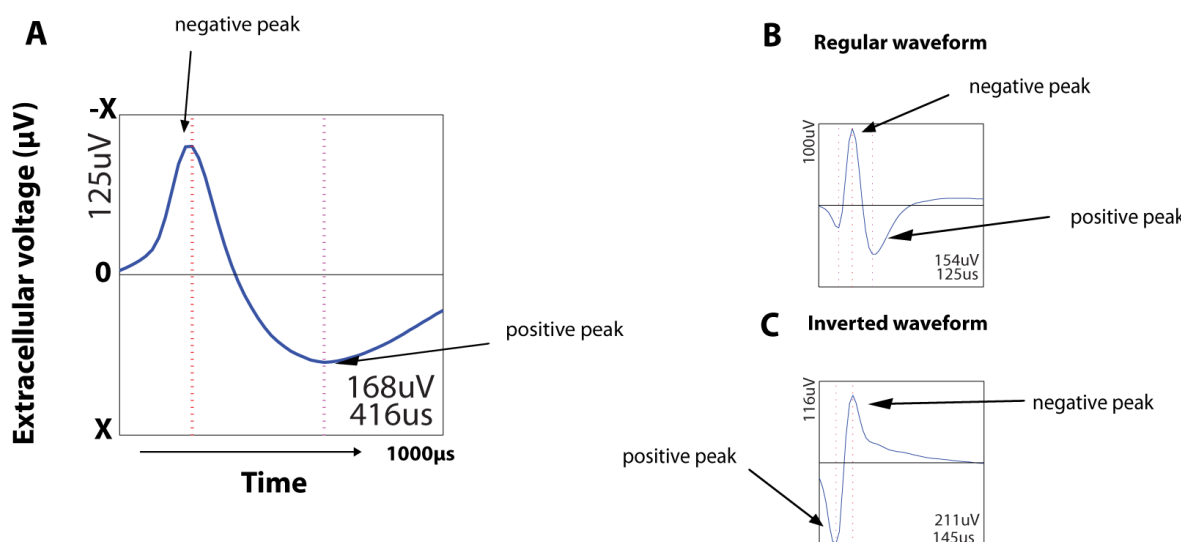


Figure 3.12.1. Waveform illustration

A) Gives an illustration of the waveform graph. The X axis shows the voltage, the Y axis shows time. The waveform amplitude and interval statistics are given in the bottom right. Generally the waveform amplitude and interval are taken from the negative peak to the positive peak as shown in B. However, some cells ($n=8$) demonstrated inverted waveforms where the positive was higher in amplitude than the negative peak. In these cases the positive peak to negative peak was used to characterise the cells waveform characteristics.

3.12.2 Figures showing spatial firing

This thesis shows locational firing rate maps and directional polar plots for all the cells of the following categories: grid cells, boundary vector cells, boundary off cells, and head direction cells. It also shows locational firing rate maps for non-grid periodic cells.

All locational firing rate maps shown in the Figures of the present thesis were constructed from 3 x 3 cm binned data, smoothed using a 5x5 bin square around each bin (boxcar filter). For a given cell, firing rates in each bin were calculated by dividing the total number of spikes during occupancy of the bin by the total duration of occupancy (dwell time). Example rate maps for a BVC and grid cell are given in Figure 3.12.2 (A and B). The spike count was divided by dwell time to give the firing rate per bin. These rate maps were auto-scaled false colour maps; each colour representing a 20%-band of peak firing rate, from dark blue (0-20%) to red (80-100%). Unvisited bins are shown in white. For all rate maps the peak rate (after smoothing) is shown top left of the map (see Figure 3.12.2A and B).

Polar plots were also created in order to show each cell's directional activity. Firing rate is shown for each directional bin of 5.6°, each bin was smoothed by the two bins around it in both directions (i.e average of 5 bins centred on the current bin). See Figure 3.12.2C. The peak firing rate was the highest firing rate shown in any directional bin. The preferred direction of a cell is the mean direction.

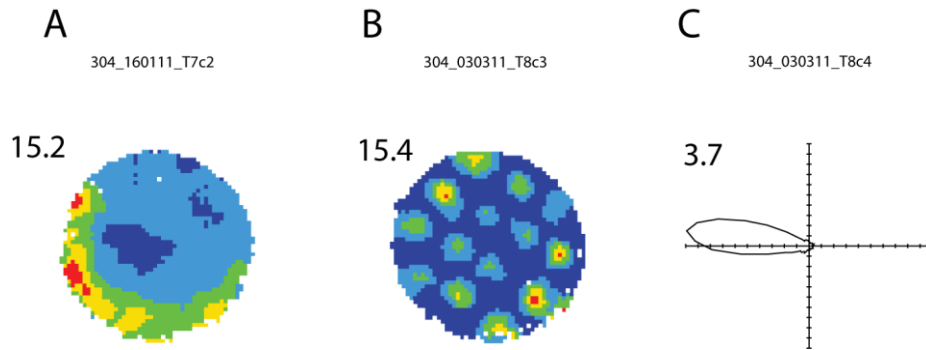


Figure 3.12.2. Example locational rate maps and polar plots for spatial cells.

Figure presents locational rate maps for a BVC (A), grid cell (B) and a polar plot for a head direction cell (C). Above the maps is the cell identification number which gives: rat number_testing day_tetrode (T) and cell (c) numbers. To the top left of the maps is the peak firing rate given in Hz. A and B) The rate maps are auto-scaled false colour maps; with each colour representing a 20%-band of peak firing rate, from dark blue (0-20%) to red (80-100%). Any white pixels represent unsampled areas. C) To plot directional activity the rats heading direction is plotted on a circular graph to create a polar plot. This plot divides the animals head direction into 60 bins of 6°. The peak firing rate was the firing rate in the peak bin.

Table 3.12.1 Table of measures used to characterise cell firing.

The table presents the measures used to assess cell firing, the cells which these analyses apply to, the source of information from which the calculation is based, the methods section to consult for more information and the results section in which they are applied.

Measure	Applied to which cells	Summary of source	See methods section	See results
Waveforms (amplitude μV and interval μs)	All cells	Averaged waveform (LWC or LWS)	3.12.1.1	4.4; 4.4.3; 5.3.3
Global mean rate	All cells		3.12.2	4.4; 5.1; 5.1.3.1; 5.2.2 5.3.3
Theta modulation score	All cells	500ms temporal autocorrelation	3.12.3.1	4.4; 4.4.4 5.3.3
Directional information (comparing different cell types)	All cells	Unsmoothed polar plots (bin size 5.6°)	3.12.3.2	4.4; 4.4.2 5.3.3
Directional information (wall no-wall for grids)	Grid cells	Smoothed polar plots (bin size 5.6°)	3.12.3.2	5.1
Directional selectivity	All cells	Unsmoothed polar plots (bin size 5.6°)	3.12.3	4.2.3; 5.3.2; 5.3.3; 4.4.3.1 4.4.3.2
Location of the locational field peak	BVC	5x5 smoothed firing rate map (bin size 3cm x 3cm)	3.14.2	5.2.5
Locational peak rate (darkness manipulations & wall no-wall for grids)	BVCs, grid cells	5x5 smoothed rate maps (bin size 3cm x 3cm)	3.12.2	5.1; 5.1.3.1; 5.2.2
Locational selectivity	BVCs, boundary-off cells	Unsmoothed firing rate map (bin size 3cm x 3cm)	3.12.3.2	4.2.3; 5.3.2

Table 3.12.1. table of measures continued

Measure	Applied to which cells	Summary of source	See methods section	Used in analyses
P,d locational information to be compared to directional information	BVCs, boundary-off cells	Unsmoothed firing rate map (LWC ; bin size 18.5cm x 18.5cm)	3.12.3.2	5.3.2
P,d directional information to be compared to locational information	BVCs, boundary-off cells	Unsmoothed polar plot (bin size 6°)	3.12.3	5.3.2
Pxd corrected locational information	BVCs	Unsmoothed firing rate map (mostly LWC , bin size 18.5cm x 18.5cm; 6 = LWS , 14cm x 14cm)	3.12.3.3	4.2.3
Pxd corrected directional information	BVCs	Unsmoothed polar plot (bin size 6°)	3.12.3.3	4.2.3
Gridness	All cells	Unsmoothed firing rate map (bin size 3cm x 3cm). Spatial autocorrelation smoothed.	3.13.1	3.13.2; 4.4.1; 4.4.2
Orientation	Grid cells	Unsmoothed firing rate map (bin size 3cm x 3cm). Spatial autocorrelation smoothed.	3.13.1 3.13.3.2	4.1.1; 4.1.3; 5.1.3
Grid scale	Grid cells	Unsmoothed firing rate map (bin size 3cm x 3cm). Spatial autocorrelation smoothed.	3.13.1 3.13.3.1	4.1.4 5.1.1

3.12.3 Quantitative measures of temporal and spatial firing characteristics

3.12.3.1 Temporal firing characteristics

Global mean rate was the number of spikes divided by the trial length (in seconds).

Theta modulation was calculated using the same methods as in Jeewajee et al., (2008). In brief the power spectrum of each cell's spike-train autocorrelogram was used to assess the extent to which each individual cell's spiking was modulated by theta. The theta-modulation score gives the ratio of average power in a narrow band (2 Hz) around the peak in the theta range (6-12Hz) to the total average power in the whole spectrum.

3.12.3.2 Directional information

For comparisons between cell types and between trials directional information and directional selectivity were calculated typically using uncorrected directional information calculations (P,D ; Skaggs et al., 1993). Information is measured in 'bits', either as 'bits per spike' which is the information provided every time the cell fires, or as 'bits per second' which is the information provided per second. Bits per spike is the most typically used measure and so was adopted here in most analyses and in the comprehensive basic properties figures (in the results). In some cases both measures were used.

To compare directional information across cell types directional polar plots were created with a bin size of 5.6°, with no smoothing. Directional information in bits per second was calculated by multiplying the directional information in bits per spike by the global mean rate. Directional selectivity (Cacucci et al, 2004) was calculated by dividing the peak rate by the mean firing rate. The Peak firing rate was taken from the directional bin with the highest firing.

Spatial information was also compared across trials. In grid cells, the directional information was compared in the wall-no wall manipulation and in the darkness manipulation. For these analyses directional polar plots were calculated using a bin size of 5.6°, each bin smoothed by the two bins around it in both directions (i.e. average of 5 bins centred on the current bin). In BVCs directional and locational information were also compared in the darkness manipulation between light and dark trials. For this analysis locational information was calculated using 5x5 smoothed rate maps.

3.12.3.3 Comparing locational and directional information in boundary cells

Using uncorrected calculations to determine spatial information can arguably produce artifactual results, because of inhomogeneous sampling of behavioural variables caused by the animal's motion. For example inhomogeneity in the sampling of places causes head-direction cells to show apparent preferential response to those places sampled most frequently with the preferred head direction. This inhomogeneity of sampling is unavoidable in freely moving animals, and is often seen at environment boundaries, where not all locations can be approached from all directions. Burgess et al., (2005) presented a method to account for this.

To correct for spurious dependencies created by inhomogeneous sampling of orientation and location I applied a procedure described in Burgess et al., (2005), hereafter called the *position times direction* (pxd) correction. Pxd correction allows for an unbiased assessment of specifically locational vs. specifically directional signalling. The correction estimates the effect of one variable (e.g. location) on firing rate when also accounting for the effect of a second variable (e.g. heading direction).

Since absolute information values are dependent on bin number, and smoothing, it was ensured that bin number and smoothing was identical where locational vs. directional signalling was assessed (specifically for the characterisation of BVCs). That is, no smoothing was applied, and the number of locational bins was matched to the number of directional bins, we have referred to this a location/direction equivalence binning. There were *always* 60 directional bins (6 degrees each) used in the directional analyses. The scaling factor of firing rate maps was adjusted such that the average number of locational bins was 60.3 ± 1.14 (range of 58-62), and thus the number of directional bins and locational bins was identical. (This is of course lower than the number of locational bins used in other analyses in the present thesis, but this is the only way of ensuring an unbiased locational vs directional comparison.)

This method of correcting for inhomogeneous sampling has been used in several studies including Cacucci et al., (2004) where CA1 place cells and presubicular head-direction cells were compared and Lever et al., (2009) used this method to compare BVCs with Cacucci et al., (2004)'s place cells and head-direction cells. Locational and directional information was also compared for Boundary-off cells, however the Pxd correction could not be run for boundary off cells. This was because for too many cells, the Pxd algorithm did not converge upon a solution and so they were analysed using the uncorrected measure (Skaggs et al., 1993). As with the BVC comparisons, the number of locational bins was matched to the number of directional bins (60 bins for both), and no smoothing was applied.

3.13 Grid cell specific analysis

3.13.1 Spatial autocorrelogram

Spatial autocorrelograms of rate maps were used to assess the periodicity, regularity, and orientation of all recorded cells and specifically those with multiple firing fields. Spatial autocorrelograms were estimated using unsmoothed rate maps; the autocorrelogram was then smoothed with a 2D Gaussian kernel with a maximal width of 10 bins and a σ set at 2.25 bins. Specifically, the spatial autocorrelogram was defined as:

$$r(\tau_x, \tau_y) = \frac{n \sum \lambda_1(x, y) \lambda_2(x - \tau_x, y - \tau_y) - \sum \lambda_1(x, y) \sum \lambda_2(x - \tau_x, y - \tau_y)}{\sqrt{n \sum \lambda_1(x, y)^2 - \left(\sum \lambda_1(x, y) \right)^2} \sqrt{n \sum \lambda_2(x - \tau_x, y - \tau_y)^2 - \left(\sum \lambda_2(x - \tau_x, y - \tau_y) \right)^2}}$$

Where $r(\tau_x, \tau_y)$ is the autocorrelation between bins with a spatial offset of τ_x and τ_y , $\lambda_1(x, y)$ and $\lambda_2(x, y)$ are equivalent for an autocorrelation and indicate the mean firing rate in bin (x, y) , and n is the number of bins over which the estimate was made. Correlations were estimated for all values of n . The six peaks surrounding the central peak on the autocorrelogram were considered to be the local maxima exceeding $r = 0$ closest to, but excluding, the central peak. The extent of each peak was defined as the contiguous set of bins around the peak with a value greater than half the value of the peak bin.

In particular, the spatial autocorrelograms constructed from the combined unsmoothed baseline rate maps were used to estimate the orientation, grid scale, and gridness of each cell (Figure 3.13.1). Orientation was the angle between a nominal horizontal reference line and an axis defined by the center of the spatial autocorrelogram and the peak closest to the reference line in a counter-clockwise direction (Figure 3.13.1D). Grid scale was the median distance from the central peak to the six surrounding peaks (Figure 3.13.1C). Gridness, a measure of spatial periodicity, was calculated by defining a mask of the spatial autocorrelation centered on but excluding the central peak bounded by a circle passing around the outside edge of the outermost of the six central peaks (Figure 3.13.1B). This area was rotated in 30° increments up to 150°, and for each rotation, the Pearson product moment correlation coefficient was calculated against the unrotated mask. Gridness was then expressed as the lowest correlation obtained for rotations of 60° and 120° minus the highest correlation obtained at rotations of 30°, 90°, or 150°.

3.13.2 Grid cell classification

Grid cells were classified by gridness score as determined by the spatial autocorrelogram (Figure 3.13.1B). High gridness relates to high periodicity. All putative grid cells were run through the spatial autocorrelation analysis. For grid cell classification gridness scores were taken from the trial with the highest gridness score, from the large walled circle (LWC), the large walled square (LWS) or the circular open platform (COP). I recorded all cells except for 4 which were taken from an unpublished dataset recorded by my supervisor Dr Colin Lever. These were tested in a smaller walled square environment only, therefore these trials were used to define these cells.

In previous studies the gridness threshold for grid cell classification was >0 (Hafting et al., 2005; Fyhn et al., 2007; Solstad et al., 2008; Boccara et al., 2010). However, for more robust analyses of environmental manipulations higher thresholds of inclusion were sometimes used (e.g. ≥ 0.3 Solstad et al., 2008; Barry et al., 2007; Wills et al., 2012). In the present study the gridness threshold was set to ≥ 0.25 . This was motivated by the following consideration. Any threshold devised for grid cell classification must exclude cells which did not show periodic firing patterns, i.e. the two neighbouring spatial populations; the BVCs and HD cells. These cell types should not be included as grid cells. A rational gridness threshold would be the mean plus 2 standard deviations of these non-grid cell types. The average mean gridness for the BVCs and HD cells plus 2 standard deviations was 0.24. Accordingly for the present thesis only cells with gridness scores of equal to or more than 0.25 gridness were included in the grid cell sample.

Arguably, this threshold is conservative. However being conservative is a sensible precaution and should ensure that the cells being characterised as subicular grid cells in the present thesis would certainly be classified as grid cells had they been recorded by others from another region. I include only definitive grid cells of equivalent or higher quality/gridness than those previously reported in the entorhinal cortex and presubiculum and parasubiculum. However, this thesis cannot meaningfully exhaustively compare all gridness measures for all given cells because other's gridness measures do not capture the periodicity of the cells. Figure 3.13.2 suggests the 0.25 threshold used here may correspond to the ~ 0.3 gridness threshold used in other studies, e.g. Wills et al., (2012) and Sargolini et al., (2010), which characterised grid cells with smaller gridscale than in this dataset. Figure 3.13.2 also shows where alternative measures do not capture the cells' periodicity perhaps because of the large grid scale seen in the subiculum grid cells recorded here (e.g. 60-70 cm). The spatial autocorrelation used in this thesis provided the best fit for the largest number of periodic cells. It is notable that many cells which show interesting periodicity show low or even negative

gridness values, as gridness indexes node hexagonality (see Figure 4.1.1). Arguably, the gridness measure fetishizes hexagonality. Cells are probably very functional for spatial representation even if the fields are more elliptical for instance. One approach to thresholding is to conduct a series of shuffles of the location and spike time data, and use a minimum value defined as 2 or 3 standard deviations above the mean gridness. However, this approach will depend on the cells that are being shuffled, and it will still overvalue hexagonality.

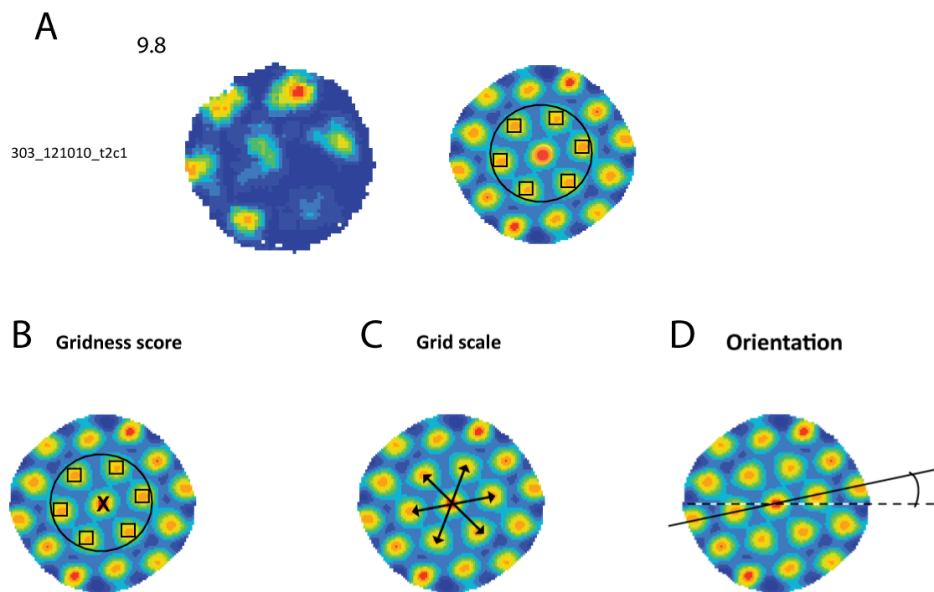


Figure 3.13.1. Spatial autocorrelation is used to determine the parameters of the grid pattern.

The figure shows an example grid cell recorded from rat 303. A) Presents the locational rate map and peak rate (Hz) and the spatial autocorrelation. B) Gridness, a measure of spatial periodicity, was calculated by defining a mask of the spatial autocorrelation centered on but excluding the central peak (marked with an x) bounded by a circle passing around the outside edge of the outermost of the six central peaks. C) Grid scale was calculated as the median distance from the central peak to the six surrounding peaks. D) Orientation was the angle between a nominal horizontal reference line (dotted line) and an axis defined by the center of the spatial autocorrelogram and the peak closest to the reference line (black line) in a counter-clockwise direction.

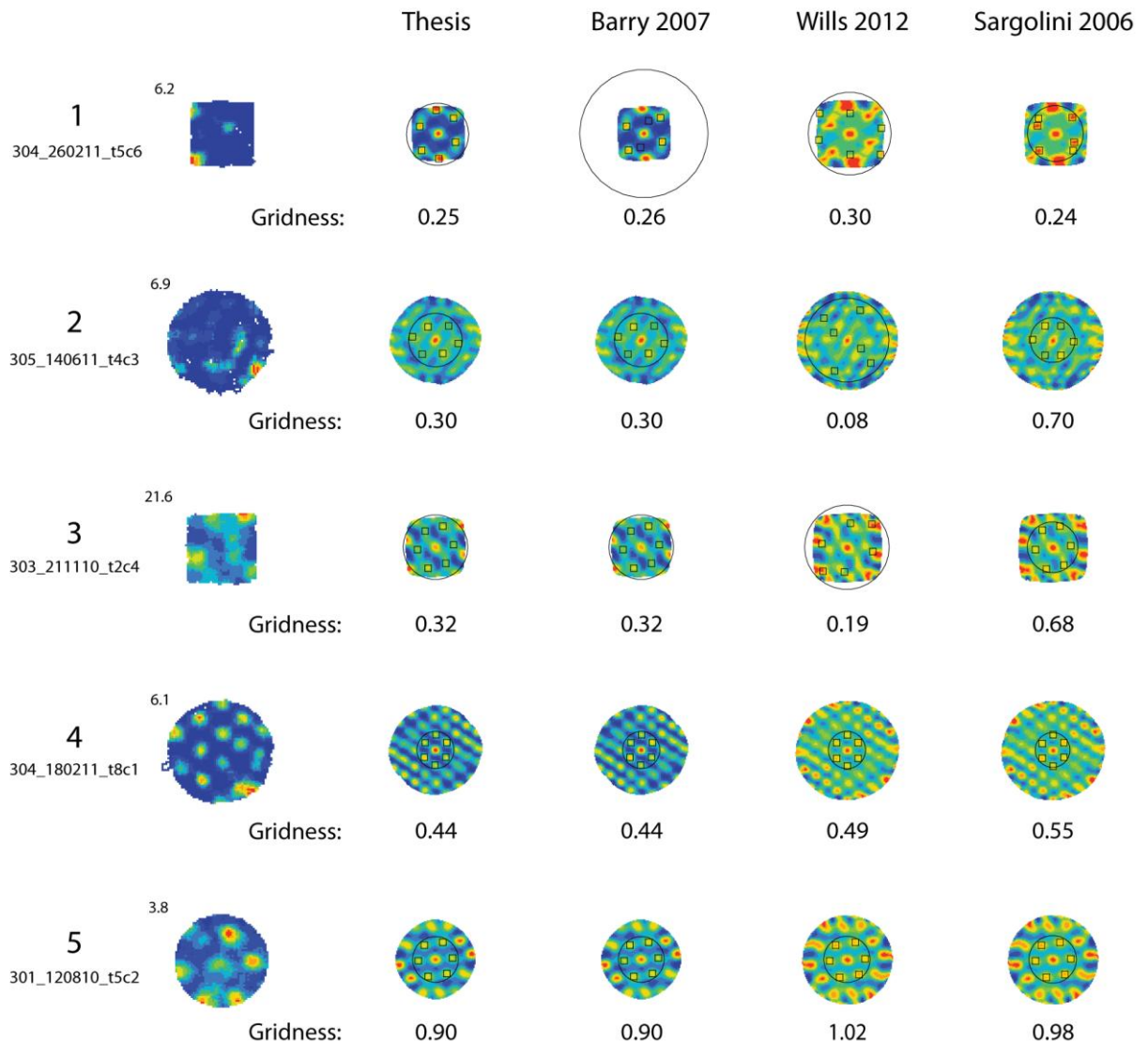


Figure 3.13.2. Gridness scores depend upon which spatial autocorrelation analysis is used.

The figure shows 5 example grid cells which were tested using spatial autocorrelation analyses from key grid cell studies. The first column gives both the number of the cell specific to this figure and the cell identification number stating rat_day_ tetrode/cell. The second column presents the rate map, with the peak firing rate (Hz) in the top left corner. The following columns present the spatial autocorrelation maps.

Our spatial autocorrelation analysis provided the best fit for the largest number of periodic cells. E.g. for cell 1 above only our spatial autocorrelation captures all the grid fields. For cells where the spatial autocorrelations do capture the grid fields the gridness scores are typically higher than those given by our spatial autocorrelation, e.g. cells 4 and 5.

3.13.3 Grid scale expansion

To measure the effect of wall removal on grid cell grid scale smoothed rate maps and spatial autocorrelations were calculated for all cell and trials in the wall no-wall manipulation.

The wall no-wall manipulation involved comparing baseline walled-environments with the circular open platform (COP). The COP was run between two trials in either the large walled circle (LWC) or the large walled square (LWS). Details of this manipulation can be found in Figure 3.9.2. Wall no-wall manipulation trial series. Figure 3.9.2.

To be included in the analysis all trials must have been recorded on the same day. Trials that were not well fit by the spatial autocorrelation were excluded from the analysis. Where the un-walled trial was not fit, either by fault of the spatial autocorrelation or because the fields broke down, that cell was removed from the analysis. For trials where only one of the baseline trials was at fault, that trial was removed but the cell remained in the analysis.

Between the walled and un-walled trials, grid cell properties including directional information, grid scale, orientation, theta modulation and gridness were compared.

3.13.3.1 Measuring grid scale change

To look at changes in grid scale between walled and un-walled trials the absolute and percentage change in grid scale was calculated. Where there were two baseline trials an average was always taken. To calculate the percentage increase in grid scale, the grid scale in the walled trials (LWS or LWC) was considered to be 100%. Then the % change between the walled and un-walled grid scales was calculated. E.g. a grid scale of 48.45 in the large walled square, this would be considered as 100% grid scale for that cell. In the walled trial if the grid scale increased to 58.50cm this would be a 10.1cm absolute increase and would represent a grid scale of 121.1%. Therefore between the walled and un-walled trials there was a 21.1% increase.

3.13.3.2 Measuring shifts in orientation

To determine whether grid orientation shifted with wall removal, the difference in orientation (in degrees) was determined between walled and un-walled trials.

To briefly recap, the orientation of the grid is defined as the angle between a nominal horizontal reference defined by the centre of the autocorrelogram (dotted line; Figure 3.13.1D) and the peak closest to the

reference line in an anti-clockwise direction (black line; Figure 3.13.1D). This gives the smallest angle between the reference line and the closest peak. The 6 peaks surrounding the central peak are separated by 60° increments, and so the orientation of the grid pattern relative to the horizontal reference line can only ever be between 0° and 60° . The difference in orientation between the baseline trials was calculated, as was the difference between average baseline and un-walled trial orientation. The smallest difference was always used. E.g. if the orientation in the first baseline trial was 10° and the orientation in the un-walled trial was 22° , the orientation change would be 12° not 72° (as this would be more than 60°). These two differences in orientation were then compared to see if the orientation shift between walled and un-walled trials was significantly larger than the orientation shift between the walled baseline trials.

3.13.4 Field inhibition in grid cells with barrier insertion

To investigate the influence of barrier insertion on the grid pattern the grid cells were tested using the barrier insertion manipulation in the large walled circle and/or the large walled square. For details see Figure 3.9.1 and Figure 3.9.3. For some of the grid cells the insertion of the barrier seemed to cause field-specific inhibition, in firing rate. This phenomenon was examined in a subset of grid cells.

Using the cluster cutting software the fields could be individually isolated. This allowed us to see the peak rates and spikes for each field. Using glass2k software, the cutting window could be made opaque so that the field location could be precisely traced from the first baseline trial onto the barrier and second baseline trial rate maps. This meant that the exact locations of specific fields could be compared between trials. The peak rates of the field locations were compared between baseline (average of the 2 baseline trials) and the barrier trial. The field locations of the 'inhibited' fields were compared, as were the locations of some stable fields. The stable fields acted as 'reference' fields, to see if the inhibition was due to a reduction in firing rate across the whole grid pattern or just for specific fields.

3.14 BVC specific analyses

3.14.1 BVC classification criteria

The BVC model predicts that when an appropriately-oriented barrier is inserted into a testing environment, a BVC would develop an additional locational field in response. Lever et al., (2009) and Solstad et al., (2008) showed this field doubling for a subset of boundary cells. Lever et al. concludes that the main determinant of BVC firing is the vector from the rat to the boundary irrespective of the boundaries qualities. In support of this Lever et al. also recorded a BVC which produced a second field following the addition of extra 'drop' boundary (wall-less edges) in an open platform environment (together-apart manipulation, Figure 3.9.4). This general property of extra locational fields developing following the creation of additional, appropriately-oriented, boundaries was present in most boundary cells. In this thesis, this property was used as a defining feature of BVC firing. If a boundary cell did not exhibit this property it was classed as a 'non-BVC boundary cell.'

Cells that showed boundary responses for the perimeter of the large walled circle and or the large walled square were given subsequent trials with the addition of a free-standing internal barrier (see Figure 3.9.1). As per the model and as seen in Lever et al., (2009) the second firing field for the inserted barrier was expected to follow the barrier on its predicted side. Only in cases where the barrier was oriented correctly to the cells preferred direction were they considered further.

To quantify the BVC response to additional boundary a firing rate threshold was set (Figure 3.14.1). To be included as a BVC a second field had to be created consisting of bins $\geq 40\%$ of the peak rate along $\geq 50\%$ of the barrier. Figure 3.14.1A gives 6 examples of BVC second fields which reach this threshold and Figure 3.14.1B shows 2 BVCs with second fields which did not reach this threshold.

Cells that did not present double firing fields with the addition of a barrier, were tested with additional drop boundaries in the together apart manipulation (Figure 3.9.4). The cells were tested on a rectangular open platform that could be pulled apart by 10 cm to create three platforms. This provided 1 perimeter drop and 2 traversable drops which the rat could voluntarily cross. If a BVC responded to the drops as boundaries it would be expected to produce 3 firing fields (one for each edge). These extra fields should be akin to the field doubling seen with the insertion of a barrier. As mentioned above cells that failed to show adequate field doubling/tripling with the addition of extra boundaries, were classed as '*non-BVC boundary cells*'.

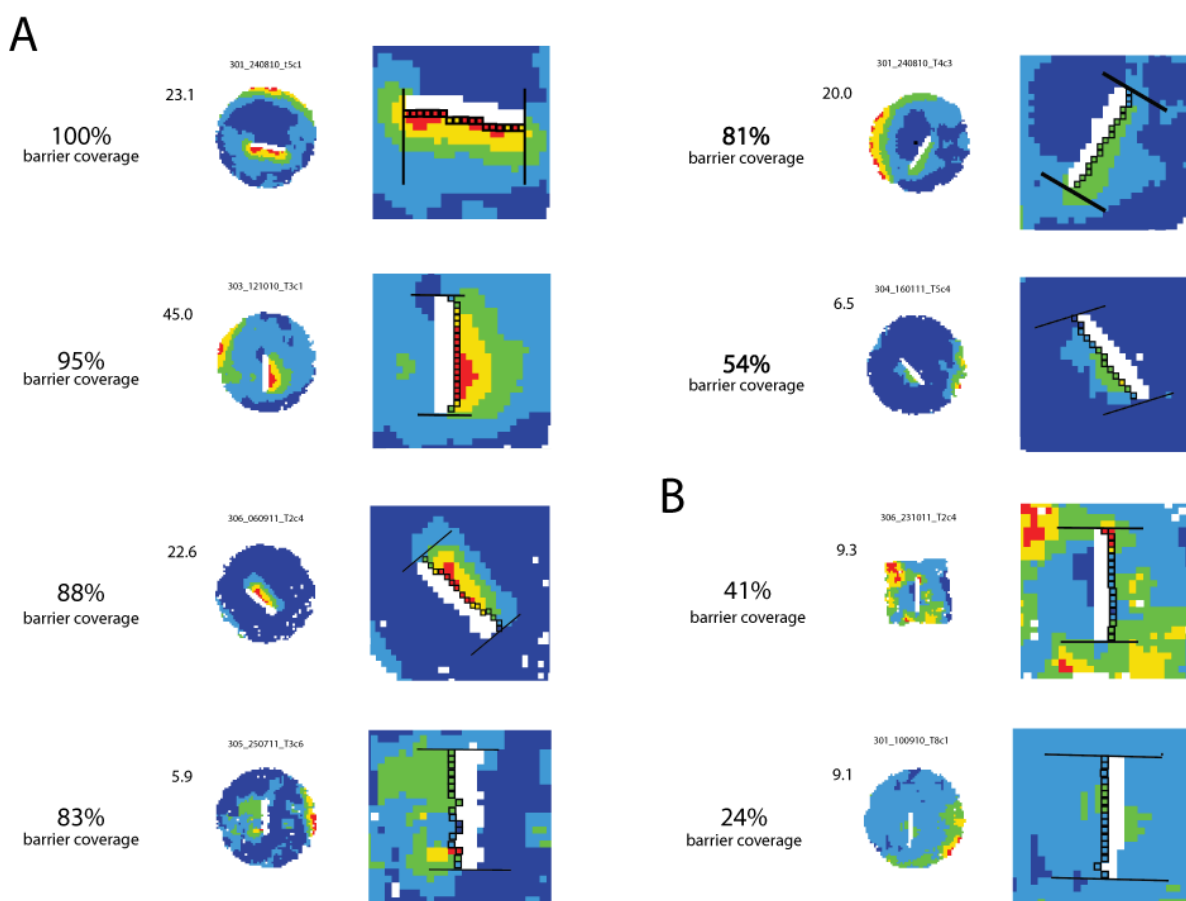


Figure 3.14.1: Representative BVCs demonstrating the selection process used to classify boundary cells as BVCs.

Figure shows 6 BVCs and 2 non-BVC boundary cells. To the left of the rate map is the percentage barrier coverage by the second locational field. To the right of the rate map is a close-up of the second field for each cell. For all putative BVCs the firing was required to be $\geq 40\%$ peak firing rate (shown on the rate maps as green pixels) across at least 50% of the barrier. This was calculated as the percentage of pixels (underneath the rate maps is the percentage pixels along the barrier. A) Shows 6 BVCs which passed the criteria B) shows 2 cells which failed to show a second field along at least 50% of the barrier. 42/46 BVCs were classified using this criteria.

3.14.2 Quantifying the effect of wall removal on BVC fields

BVCs were tested in the wall no-wall manipulation (Figure 3.9.2). To see if the peak of the BVC fields moved with wall-removal the distance in pixels from the peak to the centre of the environment for both the walled (LWC) and the un-walled (COP) trials was calculated. For this the cluster cutting software TINT was used (See Figure 3.14.2 for procedure). The distance of the 2 peaks were calculated using Pythagoras' theorem (Figure 3.14.2C). In order to see if the peak had moved between walled and un-walled trials the distance in pixels between the peaks and the environment centre were compared and converted into centimetres.

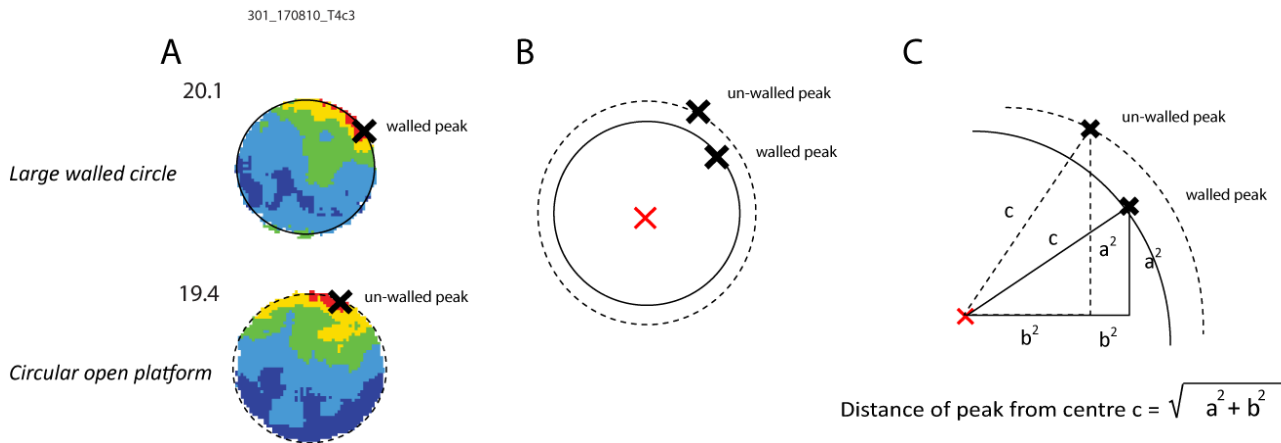


Figure 3.14.2. Do BVC field peaks move with the boundary when the walls are removed?

An example of how the shift in BVC field peaks was calculated. A) presents an example cell in the walled and un-walled circular environments (Large walled circle and circular open platform). The field peaks are marked with black crosses. B) is an illustration of the walled circle superimposed on top of the un-walled circle. This shows the relation of the field peaks to each other and the centre of the environments (red cross). C) Shows how the distance from the centre of the environments to the peaks was calculated using Pythagoras' theorem.

Chapter 4 Classification, basic properties and comparison of subicular spatial cells

4.1 Overview of the dataset

This thesis provides the first account of grid cells located in this area. Grid cells were often simultaneously recorded with Boundary Vector cells (BVCs) and head-direction (HD) cells from the subiculum, and for two rats (3 hemispheres) from the surrounding areas.

The dataset analysed in this thesis comprises 210 spatial cells (table 4.1.1.) below. I recorded all cells except for 4 which were taken from an unpublished dataset recorded by my supervisor Dr Colin Lever. The data presented here was recorded from 6 rats. Data from the subiculum was recorded from 4 rats. From 1 rat the tetrode recording locations were assigned as from locations around the subiculum. A small number of place cells were recorded from the hippocampus in one rat.

Testing and trial series were dictated by cell type and stability. Often cells were recorded across days. The average number of experimental testing days (i.e. not just screening) was 25 days for each animal. The time spent testing each animal ranged between 2 and 4 months. The number of trials per day varied but was generally around 9, taking about 8 hours to run (up to a maximum of 14 hours). Trial length was dependent upon environment size (Table 3.8.1), with the standard trial in the baseline environment (150cm-diameter walled circle) being 42 minutes in duration. Recording time per unit area was longer, to my knowledge, than in previous studies. Trials were separated by an inter trial interval (ITI) of 20minutes. This ITI was extended between manipulations on long testing days to allow the rat to rest.

Here subicular grid cells were characterised in terms of their basic properties, by using spatial autocorrelations and other spatial and temporal measures. The thesis also provides a comparison of grid cell properties with the often simultaneously recorded BVCs and HD cells.

The grid cells were tested in several environmental manipulations, to assess grid cell behaviour with environment change. These manipulations specifically investigated the effect of barrier insertion, wall removal and darkness.

This thesis also aimed to provide a detailed account of subicular BVCs leading on from Lever et al., (2009). Similar to the grid cells in this thesis BVCs were characterised using spatial and temporal measures. They were also compared to other spatial cell and were testing using a variety of environmental manipulations. Here BVCs were tested with barriers, wall removal, darkness, context change, traversable gaps and for a small sample inserted objects.

During testing a new type of boundary-specific cell was discovered, one that fires over almost the entire environment, but has a portion of inhibited firing near a boundary. When a barrier was inserted into the environment, the cells responded by producing a second inhibitory field. I have called these cell boundary-off cells. They appear to be like an inverse of BVCs. The last section of the results will attempt to characterise these cells using the measures and methods previously used for the grid cells and the BVCs.

Table 4.1.1. Spatial cells recorded and analysed in this thesis

Cell type	Number recorded
Grid cells	51
Non-grid periodic cells	25
Boundary vector cells	46
Boundary-off cells	9
Non-BVC boundary cells	18
Non-subicular boundary cells	8
Head-direction cells	30
Place cells	23
Total	210 cells

4.1 Grid cells

4.1.1 Grid cell classification criteria

Gridness is a measure of the hexagonal regularity of adjacent fields. Gridness determines the spatial periodicity of the grid pattern and is typically used in the classification of grid cells (Hafting et al., 2005; Fyhn et al., 2004; Solstad et al., 2008; Wills et al., 2010; Barry et al. 2007;2012). In brief gridness was calculated by defining a mask of the spatial autocorrelation centred on but excluding the central peak bounded by a circle passing around the outside edge of the outermost of the six central peaks (see methods for more details). This area was rotated in 30° increments up to 150°, and for each rotation, the Pearson product moment correlation coefficient was calculated against the un-rotated mask. Gridness was then expressed as the lowest correlation obtained for rotations of 60° and 120° minus the highest correlation obtained at rotations of 30°, 90°, or 150°. High gridness relates to high periodicity. All putative grid cells (n=75) were run through the spatial autocorrelation analysis. Details about the spatial autocorrellogram can be found in the methods. Gridness was taken from the trial with the highest gridness score in one of four environments; the large walled circle (LWC), the large walled square (LWS), the circular open platform (COP) or the small walled square (SWS). For putative grids gridness ranged from -0.04 to 1.30 (mean 0.47 ± 0.05). In previous studies the gridness threshold for grid cell classification was >0 (Hafting et al., 2005; Fyhn et al., 2007; Solstad et al., 2008; Wills et al., 2010). However, for more robust analyses of environmental manipulations higher thresholds of inclusion were used (e.g. ≥ 0.3 Solstad et al., 2008; Barry et al., 2007; Boccara et al., 2010). Figure 4.1.1 shows the 26 putative grid cells did not reach the gridness threshold, and were excluded from the sample. The 0.25 threshold used here may correspond to the 0.3 or higher gridness threshold used in other gridness measures. This thesis cannot meaningfully exhaustively compare all gridness measures for all given cells because some measures do not capture the periodicity of the cells. Figure 3.13.2 provides a few examples that suggest that a threshold of 0.25 in our measure likely corresponds to higher thresholds used by Wills et al. (2010) and Sargolini et al.(2010). The spatial autocorrelation used in this thesis provided the best fit for the largest number of periodic cells. However, even using this analysis some putative grid cells with clear periodic firing still had to be excluded (cells 10, 11, 18 and 20, Figure 4.1.1).

Four cells were recorded in a small-square environment only (60cm x 60cm). These cells could potentially introduce bias into some of the analyses, because only grid cells showing small grid scales can be detected in small environments.

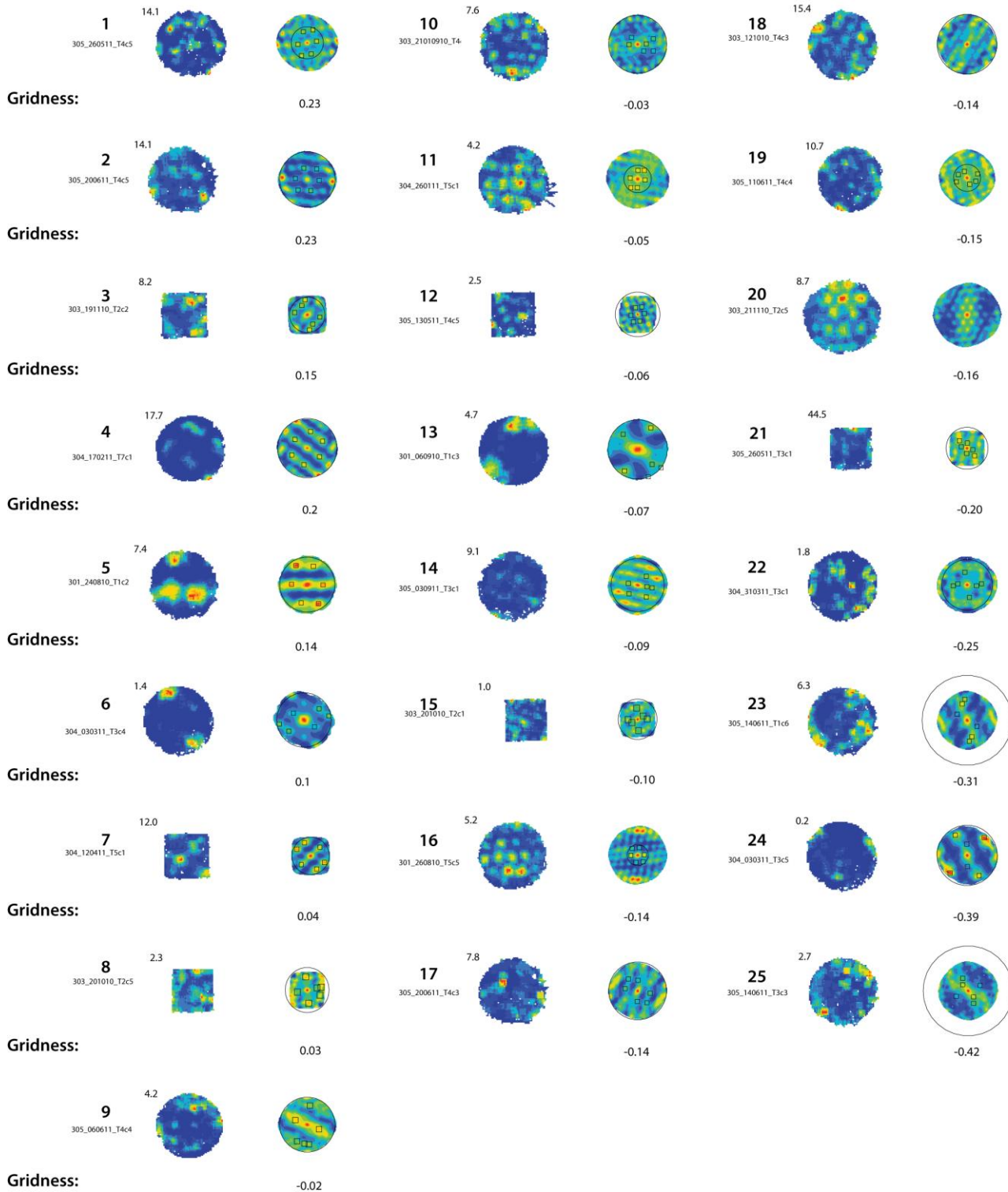


Figure 4.1.1. Periodic non-grid cells: putative grid cells with multiple peaks which did not reach the 0.25 gridness score threshold.

All putative grid cells which were identified through visual inspection were run through the spatial autocorrelation analysis. The 26 which did not reach the gridness threshold of 0.25 were excluded, these are shown here. The cells are organised by the highest gridness score (cell 1 top left) to the lowest gridness score (cell 25 bottom right).

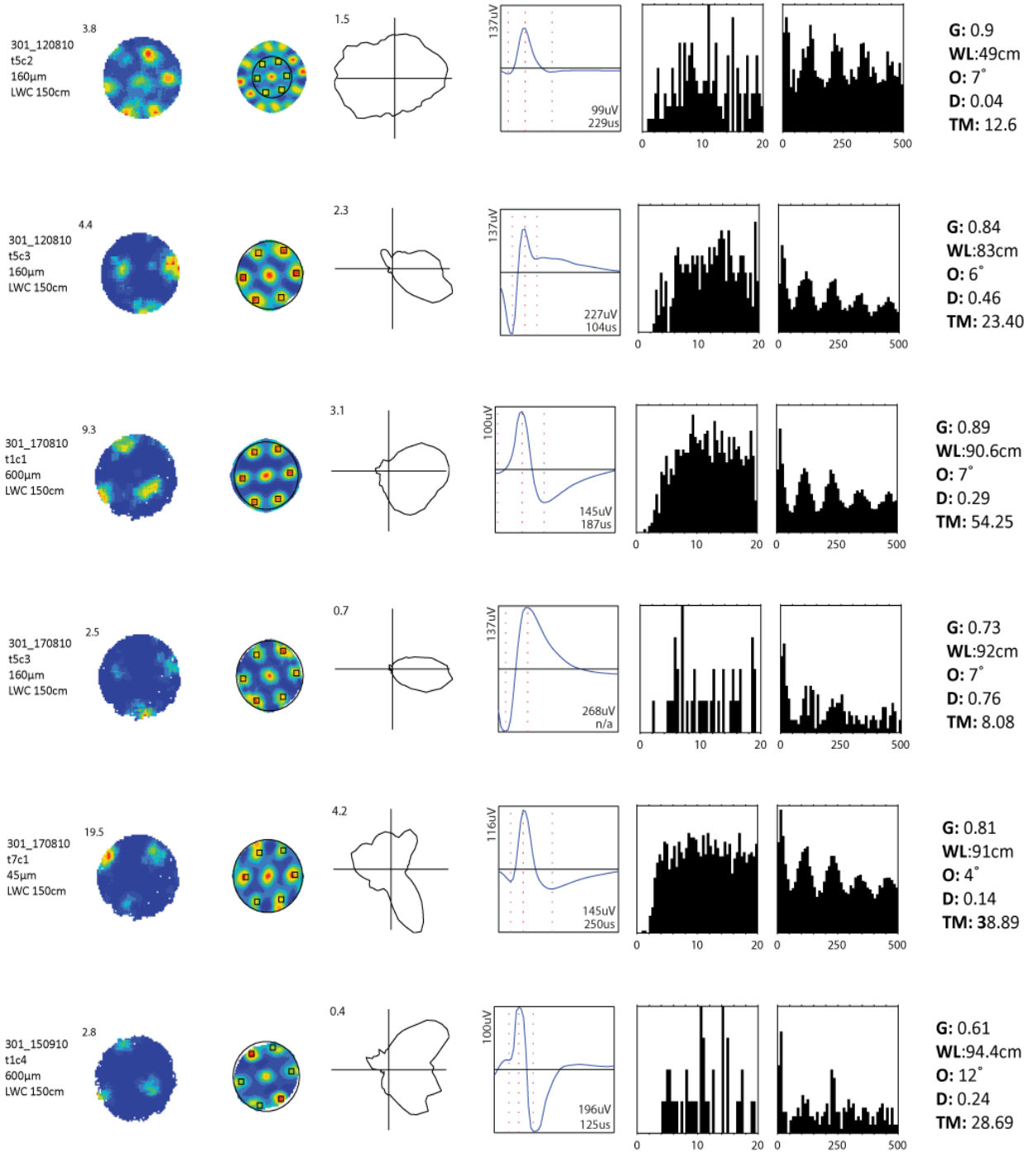


Figure 4.1.2. Basic characterisation of all grid cells; subiculum (page 1/7)

Each row shows data for one grid cell. From left to right the figure presents; text column stating rat/day, tetrode/cell, recording location in mm posterior to dorsal commissure (if subicular) and recording environment; locational rate map with peak rate (Hz); spatial autocorrelation map; directional polar plot with peak rate (Hz); spike waveform, bottom-right text stating peak amplitude (highest positive-to-negative or negative-to-positive amplitude, μV) and negative peak-to-trough interval (μs); temporal autocorrelations (0-20ms and 0-500ms). Rightmost text column gives the gridness score (G), grid scale (WL), orientation (O), directional information in bits per spike (Dir; calculated from unsmoothed polar plots. bin size 5.6°) and the theta modulation score (TM). Pages 1-4 show the subicular grid cells and pages 5-7 show the grid cells recorded outside the subiculum.

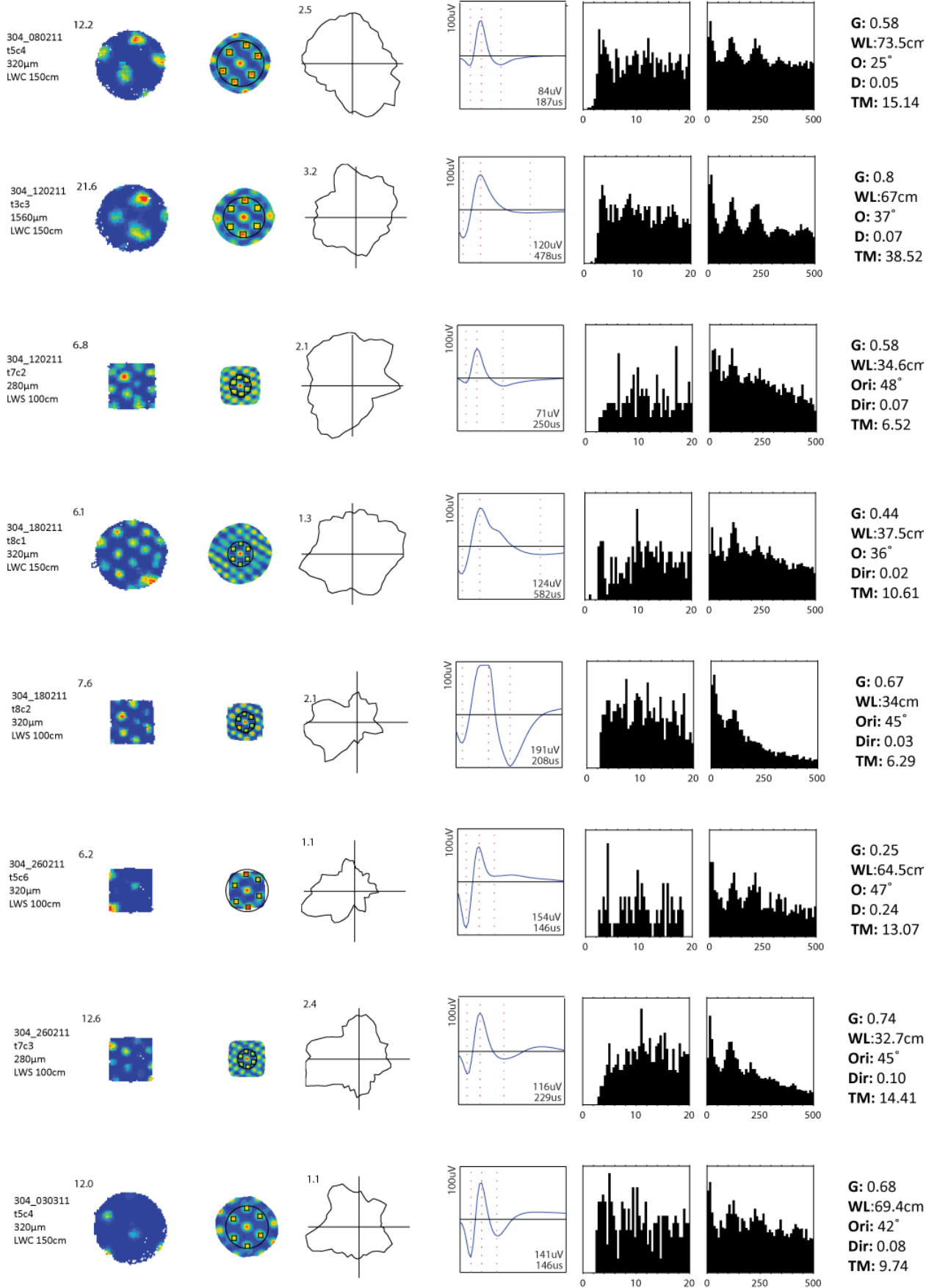


Figure 4.1.2. Basic characterisation of all grid cells; subiculum (page 2/7)

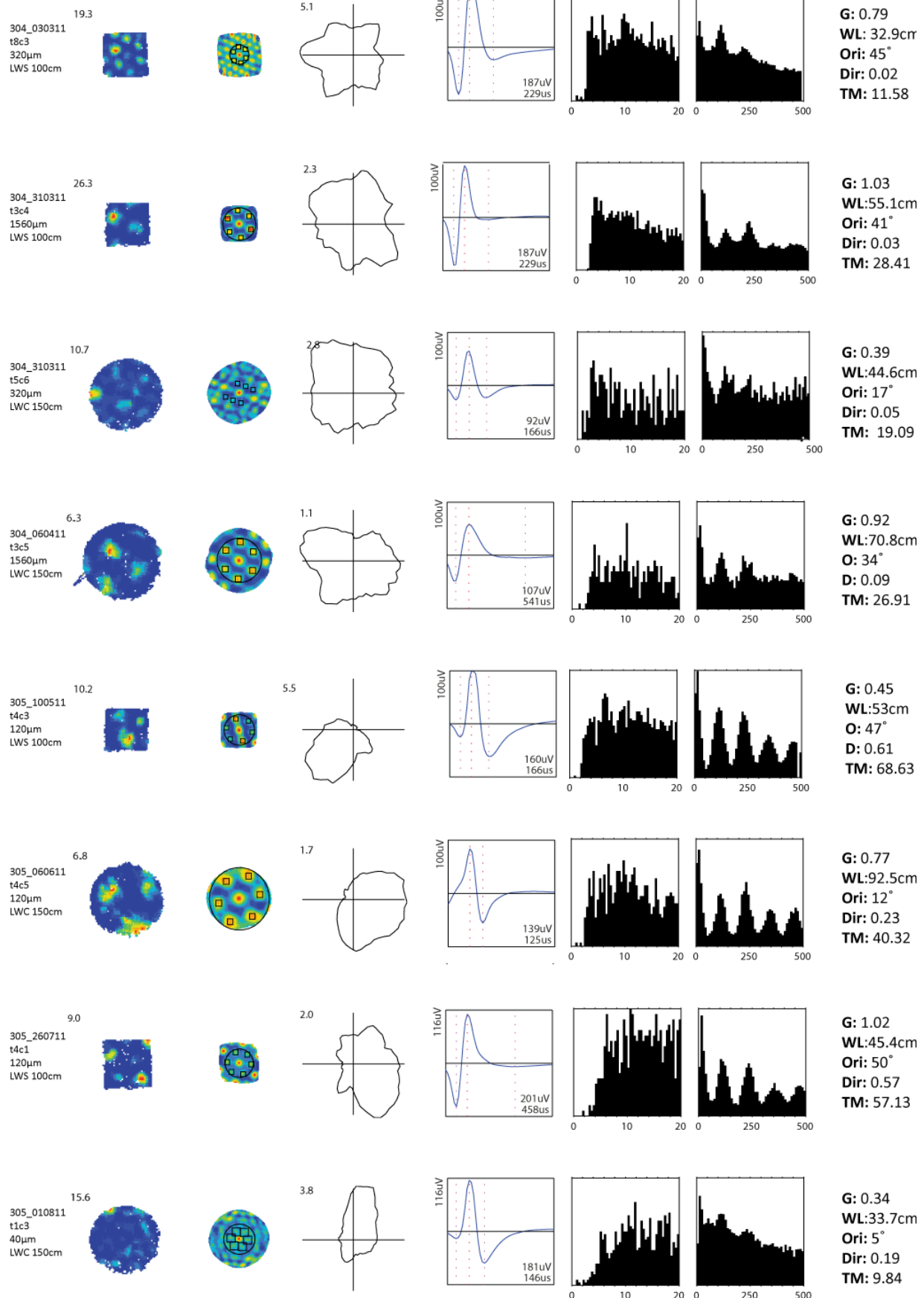


Figure 4.1.2. Basic characterisation of all grid cells; subiculum (page 3/7)

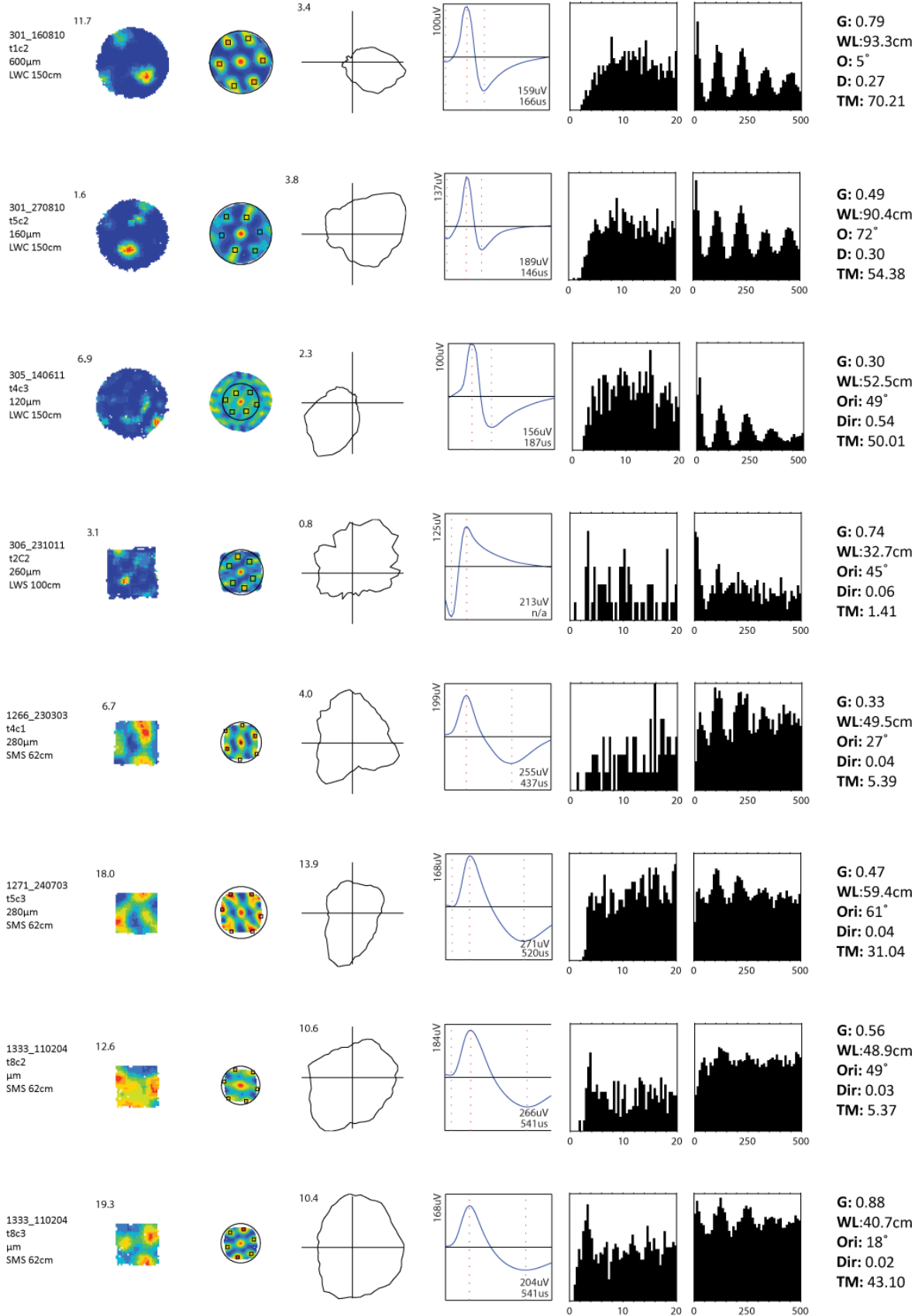


Figure 4.1.2. Basic characterisation of all grid cells; subiculum (page 4/7)

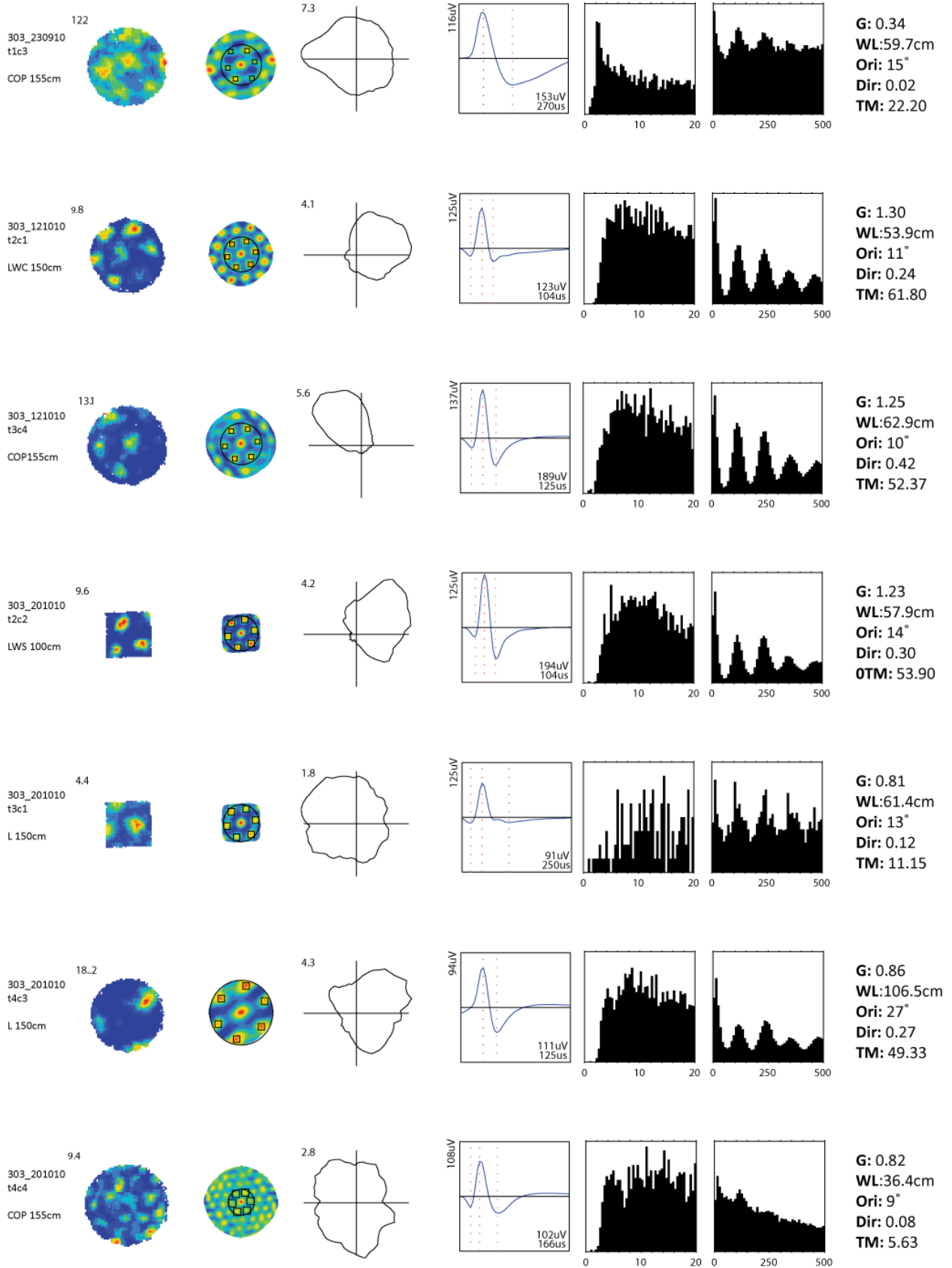


Figure 4.1.2.. Basic characterisation of all grid cells (page 5/7)

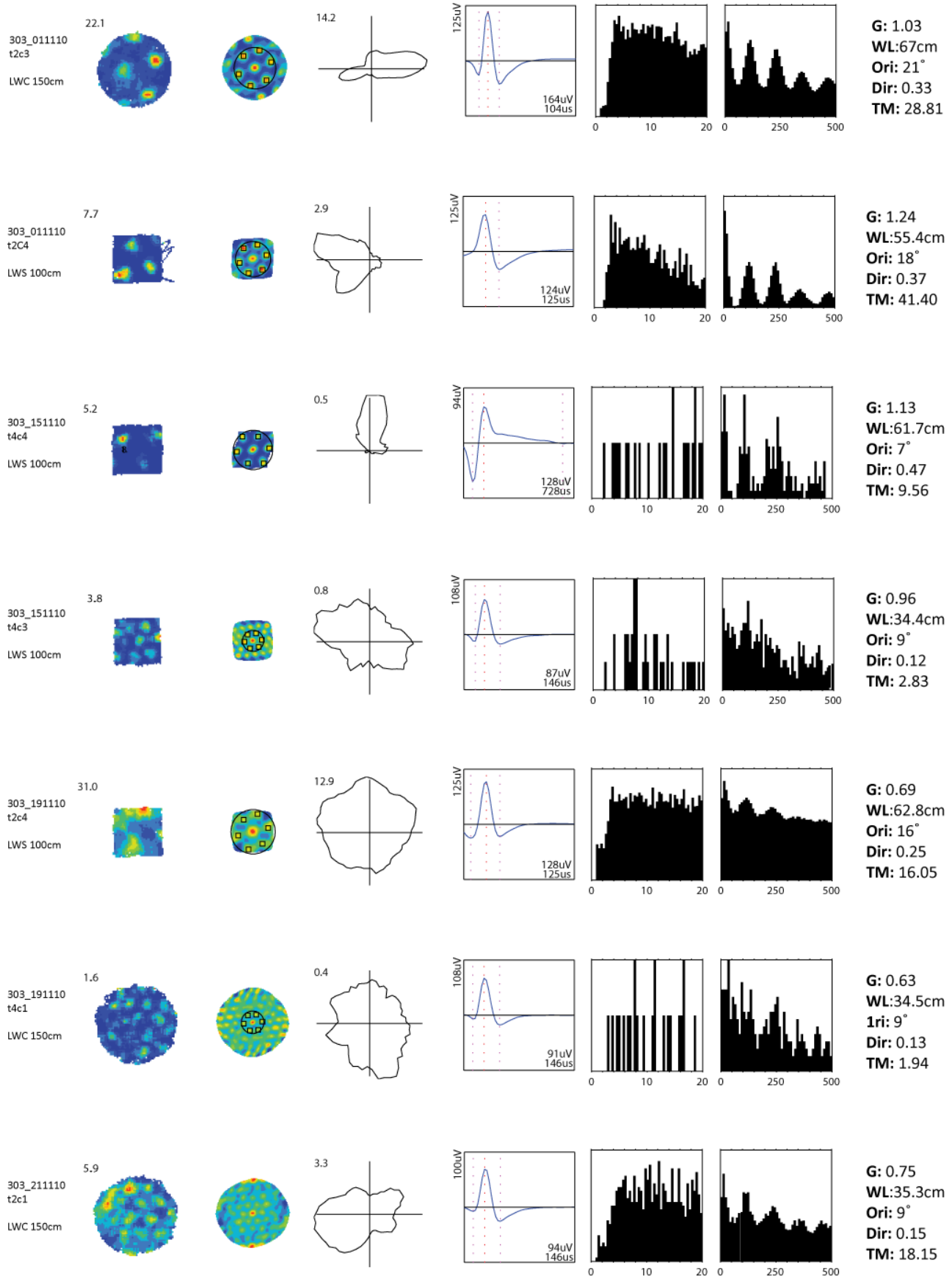


Figure 4.1.2. Basic characterisation of all grid cells (page 6/7)

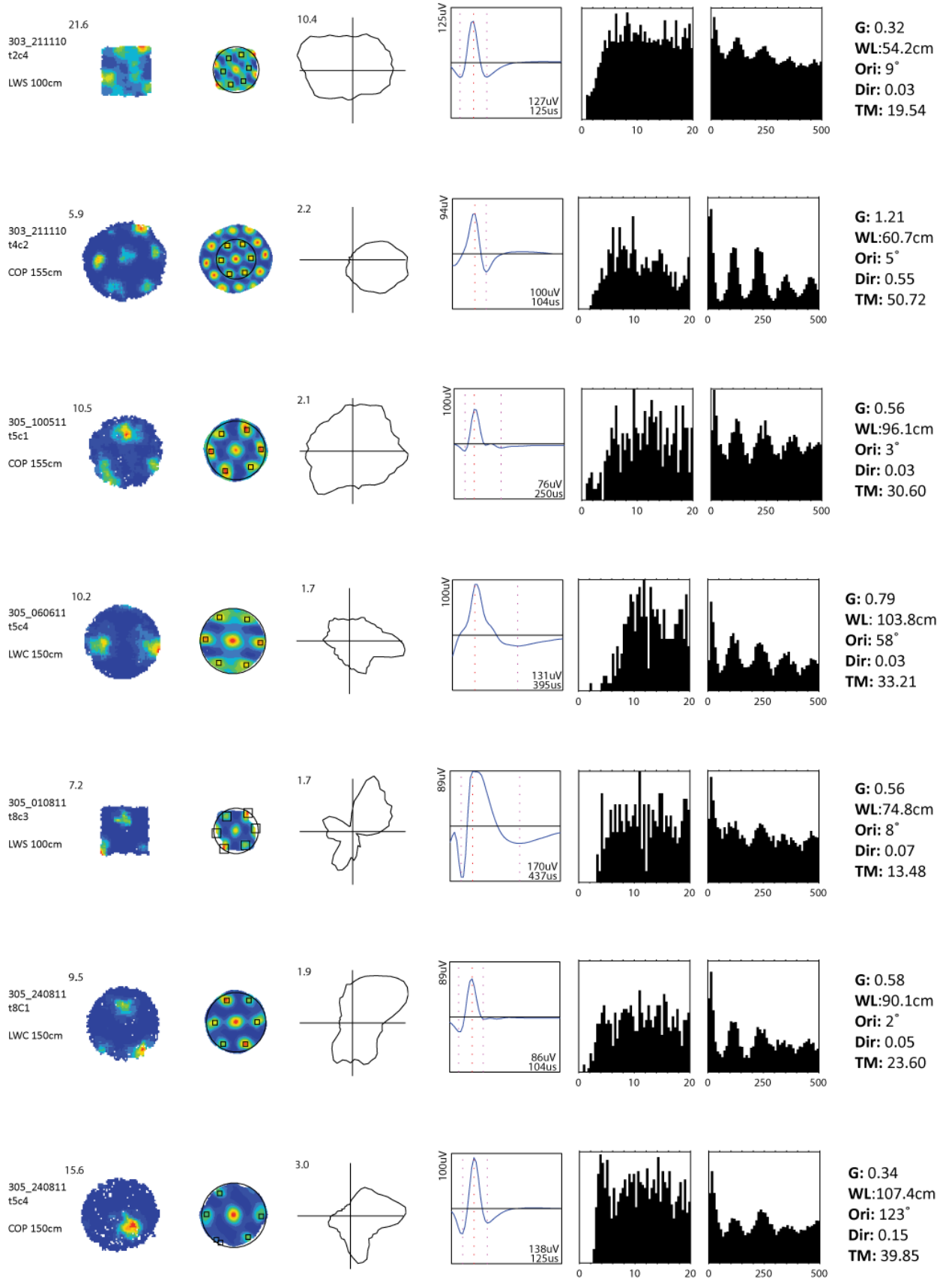


Figure 4.1.2. Basic characterisation of all grid cells (page 7/7)

2.2.2 Histology and tetrode localization

Grid cells were recorded from eight animals (11 hemispheres). For 7 of those animals subicular grid cells were recorded from at least one hemisphere (9 hemispheres in total). Subicular grid cells were recorded from both hemispheres in 2 animals. Cells recorded from 2 rats were of uncertain location nearby the subiculum. The location of these cells may be the presubiculum, the white matter above the subiculum/presubiculum and the subiculum itself. Histology and movement records were inconclusive. The results will be described for all grid cells recorded (referred to as ALLGRIDS) and then separately for the subiculum-only grid cells (referred to as SUBGRIDS). To determine where along the subicular anterior-posterior axis the cells were recorded from the distance behind the posterior end of the dorsal commissure (PDC) was calculated (in mm; see methods). At the PDC co-ordinate (0mm) the dorsal commissure breaks across the hemispheres. This corresponds to the Paxinos and Watson rat brain atlas co-ordinate -5.2mm behind bregma (Paxinos and Watson, 2007). Figure 4.1.3 shows the tetrode tracks and the estimated recording locations of the subicular grid cells.

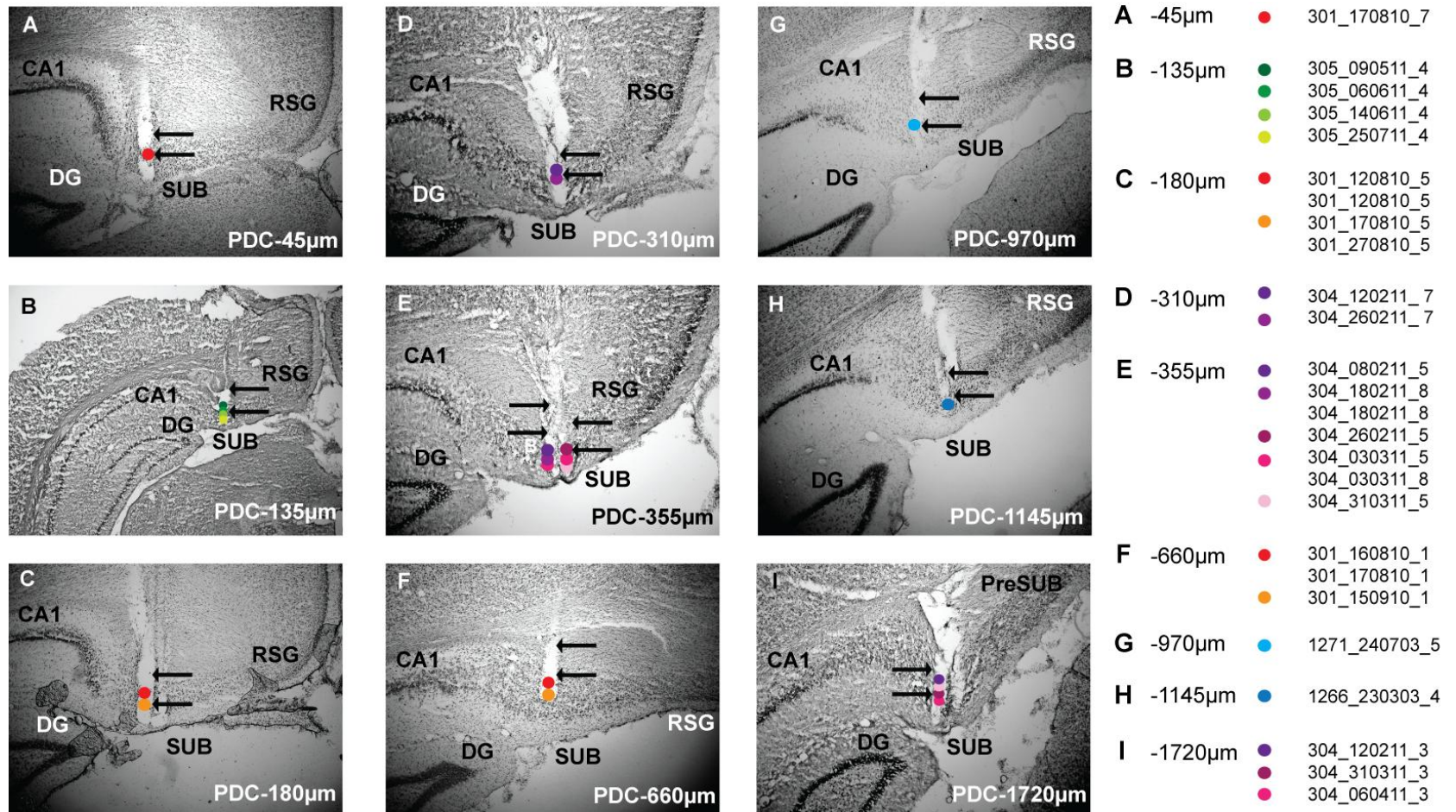


Figure 4.1.3. Estimated recording locations of grid cells.

The figure shows Nissl-stained coronal sections of the dorsal subiculum. Coloured circles indicate estimated locations of grid cells; arrows indicate tracks of recording tetrodes. Sections are arranged in anterior-posterior order (A-I), at increasing distance behind the posterior end of the dorsal commissure (PDC), which is ~ 5.2 mm posterior to bregma. SUB, Subiculum; RSG, retrosplenial cortex; DG, dentate gyrus; PreSUB, presubiculum. To the right of the sections is a key of which grid cells are at which estimated recording locations. These cell numbers correspond to those in the rate map figures. See figure 4.1.2 for rate maps and spatial autocorrelations for all grid cells.

4.1.2 Gridness: The spatial periodicity of the grid pattern

Gridness measures the hexagonal regularity of the grid pattern. The threshold for inclusion as a grid cell was set at ≥ 0.25 . For all recorded grid cells (ALLGRIDS; $n=51$) the mean gridness was 0.72 ± 0.04 and for the subiculum-only sample (SUBGRIDS; $n=30$) the mean gridness score was 0.65 ± 0.04 . The average gridness scores of grid cells recorded from nearby locations to the subiculum was higher than for the subicular grid cells. This is shown when comparing the SUBGRIDS ($n=30$) mean gridness score 0.65 ± 0.04 to the non-subicular grid cells ($n=21$) mean gridness score 0.84 ± 0.07 ; $t_{49}=2.392, p=0.023$.

4.1.3 Neighbouring grid cells share a common orientation

The mean orientation of the grid cells as determined by the spatial autocorrelation (see methods for procedure) was fairly consistent for grid cells within rat (and region) but varied between rats (see Figure 4.1.4 below). Subicular grid cells were recorded simultaneously from both hemispheres from two rats (rats 301 and 304). The mean orientation of the grid cells recorded across hemispheres did not significantly differ. For rat 301 the mean orientation of the left hemisphere grid cells ($n=4$; $8.00 \pm 1.35^\circ$) was not significantly different compared to the right hemisphere grid cells ($n=4$; $4.00 \pm 1.47^\circ$; $t_3=1.43, p=0.25$). Similarly the mean orientation in rat 304 in the left hemisphere grid cells ($n=3$; $39.66 \pm 1.33^\circ$) was also not significantly different to the right hemisphere grid cells ($n=9$; $39.00 \pm 3.55^\circ$; $n=9, t_{10}=0.10, p=0.92$). In one rat 305 grid cells were recorded from the subiculum in one hemisphere ($n=5$) and from the subiculum and surrounding regions ($n=5$) in the other. The mean orientation of the grid cells recorded from the subiculum ($40.32 \pm 8.02^\circ$) was significantly different from the mean orientation of the grid cells recorded from and around the subiculum ($n=5$; $4.4 \pm 1.75^\circ$; $t_4=4.13, p=0.015$). This suggests that orientation may not be consistent across regions. It must be noted that these cell numbers are low and therefore this data must be considered as individual cases.

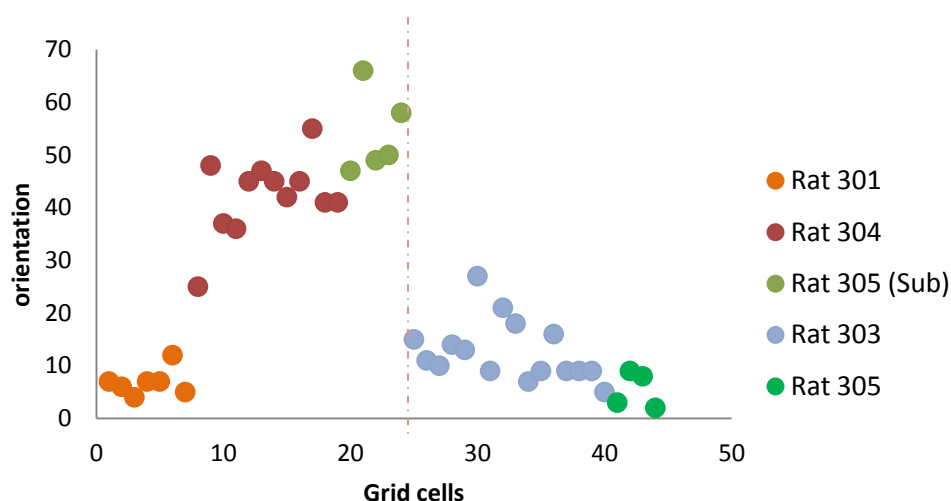


Figure 4.1.4: Grid cell orientation is fairly constant within rat but varies between rats.

Graph shows data from rats where ≥ 4 grid cells are recorded (301,303,304,305). The vertical dashed line separates the subicular cells on the left from the non-subicular cells on the right. The orientation data was taken from the highest-gridness trial (either from the large walled circular, large walled square or the circular open platform).

4.1.4 Grid scale varies across the grid cell sample

Grid scale reflects the distance between the grid fields. Grid scale was measured as the median distance from the central peak in the spatial autocorrelogram to the six surrounding peaks (see methods for more details). The grid scale varied across the sample. For example looking only at the large walled circular and square environments (LWC and LWS) the grid scale for the SUBGRIDS, $n=26$ ranged from 32.70cm to 94.40cm. See figure 4.1.2 for the grid scale for all cells in the highest-gridness trials.

4.1.4.1 Grid scale is determined by anatomical location

In hippocampal place cells and entorhinal grid cells, spatial scaling is linked to anatomical location along the long axis (Jung et al, 1994; Hafting et al., 2005) with smaller grid scales dorsally/septally, and larger grid scales ventrally/temporally. I examined the relationship between grid scale and anatomical location using distance behind the posterior end of dorsal commissure (hereafter 'PDC', ~ 5.2 mm behind bregma, Paxinos and Watson, 2007) to define a long axis through the dorsal subiculum. To avoid the sampling bias that only small-scale grids are detectable in small environments, the analysis was conducted only on cells recorded in

the large environments (LWC and LWS, $n = 26$ i.e. 4 cells excluded). I recorded more cells from anterior locations (≤ 0.3 mm PDC, $n = 19$, mean 0.24 ± 0.03 mm PDC) than from posterior locations (≥ 0.6 mm PDC, $n = 7$, mean 1.11 ± 0.21 mm PDC). As with entorhinal grids, anatomical location determined grid scale (Figure 4.1.5). The grid scale of anteriorly-located cells (56.17 ± 4.99 cm) was 20cm shorter than for the posteriorly-located cells (77.32 ± 6.98 cm; $t_{24} = 2.28$, $p = 0.032$). This was true whether I used the highest-gridness score trials (above), walled-environments only trials (LWC and LWS trials $n=26$; anterior grid scale 56.63 ± 5.2 cm; posterior grid scale 77.32 ± 6.98 cm; $t_{24}=2.16$, $p=0.041$), or environmentally-identical trials (LWC trials only $n=21$; anterior grid scale 60.88 ± 6.37 cm; posterior grid scale 80.50 ± 5.29 cm; $t_{18,29}=2.37$, $p=0.029$).

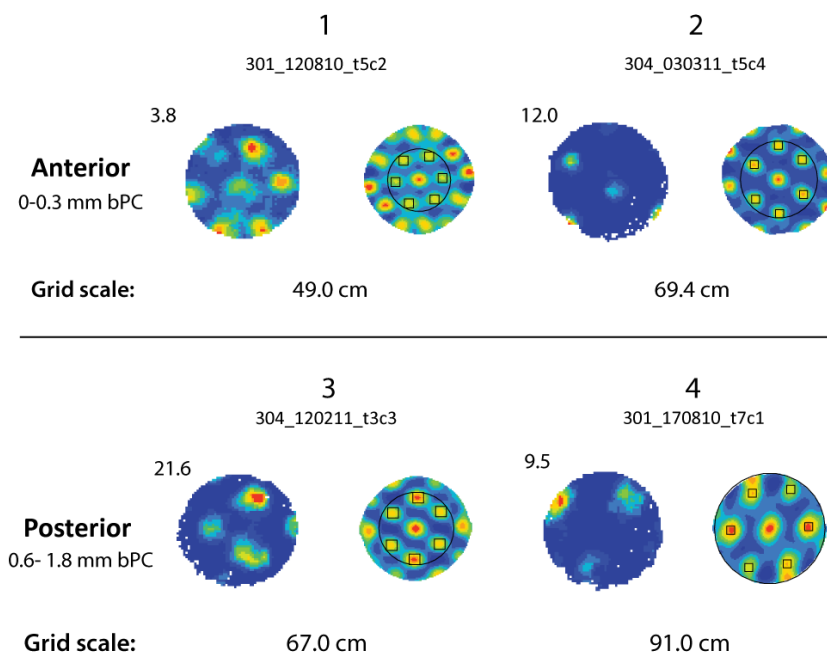


Figure 4.1.5. Anatomical position along the anterior-posterior axis determines grid scale.

Rate maps and spatial autocorrelations for two representative anterior (cells 1 and 2) and posterior (cells 3 and 4) recorded grid cells. For each location, the grid cell above (right) and below (left) the median are shown, the median taken from the environmentally-identical analysis comparing grid cells recorded in the large walled circle (14 anterior and 7 posterior).

4.1.5 Gridness correlates with theta modulation

In a comparison of different cell types in the entorhinal cortex, presubiculum, and parasubiculum, Boccara et al., (2010) make the general observation that grid cells are more theta modulated than border and HD cells (Boccara et al., 2010; see also Cacucci et al., 2004). However, no previous study has shown a direct positive correlation between gridness and theta modulation within a normal grid cell sample. Figure 4.1.6 shows a strong positive linear correlation between gridness and theta modulation (ALLGRIDS). There was a trend in the subiculum only dataset (SUBGRIDS $n=26$) however, this did not reach significance (Table 4.1.1). The positive correlation demonstrated in the ALLGRIDS sample may provide further suggestive evidence of the link between theta oscillations and grid patterns of firing (Table 4.1.1, Figure 4.1.6).

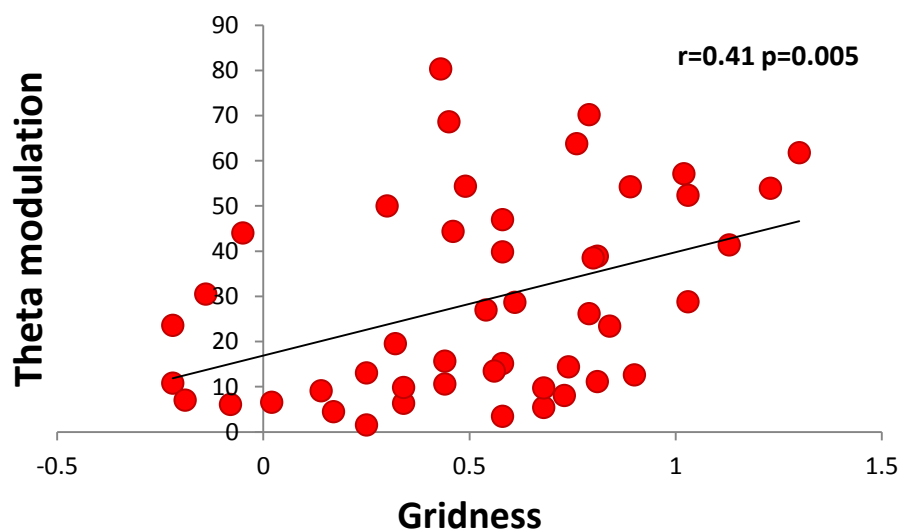


Figure 4.1.6. Gridness positively correlates with theta modulation.

There is a clear significant correlation between gridness scores and theta modulation. This data used the first large walled environments of the day (LWC or LWS) to control for the running order of the trials. Analysis includes 47/51 grid cells from the ALLGRIDS sample. 4 cells were excluded because they were run in the small environments only.

4.1.5.1 The correlation between gridness and theta modulation is not due to other factors

To ensure that the gridness score theta modulation correlation was not a by-product of other factors, gridness was also tested against locational peak rate, total spike count, global mean rate and average running speed (see Table 4.1.1 below). There was no relationship between spatial periodicity (gridness) and rate factors for either the ALLGRIDS or SUBGRIDS samples.

Table 4.1.1. Gridness correlates with theta modulation but not other factors.

For the ALLGRIDS sample gridness scores (mean gridness; 0.65 ± 0.04) correlate with theta modulation but not rate factors. There was a trend suggesting this relationship in the SUBGRIDS sample (mean gridness; 0.84 ± 0.07), however this did not reach significance. This analysis used the best gridness score trials and included only the 47 grid cells recorded in large environments. Locational peak rate was taken from unsmoothed rate maps (bin size 3cm x 3cm).

Gridness vs	Theta modulation	Locational Peak rate	Total Spike count	Global Mean rate	Average running speed
ALLGRIDS (N=47)					
Mean \pm SEM	29.00 \pm 3.17	9.15 \pm 0.81	3821.81 \pm 547.43	1.87 \pm 0.29	15.29 \pm 0.50
r value	0.41	0.10	0.04	-0.02	0.14
p value	0.005	0.49	0.81	0.87	0.36
SUBGRIDS (N=26)					
Mean \pm SEM	30.4 \pm 4.52	8.12 \pm 0.88	2761.92 \pm 453.82	1.17 \pm 0.18	14.82 \pm 0.65
r value	0.30	0.04	0.07	0.10	0.11
p value	0.14	0.85	0.71	0.62	0.59

4.2 Boundary Vector cells (BVCs)

A BVC fires whenever an environmental boundary intersects a receptive field located at a specific distance from the rat in a specific allocentric direction. The firing of a BVC depends solely on the rat's location relative to environmental boundaries and is independent of the rat's heading direction.

4.2.1 BVC classification criteria

When an appropriately-oriented barrier is inserted into a testing environment, a BVC is expected to develop an additional Locational field in response to that additional boundary. Lever et al., (2009) and Solstad et al., (2008) showed this for a subset of boundary cells. I also noted that additional Locational fields in response to additional, appropriately-oriented boundaries could be seen following the addition of extra 'drop'-type boundaries (wall-less edges). The general property of extra locational fields developing following the creation of additional, appropriately-oriented, boundaries was present in most boundary cells. In this thesis, this property was used as a defining feature of BVCs. If a boundary cell did not exhibit this property it was classed as a 'non-BVC boundary cell.'

Cells that showed boundary coding for the perimeter of the large walled circle and or the large walled square were given subsequent trials with the addition of a free-standing internal barrier. Only in cases where the barrier was oriented correctly to the cells preferred direction, were they considered further. Figure 4.2.4b shows 5 cells where the barrier was incorrectly oriented and the cells were classed as 'non-BVC boundary cells'. 57 cells showed boundary coding for the perimeter and were given a barrier in the correct orientation.

As per the model and Lever et al., (2009) the second firing field for the inserted barrier was expected to follow the barrier on its predicted side. To quantify the BVC response a firing rate threshold was set. In general boundary cell firing fields were well isolated, with little back ground firing. The fields generally consisted of spikes with >40% peak firing rate (green pixels on the rate maps), whilst background firing was less than 40% (dark and light blue on the rate maps). To be included as a BVC the second field had to consist of pixels with firing rates of over 40% along of the barrier. A threshold of coverage along the predicted side of the barrier was also set. This was calculated as the percentage of pixels showing $\geq 40\%$ peak firing rate

along cover 116 The number of boundary cells which could be classified as BVCs, varied if the barrier Id was manipulated (Table 4.2.1). For this thesis the threshold was set to 50%. Figure 4.2.1 shows the 42 BVCs were classified using this criterion. The coverage along the predicted side of the inserted barrier (at a firing rate of $\geq 40\%$) of these BVCs was $82.52 \pm 2.41\%$ (see Figure 3.14.1 in methods for examples).

Two cells were classified as BVCs which had long-range fields which were located off the boundary rather than being tightly juxtaposed (See Figure 4.2.3). As shown in Figure 4.2.3 the BVC fields double with barrier insertion but the second field is located away from the barrier. Lever et al., (2009) recorded a small number of these BVCs. However, generally short-range BVCs are more numerous than longer-ranged BVCs.

Two further cells did not present double firing fields with the addition of a barrier, but they did respond to multiple boundaries in a different manipulation (Figure 4.2.2). These cells responded to boundaries created when three platforms were pulled apart to make 10 cm gaps between them (see methods for more details). This provided 2 edges which the rat could voluntarily cross. Both BVCs treated this split platform as containing 3 north-west boundaries. In response they exhibited 3 firing fields akin to the field doubling seen with the insertion of a barrier (Figure 4.2.1).

In summary 46 cells in total were classified as BVCs. 42 produced double fields with barrier insertion, 2 had fields located off the boundary and 2 signalled the boundaries in the together-apart manipulation. Cells that failed to show adequate field doubling/tripling with the addition of extra boundaries, were classed as 'non-BVC boundary cells' (see Figure 4.2.4).

Table 4.2.1. The number of boundary cells classified as BVCs changes if the threshold of barrier coverage by the second field is varied.

To be included as a BVC a second field had to be created consisting of bins $\geq 40\%$ of the peak rate along $\geq 50\%$ of the barrier. (highlighted in the table). Initially there were 57 putative BVCs identified. By applying this threshold the number of included BVCs by this classification was reduced to 42.

	>20%	>30%	>40%	>50%	>60%	>70%
No. of cells reaching the coverage threshold	50	47	46	42	41	36

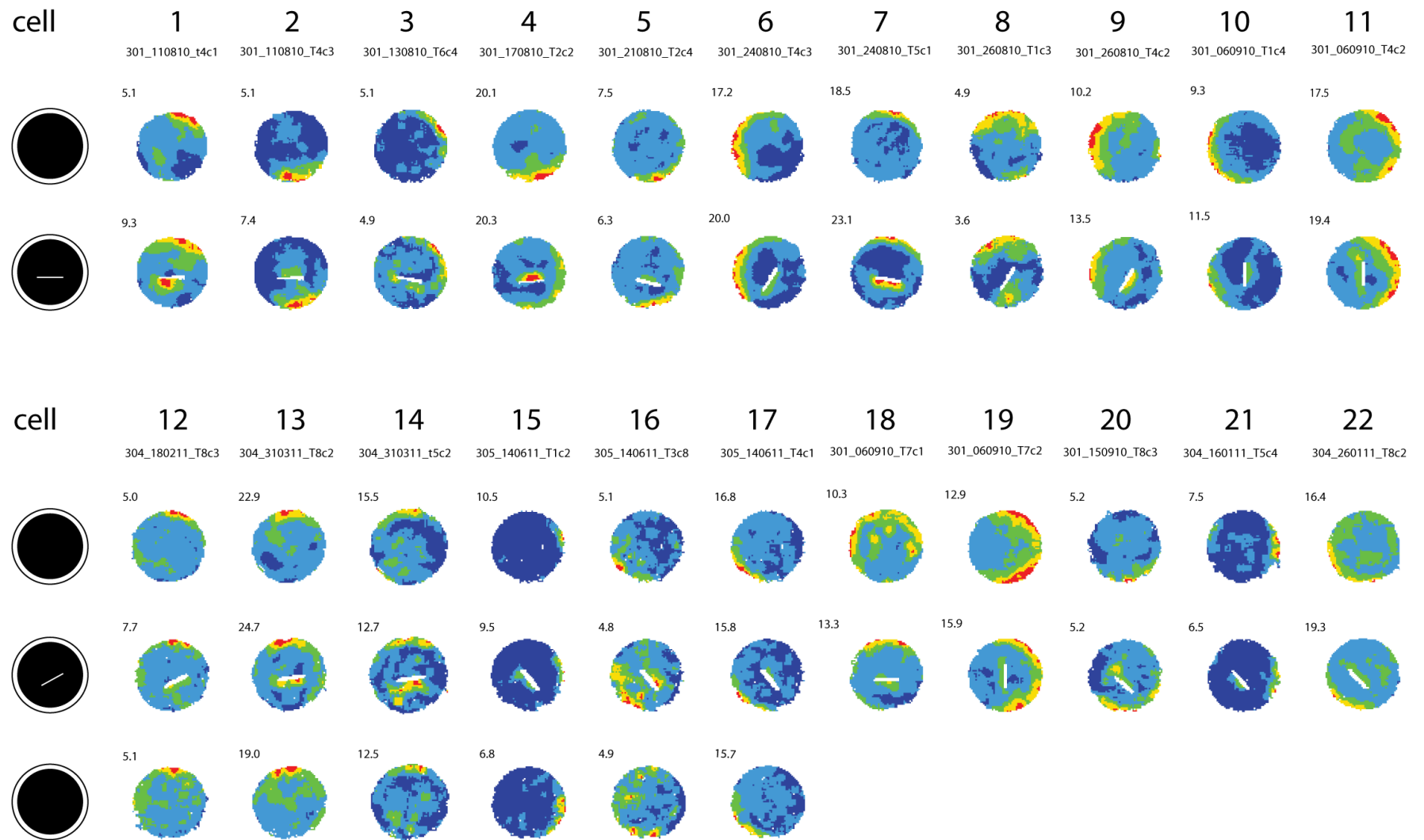


Figure 4.2.1. BVCs develop extra locational fields following the insertion of an appropriately-oriented barrier.

The production of an additional locational field with the addition of a second boundary has been used in this thesis to classify BVCs. The second field needed to consist of spikes with >40% peak firing rate (green pixels on the rate maps), along at least 50% of the additional barrier. Boundary cells which did not produce the second field were classed as non-BVC boundary cells. 42 BVCs were classified using this property. (Figure continues on the next page).

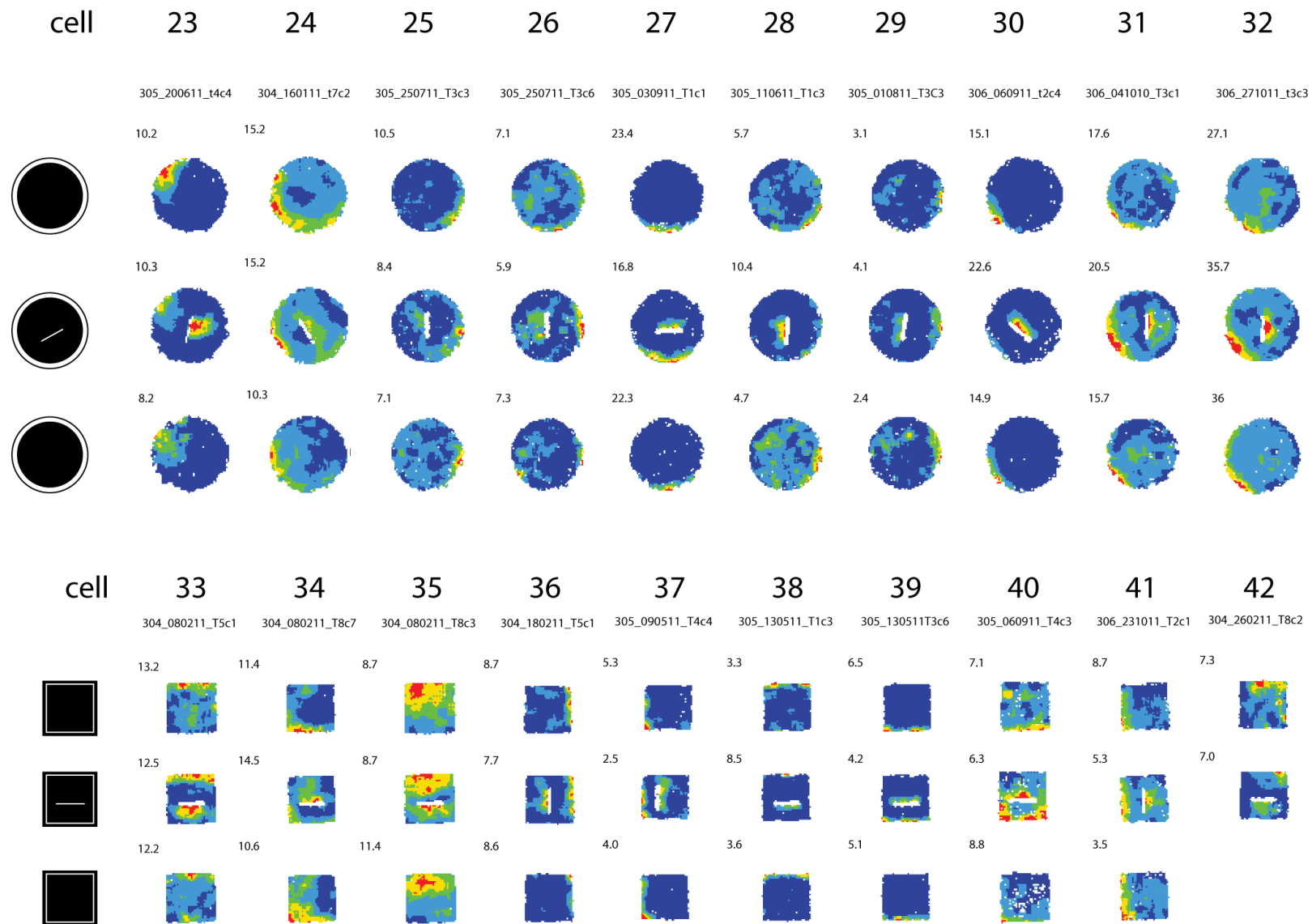


Figure 4.2.1. continued.

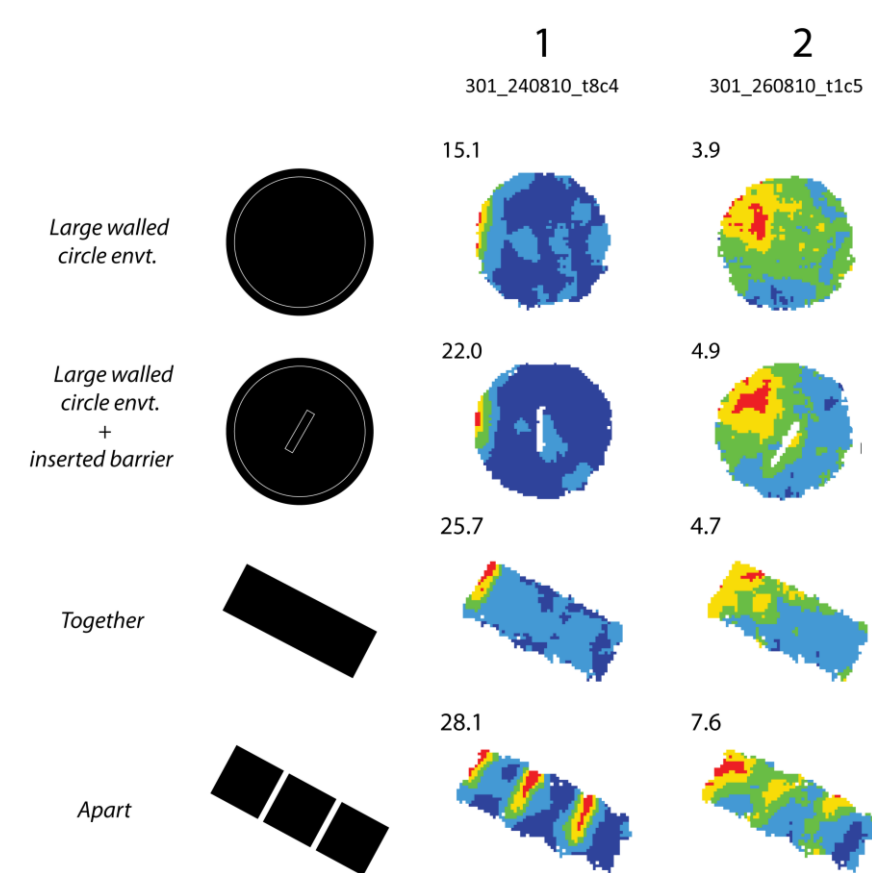


Figure 4.2.2. BVCs can respond to environment drops and traversable gaps as well as walls.

Two BVCs were classified based on their firing for environment drops and traversable gaps in the together-apart manipulation. As the figure shows neither BVCs showed a clear additional locational field for the insertion of an appropriately-orientated barrier; cell 1 did not produce a second field and cell 2's field was so broad that the addition of a second field was not clear.

However in the together-apart manipulation both cells show clear locational fields. The 'together' trial is in a rectangular open platform consisting of 3 square platforms. In this environment both cells demonstrate a clear second field in response to the environment drop. When these platforms were separated by 10cm in the 'apart' trial two additional boundaries were created. In this trial both cells responded by providing two additional fields for these additional boundaries.

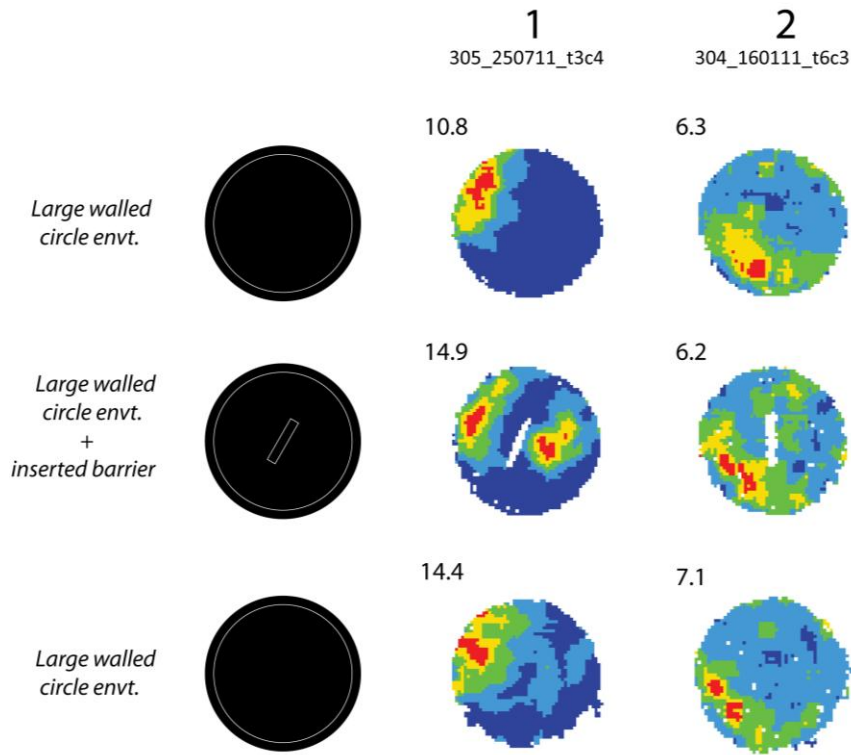


Figure 4.2.3. Two BVCs had long-range fields.

Two BVC had long-range fields which were located away from the boundaries. For both BVCs, the locational fields were located away from the boundary when responding to the perimeter wall and the inserted barrier.

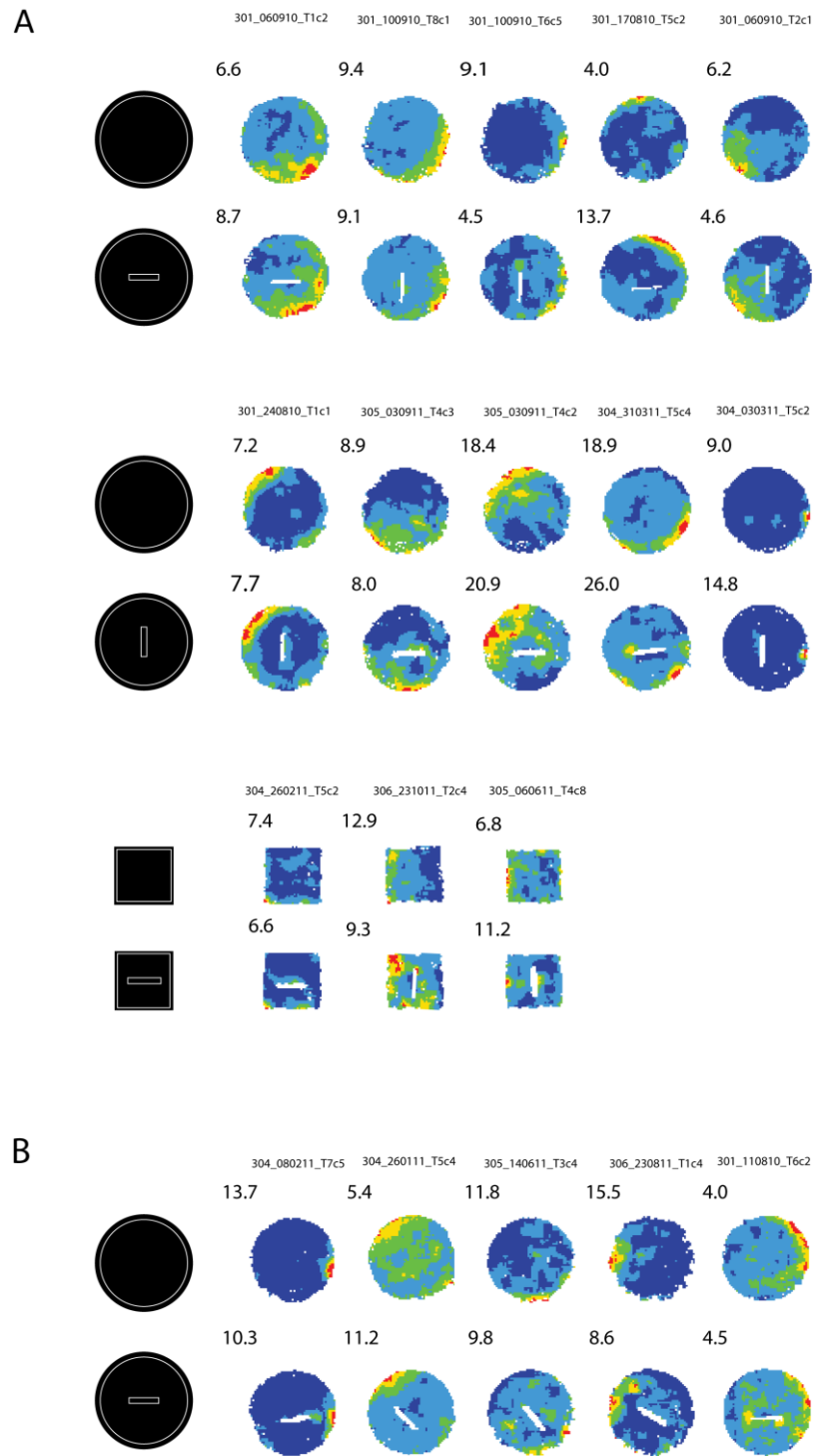


Figure 4.2.4. Non-BVC boundary cells: Boundary cells which did not show sufficient field doubling with boundary insertion were classed as non-BVC boundary cells.

Boundary cells were identified using visual inspection of rate maps. 18 boundary cells were excluded because they did not produce a second field with the insertion of an internal barrier. A) shows 13 boundary cells which failed to produce a second field at >40% peak firing rate along 50% of the barrier and B) shows 5 cells for which the barrier was not placed in the correct orientation. These boundary cells could not be tested as candidate BVCs.

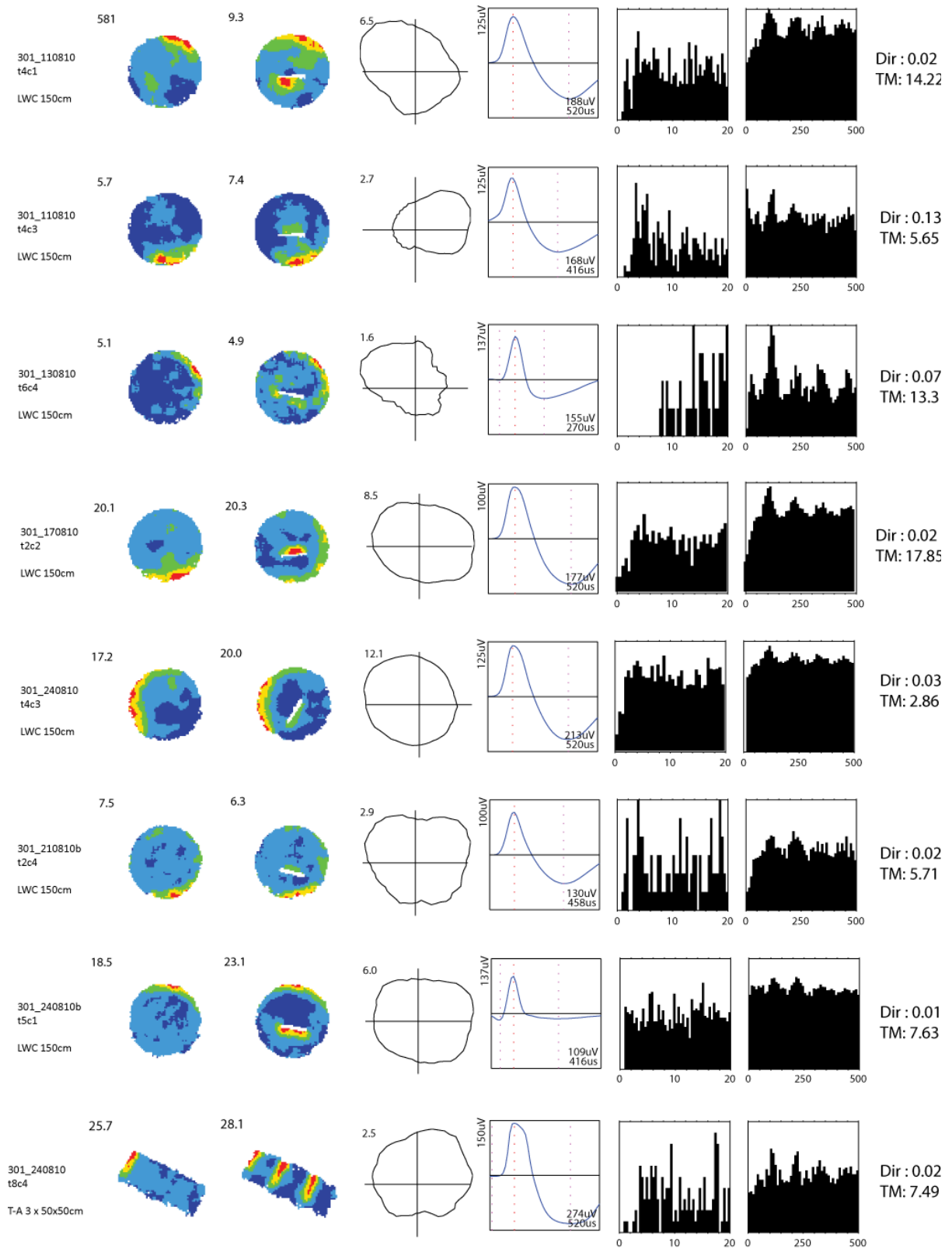


Figure 4.2.5. Basic characterisation of all BVCs (page 1/6)

Figure legend at the end of figure.

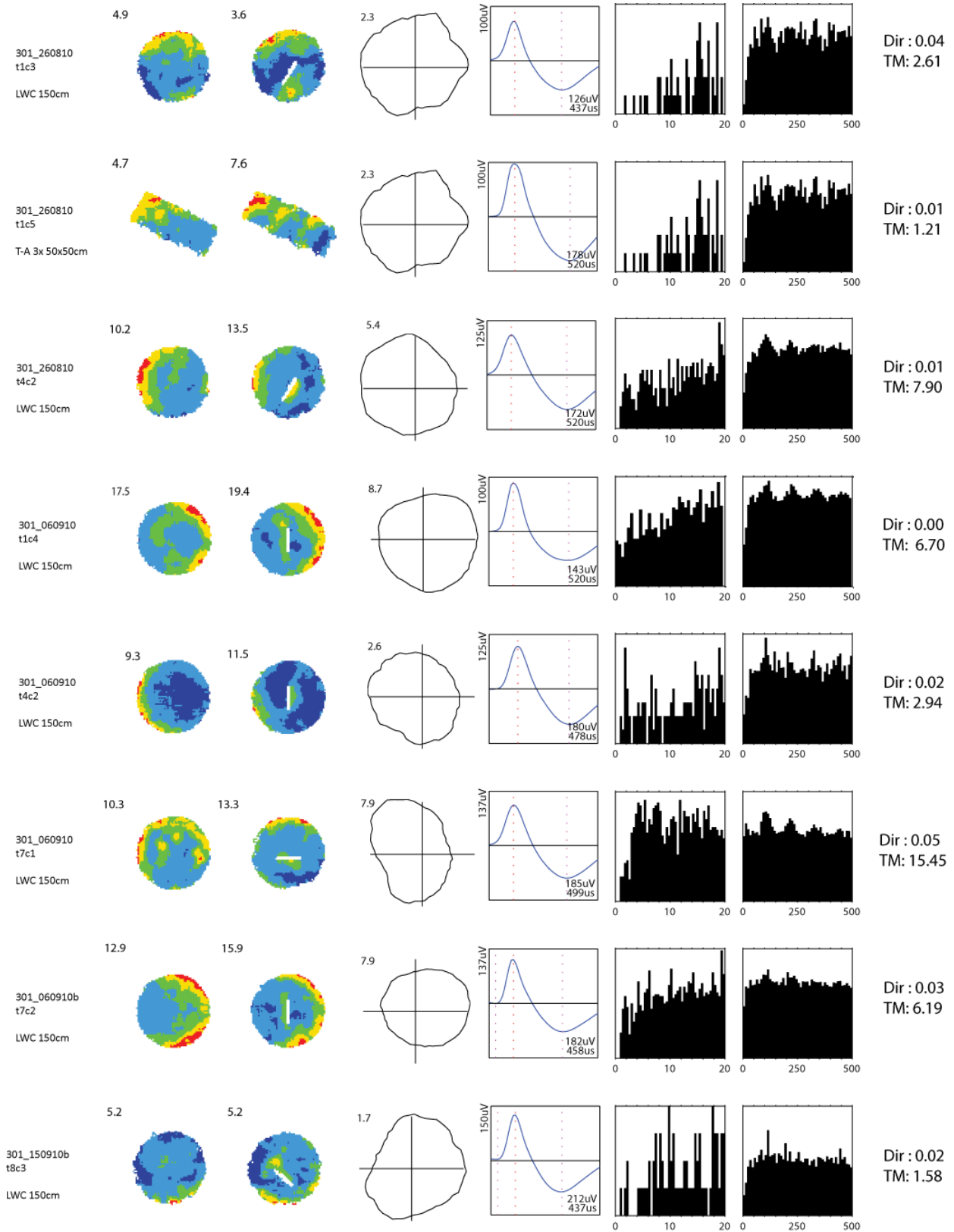


Figure 4.2.5. Basic characterisation of all BVCs (page 2/6)

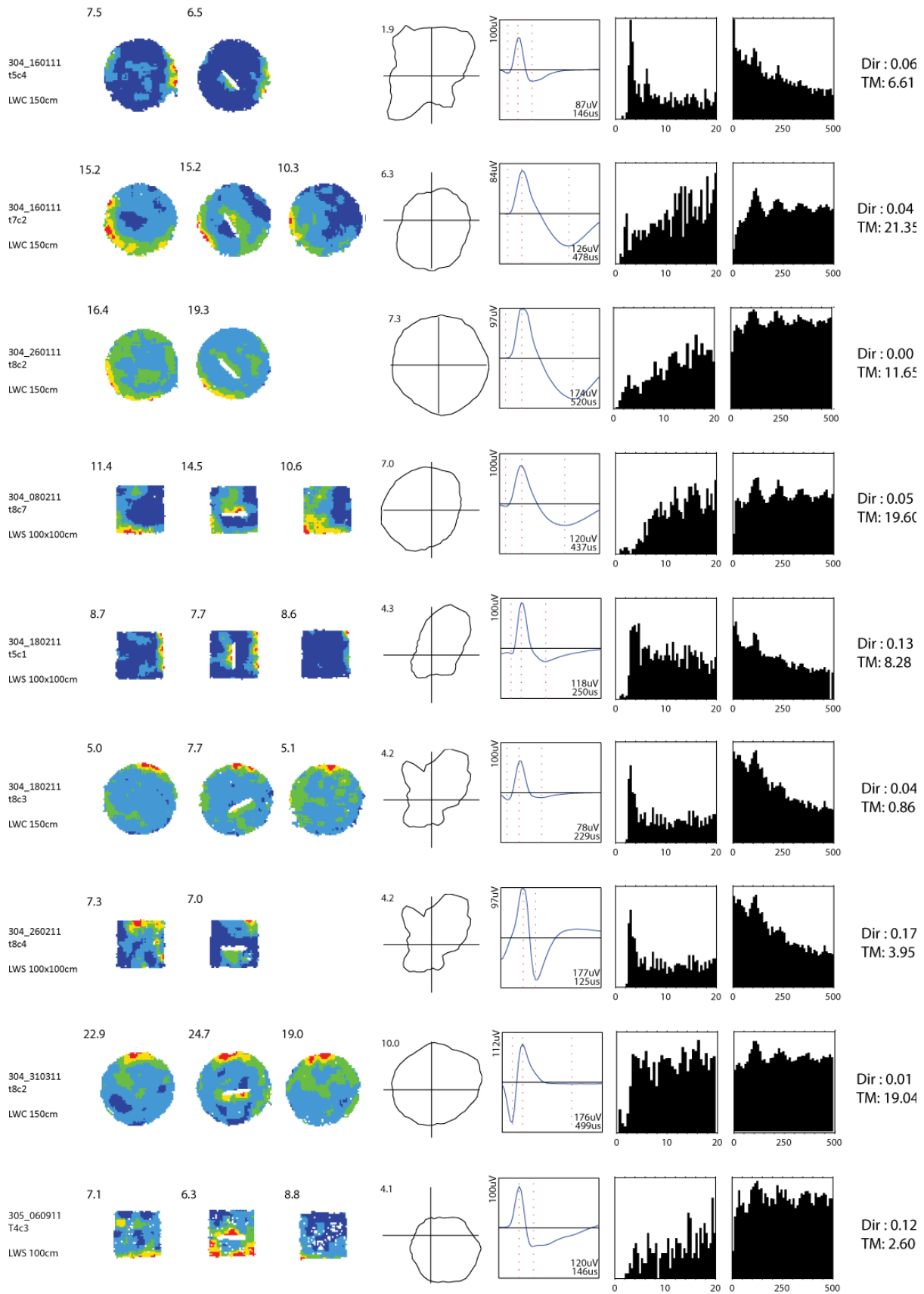


Figure 4.2.5. Basic characterisation of all BVCs (page 3/6)

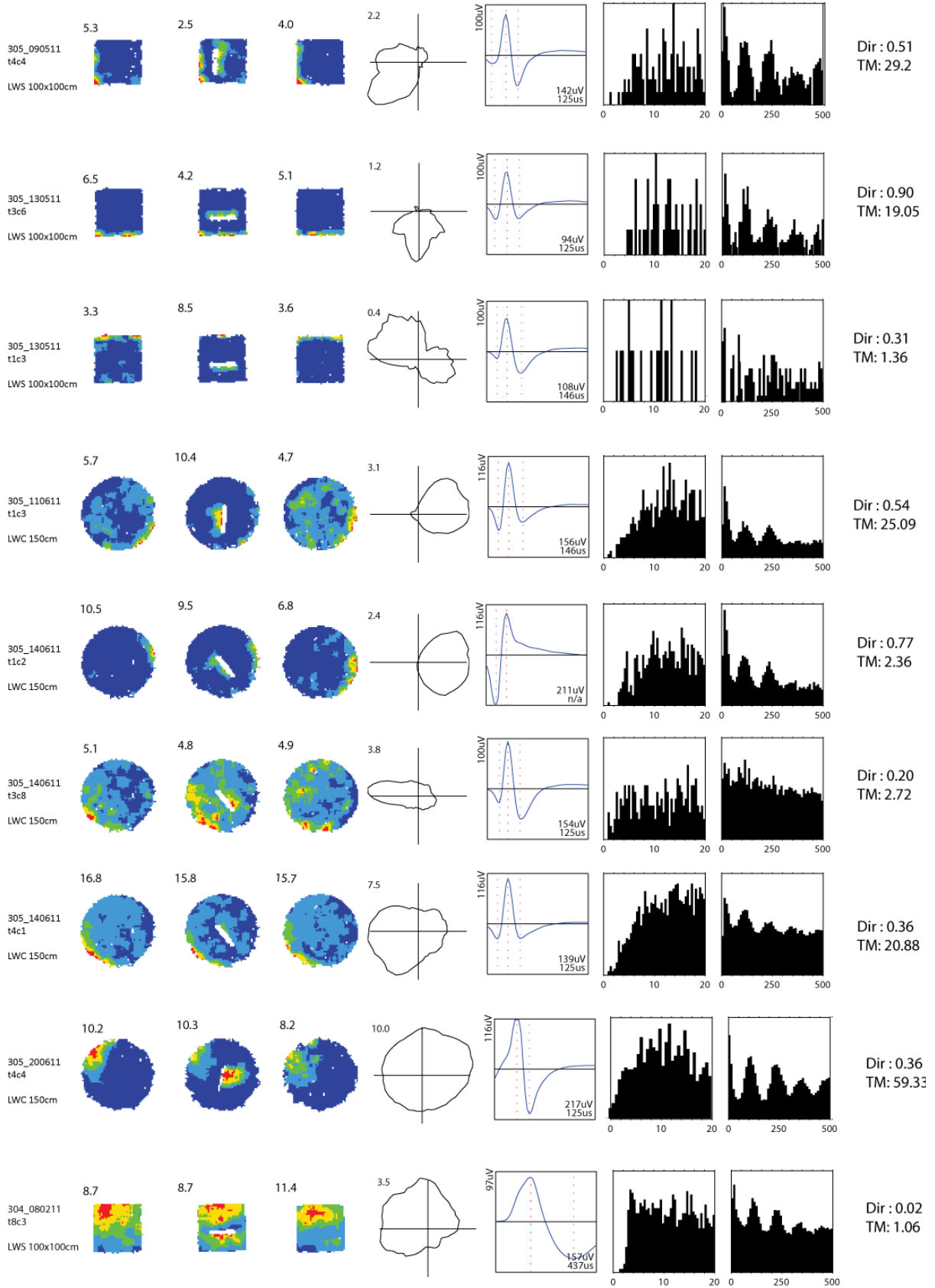


Figure 4.2.5. Basic characterisation of all BVCs (page 4/6)

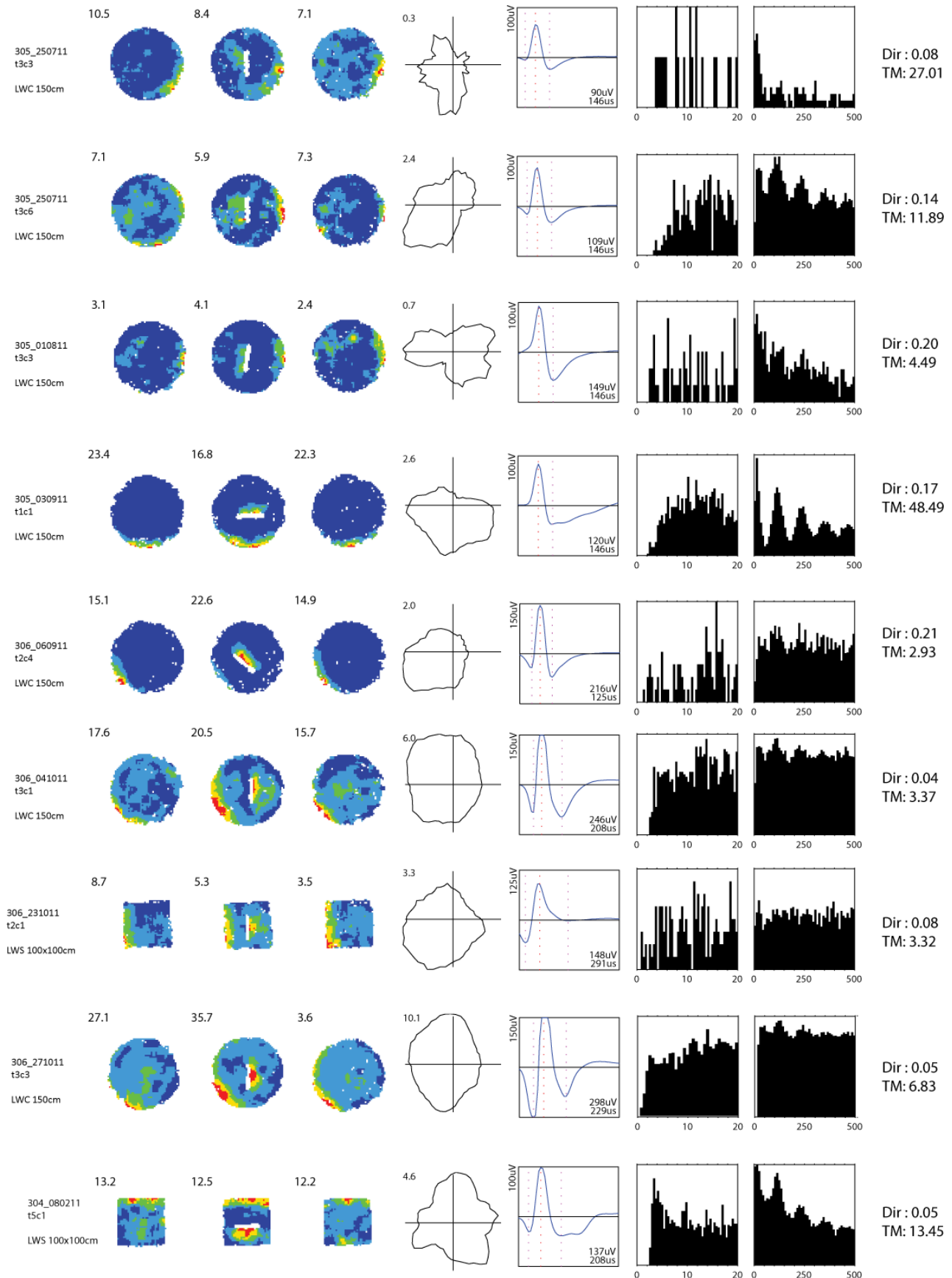


Figure 4.2.5. Basic characterisation of all BVCs (page 5/6)

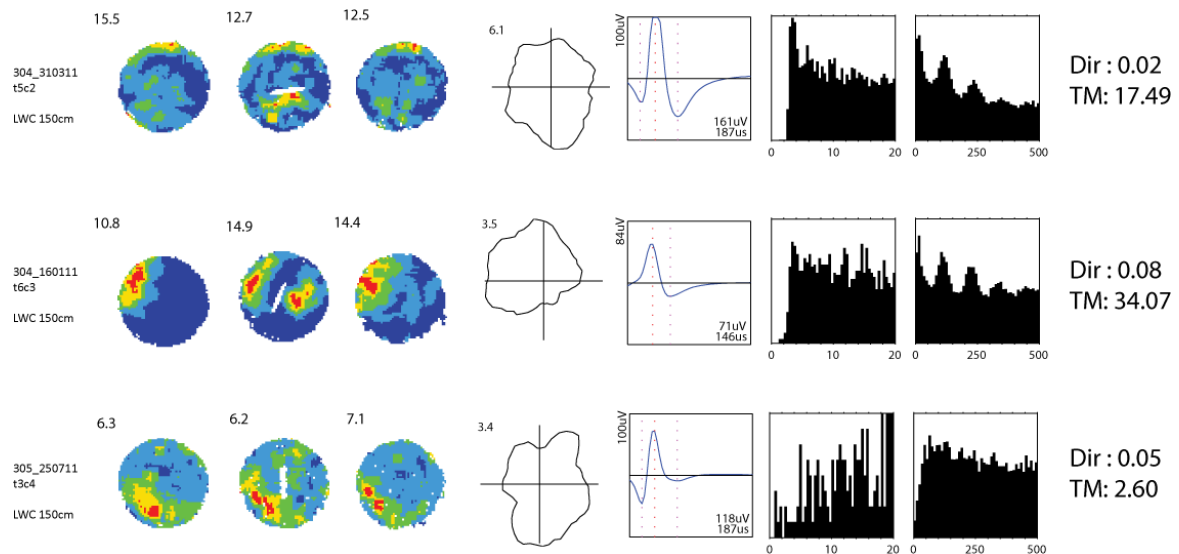


Figure 4.2.5. Basic characterisation of all BVCs cells (page 6/6)

Each row shows data for one BVC. From left to right the figure presents; text column stating rat/day, tetrode/cell, and the recording environment; locational rate map with peak rate (Hz); spatial autocorrelation map; directional polar plot with peak rate (Hz); spike waveform, bottom-right text stating peak amplitude (highest positive-to-negative or negative-to-positive amplitude, μV) and negative peak-to-trough interval (μs); temporal autocorrelations (0-20ms and 0-500ms). Rightmost text column gives the directional information in bits per spike (Dir; calculated from unsmoothed polar plots, bin size 5.6°) and the theta modulation score (TM).

4.2.2 Histology and tetrode localization

BVCs were recorded throughout the subiculum, along the subicular anterior-posterior axis at all depths. BVCs were recorded from 4 rats and from 6 hemispheres. Only boundary-related cells recorded from the subiculum were considered for analysis. As with the grid cells above to determine where along the subicular anterior-posterior axis the BVCs were recorded the distance behind the posterior end of the dorsal commissure (PDC) was calculated (in mm; see methods). As detailed above at the PDC co-ordinate (0mm) the dorsal commissure breaks across the hemispheres. This corresponds to the Paxinos and Watson, (2007) co-ordinate -5.2mm behind bregma (Paxinos and Watson, 2007). Figure 4.2.6 shows the tracks of the recording tetrodes and indicates the estimated recording locations for 41 of the 46 BVCs.

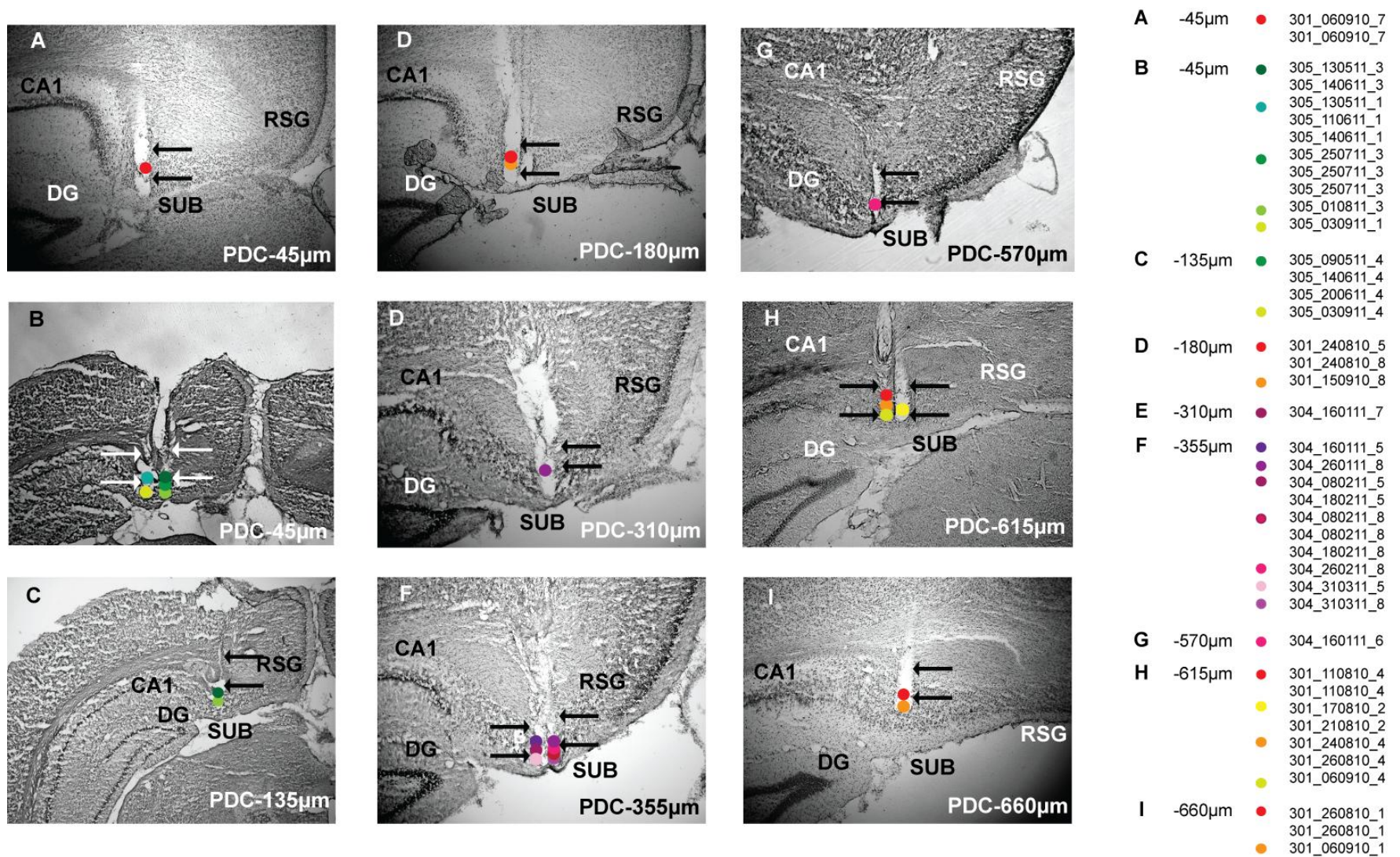


Figure 4.2.6. Estimated recording locations of BVCs.

Nissl-stained coronal sections of the dorsal subiculum. Coloured circles indicate estimated locations of BVCs; arrows indicate tracks of recording tetrodes. Sections arranged in anterior-posterior order (A-I), at increasing distance behind the posterior end of the dorsal commissure (PDC), which is ~5.2mm posterior to bregma. SUB, Subiculum; RSG, retrosplenial cortex; DG, dentate gyrus. To the right of the sections is a key of which BVCs are at which estimated recording locations. These cell numbers correspond to those in the rate map figures. See Figure 4.2.5 for rate maps and spatial autocorrelations for all BVCs.

4.2.3 BVCs carry more locational than directional information

The firing of a BVC depends solely on the rat's location relative to environmental boundaries and is considered to be entirely independent of the rat's heading direction. Lever et al., (2009) found that BVCs carried more locational than directional information. To compare Locational vs directional information within the BVC sample the rate maps and polar plots were corrected for spurious dependencies created by inhomogeneous sampling of orientation and location (described in methods section 3.12.3.3; Burgess et al., 2005; Lever et al., 2009).

Table 4.2.2 shows that BVCs had double the amount of locational information compared to directional information (in both bits per spike and bits per second). Table 4.2.2 also shows that BVCs also had three times more locational selectivity (max. firing rate across 60 bins divided by the mean rate) compared to directional selectivity. This suggests that BVCs have much stronger locational signalling than directional signalling.

Table 4.2.2. BVCs carry more locational than directional information.

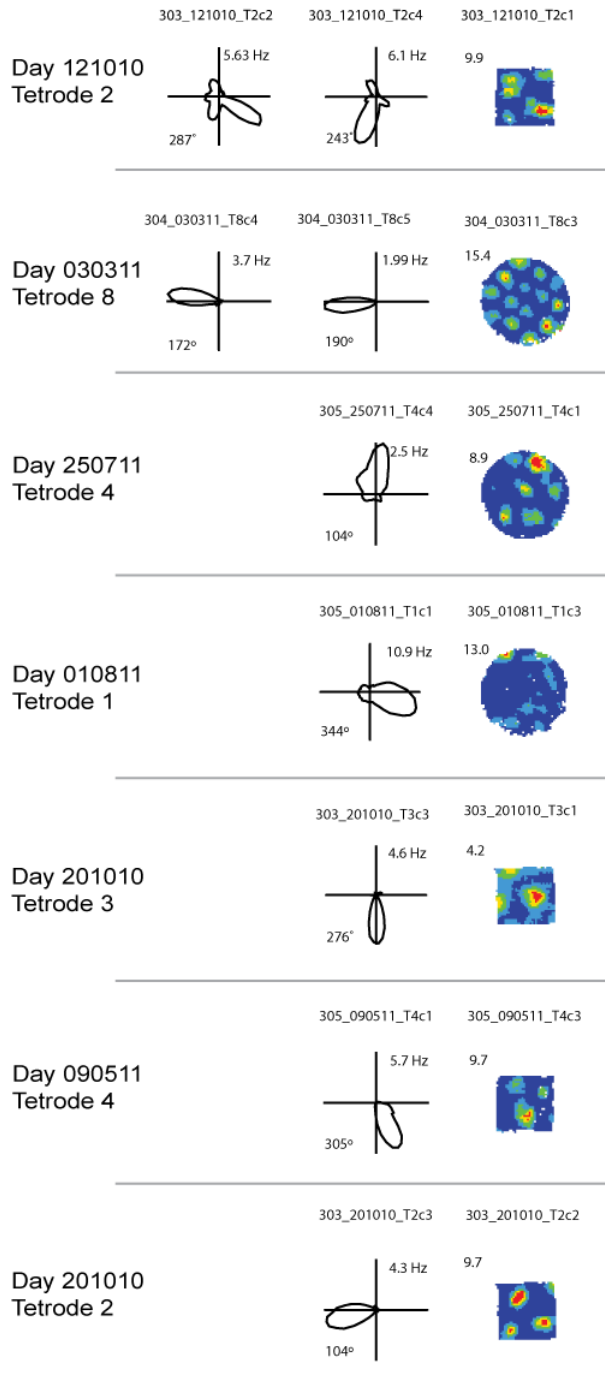
Spatial information is calculated using a corrected analysis (Burgess, 2005) to estimate the locational/directional mutual information in seconds. Spatial information was calculated using locational/directional equivalence binning (60 bins each) from unsmoothed polar plots (bin size 6°) and unsmoothed rate maps (bin size LWC, 18.5cm x 18.5cm; LWS 14cm x 14cm). Selectivity is calculated by dividing the peak firing rate across (Locational/directional) bins by the mean firing rate. Analysis was conducted using the full BVC sample (n=46) in the first large walled circle or large walled square of the day (LWC or LWS).

	MEANS ± S.E.		
	Spatial information Bits/spike	Spatial information Bits/sec	Spatial Selectivity
LOCATIONAL	0.21 ± 0.04	0.40 ± 0.04	5.47 ± 0.96
DIRECTIONAL	0.12 ± 0.03	0.16 ± 0.03	1.76 ± 0.11
p value	P=0.012	p<<0.001	P<< 0.001

4.3 Head direction cells were sometimes recorded simultaneously with grid cells and BVCs

Grid cells and BVCs in the subiculum and in nearby locations were sometimes simultaneously recorded with head-direction cells (HD cells). In total 30 HD cells were recorded from 5 rats. For the basic characterisation of the HD cells see Figure 4.3.2. All HD cells were recorded from the same hemispheres as recorded BVCs and grid cells. 24/30 were recorded from the same tetrodes that recorded BVCs and grid cells. 9 HD cells were recorded simultaneously on the same tetrode with grid cells (Figure 4.3.1A) and, 4 HD cells were recorded simultaneously on the same tetrode with BVCs (Figure 4.3.1B).

A



B

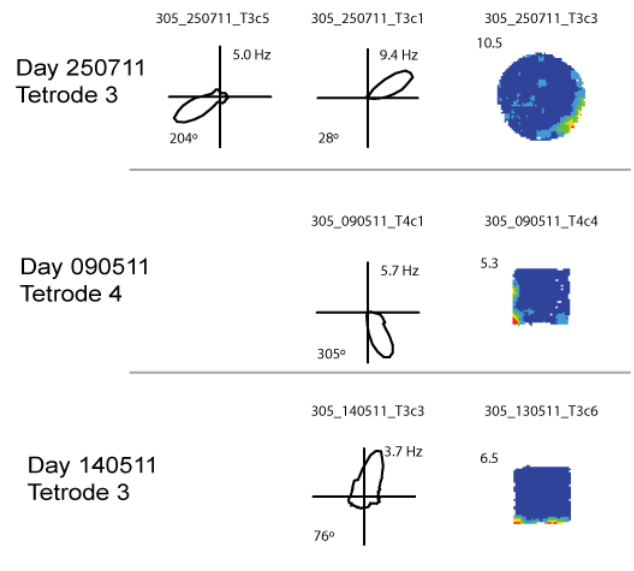


Figure 4.3.1. Head direction cells were sometime recorded simultaneously on the same tetrodes as grid cells and BVCs.

The figure presents the polar plots of the HD cells and peak rate maps of the simultaneously recorded grid cells and BVCs. Each row shows a different recording session. A) 9 HD cells recorded simultaneously on the same tetrode as a grid cell. B) 4 HD cells recorded simultaneously on the same tetrode as BVCs.

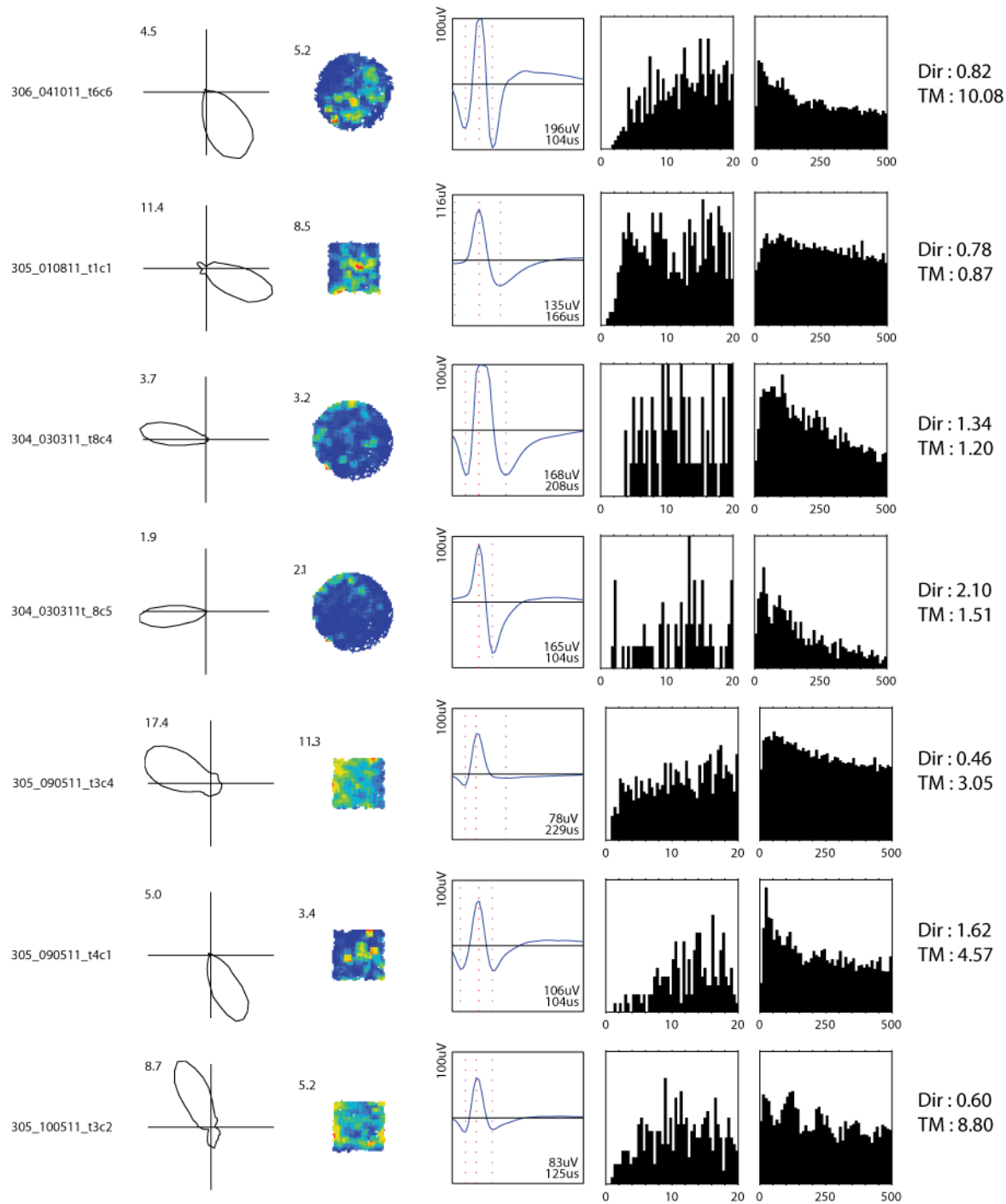


Figure 4.3.2. Basic characterisation of all HD cells (page 1/4)

Each row shows data for one HD cell. From left to right the figure presents; text column stating rat/day, tetrode/cell; locational rate map with peak rate (Hz); spatial autocorrelation map; directional polar plot with peak rate (Hz); spike waveform, bottom-right text stating peak amplitude (highest positive-to-negative or negative-to-positive amplitude, μV) and negative peak-to-trough interval (μS); temporal autocorrelations (0-20ms and 0-500ms). Rightmost text column gives the directional information in bits per spike (Dir; calculated from unsmoothed polar plots, bin size 5.6°) and the theta modulation score (TM).

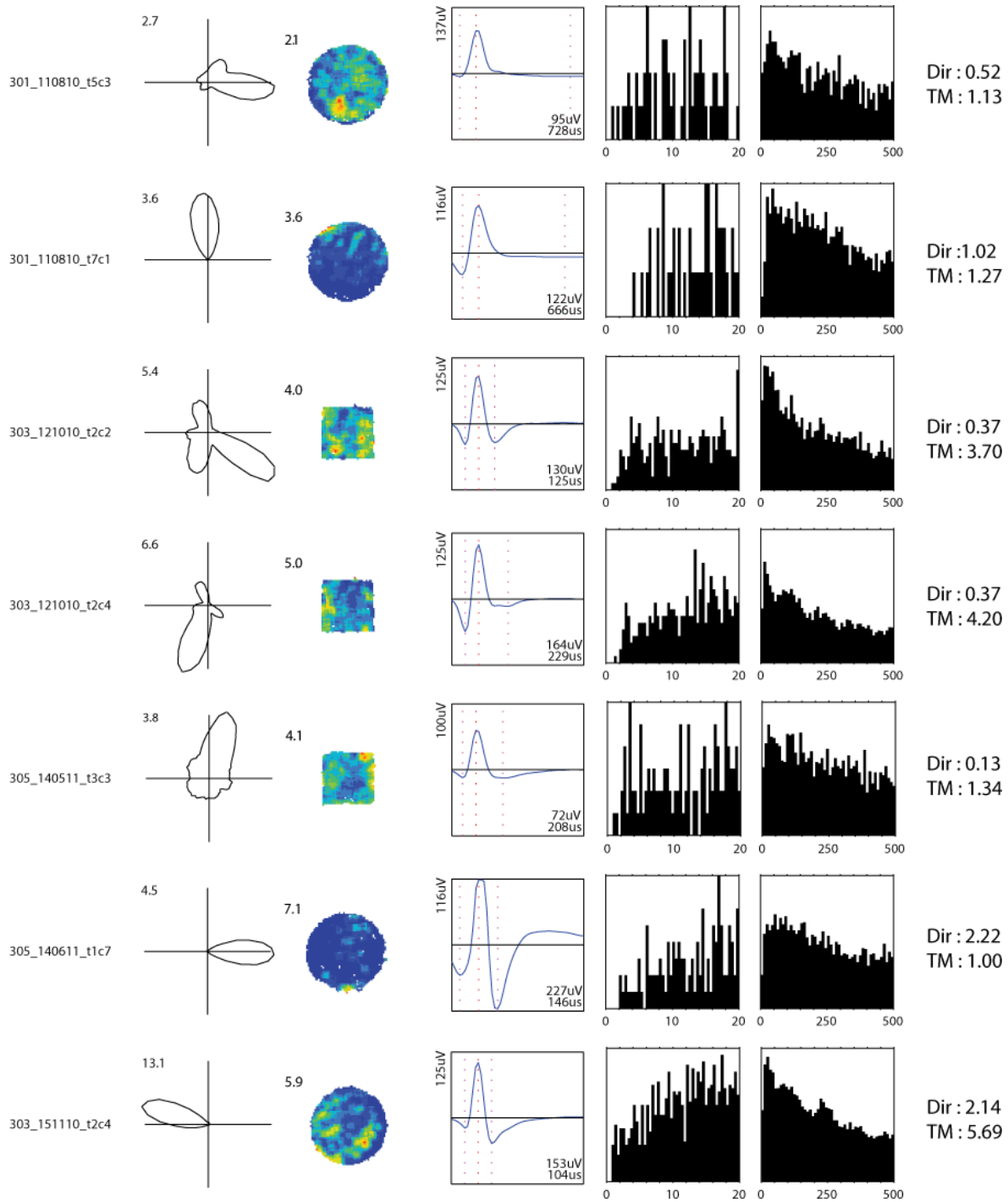


Figure 4.3.2. Basic characterisation of all HD cells (page 2/4)

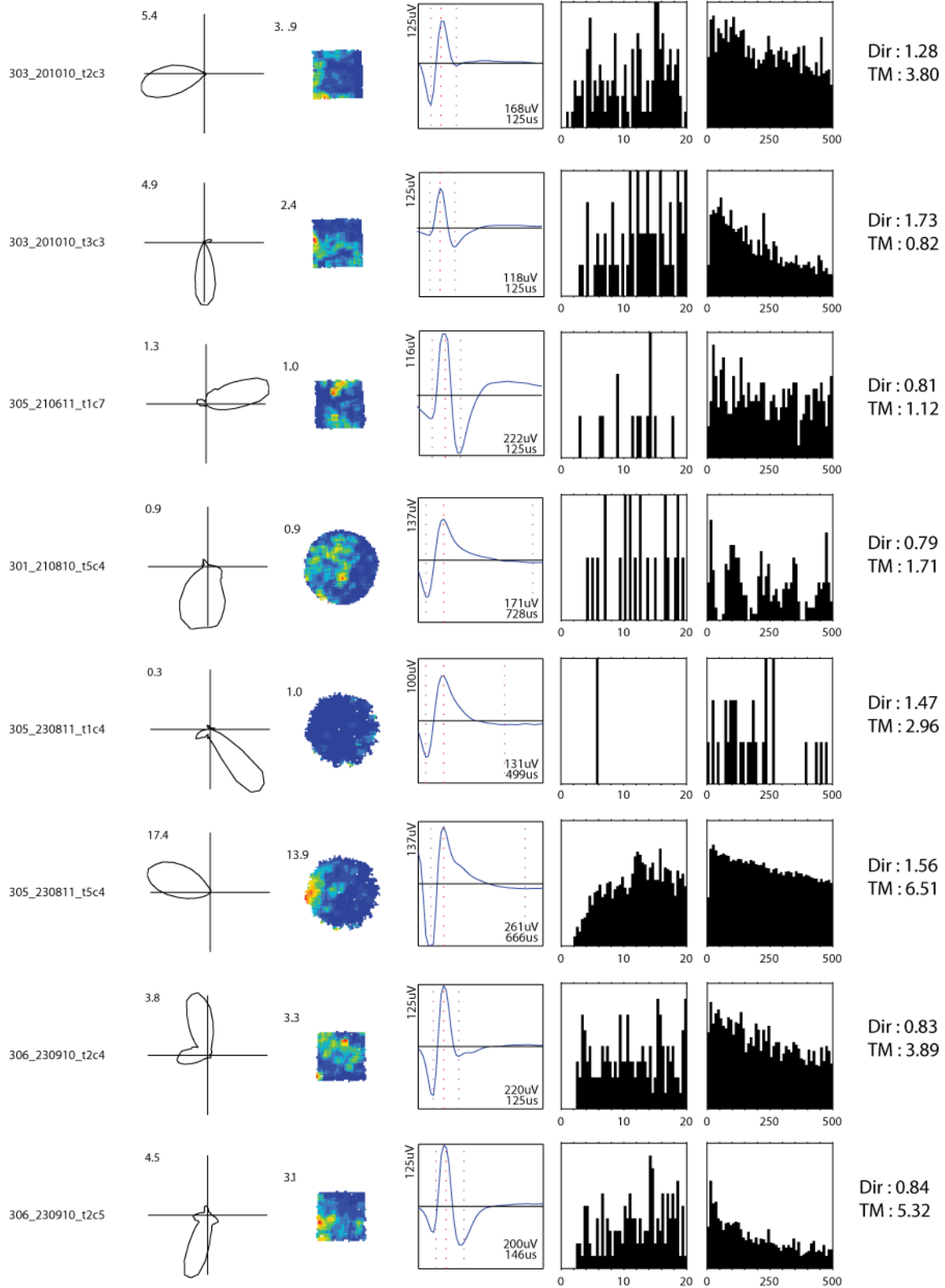


Figure 4.3.2.. Basic characterisation of all HD cells (page 3/4)

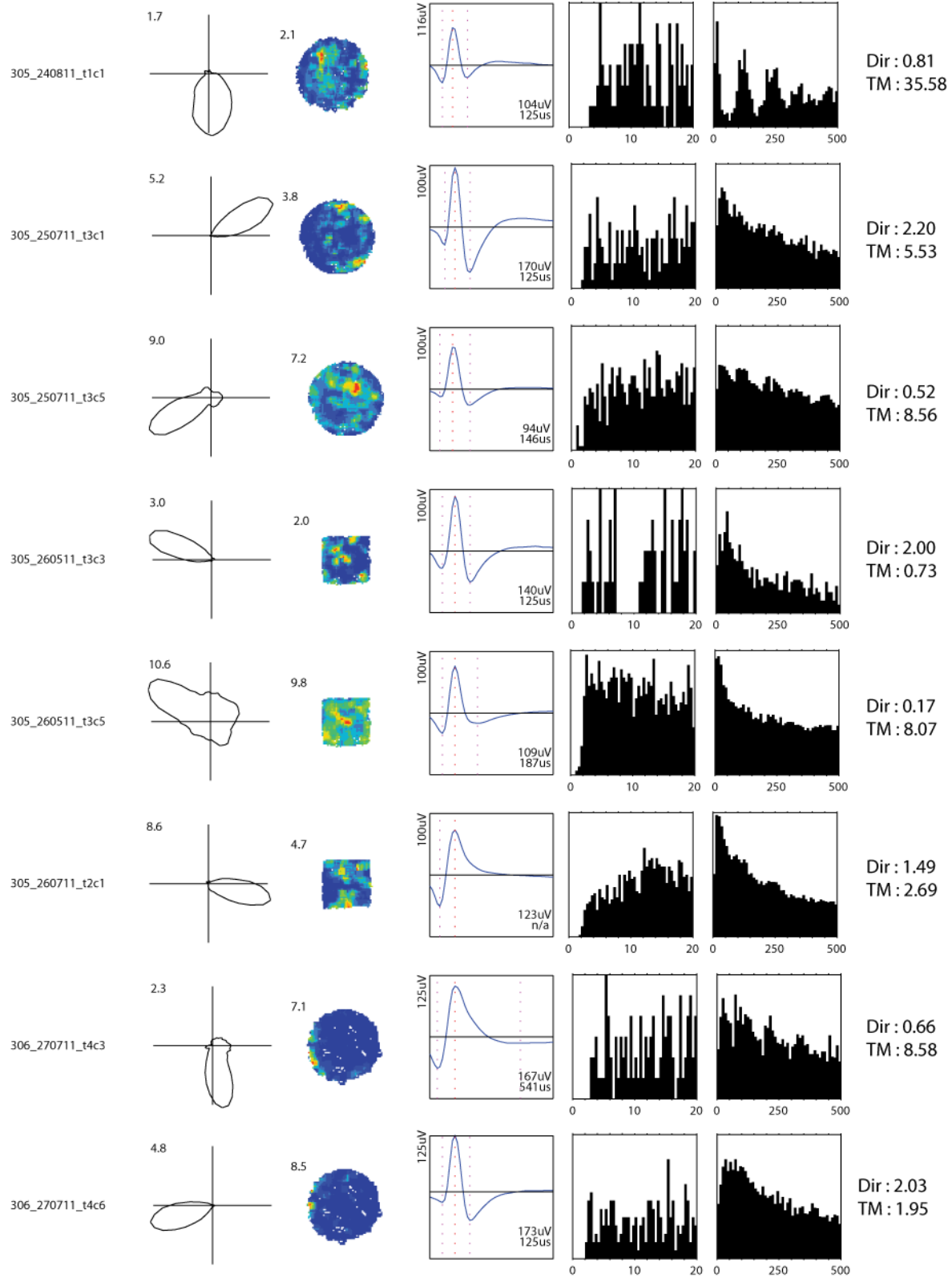


Figure 4.3.2. Basic characterisation of all HD cells (page 4/4)

4.4 Comparison between grid cells, BVCs and HD cells

Grid cells and BVCs in the subiculum and in nearby locations were sometimes also simultaneously recorded with head-direction cells (HD cells). In the next section this thesis compares these three cell types. Table 4.4.1 presents the basic properties of the grid cells (ALLGRIDS and SUBGRIDS), the BVCs and the HD samples. As would be predicted the gridness scores, directional information and theta modulation of the different cell types differed.

Table 4.4.1. Comparison of characteristics between grid cells, BVCs and HD cells.

Data was taken from the first large environment trial of the day (LWC or LWS) to control for trial order and environment effects. Directional information was calculated from unsmoothed polar plots (bin size 5.6°).

	MEAN ± SEM				
	Gridness score	Directional Information (Bits/spike)	Theta modulation score	Waveform duration (interval in μ s)	Global Mean rate (Hz)
ALLGRIDS N=51	0.72 ± 0.04	0.19 ± 0.03	28.70 ± 2.85	225.95 ± 19.89	2.30 ± 0.34
SUBGRIDS N=30	0.65 ± 0.04	0.19 ± 0.04	27.54 ± 3.71	264.85 ± 28.64	2.15 ± 0.43
BVCs N=46	-0.30 ± 0.03	0.21 ± 0.04	11.96 ± 1.84	294.37 ± 24.17	3.17 ± 0.34
HDs N=30	-0.18 ± 0.05	1.16 ± 0.12	4.96 ± 1.24	223.95 ± 35.28	1.35 ± 0.21

4.4.1 No BVCs met the gridness threshold

As mentioned above the mean gridness for putative grid cells ($n=75$) was 0.47 ± 0.05 . Once the gridness threshold for accepting putative cells as grid cells was set at ≥ 0.25 the mean gridness increased to 0.72 ± 0.04 for the ALLGRIDS sample and to 0.65 ± 0.04 for the SUBGRIDS sample. In contrast, out of the BVC sample only 2/46 BVCs had positive gridness scores with the highest gridness value being 0.10. There was therefore no overlap in gridness scores between the classified grid cells and BVC samples.

To compare the gridness scores between the BVCs and the grid cells an independent t-test was run. In order to control for any environment differences gridness scores were compared between the first large walled circle (LWC), large walled square (LWS) or small walled square (SWS) trials of the recording days (LWS and SWS used only when there is no LWC trial). As expected grid cells had much higher gridness scores (ALLGRIDS; 0.72 ± 0.04 ; SUBGRIDS, 0.65 ± 0.04) compared to the BVC dataset (-0.30 ± 0.03 ; $t_{89.38} = 21.01$, $p < 0.0001$; $t_{74} = 19.75$, $p < 0.0001$ respectively).

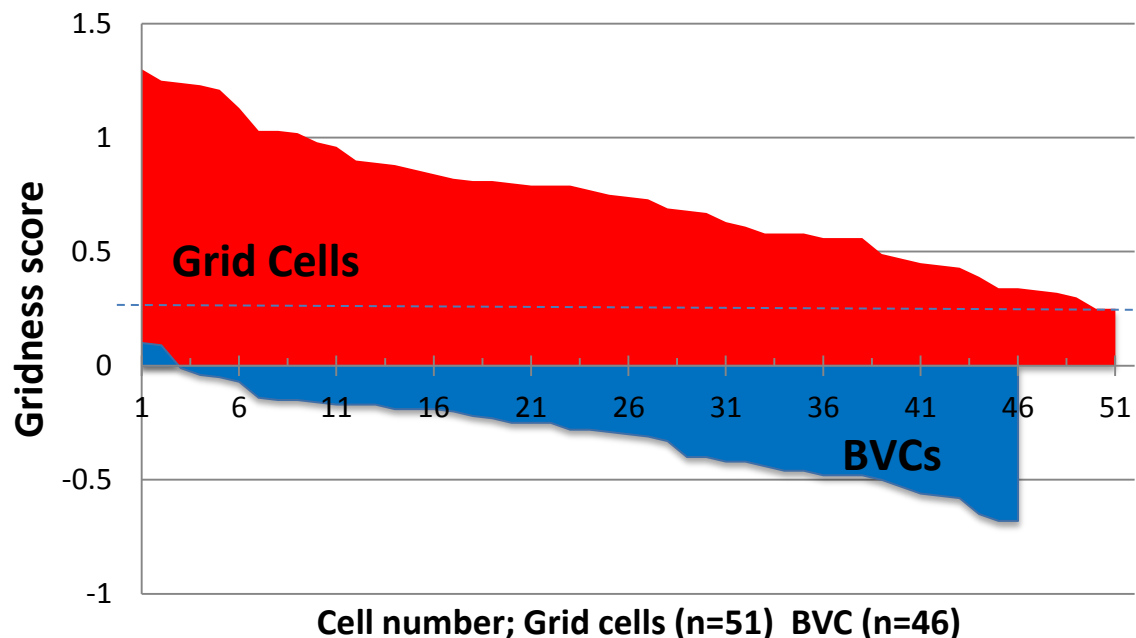


Figure 4.4.1. The BVC sample has significantly lower gridness scores than grid cells.

This figure presents the gridness scores of all recorded grid cells (red) and BVCs (blue). In order to be classified as a grid cell, the cell had to achieve a gridness score of ≥ 0.25 ; threshold indicated by the dotted line. No BVC gridness scores reached this threshold. All BVCs except 2 had grid scores < 0 .

4.4.2 In general HD cells also did not meet the gridness threshold

Of the 30 head direction cells recorded 4 had gridness scores >0 and 2 of which had gridness scores which reached the grid cell classification threshold. As with the BVCs, the grid cells had much higher grid scores (ALLGRIDS; 0.72 ± 0.04 ; SUBGRIDS, 0.65 ± 0.04) in comparison to the HD dataset (-0.18 ± 0.05 ; $t_{79}=14.06$, $p < 0.001$; $t_{58}=13.37$, $p < 0.0001$ respectively).

4.4.3 The spike waveforms of grid cells are shorter in duration than those of BVCs

The grid cells (ALLGRIDS) had significantly shorter peak-to-trough intervals than the BVCs ($t_{89,60}=2.17$, $p=0.03$). However this difference in interval length was not repeated between the subiculum-only grid cells and the BVCs ($t_{74}=0.78$, $p=0.44$). There was no difference in peak-to-trough amplitude between the grid cell samples and the BVCs (ALLGRIDS, $t_{95}=1.46$, $p=0.14$; SUBGRIDS $t_{74}=0.88$, $p=0.93$).

The HD cells had spike waveforms with significantly lower peak-to-trough amplitudes than BVCs ($t_{74}=1.99$, $p=0.05$). The means in Table 4.4.2 suggest that they may also have had shorter peak-to-trough intervals, however this is likely due to low cell numbers is not statistically significant ($t_{74}=1.71$, $p=0.09$).

There were no significant differences between the grid cell samples and the HD cells in either peak-to-trough amplitude (ALLGRIDS, $t_{79}=0.56$, $p=0.58$; SUBGRIDS, $t_{58}=1.48$, $p=0.37$) or in peak-to-trough interval (ALLGRIDS, $t_{79}=0.53$, $p=0.96$; SUBGRIDS, $t_{58}=0.90$, $p=0.37$).

Table 4.4.2. BVCs have longer waveform durations than grid cells and higher amplitudes than HD cells.

Table presents the means \pm SEM of the waveform amplitudes and durations of each cell type. Independent *t*-tests were used to compare waveform statistics. Data was taken from the first large environment trial of the day (LWC or LWS) to control for trial order and environment effects.

	MEAN \pm SEM	
	Waveform amplitude (μ v)	Waveform duration (interval in μ s)
ALLGRIDS N=51	138.91 \pm 7.79	225.95 \pm 19.89*
SUBGRIDS N=30	153.41 \pm 11.57	264.85 \pm 28.64
BVCs N=46	154.55 \pm 7.23	294.37 \pm 24.17
HDs N=30	132.23 \pm 8.36*	223.95 \pm 35.28

Significantly different compared to the BVC sample * $p < 0.05$

4.4.3.1 Subicular BVCs and grid cells carry less directional information than HD cells

The directional modulation was calculated using Skaggs directional information (see methods). This information was taken ideally from the first large walled circular (LWC) environment of the day. If the cell was not recorded in a LWC environment then the first large walled square (LWS) or small walled square (SWS) environments were used (LWC, n=30; LWS, n=17; SWS, n=4). See Table 4.4.3 below for means and SEM.

Directional information (in bits per second and in bits per spike) and directional selectivity were compared between the grid cells, BVCs and the HD cells. Both the grid cells and BVCs were much less directionally modulated than HD cells (Table 4.4.3).

Table 4.4.3. HD cells carry more directional information than Grid cells and BVCs.

Independent *t*-tests were used to compare directional information and selectivity between HD cells and a) ALLGRIDS, b) SUBGRIDS and c) BVCs. Directional information was calculated from unsmoothed polar plots (bin size 5.6°).

	MEAN ± SEM			
	HDs (N= 30)	ALLGRIDS (N=51)	SUBGRIDS (N=30)	BVCs (N=46)
bits/sec				
Directional information	0.63 ± 0.12	0.34 ± 0.07***	0.21 ± 0.04**	0.14 ± 0.03***
bits/spike				
Directional information	1.15 ± 0.18	0.19 ± 0.03**	0.19 ± 0.04***	0.21 ± 0.04***
Directional selectivity	6.51± 0.52	2.20 ± 0.20***	2.47 ± 0.30***	1.88 ± 0.12***
Compared to HD cells	*p<0.05	** p<0.01	***p<0.001	****p<0.0001

4.4.3.2 Grid cells do not carry more directional information and selectivity than BVCs

Any difference in directional signalling between BVCs and grid cells are not striking (Table 4.4.4 below). Grid cells (ALLGRIDS) carry more directional information per second than BVCs ($t_{65.99} = 2.69$, $p = 0.009$). However this is not clearly repeated when looking directional information in bits per spike ($t_{95} = 0.40$, $p = 0.69$) nor when looking at the directional selectivity measure ($t_{78.56} = 1.34$, $p = 0.18$). Looking at the subiculum only grid cell sample this difference in directional information is not maintained (bits/spike, $t_{74} = 0.39$, $p = 0.70$; bits/sec, $t_{74} = 1.53$, $p = 0.13$; selectivity, $t_{38.04} = 2.14$, $p = 0.06$).

Table 4.4.4. Grid cells carry more directional information than BVCs.

Independent *t*-tests were used to compare directional information and directional selectivity between BVCs and a) ALLGRIDS and b) SUBGRIDS. Directional information was calculated from unsmoothed polar plots (bin size 5.6°).

	MEAN \pm SEM		
	BVCs (n=46)	ALLGRIDS (n=51)	SUBGRIDS (n=30)
bits/sec Directional information	0.14 \pm 0.03	0.34 \pm 0.07**	0.21 \pm 0.04
bits/spike Directional information	0.21 \pm 0.04	0.19 \pm 0.03	0.19 \pm 0.04
Directional selectivity	1.88 \pm 0.12	2.2 \pm 0.20	2.48 \pm 0.30

Compared to BVCs * $p < 0.05$ ** $p < 0.01$

4.4.4 Theta modulation

As previously mentioned Boccara et al., (2010) make the general observation that grid cells are more theta modulated than border and head direction cells (see also Cacucci et al., 2004). The present data supports this observation (Table 4.4.5). Grid cells were significantly more theta modulated than BVCs and HD cells. This was the case whether I looked at the ALLGRIDS (ALLGRIDS vs. BVC's, $t_{83.90} = 4.8$, $p < 0.0001$; ALLGRIDS vs. HD, $t_{66.56} = 7.63$, $p < 0.0001$) or the SUBGRIDS samples (SUBGRIDS vs. BVC, $t_{43.22} = 3.76$, $p = 0.001$; SUBGRIDS vs. HD, $t_{35.40} = 5.77$, $p < 0.0001$).

Also conforming to previous observations HD cells were the least theta modulated cell type (Boccara et al., 2010). Here it is shown that HD cells were significantly less theta modulation than the grid cells (above) and the BVCs (HD vs. BVC, $t_{72.16} = 3.16$, $p = 0.002$). This may provide support Boccara et al's (2010) suggestion that the representation of head direction may be uncoupled from the theta rhythm.

Table 4.4.5. Grid cells are significantly more theta modulated than either HD or BVC cells.

Grid cells are significantly more theta modulated than either HD or BVC cells. This is true when comparing both the SUBGRIDS and the ALLGRIDS samples. The BVCs are more theta modulated than the HD cells. Data was taken from the first large environment trial of the day (LWC or LWS) to control for trial order and environment effects.

	Theta modulation score
ALLGRIDS N=51	28.70 ± 2.71
SUBGRIDS N=30	27.54 ± 3.71
BVCs N=46	11.96 ± 1.84
HDs n=30	4.96 ± 1.24

Chapter 5 Responses to environmental manipulations

A number of manipulations were tested with the spatial cells to investigate the influential power of boundaries on firing patterns. The following section will look at grid cell responses to environment manipulations, followed by BVC responses to environment manipulation.

5.1 Grid cell responses to wall removal

To investigate whether wall removal had an influential effect on grid properties, the baseline walled-environments were compared with the circular open platform (COP). The COP was typically run in between two walled baseline environments, of either the large walled circle (LWC) or the large walled square (LWS). There was no significant difference in directionality, gridness, theta modulation or running speed between the walled and un-walled environments (see Table 5.1.1).

There were however significant increases in grid scale (Figure 5.1.1; Table 5.1.2 and Table 5.1.3) and significant shifts in orientation between the walled and un-walled environments (Figure 5.1.4). These results will be explored in the following section.

Table 5.1.1. Grid cell properties in walled vs un-walled conditions.

This table shows the means and S.E. of 5 properties of grid cells firing that do not significantly differ between walled and un-walled environments. Directional information is given in bits per second, but there was also no difference in bits per spike (data not shown). Directional information was calculated from smoothed polar plots (bin size 5.6°). Locational peak rate was calculated from smoothed rate maps (bin size 3cm x 3cm). Where possible the walled trial statistics are taken from an average of the two baseline trials. Wall removal did not alter directionality, gridness, theta modulation or running speed. In the ALLGRIDS sample, there was a minor increase in locational peak rate, and in the SUBGRIDS sample there was a minor reduction in global mean rate (not seen in the ALLGRIDS sample).

		MEAN ± SEM						
			Directional information (bits/sec)	Gridness scores	Theta modulation (Hz)	Locational Peak rate (Hz)	Global Mean rate (Hz)	Running speed
a) Large walled square (LWS) vs Circular open platform (COP)								
ALLGRIDS (n=26)	MEAN ± SEM	LWS:	0.42 ± 0.14	0.56 ± 0.07	25.52 ± 3.38	10.5 ± 1.23	1.86 ± 0.35	8.36 ± 0.12
		COP:	0.47 ± 0.18	0.55 ± 0.08	27.00 ± 4.17	12.44 ± 1.62	1.89 ± 0.40	8.34 ± 0.18
	p value		0.41	0.01	0.38	0.03*	0.72	0.91
SUBGRIDS (n=11)		LWS:	0.27 ± 0.08	0.49 ± 0.10	21.73 ± 5.76	10.94 ± 1.57	1.86 ± 0.29	8.04 ± 0.16
		COP:	0.24 ± 0.09	0.25 ± 0.12	22.07 ± 5.90	12.2 ± 2.24	1.64 ± 0.28	7.77 ± 0.24
	p value		0.24	0.11	0.91	0.29	0.05*	0.14
b) Large walled circle (LWC) vs Circular open platform (COP)								
ALLGRIDS (n=14)		LWC:	0.20 ± 0.06	0.49 ± 0.11	26.22 ± 5.69	10.03 ± 1.40	1.73 ± 0.27	8.67 ± 0.15
		COP:	0.27 ± 0.09	0.66 ± 0.11	28.42 ± 5.88	11.15 ± 1.76	1.78 ± 0.33	8.33 ± 0.16
	p value		0.13	0.12	0.38	0.16	0.75	0.07
SUBGRIDS (n=9)		LWC:	0.15 ± 0.05	0.35 ± 0.10	20.28 ± 6.31	10.59 ± 2.01	1.63 ± 0.32	8.75 ± 0.21
		COP:	0.19 ± 0.05	0.44 ± 0.11	24.43 ± 6.72	11.92 ± 2.57	1.65 ± 0.33	8.25 ± 0.24
	p value		0.23	0.37	0.26	0.28	0.91	0.06

5.1.1 Grid scale expanded upon wall removal

Barry (2007; 2012) has recently shown that environment manipulation can influence grid scale. When an environment is extended, the grid scale of MEC grid cells was shown to expand parametrically in the extended dimension.

In the present thesis environment wall-removal seems to have an influence on grid scale. Changes to grid scale with wall-removal was examined using two environment comparisons:

- a) The large-walled square environment vs the circular open platform (LWS vs COP; Figure 5.1.1A)
- b) The large-walled circle environment vs the circular open platform (LWC vs COP; Figure 5.1.1B).

Any changes to grid scale were calculated in both absolute (cm) and percentage (%) difference between the environments. The increase in grid scale for each cell is given underneath the rate maps in Figure 5.1.1.

The grid cells showed a clear expansion of grid scale with wall removal in both comparisons (see Table 5.1.2 for statistics and Figure 5.1.1 for rate maps). When the walls were removed the grid scale increased for both the ALLGRIDS and SUBGRIDS samples. Further, this result was maintained when a subset of the data was analysed, which included only grid cells recorded in both comparisons, lending supporting this finding (see Table 5.1.3).

Table 5.1.2. Spatial scale expands when the environment walls are removed.

Grid scale increased in cm's and percentage between walled baseline a) LWS and b) LWC and un-walled COP trials. The percentage increase in grid scale was calculated considering the walled environment had 100% grid scale.

MANIPULATION	Envt	Spatial scale MEAN ± SEM	SCALE INCREASE		
			Absolute (cm)	%	
a) Large walled square (LWS) vs Circular open platform (COP)					
ALLGRIDS	(n=26)	LWS:	48.45± 2.92		
		COP:	58.50 ±3.81	10.1cm (p<0.0001)****	21.1% (p<0.0001)****
SUBGRIDS	(n=11)	LWS:	39.94 ± 3.00		
		COP:	53.22 ± 4.26	13.3cm (p<0.0001)****	33.2% (p<0.0001)****
b) Large walled circle (LWC) vs Circular open platform (COP)					
ALLGRIDS	(n=14)	LWC:	58.08± 6.64		
		COP:	63.07 ± 6.25	5.0 cm (p=0.08)	11.5% (p= 0.007)**
SUBGRIDS	(n=9)	LWC:	56.23± 8.54		
		COP:	64.21± 8.93	8.0cm (p= 0.003)**	16.1% (p= 0.02)*

Comparison between large walled environments (LWS or LWC) vs. Circular open platform *p< 0.05 ** p< 0.01 ***

p< 0.001 **** p< 0.0001

Table 5.1.3. Grid cell same day subset: Spatial scale expands when the environment walls are removed.

Subset of grid cells for which the trials in the walled vs. un-walled comparisons were recorded on the same day. Spatial scale is significantly increased when the environment walls are removed. Grid scale increased in cm's and percentage between walled baseline a) LWS and b) LWC and un-walled COP trials. The percentage increase in grid scale was calculated considering the walled environment had 100% grid scale.

MANIPULATION	Envt	Spatial scale MEAN ± SEM	SCALE INCREASE	
			Absolute (cm)	%
a) Large walled circle (LWC) vs circular open platform (COP)				
ALLGRIDS	(n=11)	LWC: 50.87± 6.25 COP: 56.46 ± 5.37	5.60cm (p=0.035)	13.5% (p=0.004)**
SUBGRIDS	(n=7)	LWC: 44.89 ± 5.20 COP: 53.14 ± 6.30	8.26cm (p=0.003)	18.43% (p=0.001)***
b) Large walled square(LWS) vs circular open platform (COP)				
ALLGRIDS	(n=11)	LWS: 46.10 ± 4.81 COP: 56.46 ± 5.37	10.37cm (p=0.002)	24.4% (p=0.001)***
SUBGRIDS	(n=7)	LWS: 39.39 ± 4.14 COP: 53.14 ± 6.30	13.80cm (p=0.002)	34.3% (p=0.001)***

Comparison between large walled environments (LWS or LWC) vs. Circular open platform *p< 0.05 ** p< 0.01

*** p< 0.001 **** p< 0.0001

A Large walled square vs circular open platform

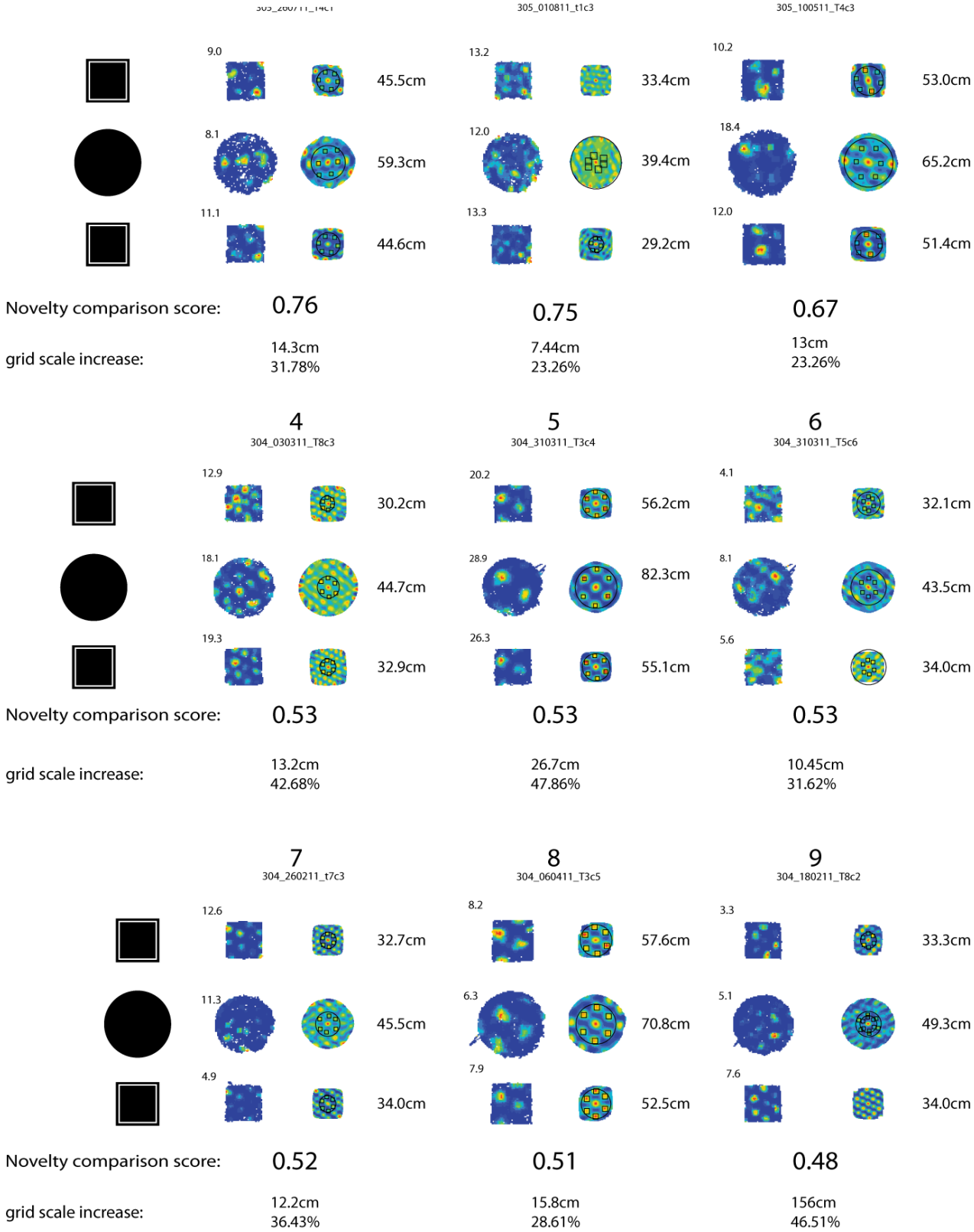


Figure 5.1.1. Grid scale expands with wall removal (page 1/5)

Figure legend at the end of figure

A *cont.*

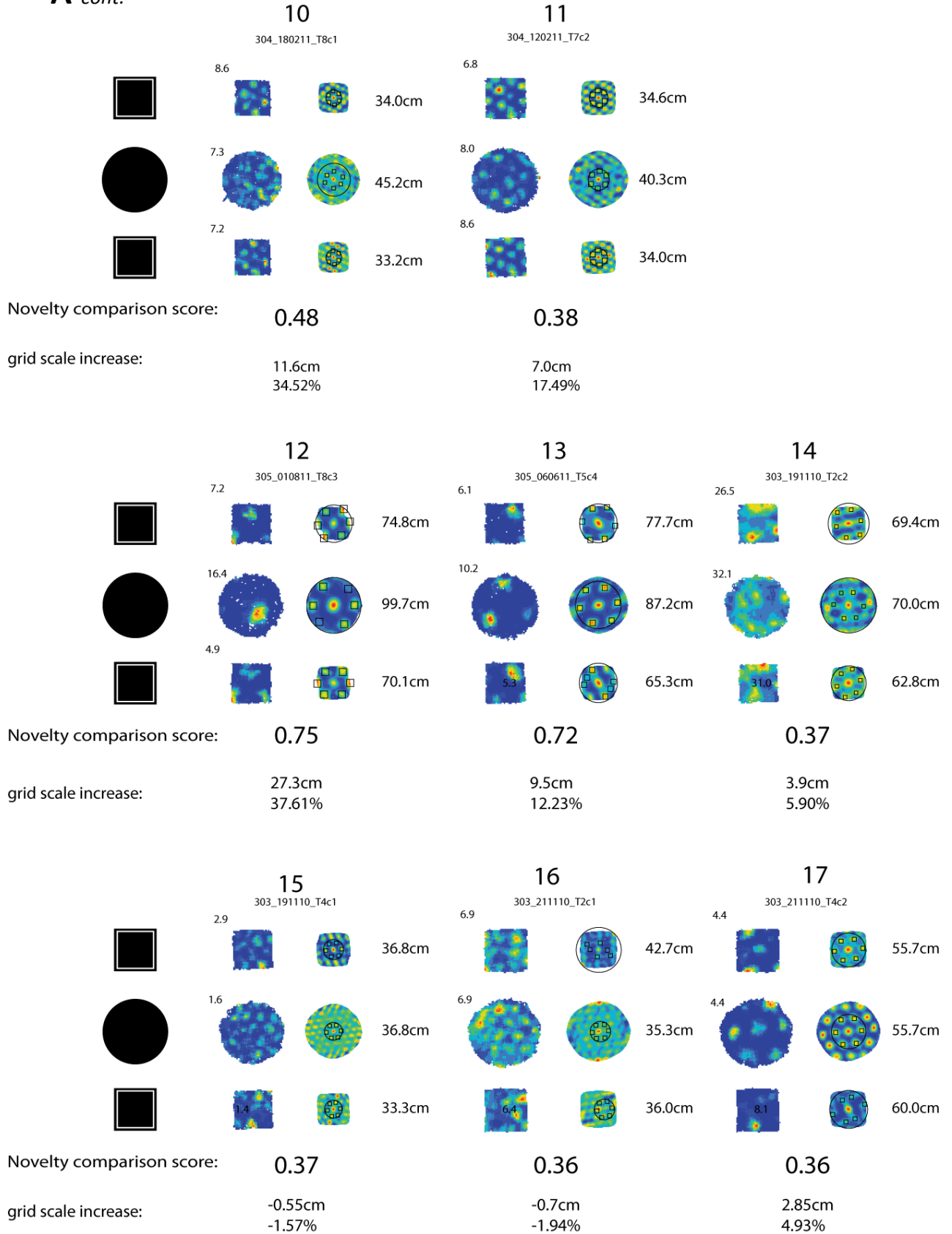


Figure 5.1.1. Grid scale expands with wall removal (page 2/5)

A *cont.*

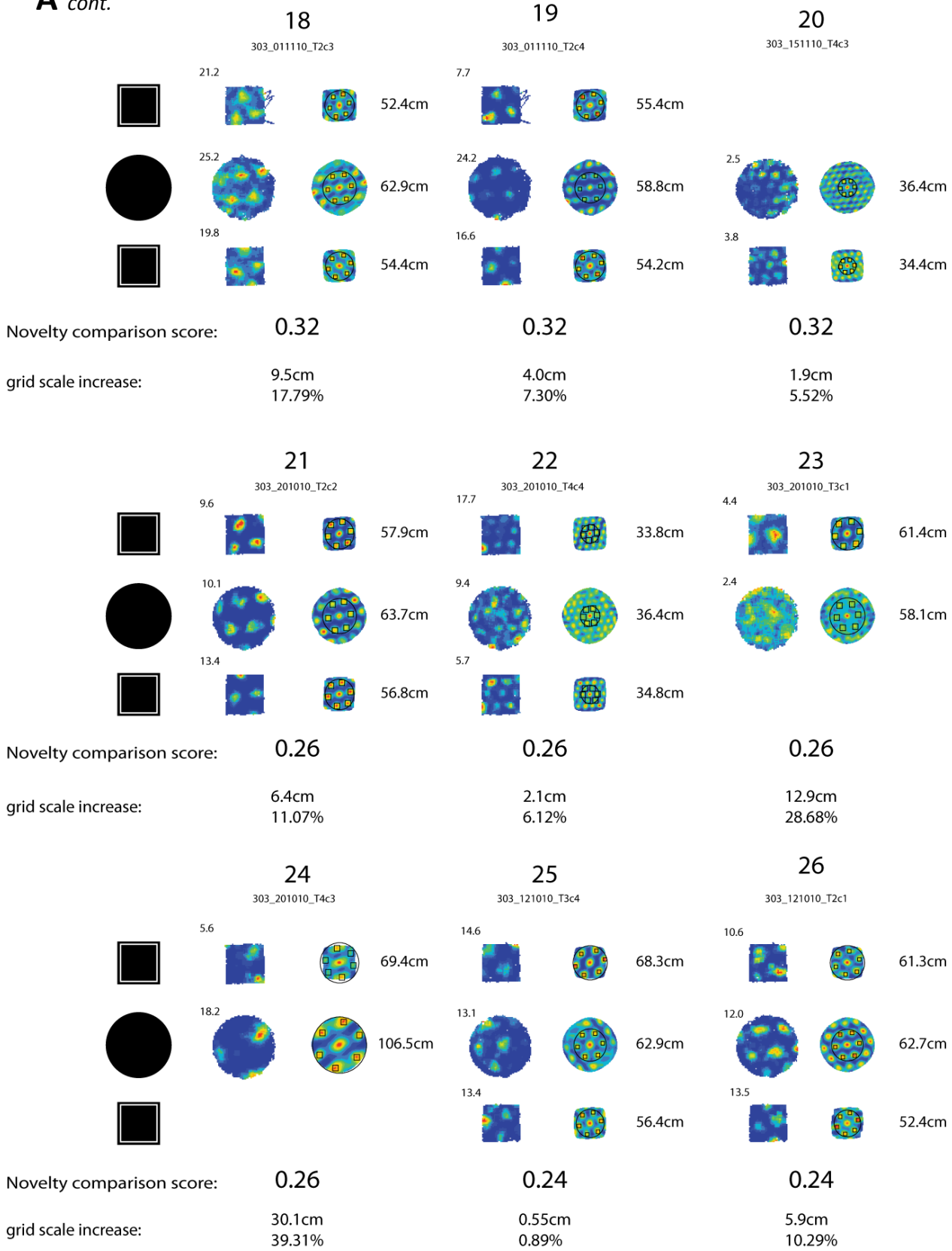


Figure 5.1.1. Grid scale expands with wall removal (page 3/5)

B Large walled circle vs circular open platform

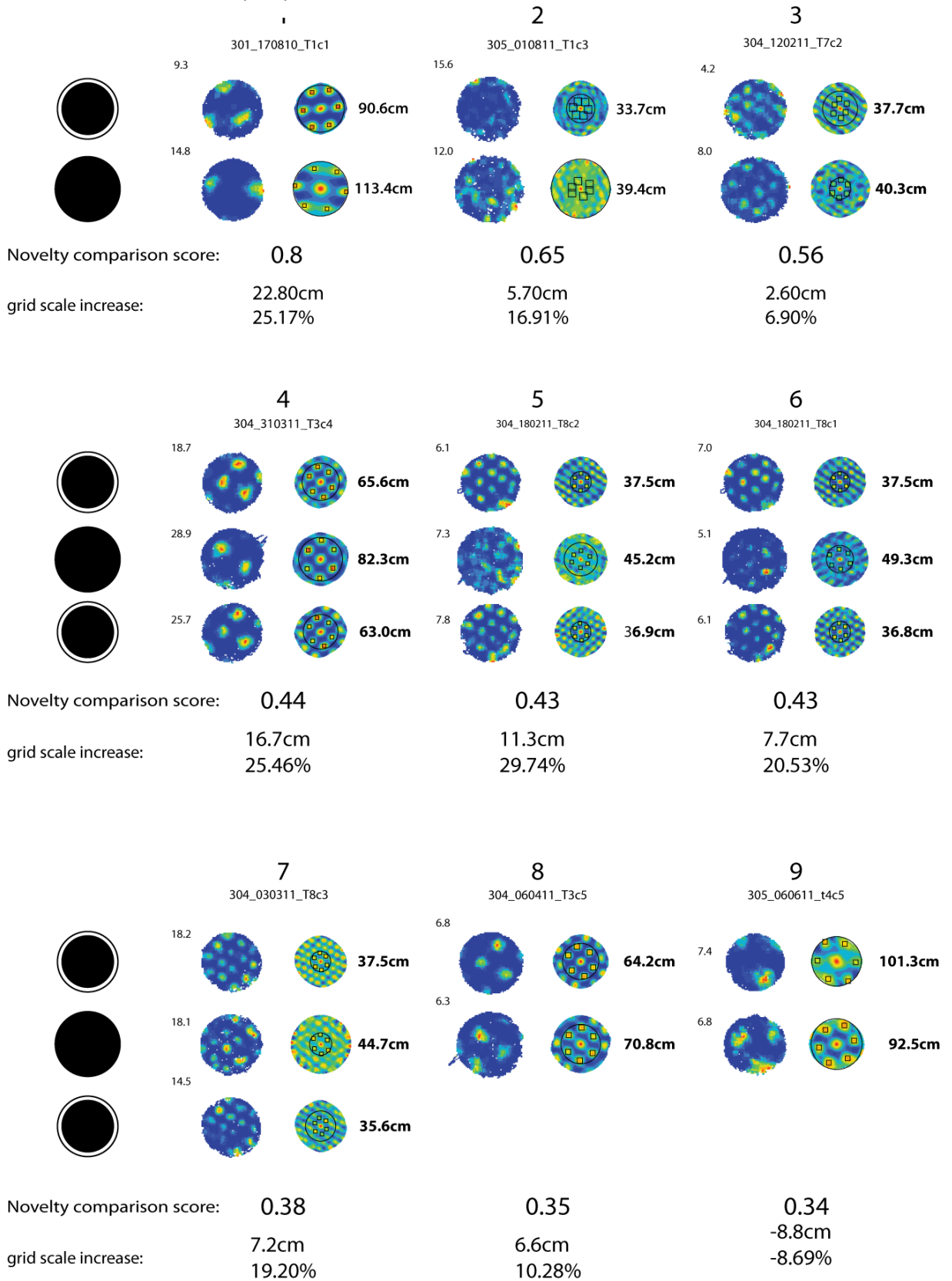


Figure 5.1.1. Grid scale expands with wall removal (page 4/5)

B *cont.*

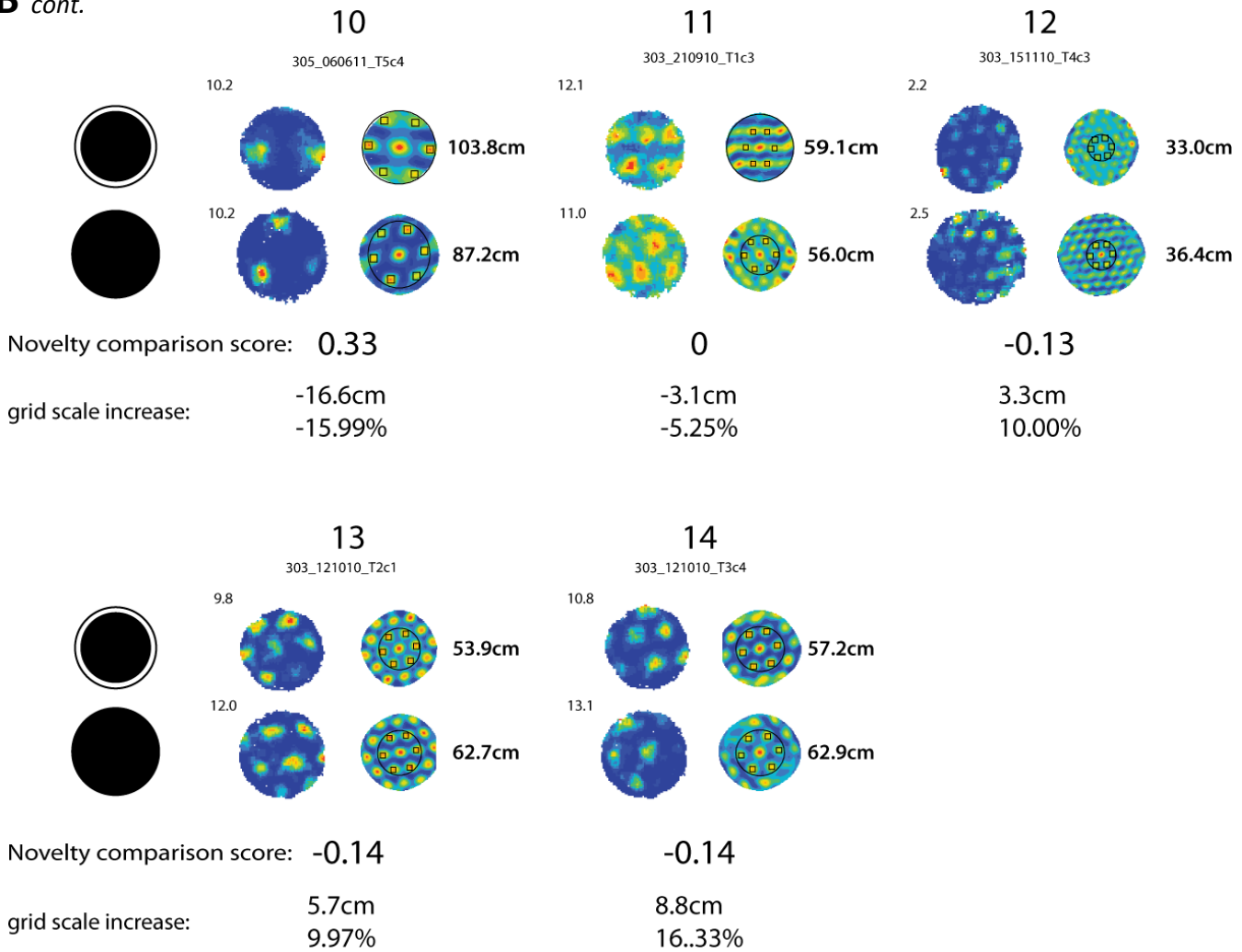


Figure 5.1.1. Grid scale expands with wall removal (page 5/5)

A) Comparison of grid scale between the large walled square vs circular open platform (LWS vs COP) B) Comparison of grid scale between Large walled circle vs circular open platform (LWC vs COP). The figure shows the rate maps and the autocorrelations for each cell tested using this manipulation. The cells are organised by Novelty comparison scores. The higher the novelty score the more novel the circular open platform was in comparison to the walled environment (A Large walled square; B Large walled circle. The grid scales for each cell in environment are given to the right of the autocorrelation maps. For each cell the average grid scale increase in cm and in % are given underneath each the maps.

5.1.2 Grid scale expansion may be modulated by novelty

Previous studies (Barry et al., 2008; 2012) suggest that grid scale expansion can be related to novelty. Upon first exposure to a novel environment grid scale has been shown to increase by 37.3% in MEC grid cells (Barry et al., 2012). With exposure the grid scale expansion reduces back towards baseline as the novel environment becomes more familiar.

In the present study the un-walled circular open platform (COP) was relatively novel in comparison to the walled environments (LWS and LWC). The rats were tested in the large walled trials significantly more than in the un-walled trials (COP). The walled environments were typically used as baseline environments for manipulations as well as for screening. In order to index how novel the un-walled environment (COP) was in comparison to the generally more familiar walled environments (LWS and LWC) a novelty comparison score (NCS) was calculated as follows:

Novelty comparison score (NCS) =

$$\frac{\text{Number of exposures to Env't X minus number of exposures to COP}}{\text{Sum of exposures to Env'ts X and COP}}$$

Sum of exposures to Env'ts X and COP

Where X is the LWC or the LWS.

In principle, the score can vary between -1 and +1. The score approaches +1 when the un-walled environment (COP) is highly novel relative to the baseline environment. Figure 5.1.1 presents each cell tested in this manipulation. Underneath the rat maps the increase in grid scale and the novelty comparison scores are given. Grid cells are organised in order of novelty comparison scores.

Grid scale expansion was positively correlated with the novelty of the circular open platform (COP) for the ALLGRIDS sample in comparison to the large walled square (LWS vs COP). Figure 5.1.2 shows that the more novel the circular open platform (compared to the large-walled square) the larger the grid scale expansion. This positive relationship was evident in both absolute centimetre increase in grid scale ($r = +0.40$, Figure 5.1.2A) as well as percentage increase in grid scale ($r = +0.47$, Figure 5.1.2B). Meaningful analysis of the

large walled circle vs. circular open platform comparison (LWC vs COP) was not possible because the sample sizes were too small.

While there was a relationship between running speed and expansion, there was no hint of a significant difference in the median running speed between the walled and un-walled trials ($t_{25}=0.12, p=0.91$). Partial correlation analysis showed that the relationship between novelty and gridscale remained when running speed was controlled for (% , $r=0.45, p=0.02$; cm, $r=0.36, p=0.07$). This suggests that running speed did not explain the positive relationship between expansion and novelty.

Table 5.1.4 There was a significant difference in the number of exposures to walled and un-walled environments

		MEAN ± SEM		
		Average number of Walled envt exposures	Average number of COP exposures	Average difference in exposures
a) Large walled square (LWS) vs Circular open platform (COP)				
ALLGRIDS	(N=26)	20.0 ± 2.2	6.8 ± 0.5	13.0 ± 2.0****
SUBGRIDS	(N=11)	24.3 ± 3.5	6.6 ± 0.8	17.7 ± 3.1 ****
b) Large walled circle (LWC) vs Circular open platform (COP)				
ALLGRIDS	(N=14)	13.0 ± 2.2	5.6 ± 0.8	8.9 ± 1.9 **
SUBGRIDS	(N=9)	17.8 ± 1.9	6.2 ± 0.9	11.6 ± 1.6 ****

*Comparison between the numbers of exposures in large walled environments (LWS or LWC) vs. Circular open platform * $p < 0.05$ ** $p < 0.01$ *** $p < 0.001$ **** $p < 0.0001$*

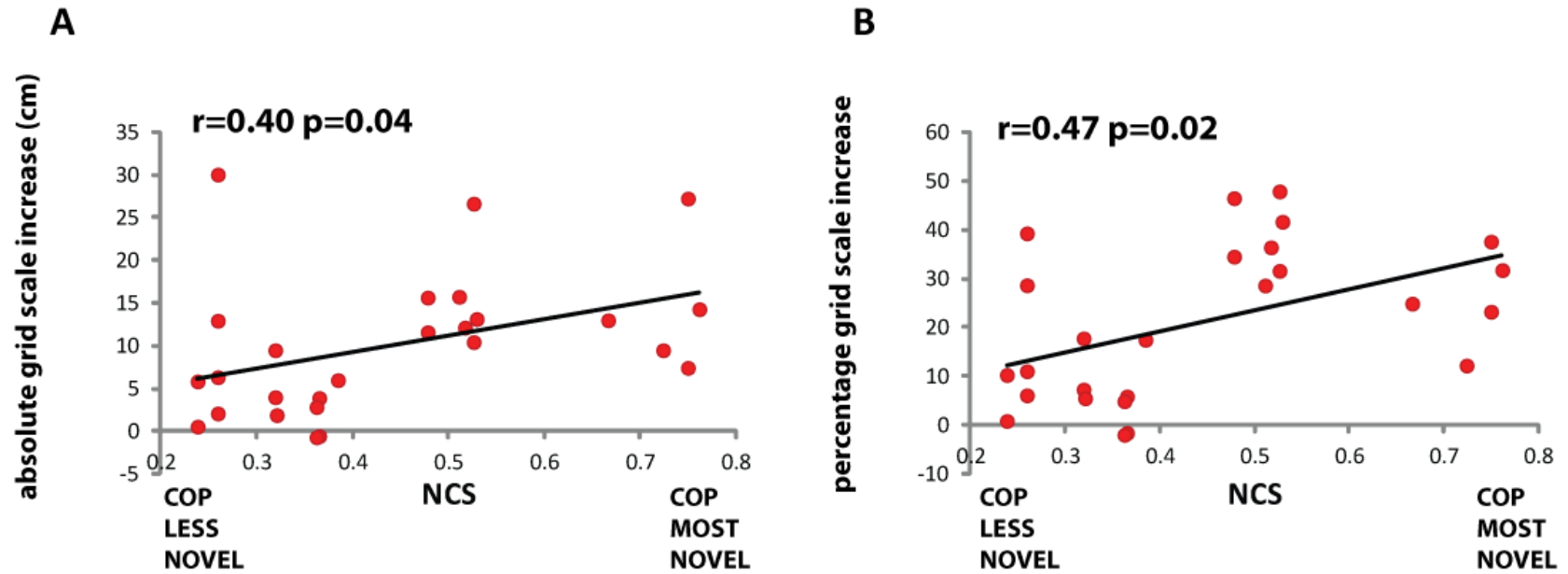


Figure 5.1.2. There is a positive relationship between grid scale and novelty.

Scatterplots showing for the ALLGRIDS sample the relationship between the a) absolute and b) percentage increase in grid scale with the novelty comparison score (NCS) between the large walled square (LWS) and the un-walled circular open platform (COP).

5.1.2.1 The relationship between the familiar grid scale and the magnitude of novelty-induced grid expansion.

In 2012 Barry et al. noted that the relationship between grid scale in the familiar environment and the magnitude of novelty-induced grid expansion was unclear. Barry et al. observed that in general the expansion in the novel environment was not random. The smaller scale grid cells tended to still be small, and in general the larger scaled grid cells expanded by a similar absolute amount to the smaller grid cells. Barry et al., (2012) considered that their data superficially suggested that grid cells of different scales tended not to expand by different amounts. Were this the case it may have provided tentative evidence for a fixed expansion amount.

The present data does not support the idea of a fixed expansion amount. Figure 5.1.3 suggests a trend towards a positive linear relationship between grid scale in the walled environment and the absolute (cm) increase in the un-walled environment ($r=0.35$, $p=0.08$). This trend implies that larger scaled grid cells expand by more centimetres than smaller scaled grid cells between the walled and un-walled environments.

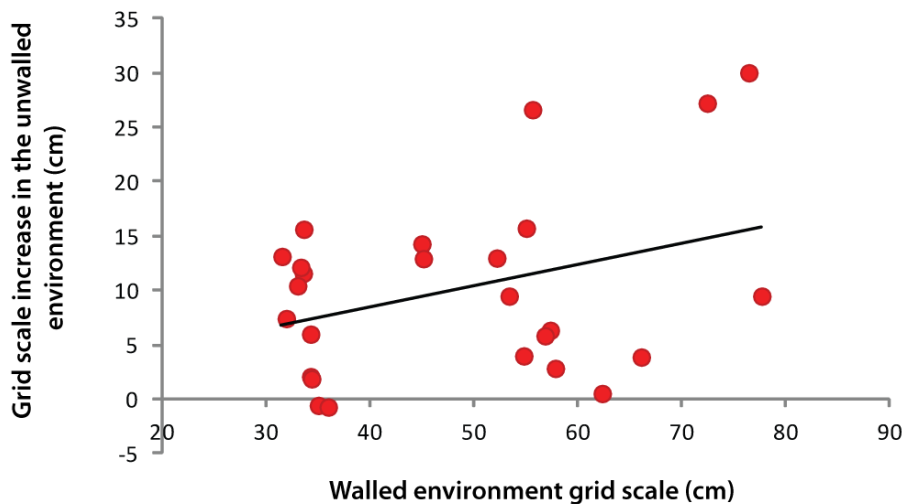


Figure 5.1.3. There is a trend towards a positive linear relationship between grid scale in the walled environment and the grid scale increase in the un-walled environment.

Using the ALLGRIDS ($n=26$) sample the scatterplot shows the relationship between grid scale in the walled square environment in comparison to the absolute grid scale increase (cm) in the circular open platform.

5.1.3 Orientation of the grid pattern shifts between walled and un-walled environments

Previous studies have shown environment changes can cause orientation to shift (hafting et al., 2005; Fyhn et al., 2007). To investigate this I tested whether wall removal had any effect upon grid orientation. Walled environments were used as baseline trials as compared to the un-walled environment as the test trial. As with the rescaling experiment above orientation shift with wall removal was examined using two environment comparisons:

- a) The large-walled square environment vs the circular open platform (LWS vs COP)
- b) The large-walled circle environment vs the circular open platform (LWC vs COP).

Grid orientation was stable across trials in the same walled environment (see Figure 5.1.4 for means \pm SEM). In the LWS vs COP comparison there was no difference in grid orientation between baseline trials in either the ALLGRIDS (n=22) and SUBGRIDS (n=13) samples ($t_{21}=1.17, p=0.254$; $t_{12}=0.61, p=0.55$ respectively). There was also no difference in orientation between baseline trials in the LWC vs COP comparison ($t_4=1.22, p=0.29$), although only five subicular grid cells were tested in two baseline trials.

Orientation however was not stable between the walled and un-walled environments. There was a significant orientation shift between walled and un-walled environments, compared to the walled environments (Figure 5.1.4). This orientation shift can be seen in the comparisons of the difference in the shift between baseline trials (average of baseline₁ and baseline₂) and the shift between average baseline and test trials. Figure 5.1.4A demonstrates the significant orientation shift between the walled environments and the un-walled environment in both the LWS vs COP comparison (ALLGRIDS, $t_{21}=3.57, p=0.002$; SUBGRIDS, n=13: $t_{12}=4.33, p=0.001$). and the LWC vs COP comparison ($t_4=4.043, p=0.016$). Across both environment comparisons the orientation shifted by $>10^\circ$ between the walled and un-walled environments compared to the walled environments. This suggests that the walls/boundaries of the environment can provide a controlling influence upon grid cell orientation.

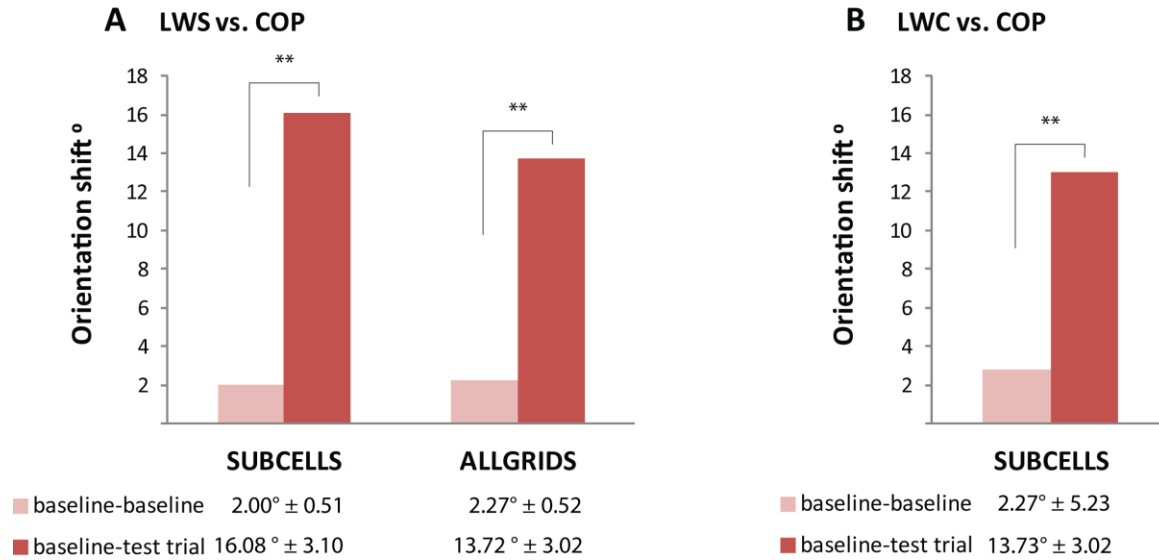


Figure 5.1.4. Grid orientation significantly shifted between walled and un-walled environments.

The shift between baseline trials (pink fill) was significantly smaller than the shift between baseline (average of baseline₁ and baseline₂) and test trial (un-walled circular open platform; COP; red fill). Histograms show the difference in orientation between A) the large walled square (LWS) vs. the COP and B) the large walled circle (LWC) vs. the COP. B) shows the SUBGRIDS sample only as only subicular grid cells were run with two LWC baseline trials. ** P ≤ 0.001

5.1.3.1 Grid cell firing patterns are maintained in complete darkness

Eight grid cells were recorded in complete darkness (see Figure 5.1.5 for rate maps). The rats were given 24 minutes in the large walled square environment as per normal protocol in the large walled square, then all light was extinguished for a further 24 minutes. For most cells this was followed after a 20 minute inter trial interval with another trial in the light condition as a return to baseline. Grid properties remained stable between the lit baseline trials (data not shown).

Table 5.1.5 shows that darkness did not disrupt grid cell firing properties. There was no alteration in directional information (bits per spike) carried by the grid cells, nor were there any significant changes in gridness, grid scale, peak firing rate or global mean rate or orientation shift between the light and dark trials (Figure 5.1.5).

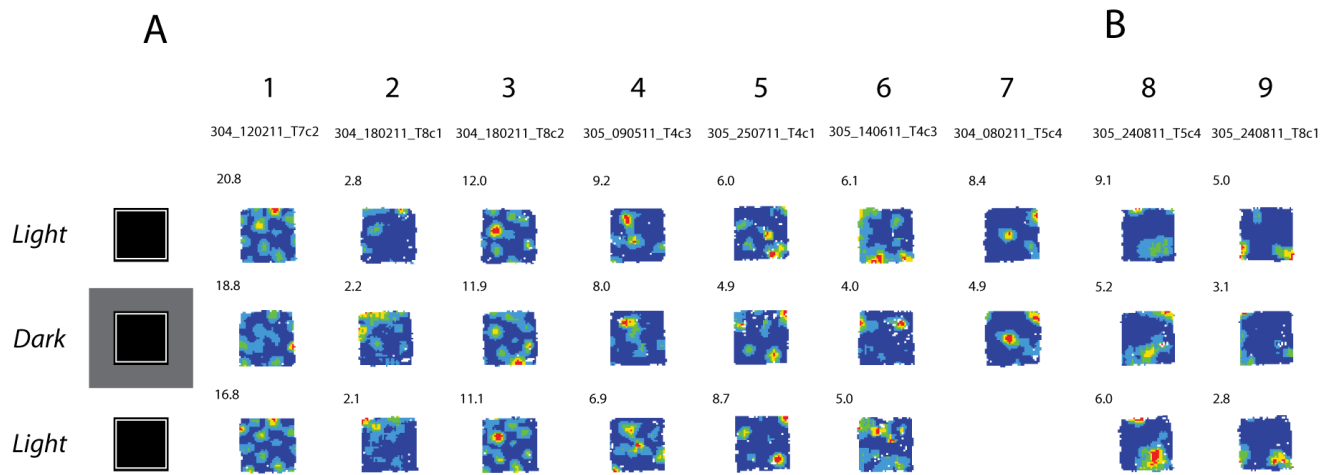


Figure 5.1.5. Grid cell firing patterns do not change between light and dark trials.

Figure shows the rate maps for all grid cells recorded in the dark manipulation. A) subicular grid cells B) non-subicular grid cells.

Table 5.1.5. Removing visual cues did not interrupt grid cell firing properties.

This table gives the means and S.E.M. of 6 properties of grid cell firing that do not significantly differ between light and dark trials. Where possible the light trial statistics are taken from an average of the two baseline trials (8/9 grid cells). Directional information was calculated from unsmoothed polar plots (bin size 5.6°). The orientation calculation only includes the cells with 2 baseline trials (ALLGRIDS, 8/9 grid cells; SUBGRIDS 6/7 grid cells). The table also presents the t-test values and p-values for comparisons of properties between light and dark trials.

	MEAN ± SEM					
	Directional Information (bits/spike)	Gridness score	Grid Scale (cm)	Locational Peak rate (Hz)	Global Mean rate (Hz)	Orientation shift (°)
a) ALLGRIDS (n=9)						
Light trials	0.34 ± 0.08	0.29 ± 0.11	49.21 ± 4.96	8.72 ± 1.73	1.50 ± 0.37	7.2 ± 5.02
Dark trials	0.34 ± 0.37	0.14 ± 0.17	51.21 ± 4.94	7.82 ± 1.93	1.38 ± 0.38	13.54 ± 5.16
p value	0.30	0.25	0.10	0.16	0.10	0.38
b) SUBGRIDS (n=7)						
Light trials	0.38 ± 0.09	0.33 ± 0.11	46.11 ± 4.97	9.88 ± 2.44	1.73 ± 0.51	6.00 ± 10.47
Dark trials	0.33 ± 0.08	0.20 ± 0.21	46.67 ± 4.41	8.72 ± 2.39	1.69 ± 0.46	7.67 ± 8.57
p value	0.32	0.97	0.31	0.08	0.30	0.80

5.1.4 Barriers can cause field inhibition in grid cells.

Similar to the BVCs the grid cells were tested with a free-standing barrier. The insertion of a barrier into the testing environment prompted a variety of grid cell responses. Out of the grid cell sample 35 grid cells were tested with an inserted barrier, ~5 seemed to show no pattern disruption whilst the rest showed a measure of disruption with barrier insertion. The most common responses to barrier insertion were a) a shift/deformation of the grid pattern (figure 5.1.6) and b) field inhibition (figure 5.1.7).

For most grid cells the insertion of a barrier caused the cell pattern to shift/deform. Figure 5.1.6 shows four representative cells whose grid patterns were disrupted in that the field locations have been displaced. For example, cell 3's grid pattern in the barrier insertion trial is unrecognisable as the same pattern seen in the baseline trials. The grid fields are still clear, but they do not occupy the same locations in the environment as in the baseline trials. Similarly cell 1 also shows a pattern shift, as the grid fields no longer seem to occupy the same locations. For cell 1 barrier insertion also seems to have caused the fields to become more diffuse.

The other common response to barrier insertion was the inhibition of individual grid fields. Figure 5.1.7A shows four representative cells where the barrier insertion seemed to cause strong firing rate reduction in certain grid fields. This suggests that the inserted barrier has an inhibitory influence upon the grid pattern. Fields which are inhibited by the barrier insertion are indicated with red arrows. Preliminary quantification of the effect of inserting a barrier is shown in Figure 5.1.8. To quantify the inhibition peak rates were compared between 'inhibited' fields (3rd column) and reference fields (4th column). For both the grid cells shown in Figure 5.1.8, the peak rates in 'inhibited' fields were around 20% of their average peak rate in baseline trials. In contrast, the peak rates in the reference fields in the barrier trials were at 98% and 90% of the values in baseline trials.

What explains the inhibition? A trivial explanation for the inhibition could be that the barrier prevents movement in precisely that direction which is the preferred direction of a directional grid cells. Could field inhibition be the by-product of directional modulation? Does the insertion of the barrier prevent the rat entering the field from its preferred direction? I inspected all the cells exhibiting this phenomenon and saw no evidence of this. Figure 5.1.7B shows polar plots for each

grid cell: it can be seen that the grid cells are not directional. Therefore it is unlikely that the field inhibition could be attributed to this. Figure 5.1.9 examines this issue in more detail. Rate maps are shown for head directions in the four cardinal directions (N, E, S, W). The cell fires broadly similarly in the four different directions. The inhibited region of firing in the barrier trial (east of the barrier) shows reduced firing relative to other nodes irrespective of whether the rat explores that space facing northwards, eastwards, southwards, or westwards.

Overall our observations suggest that the insertion of a barrier causes obvious disruption to the grid pattern. One study which shows a disruption to grid patterns with barrier insertion is that by Derdikman et al., (2009). Derdikman et al., (2009) investigated what happened to grid patterns when an open arena was discretized by multiple barriers. However, this environment forced the rats to travel around the environment using stereotypical unidirectional behaviour through narrow corridors. Derdikman et al., (2009) found that by breaking the environment up into compartments the rats formed discrete sub maps for each compartment. Whether the changes to grid pattern shown here can be related to those seen in Derdikman et al., (2009), is a question for future investigation. The only report of grid cells recorded with the insertion of a single barrier in an open foraging type paradigm permitting free movement came from Solstad et al., (2009), who showed 2 cells recorded from the same animal and reported no disruption of the grid pattern. It may be that responses to inserted boundaries provide a distinction between MEC and subicular grid cells.

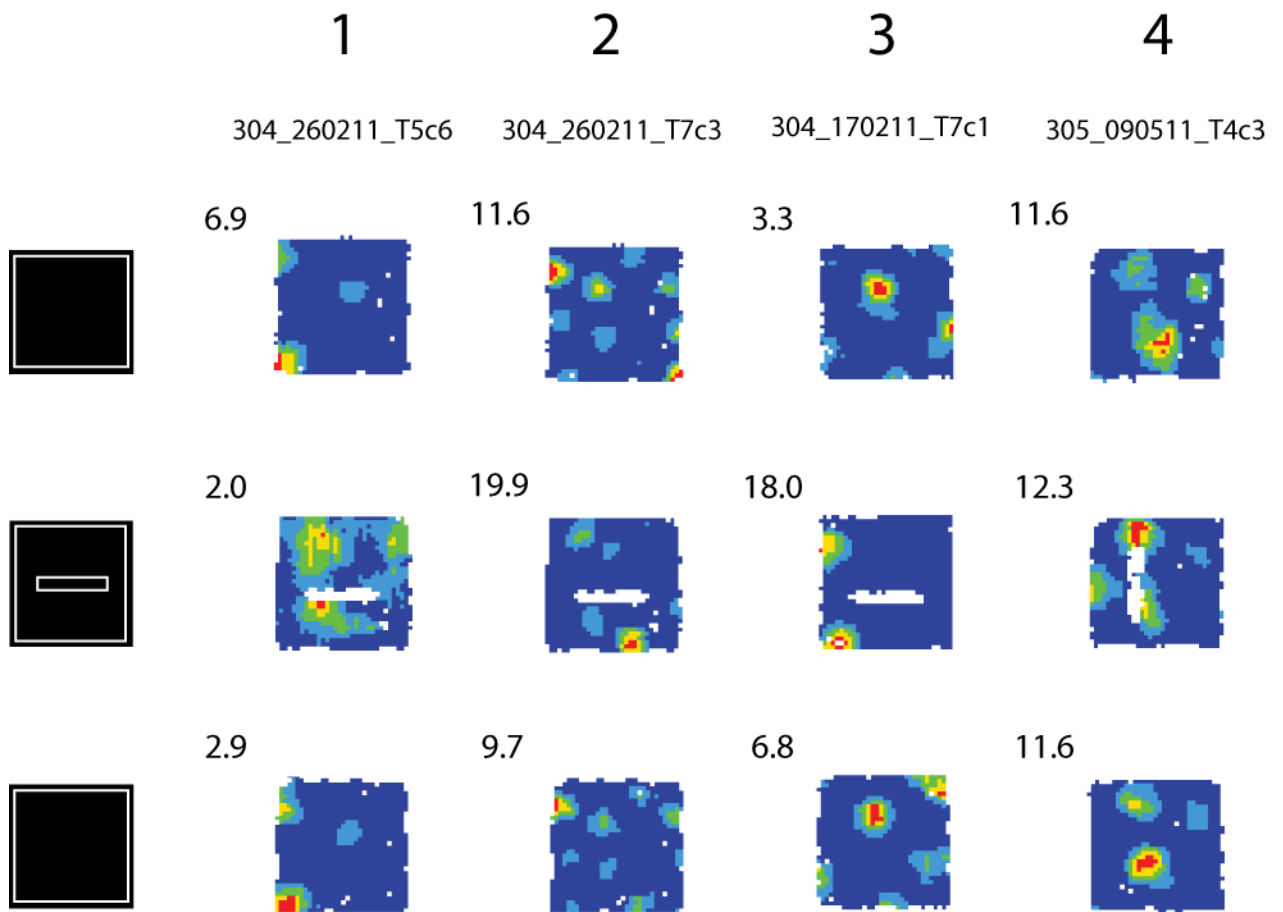


Figure 5.1.6. The insertion of the barrier causes some grid cell patterns to shift/deform

The figure presents 4 grid cells showing a shift/displacement of the grid pattern with insertion of the barrier. The grid pattern remained stable between baseline trials, however with barrier insertion the grid pattern looks similar but none of the fields are located in the same place.

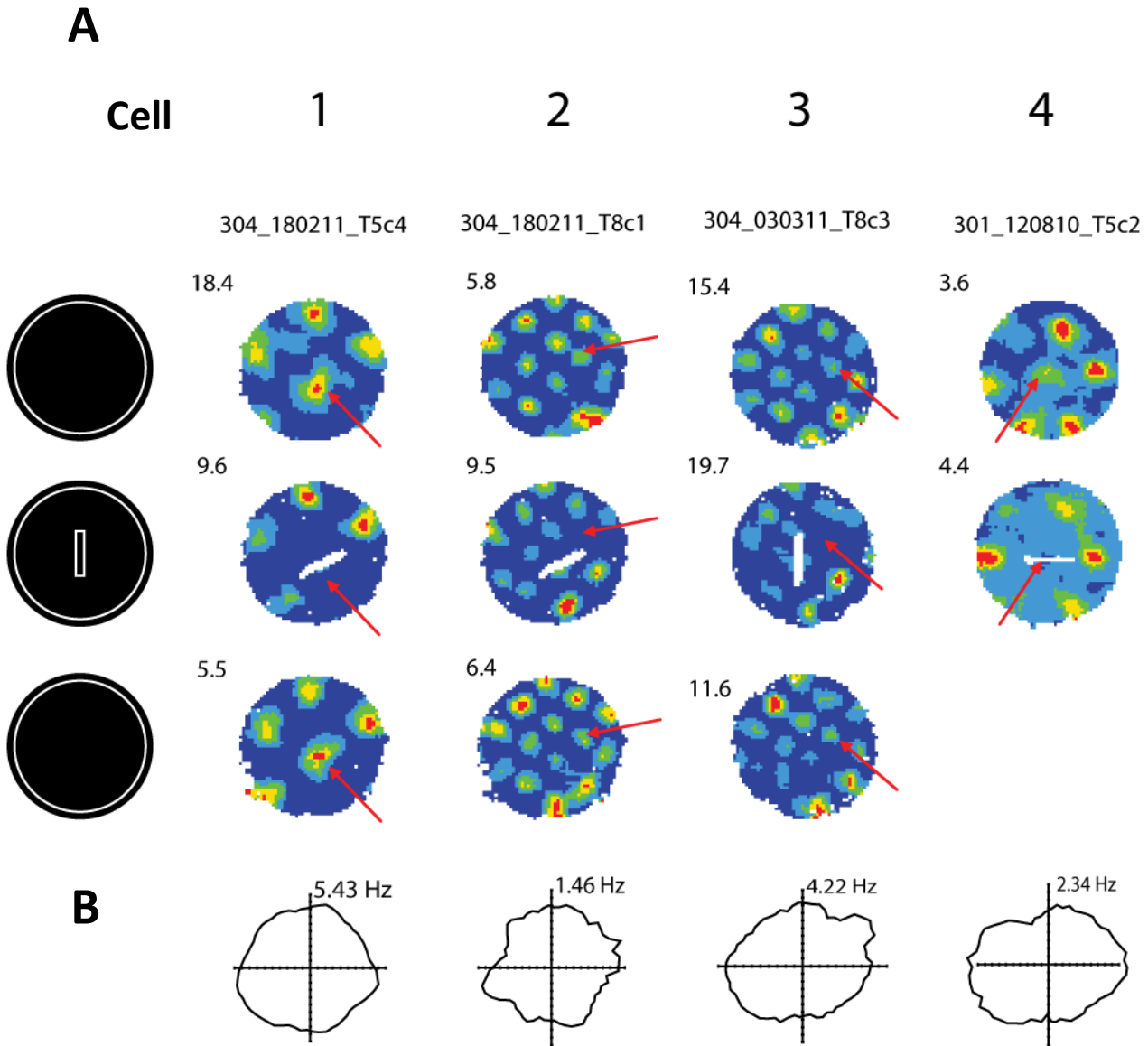


Figure 5.1.7. Some grid cells show field inhibition with the insertion of a free-standing barrier.

Figure shows 4 grid cells which demonstrate field inhibition with barrier insertion. Fields which are inhibited are indicated with red arrows in the first baseline trial rate map. Polar plots for each cell are also given underneath the rate maps. These are taken from the first baseline trial of the day.

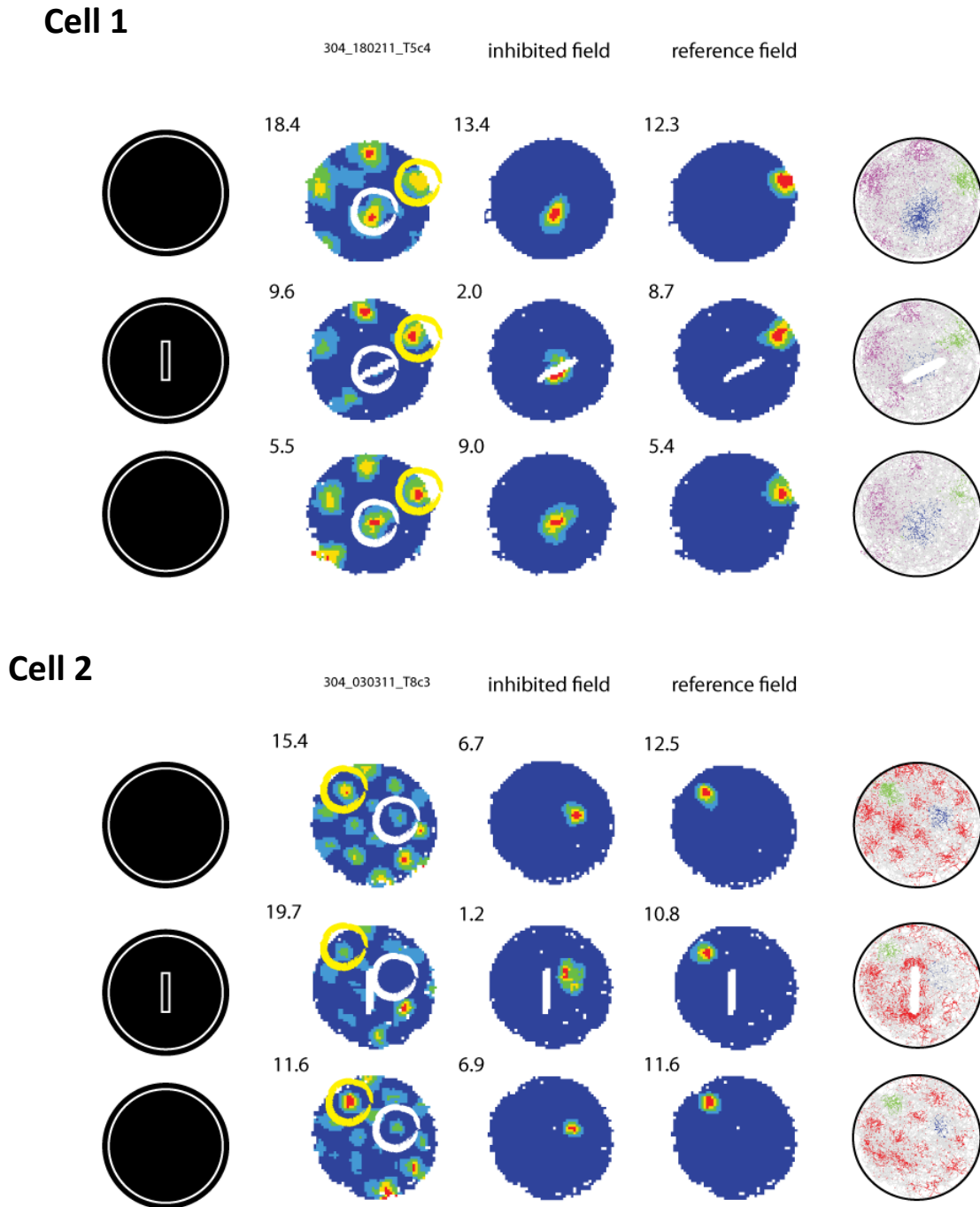


Figure 5.1.8. Quantifying field inhibition with barrier insertion.

This figure shows 2 grid cells which demonstrate field inhibition with the barrier insertion. As per all rate map figures to the left is a schematic representation of the testing environment, and the peak rates are given top left of each map. The second column gives the rate maps. The inhibited field is indicated with a white circle and the reference field is indicated with a yellow circle. The isolated inhibited field is given in the third column and the isolated reference field is given in the fourth column. The most right column gives the spike maps. Each coloured dot is a cell spike. The blue spikes are from the inhibited field and the green spikes are from the reference field. The reduction in firing rate with barrier insertion can be seen in the reduction of peak rate in the second column, and the reduction in spikes in the most right column.

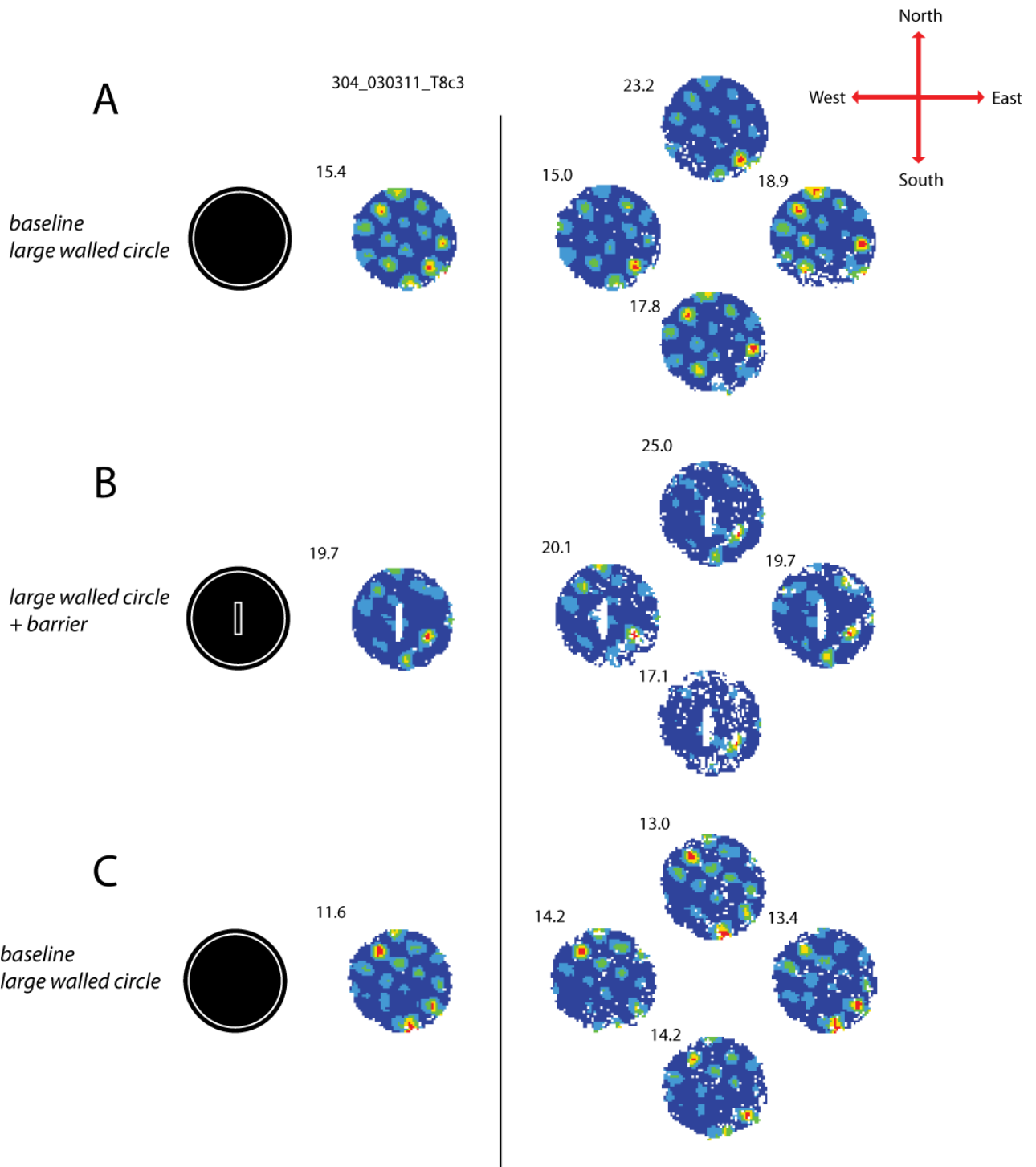


Figure 5.1.9 Representative example showing grid field inhibition relative to other grid fields irrespective of the head direction (and likely movement direction) of the rat.

Figure shows that the inhibited region of firing in the barrier trial (east of the barrier) shows reduced firing relative to other nodes irrespective of which direction the rat's head is facing. A) shows first baseline trial, B) barrier trial, and C) second baseline trial. In each of parts A, B, C, leftmost column depicts trial type; rate map to left of vertical line shows rate map for all sampled head directions; and cluster of 4 rate maps right of vertical line are sub-sampled to show data only when the rat faces 90 degrees either side of the cardinal direction in question. Northward direction is at the top, eastward to the right, southward at the bottom, and westward to the left. Peak firing rate is shown at the top right of each rate map.

5.1.5 Summary of grid cell responses to environment manipulation.

Environmental manipulation can influence grid cell firing patterns. Of particular note is that environment wall removal affects both grid scale and grid orientation. This could be seen between both the large walled square (LWS) and the un-walled circular open platform (COP) and between large walled circle (LWC) and the un-walled circular open platform (COP). When the walls were removed the grid scale expanded. In the LWS vs COP manipulation this expansion was correlated with the novelty of the COP. This supports the findings of Barry 2007; 2012 which also found that grid scale expansion correlated with novelty. The grid orientation shifted between walled and un-walled trials. This shift may support previous findings that grid orientation stability is linked to proximal environmental cues (Hafting et al., 2005). The orientation shift may be a response to wall removal abolishing these cues and subsequently un-anchoring the grid orientation.

The insertion of an extra boundary into the environment also influenced grid cells patterns. For the majority of grid cells in the insertion of a free-standing barrier disrupted the grid pattern. The grid cells showed a variety of responses to barrier insertion with the most notable being field inhibition and a shift/deformation of the grid pattern. For many of the grid cells the insertion of a barrier caused field inhibition somewhere in the environment. This inhibition was not always seen for the fields that intersected by the barrier or those close by it.

Overall environment manipulation disrupted the grid cell firing patterns; however the grid pattern remained stable in darkness. When visual cues were removed there was no difference in gridness, directionality etc. This suggests the grid pattern is not dependent upon allocentric cues, and that firing can at least to some extent be dependent upon idiothetic cues, supporting Hafting et al., (2005).

5.2 BVCs respond to environment boundaries

The BVCs were similarly tested like the grid cells through multiple manipulations in order to characterise their responses to environmental change. The BVCs were tested with a variety of differently shaped and sized environments, wall-less platforms, inserted barriers, inserted objects and in complete darkness. The response of the BVCs to these manipulations can provide support for and new insights into the determinants of BVC firing outlined by the BVC model and the findings of Lever et al., (2009).

5.2.1 BVCs respond to environment walls

A BVC would fire whenever an environmental boundary intersected a receptive field located at a specific distance from the rat in a specific allocentric direction. BVC firing fields were stable with repeated exposures to the same environment (see Figure 4.2.1 for examples). The BVC firing fields followed the environment walls with the long axis following the boundary irrespective of the environment shape. The fields follow the curvature of the circular environments and the straight edges in the square (Figure 5.2.1). For those cells which have directional preferences which intersect two walls both of these walls/ a portion of each are responded to e.g. cell 5 Figure 5.2.1.

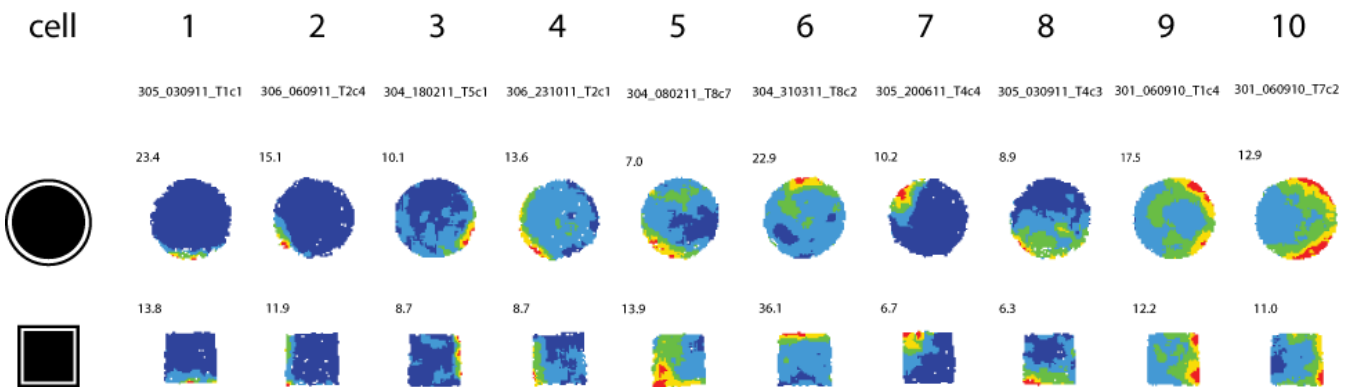


Figure 5.2.1. BVCs respond to perimeter walls of differently shaped environments.

Figure shows 10 BVCs which were recorded in the large walled circle and large walled square environments. The field locations were stable across the differently shaped environments. The fields follow the curvature of the circular environments and the straight edges in the square.

Tuning to distance and direction varied continuously within the BVC sample, albeit with a bias toward shorter distances (see Figure 5.2.2 below for a subset). Lever et al considered that BVC fields with shorter distances are produced when the BVCs receptive fields are peaked close to the animal and when the animal is close to the preferred wall (e.g. cells 1-6, Figure 5.2.2). Whereas broader BVC fields are the product of larger receptive fields which peak further from the rat, responding to the boundary further from the rats position (e.g. cells 7, 8 and 9, Figure 5.2.2).

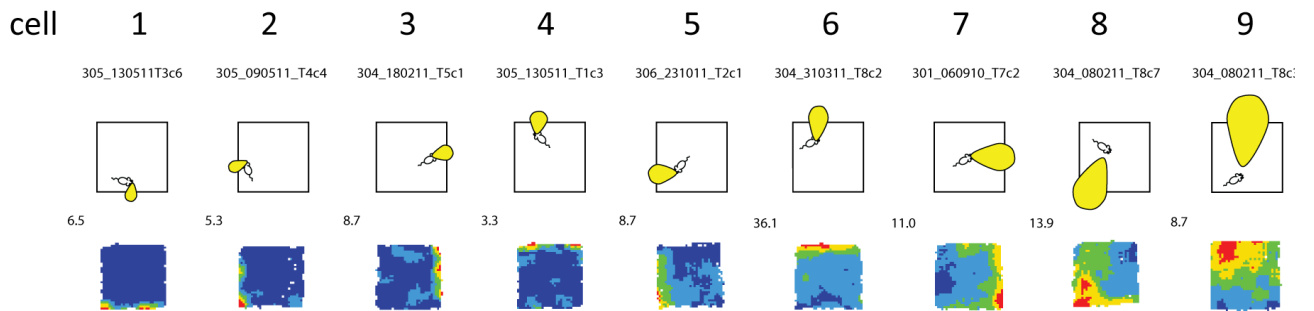


Figure 5.2.2. BVCs vary in distal and directional preference.

This figure provides a subset of the BVC sample demonstrating that distal and directional preference varies. From left to right the BVCs are organised by field thickness. Lever et al. (2009) considers that thicker/broader fields are produced by receptive fields peaking further from the rat. Above the rate maps is an illustration to suggest each BVCs receptive field. BVCs with narrower fields would have smaller receptive fields that respond to the boundary only when the rat was close to it (e.g. cell 1). Whereas the thicker fielded BVCs would have larger receptive fields which are peaked further from the rat (e.g. cell 9).

5.2.1.1 BVC fields are largely insensitive to context change

To test the stability of BVC firing fields a specific paradigm was used which prompts remapping in place cells, see Figure 5.2.3A. This paradigm consists of 4 trials, with familiar environment trials either side of a novel environment trial. Briefly after two presentations of a highly familiar circular environment the floor, the environment walls and the external cues were changed. This created a relatively unfamiliar square environment in a novel context. This trial is followed by a return to baseline in the circular environment (see methods for more details). This paradigm initiates remapping in place cells causing the place field to shift or disappear altogether in the square environment. Figure 5.2.3 shows a comparison of place cell activity and BVC activity in the remapping paradigm. The place cells demonstrate clear remapping (Figure 5.2.3A) whilst the BVCs continued to respond for the portion of the new boundary (square perimeter walls) which intersected the cells preferred distal and directional preferences. From visual inspection it can be seen that the BVC field locations remained stable across trials in the same environment, and in the changed environment test trial. The stability of BVCs across these trials supports the theory that BVCs are insensitive to context change and produce universal responses to boundaries (Lever et al 2009; Hartley et al. 2000; Barry et al., 2006).

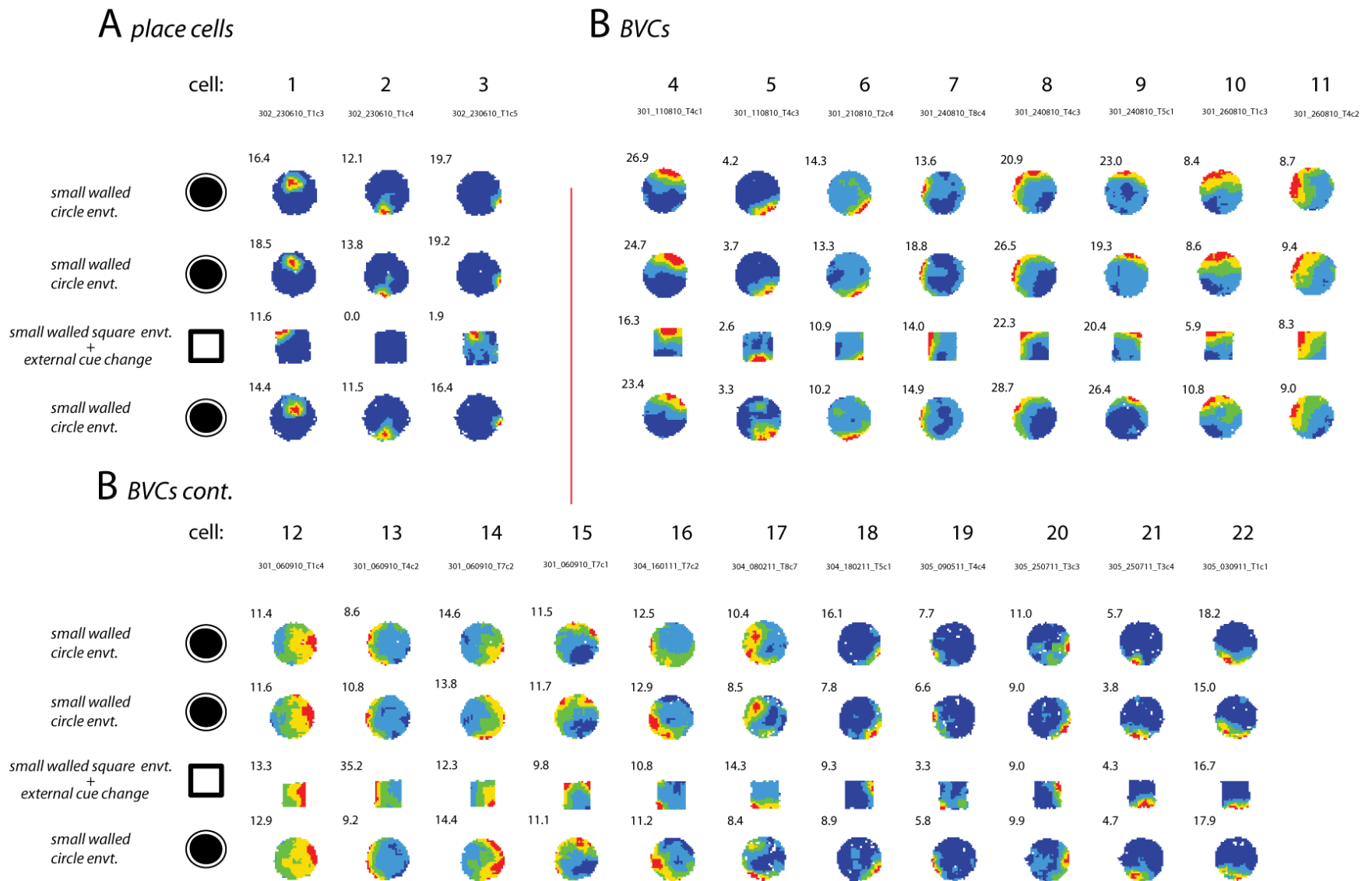


Figure 5.2.3: BVCs are not sensitive to context change.

The figure presents 3 place cells and 19 BVCs tested using the context change paradigm. The rats were run in two exposures of the familiar environment (small walled circle) and were then run in a novel environment whereby the walls, floor and external cue cards were changed (test trial; small walled square). After the test trial the BVCs were then run in another familiar environment trial as a return to baseline. A) Shows three place cells from rat 302 demonstrating clear global remapping B) shows 19 BVCs with relatively stable firing across the trials.

5.2.2 BVC fields are maintained in darkness

In order to examine whether visual input is required for BVC boundary responses, BVCs were recorded in complete darkness using the same protocol as used for the grid cells (see methods). Lever et al., (2009) recorded 3 BVCs in darkness, all of which continued to show BVC-like responses to the perimeter boundary. Lever et al., (2009) noted however that the BVC firing fields were more diffuse in darkness than in normally lit conditions.

Figure 5.2.6 shows 15 BVCs tested in darkness. Between the lit baseline trials the BVC firing properties were stable (data not shown). This stability was also maintained during the dark trial (Table 5.2.1). Between the lit baseline trials and the dark trial there was no difference in locational or directional information (bits per second), selectivity, locational peak rate, or global mean rate. This was the case whether I looked at the first and second lit baseline trials vs. the dark trial (not shown), or an average of the lit baseline trials vs. the dark trial (Table 5.2.1). Stable BVC firing properties with the removal of visual cues supports Lever et al's observation that BVC-like responses are maintained in darkness. This also suggests that BVCs do not require visual cues for boundary signalling.

Table 5.2.1. Removing visual cues does not interrupt BVC firing properties.

This table gives the means and S.E.M. of 6 properties of BVC firing that do not significantly differ between light and dark trials. Where possible the light trial statistics are taken from an average of the two baseline trials (12/15 BVCs). Directional information was calculated from unsmoothed polar plots (bin size 5.6°). Locational information was calculated from unsmoothed rate maps (bin size 3cm x 3cm). The table also presents the p-values for comparisons of properties between light and dark trials.

BVCs (n=15)	MEAN ± SEM					
	Locational Information Bits/sec	Directional Information Bits/sec	Locational selectivity	Directional selectivity	Locational Peak rate (Hz)	Global Mean rate (Hz)
Light trials	0.47 ± 0.07	0.30 ± 0.10	4.97 ± 0.73	1.83 ± 0.14	8.14 ± 0.97	2.03 ± 0.37
Dark trials	0.49 ± 0.12	0.29 ± 0.10	4.72 ± 0.62	1.98 ± 0.21	7.8 ± 1.01	1.98 ± 0.33
p value	0.81	0.88	0.66	0.33	0.50	0.80

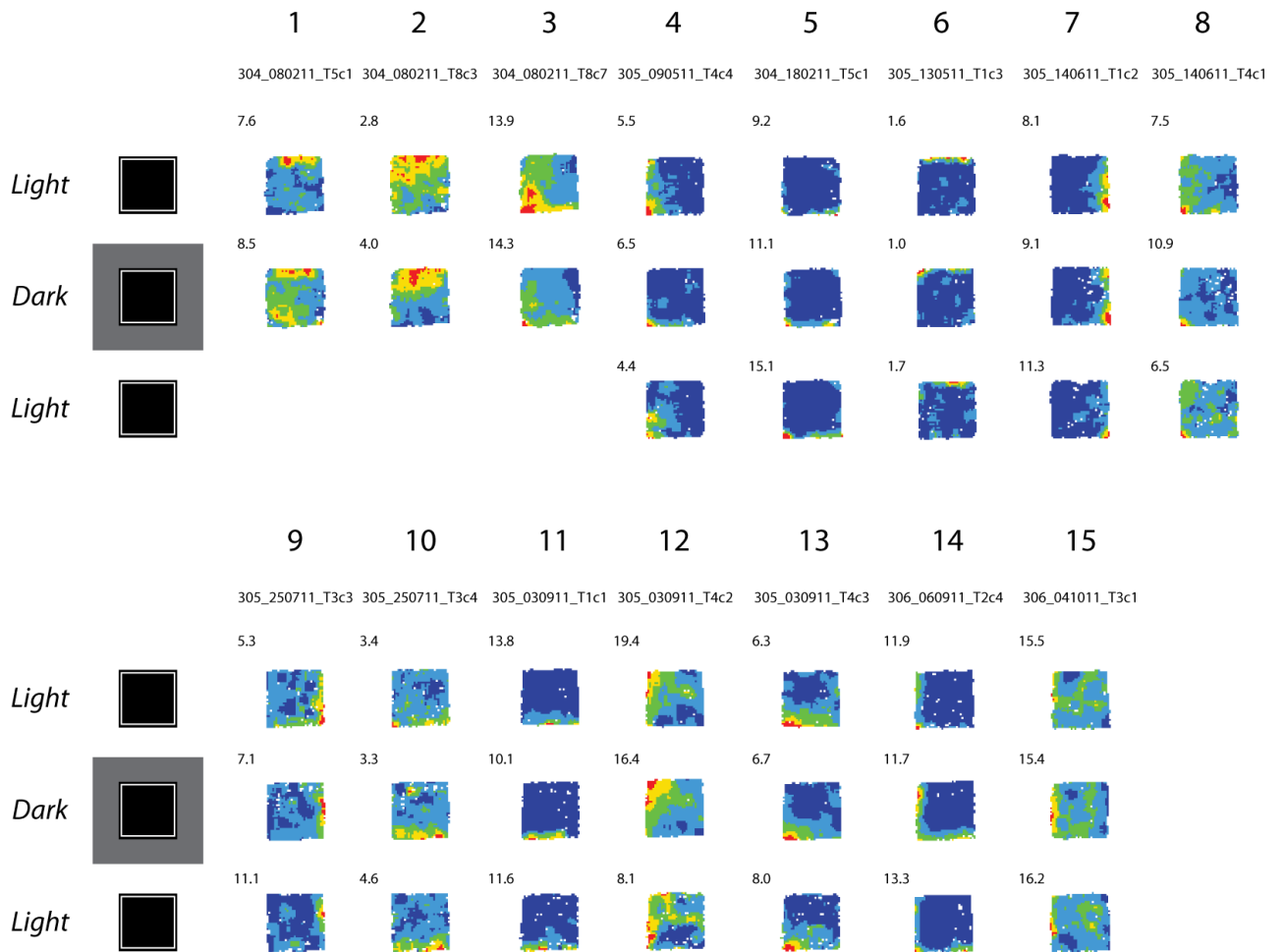


Figure 5.2.4: BVC firing properties are not disrupted between light and dark trials.

The figure shows the full sample of BVCs tested in darkness (from three rats). There was no difference in spatial information or rates between the light and the dark trials (see Table 5.2.1 for statistics).

5.2.3 BVCs respond to internal barriers and objects

The predicted doubling of the BVC firing fields in response to the insertion of an appropriately oriented barrier is demonstrated in Figure 4.2.1. The doubling of BVC fields following the creation of additional, appropriately-oriented boundaries was a key prediction of the original model. This was demonstrated with only 3 cells in Lever et al., (2009). As detailed earlier in this thesis, this property was used as a defining feature for BVCs recorded here.

To briefly recap, a BVC was classed as such if, with the addition of an internal barrier it produced a second field covering for 50% at least of the predicted side of the barrier at a firing rate of $\geq 40\%$. Of the 57 putative BVCs identified by visual inspection 42 were classified using this method (Figure 4.2.1). The inserted barrier shared qualities with the perimeter wall. It was of equal height, and when used with the large walled circle and square environments it was the same colour as the floor. The barrier was also made of the same materials the large walled square (LWS). Could the doubling of the firing field with the insertion of the barrier be in response to the barrier's shared qualities with the familiar walls?

Three BVCs (from 2 rats) were tested with an additional boundary created using a linear array of bottles (see Figure 5.2.5 and methods for more details). They produced a second locational field on the expected side of the linear array-boundary similar to that seen with the insertion of the appropriately oriented barrier. If the linear array of bottles was deconstructed the second firing fields persisted for a two bottle array in all 3 BVCs. Two of the cells (cell 2 and cell 3) also produced a second firing field when only a single bottle remained in the environment. When an even smaller object (cylindrical measuring tube, Figure 5.2.5C) was introduced, the two cells which were still being recorded, responded to it as a boundary and produced a second firing field (Figure 5.2.5). This suggests that the length of the inserted boundary be it a wall, an array of bottles, a singular bottle or a thin object may not be the determining factor controlling the production of a second BVC locational field.

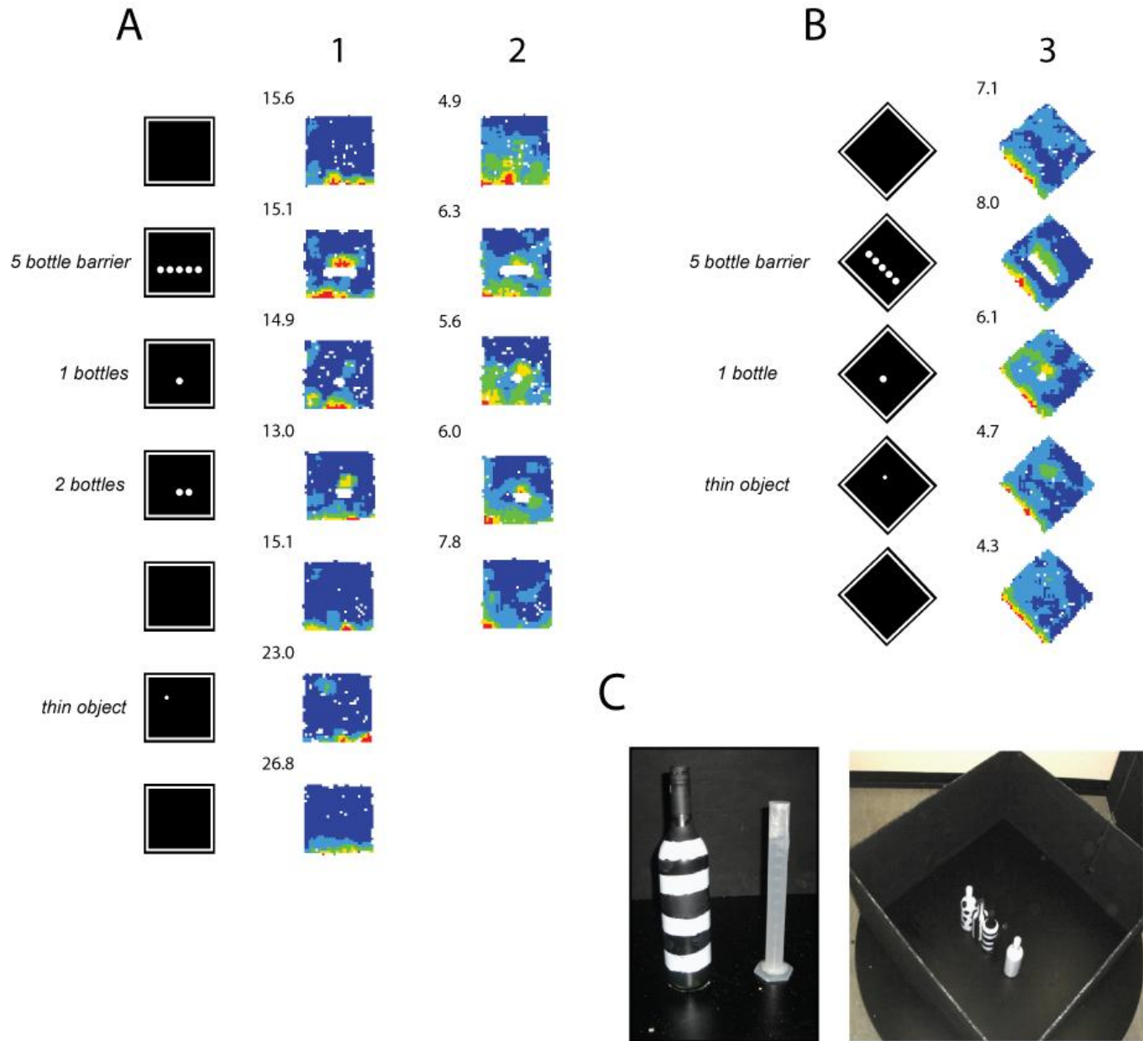


Figure 5.2.5: BVCs code for objects as well as for linear boundaries.

3 cells were recorded with linear arrays and individual objects (bottles). A) Shows two cells from rat 305. These were simultaneously recorded. B) Shows one cell recorded from rat 306. C) Between baseline trials, the cells were recorded with individual objects and arrays of objects. Left shows example objects; they were either bottles or a ‘thin object’ which was a measuring cylinder. Right shows 5 bottles made into a linear array creating a boundary to the south-west in the large walled square environment. This was the trial set up for the 5 bottle barrier trial used to test cell 3 (B). All 3 cells produced a clear second field for the 5 bottle barrier, and cells 2 and 3 produced second fields for the 1 bottle barrier. Cells 1 and 3 also produced second fields for the thin object. See methods for manipulation details.

One cell was recorded with the standard barrier and two objects during darkness (Figure 5.2.6). The method was the same as used above for the grid cells and the BVCs, but with the addition of a barrier/objects.

Figure 5.2.6A reveals that when the lights were extinguished the BVC maintained its second firing field for the inserted barrier. In Figure 5.2.6B both the thin object and a single bottle were inserted into the environment during the same trial (objects shown in Figure 5.2.5C *left*). In the light trials the cell produced a second field for the bottle, but in the dark trial the firing rate of the second field was diminished leaving only a small portion of field with a weakened firing rate of 20-40%. This BVC did not produce a second firing field for the thin object, in either the light or dark trials on this day.

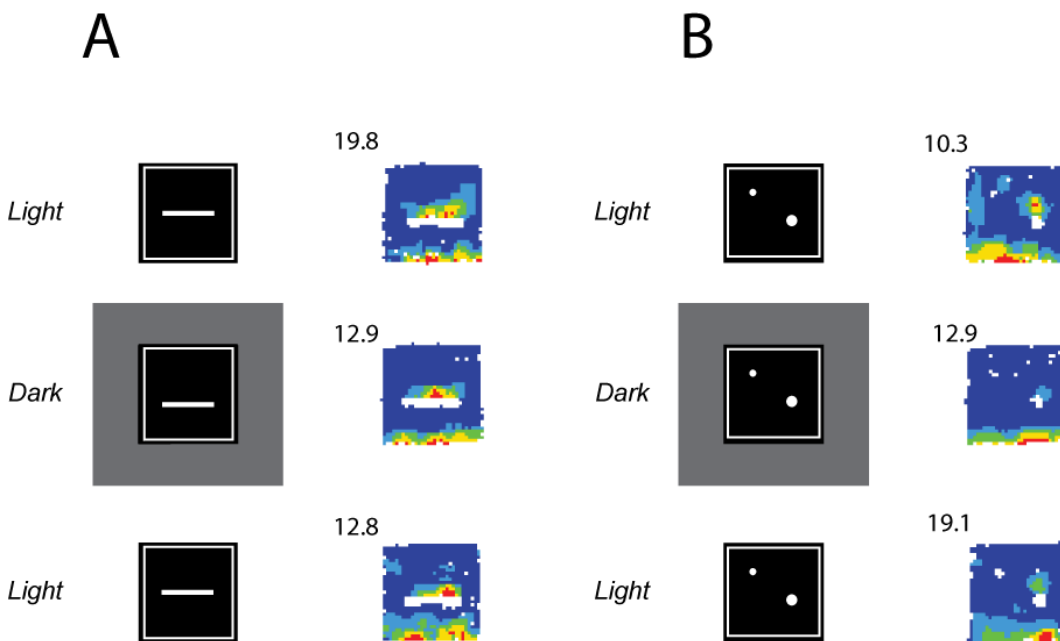


Figure 5.2.6. BVCs can produce second firing fields in darkness.

This figure shows 1 cell recorded from rat 305 in the darkness paradigm with inserted barriers/objects. A) Shows the BVCs response to the standard barrier. The BVC produced a second firing field (along at least 50% of the barrier at $\geq 40\%$ peak firing rate) for the standard barrier in the absence of visual cues. B) Shows the cells response to two objects: the thin measuring cylinder (top left) and a single bottle (bottom right). The BVC ceases to produce a second firing field with $\geq 40\%$ firing rate for the single bottle object when visual cues are removed. However, a second field is evident in both the light trials. The thin object did not instigate the production of a second field in any of the trials.

5.2.3.1 BVC firing may depend upon boundary height

BVCs were also able to produce second fields for boundaries that varied in height and width as well as length. Two of the BVCs received further trials with 2 short barriers which were traversable (Figure 5.2.7). The first traversable barrier was 4.5cm high, 10cm wide and 20cm long (Figure 5.2.7A). The second was 2.5cm high and wide and 50cm long (Figure 5.2.7B). Both cells produced a second field for the 4.5cm high barrier, but not for the for the shorter 2.5cm high barrier. This may suggest that that the 'height' and 'breadth' of a boundary may be a fixed factor in determining what a BVC treats as a boundary (for more details see methods).

5.2.4 BVCs respond to objects of varying heights and widths as boundaries: summary

These few cases outlined above suggest that BVC firing is not restricted to only the environment perimeter and that there may be a quantitative way to establish what BVCs treat as a boundary. Here the height and width of the boundaries was varied and saw that even for a few cases the fields doubled (Figure 5.2.5; Figure 5.2.7). The ability of BVCs to respond to individual objects and to traversable ridges suggests that boundaries may be defined by sensory cues and limitations to movement that are not restricted to walls.

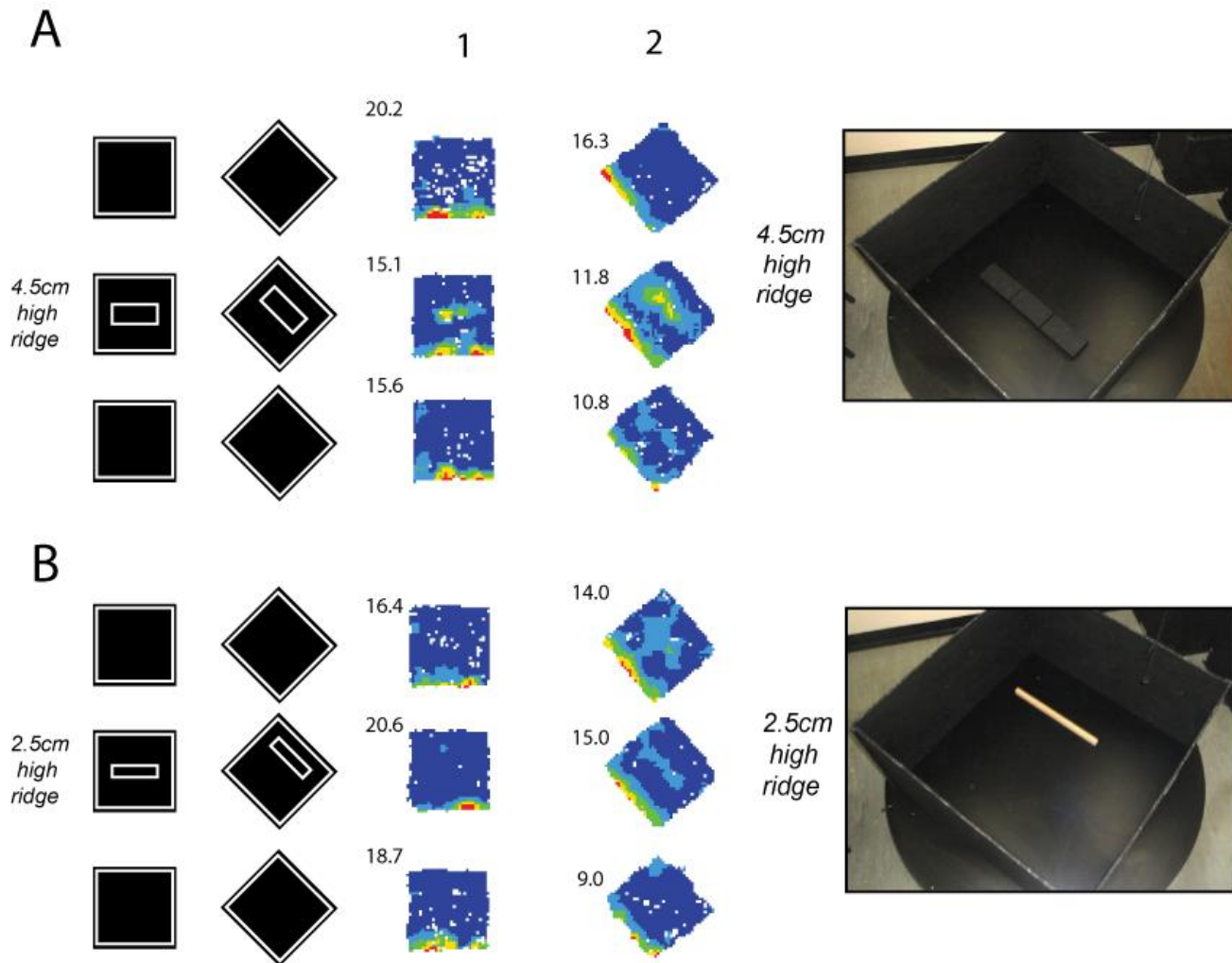


Figure 5.2.7: The height and width of a traversable barrier determines whether it is treated as a boundary.

This figure shows 2 cells from 2 rats. For cell 2 the environments were rotated so that the cells preferred direction would not intersect two walls. Environments and rate maps are shown in running order from top to bottom. A) An inserted barrier 4.5cm high and 10cm wide was inserted into the environment (see illustration, left; and photo, right). Both cells produced a second field for the barrier. B) When a shorter and thinner barrier was inserted (height and width 2.5cm; see illustration, left; and photo, right) neither cell produced a second field. However for cell 2 a shadow of the second field remained from exposure to the 4.5cm barrier.

5.2.5 BVCs maintain their firing fields with wall removal

In a walled environment the boundary is obvious, but when the walls are removed the boundary becomes less clear. Arguably in a wall-less environment the boundary can be either the platform drop, the extent of explorable space over the drop, or both. In Lever et al., (2009) for the 17 BVCs recorded in wall-less environments there was a mixture of responses (see Figure 2.3.2 in the introduction). Some BVCs demonstrated responses to the platform edge (e.g. cell 5K). Some coded for the extent of explorable space (e.g. cell 1a) and for some BVCs the fields disintegrated with wall removal (e.g. 5g).

As the BVC model predicts BVCs will produce fields for any boundary in their preferred direction and distance, irrespective of changes to the environment. For example between circular and square environments a BVC will produce a field which follows the curvature of the circular wall in the large walled circle (LWC), and the straight edge of the straight wall in the large walled square (LWS; see Figure 5.2.1).

This thesis shows that in grid cells the grid scale expands in a relatively novel wall-less environment when compared to a familiar walled environment. It has been suggested that BVCs anchor grid cells to the geometric boundaries of the environment (Moser and Moser, 2008). If this is the case then would the expansion of grid cell grid scale be accompanied by a BVC field shift with wall removal?

Figure 5.2.8 provides a comprehensive illustration of the BVCs recorded in the walled (LWC) and un-walled (COP) circular environments. 16 cells were recorded in this manipulation with one cell being recorded on two occasions five days apart (cell 1). The peak rate pixels are indicated in the figure with an 'x'. For two of the cells alternative peaks had to be created because the peaks were not located in the BVC field (see methods). The peaks for these trials are circled on the rate maps. Where possible when there are 2 baseline walled trials the average location of the peak pixels was taken (5 cells). 12 BVCs (one was run through with both days) with clear fields in the COP were included in the analysis; see Figure 5.2.8A. Cell 1 was tested in this manipulation on two days both of which were included in the analysis.

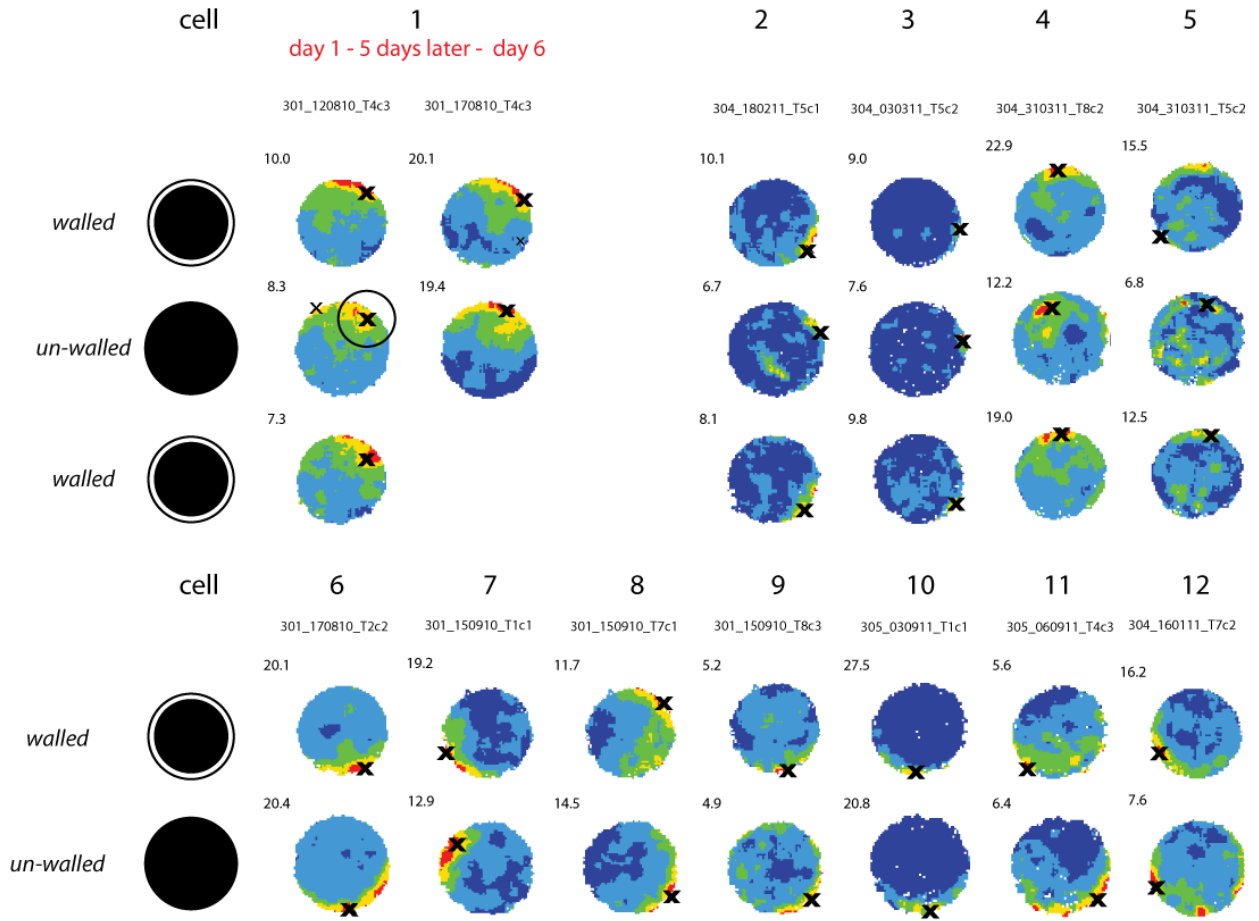
Figure 5.2.8B shows 4 cells which were excluded from the analysis. When the walls were removed these cells stopped demonstrating evidence of boundary signalling. For 3 of them the field disintegrated (cells 14-16), and for the other BVC the field moved and became more 'place-like' (cell 13). For this cell boundary signalling returned in a subsequent return to baseline walled trial.

To see if the peak of the BVC fields moved with wall-removal the distance in pixels from the peak to the centre of the environment for both the walled (LWC) and the un-walled (COP) trials was calculated. This was calculated using the cluster cutting software (TINT, Axona). The distance in pixels between the peaks and the environment centre were compared and the pixel distance was then converted into cm's (see methods for more details and diagram).

The BVC peaks did not move significantly further away from the environment centre with wall removal ($3.5 \pm 1.23\text{cm}$; $t_{12}=1.22$, $p=0.25$). If the peaks were to have shifted outward to the extent of explorable space then it would be expected for the BVC fields to have shifted $\sim 10\text{-}15\text{cm}$ further away from the environment centre.

The observed evident grid expansion between the walled and un-walled environments presented in section 5.1.1 above was around 11.5% (higher in SUBGRIDS sample). A simple view in which grid expansion was tied to the extension of the perimeter by boundary cells would predict an expansion of 3.5 cm divided by 75 cm, i.e. around 4.6%. Thus grid expansion appears to exceed BVC field centrifugal extension. In addition to the fact that grid expansion is partly determined by novelty, this appears to rule out any simple hypothesis linking grid expansion to perimeter extension.

A *BVCs included in the wall no-wall analysis*



B *Wall removal can cause BVC fields to disintegrate*

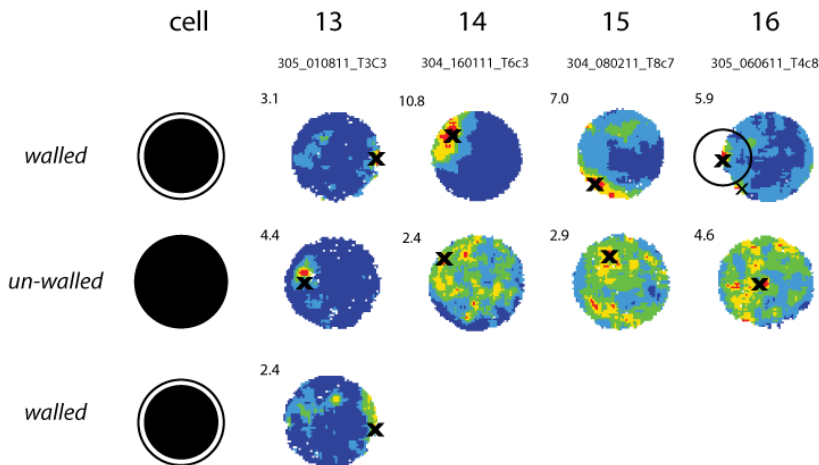


Figure 5.2.8: BVCs respond for environment drops as well as walls.

16 BVCs were recorded in walled (large walled circle) and un-walled (circular open platform) environments. A) Shows 12 BVCs which maintained stable fields in both the walled circle and the un-walled circular open platform (COP). B) Shows 4 BVCs which stop demonstrating boundary signalling when the environment walls are removed. 'X' indicates the location of the peak rate pixel for each trial. Cells 1 and cell 16 have two 'X's' in two of their trials the circled 'X' is the peak pixel located in the BVC firing field and used for analysis.

5.2.6 BVCs respond to traversable gaps as boundaries

BVCs can also respond to boundaries produced by the creation of traversable drops (Figure 5.2.9). Lever et al., (2009) reported a single BVC which responded to both the perimeter drop of an open platform and a traversable gap of 13cm created between 2 open platforms. This gap was such that the rat voluntarily crossed the single traversable gap 3 times but had to be carried over 5 times.

In the present study two trials were presented with a rectangular open platform that could be pulled apart to create two 10cm gaps separating 3 square platforms (Figure 5.2.9). The first trial consisted of the three square platforms *'together'* creating a rectangular open platform. This was oriented so that one of its short edges was in the BVCs preferred direction. In the second trial the three platforms were pulled *'apart'* to produce two 10cm gaps. This created three drops, two of which were traversable. The gap of 10cm was easily crossed by the rat.

Figure 5.2.9A shows 9 BVCs which produced a tripling of their fields in response to both the perimeter drop and the traversable drops. Two cells were classified as BVCs based on their behaviour in this manipulation. These 2 BVCs did not produce a second field with the addition of an appropriately-oriented internal barrier, however they did produce a tripling of their fields in response to appropriately-oriented *'drops'* in this manipulation. Both cells treated the gaps as three north-west boundaries (cells 2 and 3 Figure 5.2.9A).

Not all BVCs shared the same response to this manipulation. Figure 5.2.9D shows 3 BVCs which did not respond to the perimeter or gap boundaries. Of the 19 BVCs recorded in this manipulation only those shown in Figure 5.2.9A and the two cells with all-boundary fields in Figure 5.2.9B responded to the perimeter drop in the *'together'* trial. Three BVCs which did not produce fields responding specifically to the perimeter drop did however produce double fields for the traversable drops in the *'apart'* trial (Figure 5.2.9C).

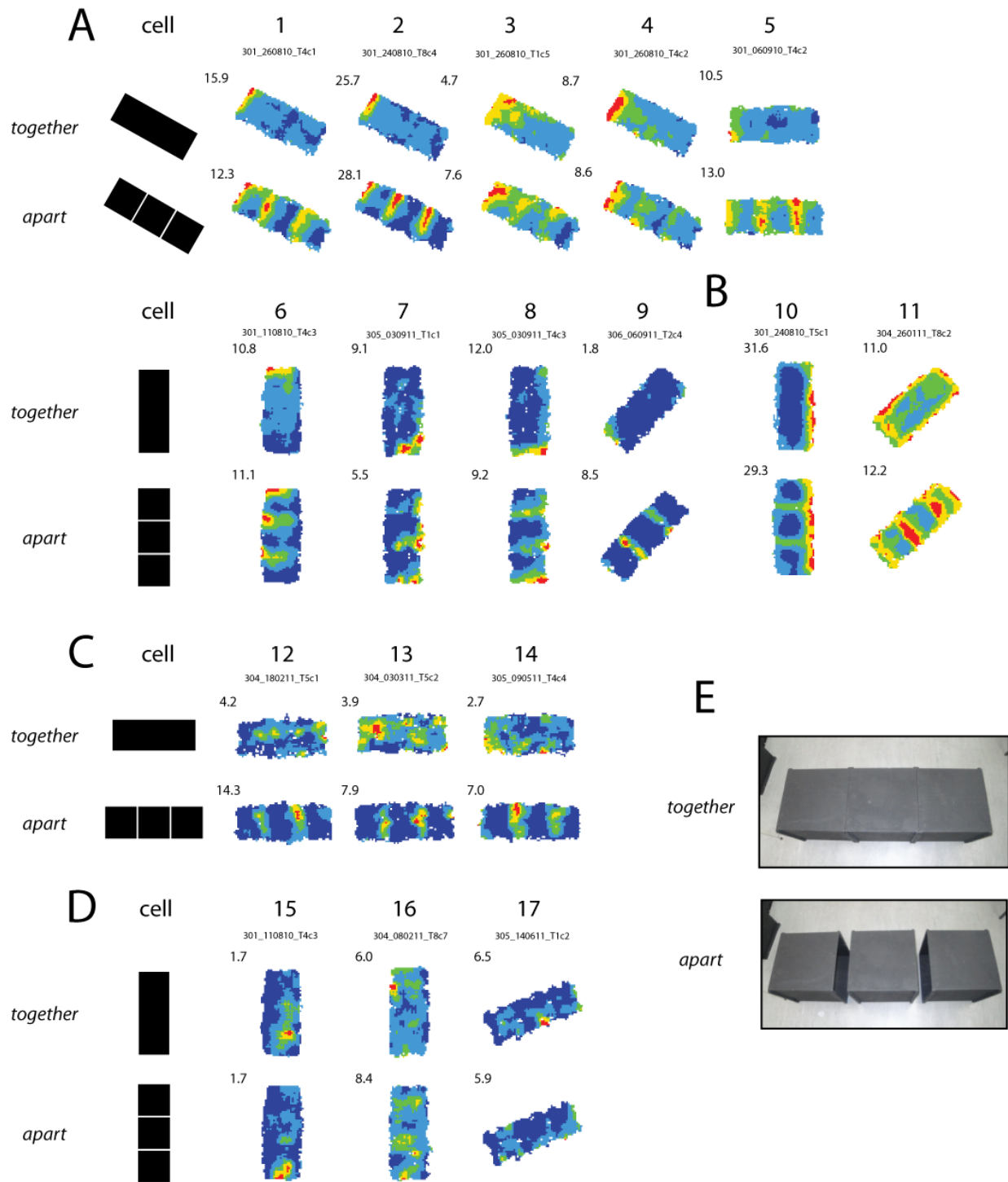


Figure 5.2.9: BVCs can treat traversable drops as boundaries.

This manipulation includes two trials, the ‘together’ trial, which is a rectangular open platform made up of 3 square platforms, followed by the ‘apart’ trial where these platforms are separated by two 10cm gaps (E for photos). The environment was orientated so that one of the short edges was in the BVCs preferred direction. A) 9 BVCs responded to both the perimeter drop in the ‘together’ trial, and the addition of two new drops in the ‘apart’ trial. B) 2 BVCs demonstrated all-boundary fields for both the perimeter and traversable drops. C) 3 BVCs which did not show boundary signalling in the ‘together’ trial, but produced firing fields for the traversable drops in the ‘apart’ trial. D) 3 BVCs which did not code for the perimeter or traversable drops. E) provides photographs of the environments; ‘together’ (top) and ‘apart’ (bottom).

5.2.6.1 BVCs respond to traversable gaps as small as 3cm

For over half of the BVCs tested in the together-apart manipulation a traversable gap of 10cm was responded to as a boundary similar to the perimeter edge. For 3 cells from 2 rats a series of trials were run in an attempt to quantify what size gap was required to be signalled as a boundary (Figure 5.2.10). All three BVCs previously produced triple fields in the *'together-apart'* manipulation with a gap of 10cm (cells 7, 8 and 9 Figure 5.2.9). Two different trial series were used between rats. In cell 1 the gap was reduced over trials and in cell 2 and 3 it was increased. Figure 5.2.10A shows three photos of the together trial, the 1cm gap trial and the 3cm gap trial. Cells 2 and 3 show clear field doubling for the 10cm gap and the 5cm gap but weaker second fields for the three cm and 1cm gaps. For these two trials cell 3's second field included a portion of 40-60% peak firing rate along the traversable drop (green on the rate map). However the appearance of a second field for this BVC is hard to judge because the firing fields generally became more diffuse through the series of trials.

Cell 1 showed a clear second field for the 3cm gap trial, and no second field for the 1cm gap trial, suggesting for this cell that 3cm was treated as a boundary, whereas 1cm was not. The strength of the second fields for cells 2 and 3 diminished as the gap was reduced in size. As the gaps got smaller fields responding to the traversable gaps were hard to dissociate from background firing as the fields became more diffuse through the trial series (Figure 5.2.10).

Overall, looking at the response of these 3 BVCs, it seems that as the size of the traversable gap is reduced, so does the BVC response to it. As seen when the width and height of the barrier is altered, the size of traversable gap which constitutes a boundary may be quantifiable.

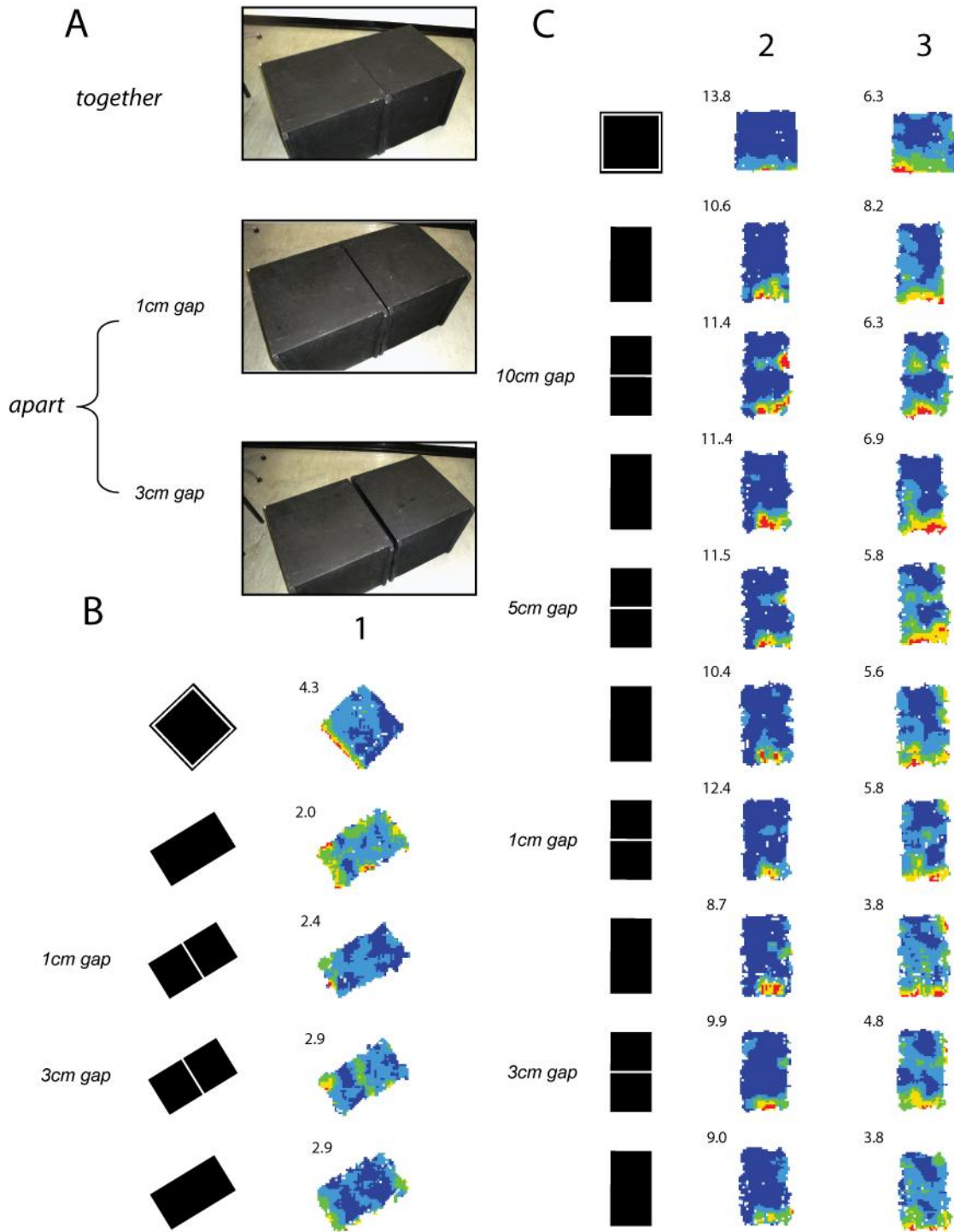


Figure 5.2.10. The size of the traversable drop determines whether BVCs treat it as a boundary.

A) Shows example photo's of the traversable gap environments. The top photo shows the 'together' trial where two square platforms create a rectangular open platform. The middle and bottom photos show two of the 'apart' trials where the square platforms are separated by a 1cm and 3cm gap respectively. B) shows one cell from rat 306, which treated a 3cm gap as a boundary but not a 1cm gap. C) shows 2 cells from rat 305. Both cells show a clear second field with 10cm and 5cm gaps, and a weak field for both the 3cm and 1cm gaps.

5.2.7 Summary of BVC responses to environment manipulations

BVCs signal boundaries that are located in their distal and directional preferences. They follow the environment shape, and if their preferred direction intersects two walls, the BVC will fire for a portion of each. BVCs maintain their directional and distal preferences across strikingly different environments, and remain stable in manipulations which induce global remapping in place cells. BVC field stability is also maintained in darkness, with no evidence of BVC properties changing between light and dark trials. BVCs signal perimeter boundaries and internal boundaries. When an appropriately-oriented free-standing barrier is inserted into the environment a BVC will produce a second firing field on the predicted side of the barrier. BVCs also signal a second boundary when a linear array of bottles is inserted into the environment. Signalling is maintained as the bottle barrier is reduced in size, with some BVCs being able to signal a singular bottle, and an even smaller object as boundaries.

The BVCs also produced fields for environment edges of open platforms (environment drops). The BVC firing fields in general continued to signal the environment edge and did not expand to the extent of explorable space. BVCs also produced boundary signalling to traversable gaps between open platforms. When three open platforms were pulled apart by 10cm some of the BVCs signalled these gaps similarly to the perimeter platform edge. Some BVCs also respond to smaller gaps between open platforms. Looking at a small sample of BVCs, it was evident that gaps as small as 3cm can be signalled as boundaries.

The variable responses of BVCs to boundary manipulations suggest that the BVC population may treat different boundaries differently. In 2009 Lever et al., concluded that what a BVC may consider is a boundary may depend on many factors. Like shown in Lever et al., (2009), the BVCs presented here show a variety of responses to wall removal, as well as to different walled boundaries. The BVC response may reflect sensory properties of environment features such as the sight or feel of a wall or an extended edge. Boundary-signalling may also be related to restrictions to movement. Lever et al. also noted a diversity of differing representations of the un-walled environment boundary and considered that the properties which determine a boundary may vary in importance across the BVC population. Certainly our results support this consideration.

5.3 New class of boundary-correlated cell: Boundary-off cells

Some of the subicular cells recorded during the above experiments, showed large fields covering almost the entire environment floor (e.g. cell 1 Figure 5.3.1). For these cells the portion of the environment *without firing* was a thin area located at the boundary edge (Figure 5.3.1 and Figure 5.3.2). Lever et al., (2009) considered that BVCs with large fields may be cells with more distal distance tuning (see Figure 2.3.2 in the introduction). However, the cells in Figure 5.3.2 are better characterized as having an ‘inhibited’ zone of firing like that of the region of peak firing in a BVC (cell 1 Figure 5.3.1). I have called these boundary-off cells.

Figure 5.3.1 shows the simultaneous recording of a boundary-off cell, a BVC and a HD cell. The BVC clearly shows a firing field which follows the boundary, and the boundary-off cell shows a crescent of inhibition along the boundary. When an appropriately-oriented barrier was inserted into the environment the BVC characteristically produced a second firing field on the predicted side of the barrier. The boundary-off cell also responded to the barrier insertion with the appearance of a second inhibited field (see Figure 5.3.1 and Figure 5.3.2). These cells seem to show the inverse response to boundaries, that are seen in BVCs. The appearance of a boundary does not initiate cell firing but rather inhibits it. The cell appears to fire everywhere except near the boundary.

I report 9 examples of boundary-off cells recorded from 3 rats (see figure 5.3.3 for the basic properties of each boundary-off cell). To be considered a boundary-off cell, cells had to show a) an inhibition of firing for the preferred boundary and b) a second inhibitory field with the addition of an appropriated-oriented barrier. Boundary-off cells were recorded from the same tetrodes as BVCs, grid cells and HD cells. On some occasions they were simultaneously recorded, as shown in Figure 5.3.1. All cells shown in Figure 5.3.2 demonstrated clear inhibition for both the perimeter wall and the appropriately-oriented barrier. For 6 of the cells this was shown in both the large circular and square environments (Figure 5.3.2).

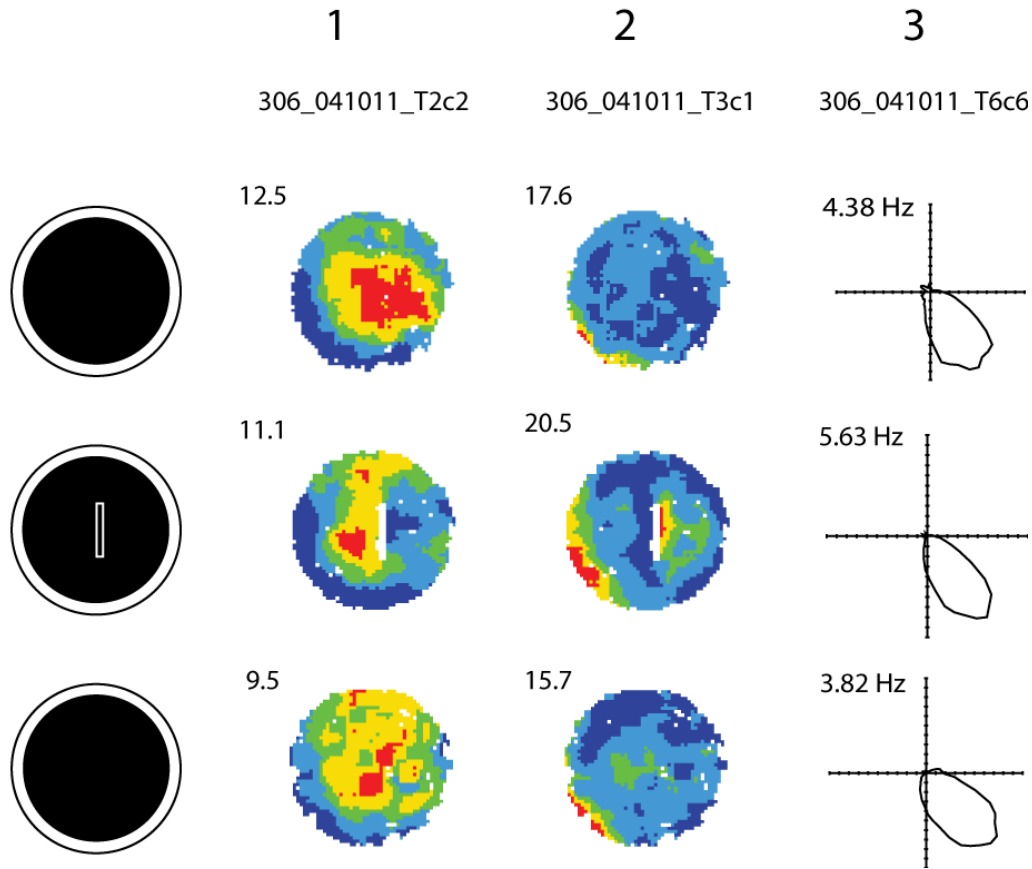


Figure 5.3.1: Boundary-off cells were sometimes simultaneously recorded with other spatial cells.

The figure shows the simultaneous recording of a boundary-off cell (1), a BVC (2) and a HD cell (3). The firing pattern of the boundary-off cell is very similar to the inverse of the BVC.

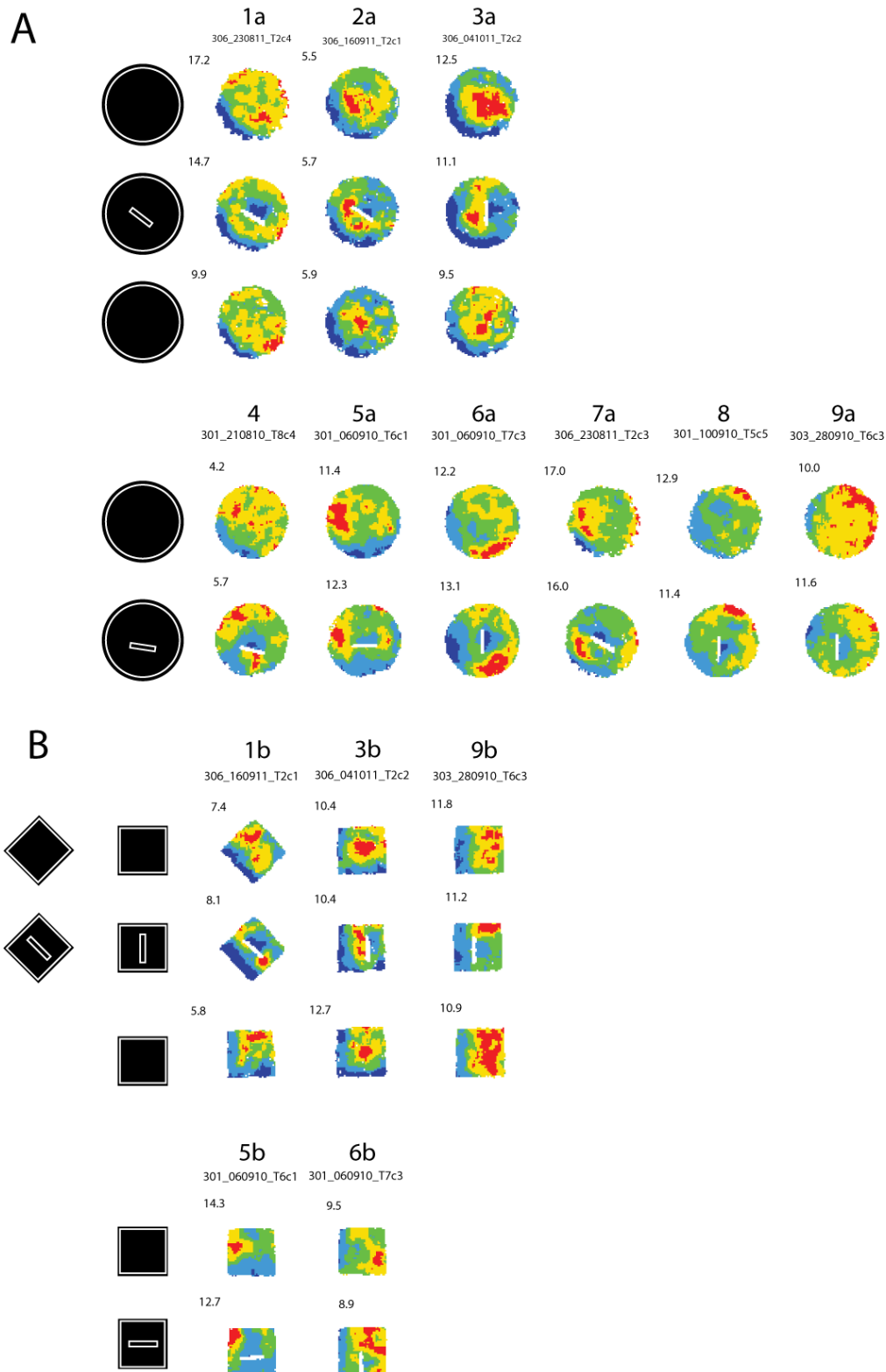


Figure 5.3.2: Boundary-off cells show an inhibitory response to barrier insertion.

The figure provides the full sample of boundary-off cells tested with barrier insertion. A) Shows all 9 cells tested with a barrier inserted into the large walled circle. B) Shows 6 of the cells which were also tested with the barrier in the large walled square. Each boundary-off cell is given a number as in previous figures. If the cell was tested with the barrier in both the square and circular environments this is indicated with an 'a' and a 'b' e.g. 1a in section A and 1b in section B are the same cell recorded in both manipulations.

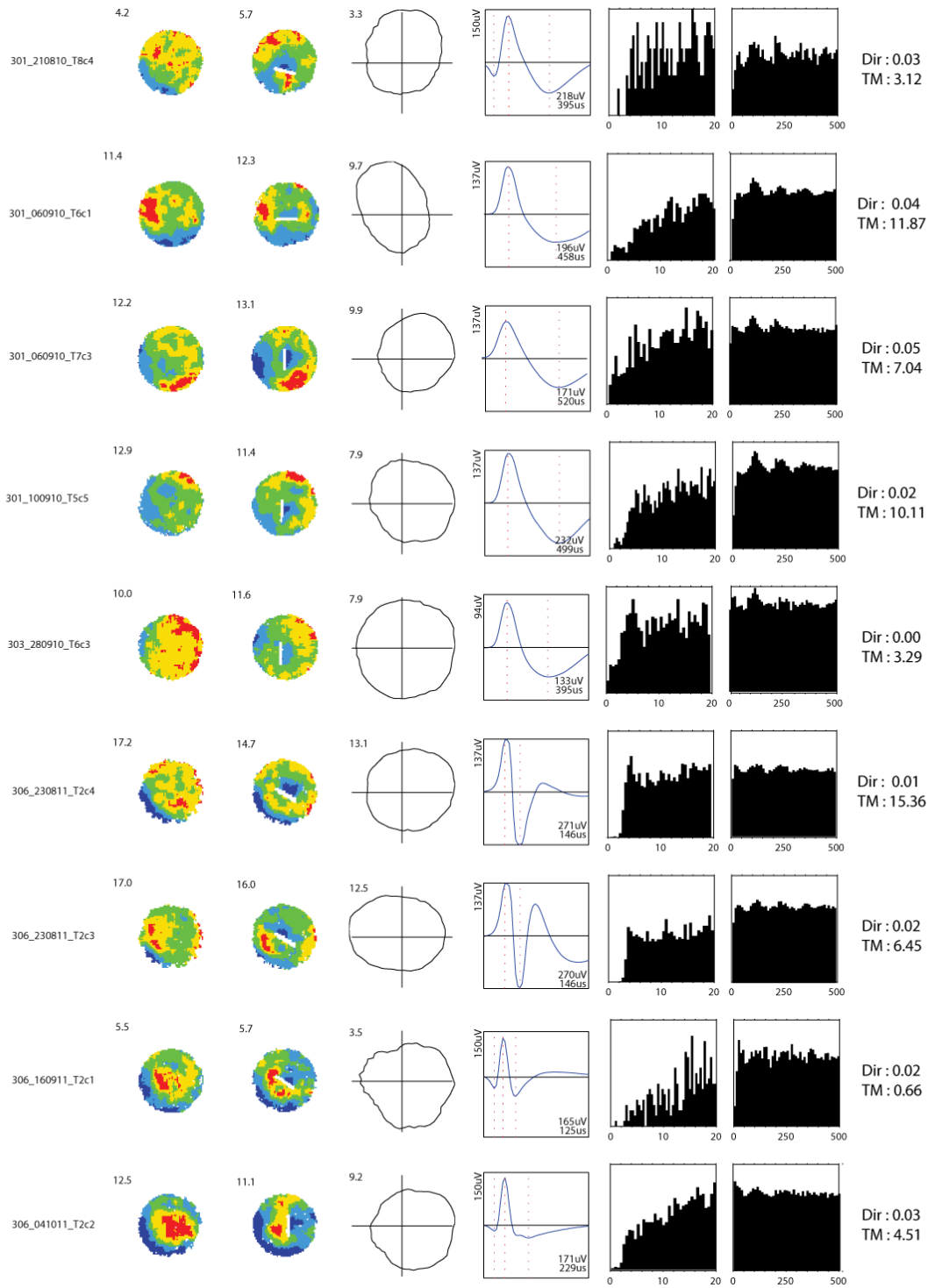


Figure 5.3.3. Basic characterisation of all boundary-off cells.

Each row shows data for one boundary-off cell. From left to right the figure presents; text column stating rat/day, tetrode/cell; locational rate map with peak rate (Hz); spatial autocorrelation map; directional polar plot with peak rate (Hz); spike waveform, bottom-right text stating peak amplitude (highest positive-to-negative or negative-to-positive amplitude, μV) and negative peak-to-trough interval (μS); temporal autocorrelations (0-20ms and 0-500ms). Rightmost text column gives the directional information in bits per spike (Dir; directional information calculated from unsmoothed polar plots, bin size 5.6°) and the theta modulation score (TM). Data comes from the first large walled circle trial of the day.

5.3.1 Boundary-off cells maintain their firing fields in darkness

The firing pattern of the boundary off cell is very similar to the inverse of the BVC. The inhibited field follows the boundary, in the circular and in the square environments (Figure 5.3.2). Like BVCs boundary-off boundary responses are not disrupted in darkness (Figure 5.3.4). Only 3 cells were recorded in the darkness manipulation, however in Figure 5.3.4 the rate maps do not show any evident disruption of the boundary-off fields. The inhibitory fields continue to remain along the same portions of the perimeter walls.

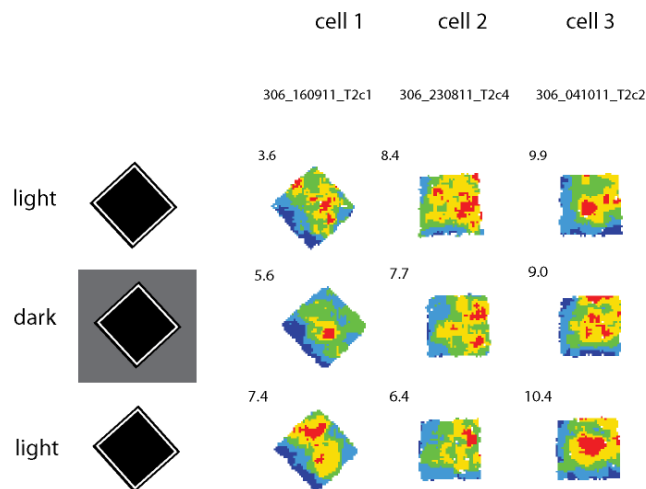


Figure 5.3.4: Boundary-off cells like BVCs and grid cells maintain their firing patterns in the absence of visual cues.

5.3.2 Boundary-off cells carry more locational than directional information.

Table 5.3.1 shows that Boundary-off cells carried significantly more locational than directional information in both bits per spike and in bits per second. However they did not show more locational than directional selectivity.

Locational and directional information was compared between boundary-off cells and BVCs (Table 5.3.2). There was no difference in locational or directional information over time (bits per second). However, BVCs carried more locational and directional information per spike and were more locationally and directionally selective than the boundary-off cells. Boundary-off cells had large fields covering almost the entire environment and a higher global mean rate than the BVCs (Table 5.3.3). Which would account for boundary off cells carrying less spatial information per spike and being less spatially selective than BVCs.

Table 5.3.1. Boundary-off cells carry more locational than directional information.

Spatial information is calculated to estimate the mutual locational/directional information in seconds. Selectivity is calculated by dividing the peak firing rate across bins by the mean firing rate (calculated for locational and directional). Spatial information was calculated using locational/directional equivalence binning from unsmoothed polar plots (bin size 6°) and rate maps (bin size 18.5cm x 18.5cm). Analysis was conducted using the full boundary-off sample (n=9) in the first large walled circle of the day (LWC).

	MEAN ± SEM		
	Spatial information Bits/sec	Spatial information Bits/spike	Spatial Selectivity
Locational	0.06 ± 0.01	0.40 ± 0.10	1.65 ± 0.20
Directional	0.02 ± 0.00	0.15 ± 0.03	1.35 ± 0.07
p value	0.01	0.02	0.19

Table 5.3.2. Boundary-off cells carry less spatial information per spike and less spatial selectivity than BVCs.

Spatial information was calculated using locational/directional equivalence binning (60 bins each) from unsmoothed polar plots (bin size 6°) and unsmoothed rate maps (bin size **LWC**, 18.5cm x 18cm; **LWS**, 14cm x 14cm).

	MEAN ± SEM					
	Locational			Directional		
	Locational information Bits/spike	Locational information Bits/sec	Locational Selectivity	Directional information Bits/spike	Directional information Bits/sec	Directional Selectivity
Boundary-off N=9	0.06 ± 0.01	0.40 ± 0.10	1.65 ± 0.20	0.02 ± 0.00	0.15 ± 0.03	1.35 ± 0.07
BVC N=46	0.21 ± 0.04	0.43 ± 0.04	5.72 ± 1.00	0.13 ± 0.03	0.20 ± 0.03	1.79 ± 0.11
p value	0.0002	0.80	0.07	0.002	0.53	0.002

5.3.3 Boundary-off cells have basic properties which are distinct from other spatially recorded cells

Table 5.3.3 shows that like BVCs and grid cells boundary-off cells carried significantly less directional information than locational information. However, boundary-off cells can be distinguished from BVCs because per spike they are less locationally and directionally modulated and they are less spatially selective (Table 5.3.2 and Table 5.3.3). Due most likely to the size of the spatial fields the boundary-off cells also had much higher global mean rates than the other cell types (Table 5.3.3).

Similar to BVCs and grid cells, Table 5.3.3 shows that boundary-off cells carry much less directional information than HD cells. The table also shows that like BVCs boundary-off cells are distinct from grid cells because they had much lower gridness scores and theta modulation scores than the grid cells.

Of the 4 types of cells recorded here boundary-off cells had the highest firing rate and higher global mean rate than BVCs, grid cells or HD cells (Table 5.3.3). Boundary-off cells also had larger peak-to-trough amplitudes than any of the other cell types (Table 5.3.3). Looking at the means in Table 5.3.3, boundary-off cells also have longer waveform durations than the other cell types however this is not statistically significant. The absence of a significant difference is likely to be due to the small sample of boundary-off cells.

5.3.4 Boundary-off cell summary

This new boundary-related cell type is located in the subiculum and can be simultaneously recorded with BVCs, grid cells and HD cells. Boundary-off cells have a firing pattern which is similar to the inverse of BVCs. They fire for the entire environment except for a portion located along a wall. Like BVCs the boundary-off cells respond to the insertion of an appropriately-oriented barrier, and produce a second inhibitory field along the barrier.

Boundary-off cells are distinct from other spatial cells. They carry less spatial information and are less spatially selective than BVCs. They have very low grid scores distinguishing them from grid cells, and they carry much less directional information than head direction cells.

Table 5.3.3. Boundary-off cells are distinct from other spatial cells.

Data was taken from the first large environment trial of the day (LWC or LWS) to control for trial order and environment effects. Directional information was calculated from unsmoothed polar plots (bin size 5.6°).

	MEAN ± SEM						
	Gridness score	Directional Information (Bits/spike)	Directional Information (Bits/sec)	Theta modulation score	Waveform amplitude (in μv)	Waveform duration (intervals in μs)	Global Mean rate (Hz)
Boundary-off cells N=9	-0.57 ± 0.04	0.02 ± 0.01	0.15 ± 0.03	6.94 ± 1.58	203.09 ± 16.11	323.55 ± 53.94	6.20 ± 0.89
ALLGRIDS N=51	0.72 ± 0.04***	0.19 ± 0.03	0.34 ± 0.07	28.70 ± 0.04***	138.91 ± 7.79*	225.95 ± 142.05	2.30 ± 0.34***
SUBGRIDS N=30	0.65 ± 0.04***	0.19 ± 0.04	0.21 ± 0.04	27.54 ± 3.71***	153.41 ± 11.57*	264.85 ± 28.64	2.15 ± 0.43***
BVCs N=46	-0.30 ± 0.03***	0.21 ± 0.04*	0.14 ± 0.03	11.96 ± 1.84	154.55 ± 7.23*	294.37 ± 24.17	3.17 ± 0.34***
HDs n=30	-0.18 ± 0.05***	1.15 ± 0.18***	0.63 ± 0.70**	4.96 ± 1.24	132.23 ± 8.36*	223.95 ± 35.28	1.35 ± 0.21***

Compared to Boundary-off cells *p< 0.05 ** p< 0.01 *** p< 0.001 **** p< 0.0001

Chapter 6 Discussion

6.1 Overview of results

This thesis presents novel research identifying and characterising spatial cells located in the subiculum. Of particular importance is the discovery of subicular grid cells. The thesis also extended the work of Lever et al., (2009), by presenting a detailed investigation and characterisation of subicular BVCs. Building upon this earlier work, the present thesis sets a plausible empirical classification criterion, and provides a further characterisation for this relatively unknown cell type. In particular, the thesis also investigates the influence of environment boundaries on subicular grid cell and BVC firing.

This thesis reports a variety of functionally and morphologically diverse spatial cells recorded from the subiculum. I recorded grid cells, BVCs, HD cells and a new type of boundary signalling cell the boundary-off cell. Each of these cell types had distinct properties. Only the grid cells had gridness scores reaching the classification threshold. Only BVCs produced a second firing field for the insertion of an appropriated-oriented barrier and HD cells carried significantly more directional information than any other spatial cell type.

Below is a summary of results presented in this thesis:

1. Grid cells exist in the subiculum.
 - a) The subicular grid cell sample showed periodic firing patterns with gridness scores comparative to grid cells recorded in the MEC and the pre- and parasubiculum.
 - b) Neighbouring subicular grid cells tended to share common grid scales and orientations. As with MEC grid cells and CA1 place cells the spatial scale of the grid cells varied along the long subicular axis, with larger grid spacing in the posterior subiculum and smaller in the anterior subiculum.
 - c) Subicular grid cells carried much less directional information than head direction cells.
 - d) Grid scale and orientation were altered by wall removal. When the environment walls were removed the grid scale expanded. Similar to Barry et al., (2007) who found rescaling between different environments; I show that the increase in grid scale was also related to the novelty of the un-walled environment. In addition there was also a significant shift in

the grid orientation between walled and un-walled environments, which was not evident between trials in the same walled environment.

- e) When a barrier was inserted into the environment it altered the grid cell firing. Grid cells showed variable responses to barrier insertion, the most notable of which were the inhibition of grid fields and a shift/displacement of the grid pattern.
- f) Supporting previous findings of MEC grid cells, subicular grid cell firing patterns remained stable in darkness.

2. BVCs were often recorded simultaneously with grid cells

- a) This thesis has extended upon the work of Lever et al., (2009) and created a BVC classification criterion based upon the doubling of the BVC firing field with the insertion of an appropriately-oriented barrier. A minority of boundary-responsive cells did not show boundary signalling for additional barriers but rather seemed to code specifically for perimeter walls and were classified as non-BVC boundary cells.
- b) None of the BVCs could be classified as grid cells based on the spatial autocorrelogram, nor did they show any preference for directional signalling.
- c) BVCs provided significantly more locational than direction information supporting Lever et al., (2009) and the BVC sample carried significantly less directional information than the HD cells.
- d) This thesis provides corroborative evidence that BVCs signal qualitatively different boundaries. Using a variety of manipulations I tested what qualified as a boundary. BVCs responded to walls, barriers, ridges and objects arranged in a linear array and individually. By varying the height and width of the boundaries it may be possible to quantify what a BVC responds to as a boundary.
- e) Similarly the thesis provides evidence that BVCs also respond to drops and traversable gaps as boundaries.
- f) Like GC firing patterns BVC boundary signalling was also not disrupted in darkness (supporting Lever et al., 2009).

3. I recorded a new type of subicular boundary responsive cell; the boundary-off cell

- a) These cells have firing patterns which can be considered very similar to the inverse of a BVC. Boundary-off cells have large fields which cover the entire environment apart from an 'inhibited field' which follows the boundary. When a barrier was inserted into the

environment, the boundary-off cells responded by creating a second inhibited field on the predicted side of the barrier.

- b) Like BVCs they carried significantly more locational than directional information, and were not disrupted in darkness. They were also distinct from grid cells and HD cells, in that they did not reach the gridness threshold as determined by the spatial autocorrelogram and they carried significantly less directional information than HD cells.

6.2 Wealth of spatial cells in the subiculum

The Subiculum has been a rather under-explored and a relatively unknown structure of the hippocampal formation. For a long time the subiculum was considered to be simply a bidirectional relay region interposed between the hippocampus and the temporal cortex (Witter et al., 2000; Menendez de la Prida et al., 2006). However in recent years a role for the subiculum in spatial mapping has emerged. Early recording studies showed that the subiculum encodes a universal location-specific map independent of the size and the shape of the environment (Sharp, 1997). Firing fields of subicular cells were shown to be larger and more stable across different environments than those of CA1 pyramidal cells. Also distinguishing subicular cells from CA1 place cells subicular cells fired throughout the testing environment and had multiple peaks of activity rather than just the one which is typical of CA1 cells (Sharp and Green, 1994).

Our present study shows that the subiculum houses boundary-related cells, grid cells and head-direction cells. The multiplicity of the spatial representation reported here is similar to that seen in the MEC, the presubiculum and the parasubiculum (Boccaro et al., 2010).

6.2.1 The different spatial cells were functionally and morphologically distinct.

This thesis investigated the basic properties of the spatial cells as well as their responses to environment manipulation. Through looking at the basic properties this thesis shows that the cells are functionally and morphologically distinct.

Using the spatial autocorrelogram cells with periodic firing patterns could be classified as grid cells (gridness scores of ≥ 0.25). The BVCs, HD cells and boundary-off cells were also run through the spatial autocorrelogram. However none of them had gridness scores which reached the inclusion threshold, therefore distinguishing them from the grid cells. Also distinguishing the grid cells was their high theta

modulation scores. The results show that grid cells had significantly higher theta modulation scores than all the other cell types. This supported previous observations, that MEC grid cells are high and head direction cells are low in theta modulation (Sargolini, et al. 2006; Boccara et al., 2010; Brandon et al., 2011).

Grid cells, BVCs and boundary-off cells were clearly distinct from HD cells. As in comparison they all carried significantly less directional information. BVCs were also easily distinguishable because they were the only cells to produce a second firing field for the insertion of a barrier. Neither the grid cells nor the HD cells showed firing patterns that indicated they were signaling boundaries. The BVCs also had different waveforms than the HDs and grid cells. BVCs had longer waveform durations than the grid cells (ALLGRIDS), and had larger peak-to-trough amplitudes than the HD cell sample.

BVCs were also easily distinguishable from boundary-off cells. Boundary-off cells produced a firing pattern which was the inverse of the BVC firing pattern. Further, boundary-off cells carried less locational information per spike and were less locationally selective than BVCs. Boundary-off cells were also dissociable from the other recorded cell types because they had larger peak-to-trough amplitudes and higher firing rates. Also, due most likely to the size of the spatial fields the boundary-off cells had much larger global mean rate than the other cell types.

6.3 Grid cells exist in the subiculum

This thesis provides the first report of grid cells located in the subiculum. Up until relatively recently the subiculum had been a comparatively unexplored structure of the hippocampal formation. Whilst cells with multiple peaks had been noted in early studies (Sharp and Green, 1994), this was prior to the discovery of grid cells in 2004 (Fyhn et al., 2004; Hafting et al., 2005). Additionally, early subicular studies used small environments which would have struggled to capture the multiple fields characteristic of grid cells. This is especially true if the electrodes were recording from the posterior subiculum, which as demonstrate here contains grid cells with predominantly large grid scales. In these cases, in small environments grid cells with large fields may have looked like place cells with large locational fields firing for the entire environment.

Whilst trying to record BVCs from the subiculum, I also recorded grid cells. These subicular grid cells had multiple fields, with firing patterns similar to grid cells recorded from the MEC. Typically grid cell classification requires the use of a spatial autocorrelogram to generate a gridness score for each cell. This score indicates the regularity of the gridness pattern; high gridness scores indicated high

periodicity. In the present thesis 51 grid cells from 5 animals were classified using gridness scores. Histology clearly consigned 30 of the grid cells to the subiculum. The recording locations of the other 21 were much less clear. They may have been recorded from the presubiculum, the white matter above the subiculum/presubiculum and/or from the subiculum itself. Throughout the results section the grid cells were analysed as both the full sample (ALLGRIDS) and as a subiculum only sample (SUBGRIDS).

6.3.1 Subicular grid cells share properties with grid cells recorded from the parahippocampal formation.

6.3.1.1 Subicular grid cells can be identified using gridness scores

Grid cells were defined based on their degree of spatial periodicity (gridness) as per the methods used in previous grid cell studies (Hafting et al., 2005; Barry et al., 2007;2012; Wills et al., 2010; Solstad et al., 2009; Boccara et al., 2010; Yartsev et al., 2011; Stensola et al., 2012). Gridness is determined for each cell by taking a circular sample of the autocorrelogram centered on the central peak (but with the central peak excluded), and comparing correlations across rotated versions of this sample. Between labs and between studies there are subtle differences in the spatial autocorrelogram used, which will be reviewed in more detail later in the discussion.

The putative grid cells were ran through several spatial autocorrelograms and I found a slightly modified version of the one used by Barry (2007; 2012) gave the best fit the majority of periodic cells. Gridness inclusion thresholds vary throughout the literature, with higher thresholds being used for robust analyses of environmental manipulation (Solstad et al., 2008; Barry et al., 2012; Boccara et al., 2010).

The gridness scores of the grid cells definitely consigned to the subiculum was 0.65 ± 0.04 . Those recorded from locations inside and outside the subiculum had a mean gridness score of 0.84 ± 0.07 . Boccara et al., (2010) compared the gridness scores of grid cells recorded across regions (and rats). The highest gridness scores were recorded from grid cells in the MEC with an average of 0.94 ± 0.02 , followed by parasubiculum 0.85 ± 0.03 and the lowest in the presubiculum 0.72 ± 0.03 . If the gridness scores of the subicular grid scores recorded here were compared with those reported by Boccara et al., (2010) it could be considered that gridness was lowest in the subicular grids. However, this could be explained by differences in gridness measures. This issue is discussed in more detail in the research limitations section below.

6.3.1.2 Neighbouring grid cells share a common orientation

This thesis reports that neighbouring subicular grid cells shared a common orientation. This supports similar findings in MEC grid cells (Hafting et al., 2005; Barry et al., 2007; Boccara et al., 2010) and pre- and parasubicular grid cells (Boccara et al., 2010). Like Hafting et al., (2005) this thesis showed that a range of orientations was represented across animals, whilst in general, within rat, locally recorded grid cells shared a common orientation.

6.3.1.3 Spatial scale increases along the subicular anterior-posterior axis

Place field size in CA1 place cells and grid scale in MEC grid cells has been shown to increase along the dorsal-ventral axis (Jung et al, 1994; Hafting et al, 2005; Brun et al., 2008; Barry et al., 2007; Royer et al., 2010; Stensola et al., 2012). Here this thesis shows that grid scale in subicular grid cells also varied throughout the subiculum. Grid scale increased along the anterior-posterior axis of the subiculum with posteriorly-recorded cells having on average grid scales 20cm larger than grid cells recorded 1mm anterior to them.

Recently Couey et al. (2013) reported that neighbouring MEC layer II grid cells generate firing patterns that exhibit similar spacing and orientation, suggesting that adjacent grid cells may influence each other through local microcircuits. Couey et al., (2013) conducted simultaneous whole-cell recordings in clusters of three or more MEC layer II neurons in rat brain slices. In total, they assessed the connectivity between over 600 pairs of stellate cells, which are the candidate grid cells in the MEC. They found that stellate cells of MEC layer II are connected by interneurons that are activated by the synchronous activity of the stellate cells. When 3 cells out of a cluster of 4 were stimulated there was a 64% chance of the unstimulated cell also producing an inhibitory response, whereas if only 1 cell was stimulated there was only a 4% chance of eliciting an inhibitory response in a paired cell. On the basis of these findings, the authors constructed a theoretical network in which adjacent stellate cells were connected to each other via inhibitory connections with unstructured all-or-none connectivity. This model was able to generate stable grid-like firing patterns resembling the experimental data when each stellate cell also received a constant, uniform excitatory input. The neighbouring subicular grid cells recorded in this thesis also shared common spatial scales and orientations, which may suggest that grid scale and orientation may also be dependent upon local microcircuits in the subiculum.

6.3.2 Gridness correlates with theta modulation

The results showing a positive correlation between gridness and theta modulation might appear to lend some support to theories linking theta to self-motion and grid formation (Burgess et al., 2007, Burgess et al., 2008; McNaughton et al., 2006). In particular the oscillatory interference models of grid cell firing assume that theta oscillations are necessary to produce grid cell firing (Burgess et al., 2007; Burgess, 2008; Hasselmo et al., 2008b). Consistent with this, previous studies have shown that disruption to septo-hippocampal theta by inactivating the medial septum strongly reduces gridness in MEC grid cells (Brandon et al., 2011; Koenig et al., 2011).

However, recent evidence casts some doubt on the link between theta oscillations and grid mechanisms. A study looking at MEC grid cells in bats showed cells which looked like lower-quality rat grid cells but without theta oscillation (Yartsev et al., 2011). The existence of MEC grid cells without theta oscillation argues against the interpretation that continuous theta oscillation is an obligatory requirement for grid cell patterns (Yartsev et al., 2011). Another recent study of a large volume of rat grid cells shows no correlation between intrinsic theta frequency and grid scale (Stensola et al., 2012).

Further, the medial septum inactivation studies above (Brandon et al., 2011; Koenig et al., 2011) may not provide solid evidence for a mechanistic link between theta and grid patterns. The key objection to these studies as supporting the oscillatory interference model of grid cell firing is that to disrupt septo-hippocampal theta the whole of the medial septum was inactivated. By inactivating a whole structure, numerous other processes would have been disrupted beyond the theta inputs to the MEC. Thus this evidence alone cannot provide convincing support for oscillatory interference models of grid cell firing.

6.3.3 Grid cells respond to environment manipulation

It is generally agreed that place and grid cells use external environmental cues to anchor their activity to the real world, as evidenced by the fact that their activity appears bound to the local environmental walls and reacts to changes in the environment (place cells: Muller and Kubie, 1987; O'Keefe and Burgess, 1996; Lever et al., 2002a; grid cells: Barry et al., 2007).

Limited evidence has until now suggested that like place cells, grid cells show some disruption to their firing patterns following environmental change (Hafting et al., 2005; Fyhn et al., 2007; Barry et al., 2007; 2012). However, this disruption is distinct between the cell types as unlike place cells grid cells are active across environments, and do not switch fields on and off as place cells do (Muller and Kubie, 1987; Hayman et al., 2003; Leutgeb et al., 2005). Reports suggest that the level of grid cell change may be

related to the extent of environment change. Barry et al., (2007) and Solstad et al., (2008) both showed evidence that MEC grid scale varied parametrically with environment change. Barry et al., (2007) showed that the grid scale expanded parametrically along the expanded dimension, with little expansion in the unchanged dimension.

The present findings support previous reports that environment manipulation can disrupt the grid patterns and also highlights the importance of boundaries to grid cell firing patterns. This will be discussed below.

6.3.3.1 Wall removal alters grid cell firing patterns

In the present thesis I compared firing patterns between walled and un-walled environments. The firing patterns were compared between the un-walled circular open platform and both the large walled circle and large walled square environments. The results show that the grid scale and the orientation of the grid pattern changed with wall removal. Wall removal caused the grid scale to expand. Across the whole sample, grid scale in the un-walled circular open platform expanded by 10 cm (21%) relative to the large-walled square environment, and by 5 cm (11.5%) relative to the large-walled circle environment. This was the first time grid expansion has been formally tested following wall removal. The results also show that wall removal caused an appreciable shift in grid cell orientation. Between the walled and un-walled environments there was 10-14° more shift than between trials in the same walled environments.

This expansion and orientation shift with wall removal supports the findings of Fyhn et al., (2007) and Barry et al., (2007; 2012). Fyhn et al., (2007) showed that large changes to the environment could cause both shifts in the grid patterns, including grid scale and orientation. Whilst small changes (e.g. changing the enclosure but not the room) did not affect grid patterns at all. Fyhn et al., (2007) recorded grid cells simultaneously with place cells and found that changes in grid pattern were accompanied by place cell remapping.

Fyhn et al., (2007) reported a small but significant grid scale expansion of 4.9% between differently shaped- walled environments in 25% of cells; in this study grid expansion wasn't large or common. This result is unlike in ours, where the majority of grid cells demonstrated expansion with wall removal. Perhaps, the expansion seen in Fyhn et al., (2007) is smaller because their alternative environments were different but not novel.

Barry et al., (2007) and Solstad et al., (2008) also recorded MEC grid cells demonstrating expansion. Both studies showed that the grid scale expanded parametrically with environment expansion, however Solstad et al., (2008) reports only two cases. Barry et al., (2007) considered that the parametric changes in grid scale reflect an interaction between intrinsic, path-integrative calculation of location and learned associations to the external environment. In the present thesis when the environment walls were removed the extent of explorable space was increased, allowing the rats to reach ~10-15cm over the environment edge. Conceivably the grid expansion reported here could be related to this environment expansion. The results show grid expansion between the walled and un-walled environments of around 11.5%. If grid expansion was tied to the extension of the perimeter by BVCs we would predict a similar extension from the BVCs, however, with wall removal the BVC field peaks shifted only 4.6%. Thus grid expansion appears to exceed BVC field centrifugal extension. In addition to the fact that grid expansion is partly determined by novelty, this appears to rule out any simple hypothesis linking grid expansion to perimeter extension. This dissociation of response can potentially be characterised in terms of the response to novelty by suggesting that boundary cells are not especially sensitive to novelty (Lever et al., 2009), whereas grid cells are (Barry et al., 2007; 2012).

These results suggest that grid scale changes may not be signalling environmental geometric changes per se. Overall across studies it can be seen that scale increases can be seen between differently shaped walled environments (Fyhn et al., 2007), expanded walled environments (Barry et al., 2007), environments with non-geometric changes (Barry et al., 2012), and with wall removal (shown here in this thesis). One thing that these manipulations may have in common is the novelty of the changed environments. Like seen in Barry et al., (2007; 2012) this thesis also shows a relationship between grid scale expansion and novelty. It maybe that grid expansion reflects an increase in uncertainty (Barry, personal communication).

6.3.3.2 Grid rescaling is related to environment novelty

It has been suggested that the grid pattern maybe anchored by environment boundaries, which would aid stability of the grid pattern (Hafting et al., 2005; Moser and Moser, 2008; Derdikman et al., 2009). With the co-location of grid cells and BVCs in the subiculum, it is likely that the BVCs would similarly be able to anchor the grid pattern to the boundaries. However, in this thesis we report that grid expansion was evident in excess of BVC extension.

The relationship of grid scale expansion and the novelty of the un-walled environment shown in this thesis supports Barry et al., (2007; 2012), who also reported that expansion was to some extent

experience-dependent and correlated with novelty. Barry et al., (2007) reported that grid scale expansion was correlated with the novelty of the stretched environments. In a follow up study Barry et al., (2012) again reported grid expansion when the grid cells were recorded in novel environments varying in colour, material, scent and lighting. Barry et al., (2012) found that when grid cells were recorded between familiar and relatively novel environments grid scale, gridness and orientation changed. In 2012 these changes were also accompanied by place cell global remapping.

In 2012 Barry et al. noted that the relationship between grid scale in the familiar environment and the magnitude of novelty-induced grid expansion was unclear. The authors observed that in general the expansion in the novel environment was not random. In general the larger scaled grid cells expanded by a similar absolute amount to the smaller scaled grid cells. Barry et al., (2012) tentatively considered that their data suggested that grid cells of different scales tended to expand by similar amounts. The present data however does not support the idea of a fixed expansion amount. Indeed, the present results imply that larger scaled grid cells in fact expand by more centimetres than smaller scaled grid cells.

Barry et al., (2012) considers that rescaling has a functional role in novelty signalling which can contribute to place cell remapping. They demonstrate that expansion reduces with experience, and so rescaling could provide a temporary signalling of novelty to place cells. Novelty would be signalled by the temporary mismatch with other grid cells with different scale expansions and with other inputs e.g. boundary inputs. Barry postulates that the stability of BVC firing contributes to this novelty signalling. Certainly our results support this theory.

6.3.3.3 Why rescaling had not been seen in previous studies

If rescaling is a common property of grid cell behaviour then why was it not reported in Hafting et al., (2005)? Hafting et al., (2005) did not find any parametric rescaling. However, it has been noted that in the study the large and small environments were physically different boxes which were both already very familiar to the rats (Barry et al., 2007, personal communication with E. Moser). Thus the switch from one box to the other would have acted more like a change to a new environment than a deformation of the same environment (possibly causing grids to shift and place cells to remap rather than deforming). Indeed supporting this, Barry et al. (2007) provided qualitative observations suggesting that asymmetric grid expansion induced by deforming a familiar environment could be extinguished in a new environment of the deformed shape.

This might suggest that rescaling was due to the novelty of deformed environments, i.e. with parametric extension (Barry et al., 2007; Solstad et al., 2008), or with non-geometric changes (Barry et al., 2012). Maybe the rescaling shown in this thesis between the walled and un-walled environments is because the wall removal acts as a deformation of the same environment rather than as switching between environments. Certainly in the large walled circle compared to the circular open platform manipulation the only change was the wall removal which happened in the ITI with the rat removed from the environment. Arguably the changes between the large walled square and the circular open platform could have also acted like a deformation, as the floor was unwashed and remained the same between trials. That said the rescaling seen in Fyhn et al., (2007) was not because of environment deformation. The grid scale expanded between two different environments with changed walls and floors. Whether rescaling was due to the novelty of deformed environments in particular or with novelty more generally, what is clear is that some environmental manipulation can have dramatic influences in grid cell patterns.

6.3.3.4 Addition of a barrier also disrupts grid patterns

The insertion of an extra boundary into the environment also exerted some influence on grid cell patterns. The results show that the grid cell open field pattern can be changed by the barrier insertion. For many of the grid cells the insertion of a barrier caused field inhibition somewhere in the environment, and/or a shift/deformation of the grid pattern. Barriers causing a change in grid field structure has been already been shown by Derdikman et al. (2009). However that study involved a lot of barriers such that movement was only possible as largely unidirectional travel through relatively narrow corridors. This environment only allowed very stereotyped movement. Here I show powerful deformation and inhibition effects of a single barrier despite the lack of stereotyped unidirectional movement.

This is not the first time inserted single barriers have had an inhibitory effect on spatial cells. Place cells have also been shown to respond to inserted barriers. The insertion of a barrier into a place field often causes an inhibition of firing (Muller and Kubie, 1987; Cressant et al., 1997; Rivard et al., 2004; Barry et al., 2006). Generally inserted barrier affect only those located close to it. Here the results show that inserted barriers can inhibit grid fields that are both intersected and located away from the barrier.

6.3.3.4.1 Boundary cells could explain grid field inhibition

The disruption of the grid field with inserted barriers further highlights the influential nature of boundaries upon grid patterns. As mentioned above it is likely that BVCs such as those co-located in the subiculum provide boundary inputs to subicular grid cells (and perhaps to cells of other regions).

Inserted barriers elicit a second field in the BVCs, as abundantly shown in this thesis. The inhibition of some grid cell firing fields following barrier insertion may indicate that BVCs are directly or indirectly inhibiting the firing the grid cells in and near the barriers. This could happen indirectly via interneurons which are BVC-like. Interestingly, some of the BVCs in this thesis show interneuron-like waveforms.

Boundary-off cells could be explained as pyramidal cells firing everywhere except when inhibited by BVC interneurons. In summary, then, the same population of cells could be providing the barrier-elicited inhibition of firing to grid cells and boundary-off cells.

6.4 Boundary responsive cells exist in the subiculum

The present study extended upon the work of Lever et al., (2009) by recording the largest sample of BVCs to date and by testing them on a variety of environmental manipulations. 46 BVCs were recorded from the subiculum. These cells had firing patterns which had characteristics consistent with those predicted by the model and reported in Lever et al., (2009). Overall these cells had long waveform intervals and high peak-to-trough amplitudes consistent with BVCs being pyramidal cells. The BVCs also had significantly more locational than directional information supporting the findings of Lever et al., (2009).

6.4.1 Development of a BVC classification criteria

The classification of BVCs previously relied upon putative cells conforming to general characteristics set by the model. This consisted of showing boundary responsive firing fields for any boundary in the cells preferred distance and direction which were stable across environments and over time. The discovery of boundary responsive cells which had qualities differing from these characteristics has meant that a more stringent and quantifiable classification of BVCs is required.

According to the model the defining characteristic of a BVC is that it fires whenever an environmental boundary intersects a receptive field located at a specific distance from the rat in a specific allocentric

direction. Therefore a BVC would produce firing fields for perimeter boundaries and for additional free-standing barriers alike.

When an appropriately-oriented barrier is inserted into a testing environment, a BVC would be expected to develop an additional locational field in response to that additional boundary. This response was used as a classification criterion. To be included as a BVC the second field had to consist of bins with firing rates of over 40% of peak rate along at least 50% of the barrier. Cells which showed boundary signalling but did not reach this threshold were classified as non-BVC boundary cells. From looking at those cells which did not produce second fields for the barrier, it may be that some boundary responsive cells are only tuned to perimeter boundaries. Certainly it seems that what a BVC/boundary cell considers is a boundary may not be standard across the boundary-responsive population. The next section explores this issue.

6.4.2 What is a boundary?

To try to qualify what a BVC considers is a boundary BVCs were tested on a wide range of environmental manipulations. In 2009 Lever et al. showed that BVCs could respond to perimeter walls of differently shaped environments, wall-less edges, and for a couple of cells found that a second field was produced for a free-standing barrier, and a traversable drop. The aim was to extend upon these findings to understand better what a BVC considers to be a boundary.

As predicted by the model, A BVC fired whenever an environmental boundary intersected the cells receptive field located at a specific distance from the rat in a specific allocentric direction. Across differently shaped walled environments the location of fields remained stable, even in manipulations which are shown to induce remapping in place cells.

BVCs responded to free-standing barriers similarly to perimeter walls. This response to the addition of an appropriately-oriented barrier was such a common feature that it formed the BVC classification criteria. I also showed for a few BVCs tested that a linear array of bottles is treated as a boundary. BVC boundary responses remained stable in darkness, including the appearance of a barrier-elicited second field for those cells tested.

In an attempt to quantify the responses of BVC firing to boundary manipulation, the height, width and qualities of additional barriers were manipulated. The results showed that boundary signalling could be maintained when the bottle barrier is reduced in size, with some BVCs able to treat single objects (≤ 5 cm wide) as boundaries. In a couple of cells there was still clear field doubling even when the height of the

barrier was drastically reduced. Cells continued to signal a boundary when the height of the barrier was 4.5cm making it easily traversable. However, if this barrier height was further reduced then the production of a second field ceased. Whilst these manipulations were tested with only a couple of BVCs, these responses to barrier height suggest that there is a minimum cue height for that cue to function as a boundary.

The results also confirmed Lever et al., (2009)'s reports that BVCs responded to environment drops similarly to environment walls. In Lever et al., (2009), the cells seemed to be signalling either the environment edge or the extent of explorable space. Our results here suggested that the BVCs primarily responded to the material edge of the environment, because the peaks of the firing fields did not seem to shift outwards much between walled and un-walled trials.

In 2009 Lever et al. reported a single BVC which responded to both the perimeter drop of an open platform and a traversable gap of 13 cm created between 2 open platforms. This finding was confirmed and extended by showing that the majority of BVCs tested in a similar manipulation also produced fields for traversable drops. Compared to the manipulation used by Lever et al., (2009) the number of platforms was increased to three and reduced the size of the gaps between them to 10 cm. The majority of BVCs showed signalling for the traversable gaps, however across the sample there were a variety of responses. Some of the cells showed no responses for any of the drops, some only signalled the drops not the perimeter, and, some demonstrated all-boundary fields for both the perimeter and the traversable drops. As with the variable barriers/objects manipulations, I also tried to quantify how large a traversable gap would be required to provoke BVC signalling. As with the varying height and width of barriers manipulations, this was only investigated with a small sample. However, the results did suggest that gaps as small as 3cm could be considered as boundaries.

BVCs respond to differently shaped environments, un-walled environments, barriers and objects of varying heights/ widths and in complete darkness. The multiplicity of the BVC representation makes 'What constitutes a boundary?' a difficult question to answer. Perhaps the best definition of a boundary as treated as by a BVC is that it is a significant interruption of a broadly horizontal planar surface by a surface broadly perpendicular to that, whether vertically upwards (as in a wall, or a sufficiently extensive object) or downwards (as in a drop). What is considered a boundary may vary somewhat across the BVC population. Overall, what is evident is that 'boundaries' are defined by both sensory cues and limitations to movement that are not restricted to walls.

6.4.3 BVCs vs. border cells

For the subiculum to provide boundary inputs to CA1 the most obvious route is via the MEC, and so MEC border cells are well placed to pass on this information. Lever et al., (2009) suggests that border cells may be a subset of short-distance tuned BVCs. The more numerous short range BVCs is predicted by the model, so in theory if the MEC border cells are a subset of BVCs then longer range MEC BVCs should also exist. However the border cell criterion (≥ 0.5 border score) used by (Solstad et al., 2008; Boccara et al., 2010) may have excluded longer range border cells. A couple of these cells are shown in Figure 4.2.3 but this thesis is focused on short range BVCs which are easier to identify and to test.

Some of the border cells reported by Solstad et al. (2008) could not be classed as BVCs. Many of them fired along only a small portion of the wall. Also, The majority of cells tested in no-wall conditions 'remapped' and responded to a different boundary (see Figure 2.3.5 in the introduction) and thus did not conform to the universal distal and directional vector that BVCs are characterized to have.

Solstad et al., (2008) questioned if subicular BVCs reported in Barry et al., (2006) might be either entorhinal axons or are reflections of CA1 input from the MEC (Solstad et al., 2008; looking at the Barry et al., 2006 data). The BVCs reported here and those reported in Lever et al., (2009) are unlikely to be axons as the waveform durations of subicular BVCs are long like pyramidal cells than what would be expected from axons, which would have much shorter waveforms. It is also unlikely that subicular BVCs are merely reflections of entorhinal border cells. Lever et al., (2009) consider the anatomical distribution of the subicular BVCs argue against this. The MEC projects to the distal- to-CA1 part of the subiculum. Therefore, if it were the case that the subicular BVCs were actually copies of 'border cell' firing, then the majority of BVCs would be located in this projection area. However, as Lever et al., (2009) report and can be seen here in the sample in this thesis, BVCs were recorded throughout the subiculum including in the proximal- to- CA1 portion.

Differing boundary responses can be seen within the subicular BVC sample recorded here. It may be that the boundary signaling cells in the subiculum and MEC are functionally distinct. In this thesis I record cells that conform to the BVC model as well as some boundary-responsive cells which did not. Some cells were not classified as BVCs because they did not respond to the inserted barrier. It may be that these cells specifically respond to perimeter boundaries or show responses like place cells of the hippocampus proper. In general subicular BVC fields remained stable with wall removal, whilst the majority of MEC border cells did not. The tendency for the MEC border cells to switch their preferred boundary when the walls were removed may suggest that they are more sensitive to novelty, or have

some sort of remapping-sensitive component (that the subicular BVCs show less of). Further investigation of MEC and subicular boundary cells is certainly required to establish their similarities and differences.

6.4.4 New class of boundary cell: boundary-off cells

The firing patterns of the boundary-off cells are very similar to the inverse of the BVC. Rather than having a firing field which follows the environment boundaries, these cells fire over the entire environment and have an 'inhibited field' along the boundary. When a barrier was inserted into the environment, the boundary-off cells responded by creating an inhibited field on the predicted side of the barrier, demonstrating again a firing pattern similar to the inverse of the BVC. Like BVCs boundary off cells maintain their firing patterns in darkness, and carry more locational than directional information. These waveforms for these cells have long durations and high peak-to-trough amplitudes characteristic of principal cells.

Without the key manipulations the boundary-off cells could be interpreted as long-range BVCs. However, they are distinguishable. The locational fields of the boundary-off cells almost covered the entire environment. The key distinguishing feature of the boundary-off cells is that they show a portion reduced firing following the boundary. This distinction was clearest in the circular environments, BVC firing fields would be crescent shaped following the boundary, whilst boundary-off cells demonstrated firing patterns inverse of the BVCs with a crescent of inhibition. Also distinguishing the BVCs and the boundary-off cells was the basic properties of the cells. The size of boundary-off fields meant that boundary-off cells carried less locational information per spike and were less locationally selective than BVCs. Also the boundary-off cells had higher firing rates likely due to the size of the boundary-off spatial fields.

6.5 Research implications

6.5.1 The importance of boundary information for spatial signalling of spatial cells located in the hippocampal formation.

The representation of space demands the integration of idiothetic interoceptive cues with exteroceptive environment cues. The necessity of this integration can be seen in place cells (O'Keefe, 2007), head direction cells (Blair and Sharp, 1996) and grid cells (Hafting et al., 2005). Reliance on either method alone can only be successful for a short period (e.g. Burak and Fiete, 2006; McNaughton, 2006). In

general it is considered that the development of spatial firing patterns within a new environment may depend heavily upon path integrative and other idiothetic processes, but with environment experience allothetic exteroceptive cues take over (Knierim et al., 1995; Lever et al., 2002a; Hafting et al., (2005); Barry et al., 2007; 2012).

The BVC model was created to account for the boundary inputs to place cells, and these inputs are suggested to define the location and size of place fields in relation to the environment boundaries (O'Keefe and Burgess, 1996). Arguably, considering the subicular connections into and out of the hippocampal formation, BVC inputs would also be available to anchor grid cells to the environment boundaries (Derdikman et al., 2009).

6.5.1.1 Boundaries and arguably BVCs control place cell fields

Environment boundaries influence place cell firing. when the sensory qualities of two environments differ sufficiently hippocampal place cells are well known to remap (Muller and Kubie, 1987) the greater the difference between environments, the greater the remapping (Muller and Kubie, 1987; Shapiro et al., 1997; Lever et al., 2002a; Anderson and Jeffery, 2003; Wills et al., 2005). In this thesis CA1 place cells show remapping between the square and circular environments. O'Keefe and Burgess (1996) suggest that the shape and location of place fields within an environment can be modelled as the distance of the rat from the environment walls. It was speculated that this boundary information would come from inputs tuned to the boundaries located outside of the hippocampus. The BVC model was created to account for these boundary inputs to CA1 place cells.

O'Keefe and Burgess (1996) demonstrated that when a rectangular environment was stretched it caused some fields to parametrically stretch, and some fields to become bimodal (to have 2 or more peaks). Evidence from barrier insertion studies show that place cells can also become bimodal with the insertion of a free-standing barrier (Lever et al., 2002b; Barry et al., 2006; Fenton et al., 2008). The stretching of the environment walls meant that the boundary inputs signalling the environment walls were also stretched. The modification of these inputs would in turn affect the place fields, as the boundary information was shared which could result in the fields stretching and or being pulled into several fields (becoming bimodal with several peaks).

This thesis shows that BVCs provide boundary information that is not restricted to perimeter walls. The response of BVCs to free-standing barriers and to inserted objects, may explain place cell responses to inserted barriers. As detailed above barrier insertion has been shown to promote and prevent place cell

firing. This was evident for some place fields which were both intersected by the barrier and were proximal to the barrier (Muller and Kubie, 1987; Rivard et al., 2003; Barry et al., 2006). Evidence also shows that internal objects/ barriers can anchor place cell firing. Rivard et al., (2004) showed that place cells can become attached to the barrier, and that rotating/removing the barrier could cause the fields to also rotate or disappear. Cressant et al., (1999) noted that an object could only exert an influence on place fields if it was either located by the environment walls or if the objects were formed into an extended linear array with other objects. The subicular BVCs recorded here present very clear double fields responding to the perimeter and barrier boundaries. If it is considered that these cells provide the boundary inputs to CA1 cells, the signalling for the barrier with the second field would also be available to the CA1 place cells. These inputs could also supply a mechanism to explain the disruption of the place fields when intersected by a barrier.

6.5.1.2 Boundaries may be important for anchoring the grid pattern to the environment.

Like MEC grid cells it seems likely that the grid cell patterns shown in this thesis represent an interaction between sensory and path integrative cues. Hafting et al., (2005) consider that although the spatial structure of the grid pattern may be determined by self-motion cues, orientation and phase may be controlled by the specific landmarks of each environment.

One of the key roles of for environment boundaries is in anchoring the grid pattern (Hafting et al., 2005; Moser and Moser, 2008). Evidence shows that orientation and phase are determined by the environment and can shift with environment change/rotation (Hafting et al., 2005). This thesis reports that wall removal and barrier insertion can alter grid cell firing patterns. In previous studies wall removal has been shown to induce phase rotation (Hafting et al., 2005) and here this thesis demonstrates that wall removal can cause grid cell scale expansion and an orientation shift. However, as is shown here and as is clear throughout the grid cell literature environment change does not cause a complete reorganisation of the grid pattern as is seen in place cells. What does seem to be clear is that the intrinsic grid pattern can exist independently of (though be modifiable by) external cues. This has been attributed to the grid pattern being dependent upon the path integration system (Hafting et al., 2005, Savelli et al., 2008; Solstad et al., 2008; Boccara et al., 2010).

The dependence of the rigid structure of the grid pattern on path integration is consistent with our observations that the grid fields appear independently of specific landmarks and environmental configurations. It is also consistent with previous research showing the immediate appearance of the

grid pattern in new environments and the maintenance of grid patterns in darkness (Hafting et al., 2005). The results presented here in this thesis support these findings and show that the grid pattern can be maintained in the absence of visual cues. This stability in darkness can also be seen in place cells (Quirk et al., 1990), HD cells (Taube et al., 2003), grid cells (Hafting et al., 2005; Fyhn et al., 2007; present data) and BVCs (Lever et al., 2009; and present data).

The observation of BVCs located throughout the subiculum and border cells across all layers of the MEC provides evidence for the existence of boundary-responsive cortical cell populations (Barry et al., 2006; Lever et al., 2009; Hafting et al., 2005; Solstad et al., 2008; Savelli et al., 2008; Boccara et al., 2010). By defining the perimeter of the environment, boundary-responsive cells may serve as reference frames for place cells and grid cells alike. They can serve as reference frames for place cell locational representations within different environments (O'Keefe and Burgess, 1996) and perhaps as a method to anchor the grid patterns (Hafting et al., 2005; Solstad et al., 2008; Boccara et al., 2010; Moser and Moser, 2008). The discovery of border cells intermingled with grid cells in the MEC led Savelli et al., (2008) to consider that border cells could act to relay landmark information for correcting path integration calculations to correct cumulative drift error that are inevitable with using path integration (Hafting et al., 2005; O'Keefe, 2007; Savelli et al., 2008). The combination of grid and BVCs in the subiculum, suggest that subicular BVCs could also perform this service for their neighbouring grid cells.

Evidence of this anchoring is suggested by Savelli et al., (2008). They show that boundaries and subsequently boundary-responsive cells may work to align the grid cells relative to the boundaries of an environment. This alignment would keep the grid stable despite the potential accumulation of self-motion errors (McNaughton et al., 1996; Touretzky and Redish, 1996; Burgess et al., 2007). Savelli et al., (2008) co-recorded grid cells and boundary-responsive cells from the MEC. During a trial in a small walled square environment, the walls were removed in the presence of the rat to reveal the boundaries of a larger-walled box. The authors report a powerful influence of the boundaries which was clear by the changes in spatial firing. The grid patterns continued 'outwards' in the environment, and the firing fields of the boundary cells extended to the new walls in the larger box. For example a cell that fired along the east wall in the small box fired along the east wall in the large box. Savelli et al., (2008) noted that even though the rats were presumably still capable of maintaining the path-integration-based coordinate frame of the smaller environment and were still able to perceive the unaltered global visual cues, the boundaries took control of the grid cell representation. This suggests that BVCs and border cells which signal the boundaries may bind (anchor) the grid cell firing to the environment to keep the internally

generated, grid cell representation calibrated to the coordinate frame of the external world (Savelli et al., 2008).

The mechanisms behind the anchoring of the grid pattern to the geometric boundaries of the environment have not yet been identified. However, the discovery of co-located boundary-responsive cells and grid cells in the MEC, pre-subiculum, parasubiculum and now the subiculum, may suggest that this anchoring could happen locally (Solstad et al., 2008; Boccara et al., 2010).

The hippocampus has also been highlighted as a possible storage site for associations between the path integrator and the specific features of the environment (Hafting et al., 2005; O'Keefe and Burgess, 2005). This is based on the contextual specificity of the hippocampal representations (Muller et al., 1991; Colgin et al., 2008) and the enormous storage capacity of its intrinsic networks (Battaglia and Treves, 1998). It was postulated that the CA1 place cells could input to entorhinal grid cells via the backprojections to the deep and superficial layers of the entorhinal cortex (Iijima et al., 1996; van Haeften et al., 2003; Kloosterman et al., 2003; Witter and Amaral, 2004). These outputs from hippocampal place cells may also reset the entorhinal path integrator as errors accumulate during movement. In further support of this projection recent evidence from Bonnevie et al., (2013), show that grid cells destabilize after inactivation of the hippocampus (also see Bonnevie et al., 2006; Hafting et al., 2008).

The placement of the subiculum within the hippocampal circuit fits with these suggestions. The subiculum is generally considered a CA1 output area with little to no backprojection (Amaral and Witter, 1995; O'Mara et al., 2009). In view of this, communication between the subiculum and the CA1 is generally considered to be via a strong uni-directional projection from the subiculum to the EC (Kloosterman et al., 2003). Subicular spatial information could therefore reach hippocampal place cells via EC projections. If the CA1 cells can input to the EC to reset path integrator errors, it is likely that in light of it being the major output structure of the CA1, it does the same to the subiculum.

6.5.2 Implications for the spatial representation network

Spatial navigation involves a large network of brain structures. Subicular BVCs, place cells and grid cells may be important as outputs to motor systems subserving spatially guided behaviours such as navigation. If subicular BVCs and grid cells can also act as inputs to the neural circuitry representing space, the classic view of the subiculum needs some supplementation. Classically the subiculum is considered the major output region of the CA1, and is not considered to have a direct input route back

into the CA1. If its only role is as an output region then, then it would be expected that subicular firing would follow the same patterns as CA1 cells. However evidence demonstrated that subicular cells could act independently of CA1 place cells (Lever et al., 2009). In 2009 Derdikman and Moser in response to Lever et al., (2009) consider a crucial task towards understanding the relationship of CA1 place cells and BVCs, would be to record them both in a paradigm causing place cells to remap. In this thesis BVCs and place cells were recorded in the same paradigm, and the results showed that the remapping across environments seen in CA1 place cells was not replicated by BVCs.

The strong connections between the subiculum and the CA1 and entorhinal cortex, puts the structure in a privileged position to play an integral role in spatial processing. The subiculum is actually well placed to present information to the CA1 via the entorhinal cortex by virtue of its position in a physiologically active subiculum–entorhinal– hippocampus circuit (Kloosterman et al., 2003). Also, the subiculum has strong projections to parasubiculum and presubiculum, which both provide massive input to hippocampally projecting entorhinal cells (Witter and Amaral, 2004). These connections provide another route for the passage of information back into the hippocampal formation. Furthermore, the parasubiculum’s cortical input is mainly from the subiculum, its output mainly to the entorhinal cortex (Witter and Amaral, 2004). All this considered it is reasonable to assume that at least some subicular output (re)enters the hippocampal formation. The reports of border cells in the MEC and pre- and parasubiculum is consistent with the BVC model, according to which the subicular BVCs provide inputs to place cells in the hippocampus proper via entorhinal cortex.

The functionally diverse cell populations shared by the MEC, presubiculum and parasubiculum may suggest that these brain structures may also share qualities allowing them to host this variety of spatial cells. Boccara et al., (2010) consider the diversity of spatial representation in each of these areas may suggest that each region could conduct its own computations. Here it is shown that the subiculum hosts a diverse range of spatial cells too, and so if the parahippocampal structures compute their own computations then it is likely the subiculum does too.

Boccara et al., (2010) also consider the possibility that in principle, grid, direction and border patterns in pre- and parasubiculum could be inherited passively from parent cells with similar properties in the MEC (Hafting et al., 2005; Sargolini et al., 2006; Solstad et al., 2008) or, from border cells, and BVCs in the subiculum (Lever et al., 2009). They consider that inheritance from MEC to pre- and parasubiculum is unlikely due to the weak nature of the projection (Kohler, 1986; Van Groen and Wyss, 1990). Instead, they consider it more likely that projection cells in pre- or parasubiculum may impose firing patterns on

cells in MEC, because these connections are stronger (Van Groen and Wyss, 1990). The appearance of subicular grid cells may speak to these considerations. The subiculum and the MEC have a strong reciprocal connection (as outlined in the introduction). It may be that spatial cells patterns could be inherited passively either way across this connection. The subiculum also projects strongly to the pre- and parasubiculum, possibly accounting for the abundance of spatial cells located in these areas too. The subiculum has strong efferent connections to the pre- and parasubiculum, whereas returned afferent projections from these areas are much weaker. This suggests that the direction of information between these areas may more likely be from the subiculum to the pre- and parasubiculum.

6.6 Methodological issues

6.6.1 Gridness score

6.6.1.1 Problems with spatial autocorrelogram

Gridness determines the spatial periodicity of the grid pattern and is typically used in the classification of grid cells (Hafting et al., 2005; Fyhn et al., 2004; Solstad et al., 2008; Wills et al., 2012; Barry et al. 2007;2012). All grid cell studies use spatial autocorrelation to calculate gridness scores. However, each spatial autocorrelation procedure has subtle differences including when the maps are smoothed and in the bin sizes used. For instance, the Wills et al., (2010) procedure smooths the firing rate map first then runs the spatial autocorrelation. The Barry et al., (2007) procedure runs the spatial autocorrelation on the unsmoothed firing rate maps, and then smooths the autocorrelation. These dissimilarities can mean the difference between a cell whose periodic properties are well captured by the spatial autocorrelation and one whose properties are not well captured. All the cells were run through various spatial autocorrelations and found that sometimes there were fairly substantial differences in the gridness scores.

Our spatial autocorrelation procedure was a minor smoothing-related modification of Barry et al., (2007) and provided the best fit for the largest number of periodic cells. The success of the modification was probably related to the larger grid scale of subicular grid cells (~70cm) in this dataset then used by Barry et al., (2007) and Wills et al., (2012).

6.6.1.2 Gridness thresholds

In the present thesis, the gridness threshold was set relatively high for inclusion in the grid cell sample (≥ 0.25). In previous studies the threshold was generally only been raised similar to this for more robust

analyses (e.g. ≥ 0.3 Solstad et al., 2008; Barry et al., 2007; Boccara et al., 2010). In general the threshold has in the past been set to >0 (Hafting et al., 2005; Fyhn et al., 2007; Solstad et al., 2008; Wills et al., 2010). Setting the threshold high did mean that some cells which showed periodic firing did not make it into the sample. However, even had the threshold been lowered to ≥ 0 , some cells with clear periodic-like fields would have still been excluded from the analyses.

That said in general the threshold fit the data well. The threshold excluded some cells which certainly were not grid cells, and the majority of cells demonstrating periodic firing were included in the sample. Gridness is certainly a useful measure, however, it must be utilised with caution. With the recent appearance of band-like cells (Krupic et al., 2012) and grid cells with elliptical fields, it may be wise to use other measures in conjunction with gridness scores for the characterisation of periodicity.

Barry et al., (2012) notes that grid patterns can deviate from being perfectly regular in a number of ways. For example, individual fields might be shifted relative to one another, or the entire lattice might be compressed or expanded along one dimension. Both of these eventualities can result in reduced gridness scores. These considerations led Barry et al., (2012) to perform further analyses specifically testing for ellipticity, and, for whether the grid pattern had been compressed/stretched along one dimension. It may be that in future grid cell studies extra measures would be valuable, especially since the influence of boundaries on grid patterns is not always parametric (Barry et al., 2007).

6.6.2 Task design

The work in this thesis highlights the importance of using large environments for analysis of spatial cells. It could reasonably be argued that grid cells have previously been recorded in the subiculum but that they were mistaken for place cells, because of the size of their fields and the environment areas. Grid cells are hard to identify in small environments. Savelli et al., (2008) could not investigate whether grid scale increased with expansion because there were not enough fields in the small environments. Critically, Sharp and Green (2004) noted that some subicular cells showed multiple peaks, however the implications of this discovery were missed. Similarly, this problem also occurred in MEC investigations (Quirk et al., 1992).

However, there are problems caused by using large environments. The larger the environment the longer trial time is required, to ensure adequate sampling. Long trials and long testing days meant that not all cells could be tested in all manipulations. In addition, motivating the rats to explore and forage for rice over a 14 hour periods was a difficult task. However, I managed to successfully counterbalance

this problem by using a slow careful procedure to lower the electrodes into the brain. The electrodes were lowered into the brain using small slow steps, which meant that cell stability across days was optimal.

6.7 Future directions

Research is required to test the differences and similarities of the spatial cells recorded in the different structures. Do they have different roles; are there any functional differences between subicular and MEC spatial cells? The diversity of spatial representation within structures creates more research questions. For example what is the computational significance of having two separate representations of boundaries situated along the hippocampal processing loop? Do the two representations emerge independently or does one drive the activity of the other? In order to address these questions future research needs to be conducted recording subicular and MEC cells simultaneously or at least in the same manipulations. For example if the same wall removal procedure was utilised would the MEC grid cells show the same level of grid expansion?

Further exploration is required to identify why there is such a multiplicity of spatial representation in the SUB, MEC pre and parasubiculum. Boccara et al., (2010) consider that by identifying the common properties of these networks, it may be possible to determine the necessary conditions for a shared pool of spatial cells. The discovery of these conditions and shared properties, may suggest that the subiculum, has more in common with the regions of the parahippocampal system than the hippocampal formation. These are strongly connected regions, and the functional role of sharing the same spatial representations. Given that boundary-responsive cell, HD cells and grid cells are distributed widely in the circuit, this information would be accessible to the majority of grid cells also recorded throughout the circuit.

In a similar vein to above it would be interesting and telling, to see at what age subicular grid cells and BVCs begin to appear. Currently grid cells become evident at P19 (postnatal day 19; Langston et al., 2010; Wills et al., 2012) if subicular spatial cells appear earlier or later than MEC spatial cells this could provide insights into where the grid signal originates from.

Further exploration is required into the relationship of grid scale and novelty. Do subicular grid cells revert to an intrinsic grid scale with experience of a novel environment like MEC grid cells? Future work could test subicular cells using a novelty specific paradigm, similar to Barry et al., (2012). Using a similar

paradigm would also give the benefit of making the results relatively comparable across the subiculum and the MEC.

Further research is required to determine the nature of the relationship between grid cells and BVCs. So far where grid cells have been located so have boundary cells. Is it the case that subicular BVCs and MEC border cells provide necessary inputs to their respective local grid cells?

Further characterisation of grid cells and BVCs in relation to differently sized objects. This thesis makes a good contribution to understanding more what a BVC considers a boundary, however it has also raised further questions. In addition, since BVCs do not treat thin/low objects as boundaries, does it follow that these objects would not cause grid pattern shift/deformation and inhibition in grid cells?

Finally further research is required to translate single cell recording studies to humans. As it stands it remains unclear whether rodent spatial coding has a homologue in humans or whether human navigation is in fact driven by a different, visually based neural mechanism (Ekstrom et al., 2003). However, recently Doeller et al (2010) discovered grid-cell-like representations in humans visible using functional magnetic resonance imaging (fMRI), suggesting this research is translational.

References

- Amaral D.G., Dolorfo C. & Alvarez-Royo P. (1991). Organization of CA1 projections to the subiculum: a PHA-L analysis in the rat. *Hippocampus.*, 1, 415–35.
- Amaral, D.G. & Witter, M.P. (1995). Hippocampal Formation. In: Paxinos, G (Ed), *The Rat Nervous System*. San Diego: Academic Press
- Amaral, D. G., Lavenex, P. (2007). Hippocampal Neuroanatomy. In: Andersen, P., Morris, R., Amaral, D., Bliss, T., O'Keefe, J. (Eds.), *The Hippocampus Book*. Oxford: Oxford University Press.
- Anderson, M. I., & Jeffery, K. J. (2003). Heterogeneous modulation of place cell firing by changes in context. *Journal of Neuroscience*, 23(26), 8827-8835.
- Barry, C., Lever, C., Hayman, R., Hartley, T., Burton, S., O'Keefe, J. et al. (2006). The boundary vector cell model of place cell firing and spatial memory. *Rev.Neurosci.*, 17, 71-97.
- Barry, C., Hayman, R., Burgess, N., & Jeffery, K. J. (2007). Experience-dependent rescaling of entorhinal grids. *Nat.Neurosci.*, 10, 682-684.
- Barry, C., Ginzberg, L. L., O'Keefe, J., & Burgess, N. (2012). Grid cell firing patterns signal environmental novelty by expansion. *Proc.Natl.Acad.Sci.U.S.A*, 109, 17687-17692.
- Battaglia, F. P. & Treves, A. (1998). Stable and rapid recurrent processing in realistic autoassociative memories. *Neural Comput.*, 10, 431-450.
- Blair, H. T. & Sharp, P. E. (1996). Visual and vestibular influences on head-direction cells in the anterior thalamus of the rat. *Behav.Neurosci.*, 110, 643-660.
- Boccaro, C. N., Sargolini, F., Thoresen, V. H., Solstad, T., Witter, M. P., Moser, E. I. et al. (2010). Grid cells in pre- and parasubiculum. *Nat.Neurosci.*, 13, 987-994.
- Bonnevie, T., Dunn, B., Fyhn, M., Hafting, T., Derdikman, D., Kubie, J. L. et al. (2013). Grid cells require excitatory drive from the hippocampus. *Nat.Neurosci.*, 16, 309-317.
- Bruinink A, Bischoff S. (1993) Dopamine D2 receptors are unevenly distributed in the rat hippocampus and are modulated differently than in striatum. *Eur J Pharmacol* 245:157–164.

- Brun, V. H., Solstad, T., Kjelstrup, K. B., Fyhn, M., Witter, M. P., Moser, E. I. et al. (2008). Progressive increase in grid scale from dorsal to ventral medial entorhinal cortex. *Hippocampus*, *18*, 1200-1212.
- Burak, Y. & Fiete, I. R. (2009). Accurate path integration in continuous attractor network models of grid cells. *PLoS.Comput.Biol.*, *5*, e1000291.
- Burgess, N., Jackson, A., Hartley, T., & O'Keefe, J. (2000). Predictions derived from modelling the hippocampal role in navigation. *Biol.Cybern.*, *83*, 301-312.
- Burgess, N., Cacucci, F., Lever, C., & O'Keefe, J. (2005). Characterizing multiple independent behavioral correlates of cell firing in freely moving animals. *Hippocampus*, *15*, 149-153.
- Burgess, N., Barry, C., & O'Keefe, J. (2007). An oscillatory interference model of grid cell firing. *Hippocampus*, *17*, 801-812.
- Burgess, N. (2008). Grid cells and theta as oscillatory interference: theory and predictions. *Hippocampus*, *18*, 1157-1174.
- Cacucci, F., Lever, C., Wills, T. J., Burgess, N., & O'Keefe, J. (2004). Theta-modulated place-by-direction cells in the hippocampal formation in the rat. *J.Neurosci.*, *24*, 8265-8277.
- Canteras N.S. & Swanson L.W. (1992). Projections of the ventral subiculum to the amygdala, septum, and hypothalamus: a PHA-L anterograde tract-tracing study in the rat. *J Comp Neurol*, *324*, 180-94.
- Colgin, L. L., Moser, E. I., & Moser, M.-B. (2008). Understanding memory through hippocampal remapping. *Trends in Neurosciences*, *31*(9), 469-477.
- Commins, S., Aggleton, J. P., & O'Mara, S. M. (2002). Physiological evidence for a possible projection from dorsal subiculum to hippocampal area CA1. *Exp.Brain Res.*, *146*, 155-160.
- Couey, J. J., Witoelar, A., Zhang, S. J., Zheng, K., Ye, J., Dunn, B. et al. (2013). Recurrent inhibitory circuitry as a mechanism for grid formation. *Nat.Neurosci.*, *16*, 318-324.
- Cressant, A., Muller, R. U., & Poucet, B. (1997). Failure of centrally placed objects to control the firing fields of hippocampal place cells. *J.Neurosci.*, *17*, 2531-2542.
- Cressant, A., Muller, R. U., & Poucet, B. (1999). Further study of the control of place cell firing by intra-apparatus objects. *Hippocampus*, *9*, 423-431.

- Derdikman, D., Whitlock, J. R., Tsao, A., Fyhn, M., Hafting, T., Moser, M. B. et al. (2009). Fragmentation of grid cell maps in a multicompartiment environment. *Nat. Neurosci.*, *12*, 1325-1332.
- Descarries L, Lemay B, Doucet G, Berger B (1987) Regional and laminar density of the dopamine innervation in adult rat cerebral cortex. *Neuroscience* 21:807–824.
- Doeller CF, Barry C, Burgess N. (2010) Evidence for grid cells in a human memory network. *Nature*. 463(7281):657-61.
- Ekstrom A D, Kahana M J, Caplan J B, Fields T A, Isham E A, Newman E L & Fried I., (2003). Cellular networks underlying human spatial navigation. *Nature* 425, 184-188
- Felleman, D. J. & Van Essen, D. C. (1991). Distributed hierarchical processing in the primate cerebral cortex. *Cereb.Cortex*, *1*, 1-47.
- Fenton, A. A., Kao, H. Y., Neymotin, S. A., Olypher, A., Vayntrub, Y., Lytton, W. W. et al. (2008). Unmasking the CA1 ensemble place code by exposures to small and large environments: more place cells and multiple, irregularly arranged, and expanded place fields in the larger space. *J.Neurosci.*, *28*, 11250-11262.
- Fremeau RT Jr., Duncan GE, Fornaretto MG, Dearry A, Gingrich JA, Breese GR, Caron MG. (1991) Localization of D₁ dopamine receptor mRNA in brain supports a role in cognitive, affective, and neuroendocrine aspects of dopaminergic neurotransmission. *Proc Natl Acad Sci USA* 88:3772–3776.
- Fuhs, M. C. & Touretzky, D. S. (2006). A spin glass model of path integration in rat medial entorhinal cortex. *J.Neurosci.*, *26*, 4266-4276.
- Fyhn, M., Molden, S., Witter, M. P., Moser, E. I., & Moser, M. B. (2004). Spatial representation in the entorhinal cortex. *Science*, *305*, 1258-1264.
- Fyhn, M., Hafting, T., Treves, A., Moser, M. B., & Moser, E. I. (2007). Hippocampal remapping and grid realignment in entorhinal cortex. *Nature*, *446*, 190-194.
- Frank, L.M., Stanley, G.B., Brown, E.N. (2004). Hippocampal plasticity across multiple days of exposure to novel environments. *Journal of Neuroscience*, *24*(35), 7681-7689.
- Gasbarri A, Verney C, Innocenzi R, Campana E, Pacitti C (1994) Mesolimbic dopaminergic neurons innervating the hippocampal formation in the rat: a combined retrograde tracing and immunohistochemical study. *Brain Res* 668:71–79.

- Gigg, J., Finch, D. M., & O'Mara, S. M. (2000). Responses of rat subicular neurons to convergent stimulation of lateral entorhinal cortex and CA1 in vivo. *Brain Res.*, 884, 35-50.
- Golob, E. J. & Taube, J. S. (1997). Head direction cells and episodic spatial information in rats without a hippocampus. *Proc.Natl.Acad.Sci.U.S.A*, 94, 7645-7650.
- Goodridge, J. P., Dudchenko, P. A., Worboys, K. A., Golob, E. J., & Taube, J. S. (1998). Cue control and head direction cells. *Behav.Neurosci.*, 112, 749-761.
- Greene, J. R. & Totterdell, S. (1997). Morphology and distribution of electrophysiologically defined classes of pyramidal and nonpyramidal neurons in rat ventral subiculum in vitro. *J.Comp Neurol.*, 380, 395-408.
- Hafting, T., Fyhn, M., Molden, S., Moser, M. B., & Moser, E. I. (2005). Microstructure of a spatial map in the entorhinal cortex. *Nature*, 436, 801-806.
- Hafting, T., Fyhn, M., Bonnevie, T., Moser, M. B., & Moser, E. I. (2008). Hippocampus-independent phase precession in entorhinal grid cells. *Nature*, 453, 1248-1252.
- Hampson, R. E., Byrd, D. R., Konstantopoulos, J. K., Bunn, T., & Deadwyler, S. A. (1996). Hippocampal place fields: relationship between degree of field overlap and cross-correlations within ensembles of hippocampal neurons. *Hippocampus*, 6, 281-293.
- Harris, E., Witter, M. P., Weinstein, G., & Stewart, M. (2001). Intrinsic connectivity of the rat subiculum: I. Dendritic morphology and patterns of axonal arborization by pyramidal neurons. *J.Comp Neurol.*, 435, 490-505.
- Hartley, T., Burgess, N., Lever, C., Cacucci, F., & O'Keefe, J. (2000). Modeling place fields in terms of the cortical inputs to the hippocampus. *Hippocampus*, 10, 369-379.
- Hasselmo, M. E. (2008a). Grid cell mechanisms and function: contributions of entorhinal persistent spiking and phase resetting. *Hippocampus*, 18, 1213-1229.
- Hasselmo, M. E. & Brandon, M. P. (2008b). Linking cellular mechanisms to behavior: entorhinal persistent spiking and membrane potential oscillations may underlie path integration, grid cell firing, and episodic memory. *Neural Plast.*, 2008, 658323.

- Hetherington, P. A. & Shapiro, M. L. (1997). Hippocampal place fields are altered by the removal of single visual cues in a distance-dependent manner. *Behav. Neurosci.*, *111*, 20-34.
- Iijima, T., Witter, M. P., Ichikawa, M., Tominaga, T., Kajiwara, R., & Matsumoto, G. (1996). Entorhinal-hippocampal interactions revealed by real-time imaging. *Science*, *272*, 1176-1179.
- Insausti, R., Herrero, M. T., & Witter, M. P. (1997). Entorhinal cortex of the rat: cytoarchitectonic subdivisions and the origin and distribution of cortical efferents. *Hippocampus*, *7*, 146-183.
- Jeewajee, A., Lever, C., Burton, S., Keefe, J. O., & Burgess, N. (2008). Environmental novelty is signaled by reduction of the hippocampal theta frequency. *Hippocampus*, *18*(4), 340-348.
- Jeffery, K. J. (2007). Integration of the sensory inputs to place cells: what, where, why, and how? *Hippocampus*, *17*, 775-785.
- Jung, M. W., Wiener, S. I., & McNaughton, B. L. (1994). Comparison of spatial firing characteristics of units in dorsal and ventral hippocampus of the rat. *J. Neurosci.*, *14*, 7347-7356.
- Kennedy, P. J. & Shapiro, M. L. (2009). Motivational states activate distinct hippocampal representations to guide goal-directed behaviors. *Proc. Natl. Acad. Sci. U.S.A.*, *106*, 10805-10810.
- Kjelstrup, K. G., Tuvnes, F. A., Steffenach, H.-A., Murison, R., Moser, E. I., & Moser, M.-B. (2002). Reduced fear expression after lesions of the ventral hippocampus. *Proceedings of The National Academy of Sciences of The United States of America*, *99*(16), 10825-10830.
- Kloosterman, F., van, H. T., & Lopes Silva, F. H. (2000). Functional characterization of hippocampal output to the entorhinal cortex in the rat. *Ann. N.Y. Acad. Sci.*, *911*, 459-461.
- Kloosterman, F., Van, H. T., Witter, M. P., & Lopes Da Silva, F. H. (2003). Electrophysiological characterization of interlaminar entorhinal connections: an essential link for re-entrance in the hippocampal-entorhinal system. *Eur. J. Neurosci.*, *18*, 3037-3052.
- Knierim, J. J., Kudrimoti, H. S., & McNaughton, B. L. (1995). Place cells, head direction cells, and the learning of landmark stability. *J. Neurosci.*, *15*, 1648-1659.
- Koenig, J., Linder, A. N., Leutgeb, J. K., & Leutgeb, S. (2011). The spatial periodicity of grid cells is not sustained during reduced theta oscillations. *Science*, *332*, 592-595.

- Kohler, C. (1986). Cytochemical architecture of the entorhinal area. *Adv.Exp.Med.Biol.*, 203, 83-98.
- Kohler C. (1990) Subicular projections to the hypothalamus and brainstem: some novel aspects revealed in the rat by the anterograde PHA-L tracing method. *Prog Brain Res*, 83, 59–69.
- Krupic J, Burgess N, O'Keefe J. (2012) Neural representations of location composed of spatially periodic bands. *Science*.337(6096):853-7.
- Langston, R. F., Ainge, J. A., Couey, J. J., Canto, C. B., Bjerknes, T. L., Witter, M. P. et al. (2010). Development of the spatial representation system in the rat. *Science*, 328, 1576-1580.
- Lee, I., Yoganarasimha, D., Rao, G., & Knierim, J. J. (2004). Comparison of population coherence of place cells in hippocampal subfields CA1 and CA3. *Nature*, 430(6998), 456-459.
- Leutgeb, S., Ragozzino, K. E., & Mizumori, S. J. (2000). Convergence of head direction and place information in the CA1 region of hippocampus. *Neuroscience*, 100, 11-19.
- Leutgeb, S., Leutgeb, J. K., Moser, M. B., & Moser, E. I. (2005). Place cells, spatial maps and the population code for memory. *Curr.Opin.Neurobiol.*, 15, 738-746.
- Leutgeb, J. K., Leutgeb, S., Moser, M.-B., & Moser, E. I. (2007). Pattern separation in the dentate gyrus and CA3 of the hippocampus. *Science*, 315(5814), 961-966.
- Lever, C., Wills, T., Cacucci, F., Burgess, N., & O'Keefe, J. (2002a). Long-term plasticity in hippocampal place-cell representation of environmental geometry. *Nature*, 416, 90-94.
- Lever C., Burgess N., Cacucci F., Hartley T. & O'Keefe J. (2002.) What can the hippocampal representation of environmental geometry tell us about Hebbian learning? *Biological Cybernetics*, 88, 356-72.
- Lever, C., Burton, S., Jeewajee, A., O'Keefe, J., & Burgess, N. (2009). Boundary vector cells in the subiculum of the hippocampal formation. *J.Neurosci.*, 29, 9771-9777.
- Marcelin, B., Liu, Z., Chen, Y., Lewis, A. S., Becker, A., McClelland, S. et al. (2012). Dorsoventral differences in intrinsic properties in developing CA1 pyramidal cells. *J.Neurosci.*, 32, 3736-3747.

- Maurer, A. P., Vanrhoads, S. R., Sutherland, G. R., Lipa, P., & McNaughton, B. L. (2005). Self-motion and the origin of differential spatial scaling along the septo-temporal axis of the hippocampus. *Hippocampus*, *15*, 841-852.
- McNaughton, B. L., Barnes, C. A., Gerrard, J. L., Gothard, K., Jung, M. W., Knierim, J. J. et al. (1996). Deciphering the hippocampal polyglot: the hippocampus as a path integration system. *J.Exp.Biol.*, *199*, 173-185.
- McNaughton, B. L., Battaglia, F. P., Jensen, O., Moser, E. I., & Moser, M. B. (2006). Path integration and the neural basis of the 'cognitive map'. *Nat.Rev.Neurosci.*, *7*, 663-678.
- Morris, R. G. M. (1981). Spatial localization does not require the presence of local cues. *Learning and Motivation*, *12*, 239-260.
- Morris, R. G. M., Garrud, P., Rawlins, J. N. P., & O'Keefe, J. (1982). Place navigation impaired in rats with hippocampal lesions. *Nature*, *297*(5868), 681-683.
- Morris R. G. M. Schenk F., Tweedie F., Jarrard L. E. (1990). Ibotenate Lesions of Hippocampus and/or Subiculum: Dissociating Components of Allocentric Spatial Learning, *European Journal of Neuroscience*, *2* (12), 1016-1028
- Moser, E. I. & Moser, M. B. (2008). A metric for space. *Hippocampus*, *18*, 1142-1156.
- Muller, R. U., & Kubie, J. L. (1987). The effects of changes in the environment on the spatial firing of hippocampal complex-spike cells. *Journal of Neuroscience*, *7*(7), 1951-1968.
- Muller, R. U., Kubie, J. L., & Saypoff, R. (1991). The hippocampus as a cognitive graph (abridged version). *Hippocampus*, *1*, 243-246.
- Naber, P. A., Witter, M. P., & Lopes Silva, F. H. (2000). Networks of the hippocampal memory system of the rat. The pivotal role of the subiculum. *Ann.N.Y.Acad.Sci.*, *911*, 392-403.
- O'Keefe, J. & Dostrovsky, J. (1971). The hippocampus as a spatial map. Preliminary evidence from unit activity in the freely-moving rat. *Brain Res.*, *34*, 171-175.
- O'Keefe, J. (1976). Place units in the hippocampus of the freely moving rat. *Exp.Neurol.*, *51*, 78-109.
- O'keefe, J., Nadel, L. (1978). *The Hippocampus as a Cognitive Map*. Oxford: Oxford University Press.

- O'Keefe, J. & Burgess, N. (1996). Geometric determinants of the place fields of hippocampal neurons. *Nature*, *381*, 425-428.
- O'Keefe, J., Burgess, N., Donnett, J. G., Jeffery, K. J., & Maguire, E. A. (1998). Place cells, navigational accuracy, and the human hippocampus. *Philos.Trans.R.Soc.Lond B Biol.Sci.*, *353*, 1333-1340.
- O'Keefe, J. & Burgess, N. (2005). Dual phase and rate coding in hippocampal place cells: theoretical significance and relationship to entorhinal grid cells. *Hippocampus*, *15*, 853-866.
- O'Keefe, J. (2007). Hippocampal neurophysiology in the behaving animal. In P. Andersen, Morris, R., Amaral, D., Bliss, T., O'Keefe, J. (Ed.), *The Hippocampus Book*. Oxford: Oxford University Press.
- O'Mara, S. M., Commins, S., Anderson, M., & Gigg, J. (2001). The subiculum: a review of form, physiology and function. *Prog.Neurobiol.*, *64*, 129-155.
- O'Mara, S. (2005). The subiculum: what it does, what it might do, and what neuroanatomy has yet to tell us. *J.Anat.*, *207*, 271-282.
- O'Mara, S. M., Sanchez-Vives, M. V., Brotons-Mas, J. R., & O'Hare, E. (2009). Roles for the subiculum in spatial information processing, memory, motivation and the temporal control of behaviour. *Prog.Neuropsychopharmacol.Biol.Psychiatry*, *33*, 782-790.
- Paxinos G. and Watson C. (2007). *The rat brain in stereotaxic coordinates, compact 3rd ed.* CD-Rom. Academic press, San Diego.
- Paz-Villagran, V., Save, E., & Poucet, B. (2004). Independent coding of connected environments by place cells. *Eur.J.Neurosci.*, *20*, 1379-1390.
- Quirk, G. J., Muller, R. U., Kubie, J. L., & Ranck, J. B., Jr. (1992). The positional firing properties of medial entorhinal neurons: description and comparison with hippocampal place cells. *J.Neurosci.*, *12*, 1945-1963.
- Quirk, G. J., Muller, R. U., & Kubie, J. L. (1990). The firing of hippocampal place cells in the dark depends on the rat's recent experience. *J.Neurosci.*, *10*, 2008-2017.
- Ranck, J. B., Jr. (1973). Studies on single neurons in dorsal hippocampal formation and septum in unrestrained rats. I. Behavioral correlates and firing repertoires. *Exp.Neurol.*, *41*, 461-531.

- Recce M.L. & O'Keefe J. (1989). The tetrode: an improved technique for multiunit extracellular recording. *Soc Neurosci Abstr*, 15, 1250.
- Redish, A. D., Battaglia, F. P., Chawla, M. K., Ekstrom, A. D., Gerrard, J. L., Lipa, P. et al. (2001). Independence of firing correlates of anatomically proximate hippocampal pyramidal cells. *J.Neurosci.*, 21, RC134.
- Risold P.Y., Thompson R.H. & Swanson L.W. (1997). The structural organization of connections between hypothalamus and cerebral cortex. *Brain Res Rev* 19, 197–254.
- Rivard, B., Li, Y., Lenck-Santini, P. P., Poucet, B., & Muller, R. U. (2004). Representation of objects in space by two classes of hippocampal pyramidal cells. *J.Gen.Physiol*, 124, 9-25.
- Royer, S., Sirota, A., Patel, J., & Buzsaki, G. (2010). Distinct representations and theta dynamics in dorsal and ventral hippocampus. *J.Neurosci.*, 30, 1777-1787.
- Sargolini, F., Fyhn, M., Hafting, T., McNaughton, B. L., Witter, M. P., Moser, M. B. et al. (2006). Conjunctive representation of position, direction, and velocity in entorhinal cortex. *Science*, 312, 758-762.
- Savelli, F., Yoganarasimha, D., & Knierim, J. J. (2008). Influence of boundary removal on the spatial representations of the medial entorhinal cortex. *Hippocampus*, 18, 1270-1282.
- Scharfman, H. E., Witter, M. P., & Schwarcz, R. (2000). The parahippocampal region. Implications for neurological and psychiatric diseases. Introduction. *Ann.N.Y.Acad.Sci.*, 911, ix-xiii.
- Shapiro, M. L., Tanila, H., Eichenbaum, H. (1997). Cues that hippocampal place cells encode: Dynamic and hierarchical representation of local and distal stimuli. *Hippocampus*, 7(6), 624-642.
- Sharp, P. E. & Green, C. (1994). Spatial correlates of firing patterns of single cells in the subiculum of the freely moving rat. *J.Neurosci.*, 14, 2339-2356.
- Sharp, P. E. (1997). Subicular cells generate similar spatial firing patterns in two geometrically and visually distinctive environments: comparison with hippocampal place cells. *Behav.Brain Res.*, 85, 71-92.
- Sharp, P. E. (1999). Subicular place cells expand or contract their spatial firing pattern to fit the size of the environment in an open field but not in the presence of barriers: comparison with hippocampal place cells. *Behav.Neurosci.*, 113, 643-662.

- Sharp, P. E. (2006). Subicular place cells generate the same "map" for different environments: comparison with hippocampal cells. *Behav. Brain Res.*, *174*, 206-214.
- Skaggs W.E., McNaughton B.L., Gothard K.M., Markus E.J. (1993). An information- theoretic approach to deciphering the hippocampal code. In: Advances in neural information processing systems (Hanson S.J., Cowan J.D. and Giles C.L. eds). DD 1030-1037. San Mateo. CA: Kaufman.
- Solstad, T., Boccara, C. N., Kropff, E., Moser, M. B., & Moser, E. I. (2008). Representation of geometric borders in the entorhinal cortex. *Science*, *322*, 1865-1868.
- Stackman, R. W. & Taube, J. S. (1997). Firing properties of head direction cells in the rat anterior thalamic nucleus: dependence on vestibular input. *J. Neurosci.*, *17*, 4349-4358.
- Stensola, H., Stensola, T., Solstad, T., Froland, K., Moser, M. B., & Moser, E. I. (2012). The entorhinal grid map is discretized. *Nature*, *492*, 72-78.
- Staff N.P., Jung H.Y., Thiagarajan T., Yao M. & Spruston N. (2000). Resting and active properties of pyramidal neurons in subiculum and CA1 of rat hippocampus. *J Neurophysiol*, *84*, 2398–408.
- Taube, J. S., Muller, R. U., & Ranck, J. B., Jr. (1990). Head-direction cells recorded from the postsubiculum in freely moving rats. II. Effects of environmental manipulations. *J. Neurosci.*, *10*, 436-447.
- Taube, J. S. (1993). Electrophysiological properties of neurons in the rat subiculum in vitro. *Exp. Brain res.*, *96*, 304-318.
- Taube, J. S. (1998). Head direction cells and the neurophysiological basis for a sense of direction. *Prog. Neurobiol.*, *55*, 225-256.
- Taube, J. S. & Muller, R. U. (1998). Comparisons of head direction cell activity in the postsubiculum and anterior thalamus of freely moving rats. *Hippocampus*, *8*, 87-108.
- Taube, J. S. & Bassett, J. P. (2003). Persistent neural activity in head direction cells. *Cereb. Cortex*, *13*, 1162-1172.
- Taube, J. S. (2007). The head direction signal: origins and sensory-motor integration. *Annu. Rev. Neurosci.*, *30*, 181-207.

- Thompson, L.T., & Best, P.J. (1989). Place cells and silent cells in the hippocampus of freely-behaving rats. *Journal of Neuroscience*, 9(7), 2382-2390.
- Tolman, E. C. (1948). Cognitive maps in rats and men. *Psychol.Rev.*, 55, 189-208.
- Touretzky, D. S. & Redish, A. D. (1996). Theory of rodent navigation based on interacting representations of space. *Hippocampus*, 6, 247-270.
- van Groen. T. & Wyss, J. M. (1990). The connections of presubiculum and parasubiculum in the rat. *Brain Res.*, 518, 227-243.
- van, Haefen. T., Wouterlood, F. G., Jorritsma-Byham, B., & Witter, M. P. (1997). GABAergic presubicular projections to the medial entorhinal cortex of the rat. *J.Neurosci.*, 17, 862-874.
- Verwer, R. W., Meijer, R. J., Van Uum, H. F., & Witter, M. P. (1997). Collateral projections from the rat hippocampal formation to the lateral and medial prefrontal cortex. *Hippocampus*, 7, 397-402.
- Whitlock, J. R., Sutherland, R. J., Witter, M. P., Moser, M. B., & Moser, E. I. (2008). Navigating from hippocampus to parietal cortex. *Proc.Natl.Acad.Sci.U.S.A*, 105, 14755-14762.
- Wiebe, S. P., Staubli, U. V., & Ambros-Ingerson, J. (1997). Short-term reverberant memory model of hippocampal field CA3. *Hippocampus*, 7, 656-665.
- Wills, T. J., Lever, C., Cacucci, F., Burgess, N., & O'Keefe, J. (2005). Attractor dynamics in the hippocampal representation of the local environment. *Science*, 308(5723), 873-876.
- Wills,T.J., Cacucci,F., Burgess,N., O'Keefe,J. (2010) Development of the hippocampal cognitive map in preweanling rats. *Science*, 328, 1573-1576.
- Wills, T. J., Barry, C., & Cacucci, F. (2012). The abrupt development of adult-like grid cell firing in the medial entorhinal cortex. *Front Neural Circuits.*, 6, 21.
- Witter, M. (1993). Organization of the entorhinal-hippocampal system: a review of current anatomical data. *Hippocampus*, 3, 33-44.
- Witter, M. P., Naber, P. A., van, H. T., Machielsen, W. C., Rombouts, S. A., Barkhof, F. et al. (2000). Cortico-hippocampal communication by way of parallel parahippocampal-subicular pathways. *Hippocampus*, 10, 398-410

Witter M.P., Amaral D.G. (2004). Hippocampal formation. In: Paxinos G, editor. *The Rat Nervous System*, 3rd ed. San Diego: Academic Press. 637–703.

Witter, M. P. & Moser, E. I. (2006). Spatial representation and the architecture of the entorhinal cortex. *Trends Neurosci.*, 29, 671-678.

Wouterlood, F. G., Saldana, E., & Witter, M. P. (1990). Projection from the nucleus reuniens thalami to the hippocampal region: light and electron microscopic tracing study in the rat with the anterograde tracer Phaseolus vulgaris-leucoagglutinin. *J.Comp Neurol.*, 296, 179-203.

Wyss, J. M. & van Groen, T. (1992). Connections between the retrosplenial cortex and the hippocampal formation in the rat: a review. *Hippocampus*, 2, 1-11.

Yartsev, M. M., Witter, M. P., & Ulanovsky, N. (2011). Grid cells without theta oscillations in the entorhinal cortex of bats. *Nature*, 479, 103-107.

Zugaro, M. B., Arleo, A., Berthoz, A., & Wiener, S. I. (2003). Rapid spatial reorientation and head direction cells. *J.Neurosci.*, 23, 3478-3482.